

**University of Alberta**

**Cobalt(III)-Mediated Cycloalkenyl-Alkyne Cycloaddition and  
Cycloexpansion Reactions**

by

**Bryan Chi Kit Chan**

A thesis submitted to the Faculty of Graduate Studies and Research  
in partial fulfillment of the requirements for the degree of

**Doctor of Philosophy**

**Chemistry**

©Bryan Chi Kit Chan

Spring 2010

Edmonton, Alberta

Permission is hereby granted to the University of Alberta Libraries to reproduce single copies of this thesis and to lend or sell such copies for private, scholarly or scientific research purposes only. Where the thesis is converted to, or otherwise made available in digital form, the University of Alberta will advise potential users of the thesis of these terms.

The author reserves all other publication and other rights in association with the copyright in the thesis and, except as herein before provided, neither the thesis nor any substantial portion thereof may be printed or otherwise reproduced in any material form whatsoever without the author's prior written permission.

## **Examining Committee**

Jeffrey M. Stryker, Chemistry, University of Alberta

Martin Cowie, Chemistry, University of Alberta

Jillian M. Buriak, Chemistry, University of Alberta

Frederick G. West, Chemistry, University of Alberta

William C. McCaffrey, Chemical Engineering, University of Alberta

Lisa Rosenberg, Chemistry, University of Victoria

## Abstract

A comprehensive investigation of cycloalkenyl-alkyne coupling reactions mediated by cobalt(III) templates is presented. The *in situ* derived cationic  $\eta^3$ -cyclohexenyl complexes of cobalt(III) react with some terminal alkynes to afford either  $\eta^1, \eta^4$ -bicyclo[4.3.1]decadienyl or  $\eta^2, \eta^3$ -vinylcyclohexenyl products, depending on the type and concentration of the alkyne. The mechanism for this cyclohexenyl-alkyne cycloaddition reaction is consistent with the previously reported cobalt-mediated [3 + 2 + 2] allyl-alkyne coupling reaction.

The carbon-carbon bond activation/cyclopentenyl-alkyne ring expansion process was also studied using the 1,3-di-*tert*-butylcyclopentadienyl cobalt system. A modified synthetic strategy to the requisite half-sandwich cobalt(I) cyclopentadiene precursor was developed using cobalt(II) acetoacetate, avoiding the use of simple cobalt(II) halides which are prone to ligand disproportionation. Furthermore, the preparation of the cobalt(III) cyclopentenyl precursor,  $(t\text{-Bu}_2\text{C}_5\text{H}_3)\text{Co}(\eta^4\text{-C}_5\text{H}_6)$ , was accomplished via hydride addition to the easily prepared cobalticenium complex  $[(t\text{-Bu}_2\text{C}_5\text{H}_3)\text{Co}(\text{C}_5\text{H}_5)]\text{BF}_4$  and avoids the use of the thermally sensitive  $(t\text{-Bu}_2\text{C}_5\text{H}_3)\text{Co}(\text{ethylene})_2$ .

Disubstituted alkynes such as 2-butyne or diphenylacetylene undergo cyclopentenyl coupling to afford the corresponding  $\eta^5$ -cycloheptadienyl products, albeit in lower yields compared to the pentamethylcyclopentadienyl

cobalt system. The 1,3-di-*tert*-butylcyclopentadienyl ancillary ligand shows unique and unusual reactivity, coupling with *tert*-butylacetylene to afford a novel spiro[4.5]decatrienyl complex. Ultimately, the poor isolated yields of seven-membered products demonstrate that the disubstituted cyclopentadienyl ligand system is a poor candidate for future studies in this area.

A mechanistic investigation of the cobalt-mediated carbon-carbon bond activation process was performed. Cationic cobalt  $\eta^2$ -vinyl complexes were proposed as viable intermediates in the activation process and synthetic routes to these compounds were examined. However, the resulting vinyl complexes were unstable and could not be directly isolated and characterized. Preparation of cobalt vinyl complexes in the presence of cycloalkadienes did not furnish the expected cycloexpanded products, suggesting alternative routes to the cobalt vinyl intermediates are necessary. During the course of the mechanistic investigation, a high-yielding alternative synthetic procedure for  $(C_5Me_5)Co(\eta^4\text{-butadiene})$  from the easily prepared precursor,  $[(C_5Me_5)CoI_2]_n$ , was found, circumventing the use of the thermally sensitive  $(C_5Me_5)Co(ethylene)_2$ .

## Acknowledgements

First and foremost, I would like to express my gratitude to my research advisor, Professor Jeffrey Stryker, for providing a creative and encouraging atmosphere during my time here.

I also wish to acknowledge and thank former and current members of the Stryker Group that have provided me with motivation, thoughtful discussions and research insights. In no particular order, they are: Dr. Ross Witherell, Dr. David Norman, Dr. Rick Bauer, Dr. Owen Lightbody, Paul Fancy, Dr. Takahiro Saito, Kai Ylijoki, Andrew Kirk, Jeremy Gauthier, and Dr. Robin Hamilton. In particular, I would like to thank Dr. Masaki Morita for being a repository of chemical knowledge. The staff of analytical and spectral services is also thanked for their assistance in characterizing compounds, especially Drs. Bob McDonald and Michael Ferguson for the numerous X-ray structure determinations.

Lastly, I would like to thank my friends and family for their support, encouragement and understanding.

## Table of Contents

	Page
Chapter 1. Introduction and Background .....	1
Section 1. General Introduction.....	1
Section 2. Metal-Mediated Allyl-Alkyne Coupling Reactions .....	8
A. Introduction .....	8
B. Catalytic Allyl-Alkyne Coupling Processes .....	10
C. Stoichiometric Allyl-Alkyne Coupling Reactions .....	22
D. Multiple Allyl-Alkyne Coupling Reactions.....	32
E. [3 + 2] Allyl-Alkyne Cycloaddition Reactions.....	37
Conclusions .....	41
 Chapter 2. [3 + 2 + 2] Allyl-Alkyne Cycloaddition Reactions of Agostic Cobalt Cyclohexenyl Complexes.....	 42
Section 1. Introduction .....	42
A. [3 + 2 + 2] Allyl-Alkyne Cycloaddition Reactions.....	43
B. Cobalt-Mediated [5 + 2] Cyclopentenyl-Alkyne Cycloaddition Reactions Involving Carbon-Carbon Bond Activation.....	 54
C. Cobalt-Mediated Cyclopentenyl-Acetylene Cycloaddition Reactions .....	 60
D. Project Goals .....	64

Section 2. Results and Discussion.....	65
A. Cobalt $\eta^3$ -Cyclohexenyl-Acetylene Cycloaddition Reactions..	65
B. Reactions of (C <sub>5</sub> Me <sub>5</sub> )Cobalt $\eta^3$ -Cycloheptenyl and $\eta^3$ -Cyclooctenyl Complexes with Alkynes .....	88
C. Conclusions .....	92
 Chapter 3. 1,3-Di- <i>tert</i> -butylcyclopentadienyl Cobalt Complexes .....	95
Section 1. Introduction .....	95
A. Synthetic Routes to Cobaltocene Complexes .....	102
B. Project Goals .....	104
Section 2. Results and Discussion.....	106
A. Preparation of 1,3-Di- <i>tert</i> -butylcyclopentadienyl Cobalt Templates.....	106
B. Ring-Expansion Reactions of the (1,3-Di- <i>tert</i> - cyclopentadienyl)cobalt( $\eta^3$ -cyclopentenyl Complex With Alkyne .....	127
C. Reactions of the (1,3-Di- <i>tert</i> -butylcyclopentadienyl)cobalt $\eta^3$ -Cyclohexenyl, $\eta^3$ -Cycloheptenyl, and $\eta^3$ -Cyclooctenyl Complexes with Alkynes.....	139
D. Synthesis of Acyclic $\eta^5$ -Pentadienyl Complexes of Cobalt.....	143
E. Conclusions.....	153

## Chapter 4. Mechanism and Intermediates in the Cyclopentenyl/Alkyne

Carbon-Carbon Bond Activation Process.....	155
Section 1. Introduction .....	155
A. Activation of Carbon-Carbon $\sigma$ -Bonds in Strained Ring Systems .....	157
B. Carbonyl Group Activation of Carbon-Carbon $\sigma$ -Bonds .....	159
C. Nitrile Group Activation of Carbon-Carbon $\sigma$ -Bonds .....	161
D. Proximity Effects .....	164
E. $\beta$ -Carbon Elimination and Aromatization .....	168
F. Activation by Electrophilic Cobalt Complexes.....	176
G. Activation by Electrophilic Titanium Complexes .....	177
H. Mechanistic Proposals for the [5 + 2] $\eta^3$ -Cyclopentenyl- Alkyne Cycloaddition/Carbon-Carbon Bond Activation Process .....	180
I. General Formation of $\eta^2$ -Vinyl/1-Metalacyclopropene Complexes .....	188
Section 2. Results and Discussion.....	193
A. Vinyl Grignard Addition to Cobalt(III) Precursors .....	193
B. Vinyl Grignard Addition to Cobalt(II) Precursors .....	200
C. Strong Acid Addition to Cobalt Mono-Alkyne Complex .....	210
D. Conclusions and Future Goals.....	213

Chapter 5. Experimental Procedures .....	216
Chapter 2.....	218
Chapter 3.....	223
Chapter 4.....	244
Notes and References.....	248
Appendix – Crystallographic Experimental Details .....	273

## List of Tables

	Page
Table 2-1. NMR Spectroscopic Data for Bicyclic Cation <b>42</b> .....	69
Table 2-2. NMR Spectroscopic Data for Vinylcyclohexenyl Cation <b>43</b> .....	71
Table 2-3. NMR Spectroscopic Data for Cyclohexenyl Silyl Cation <b>44</b> .....	81
Table 3-1. <sup>1</sup> H NMR Spectroscopic Data for ( <i>t</i> -Bu <sub>2</sub> C <sub>5</sub> H <sub>3</sub> )Co(C <sub>2</sub> H <sub>4</sub> ) <sub>2</sub> <b>65</b> .....	112
Table 3-2. <sup>1</sup> H NMR Spectroscopic Data for ( <i>t</i> -Bu <sub>2</sub> C <sub>5</sub> H <sub>3</sub> )Co( $\eta^4$ -C <sub>5</sub> H <sub>6</sub> ) <b>72A</b> .....	120
Table 3-3. <sup>1</sup> H NMR Spectroscopic Data for (C <sub>5</sub> H <sub>5</sub> )Co( <i>t</i> -Bu <sub>2</sub> C <sub>5</sub> H <sub>4</sub> ) <b>72B</b> .....	125
Table 4-1. <sup>1</sup> H NMR Spectroscopic Data for Cobalt $\eta^5$ -Cyclohexadienyl Cation <b>110</b> .....	206

## List of Figures

	Page
Figure 1-1. Dewar-Chatt-Duncanson Description of Metal-Alkyne Bonding .....	2
Figure 1-2. Metal-Alkyne Isomerization to Metal-Vinylidene .....	4
Figure 1-3. $\eta^1$ - $\eta^3$ Metal Allyl Isomerization .....	5
Figure 1-4. Frontier Molecular Orbital Description of Metal Allyl Bonding .....	6
Figure 1-5. Examples of Isolable Allyl-Alkyne Metal Complexes .....	8
Figure 2-1. Examples of Natural Products Containing a Seven-Membered Ring .....	42
Figure 2-2. Perspective view of Bicyclic Cobalt Cation <b>42</b> .....	67
Figure 2-3. Perspective View of Cobalt Vinylcyclohexenyl Cation <b>43</b> .....	68
Figure 2-4. $^1\text{H}$ and $^{13}\text{C}$ Numbering System for Bicyclic Cobalt Cation <b>42</b> ....	69
Figure 2-5. Selected $^{13}\text{C}$ Chemical Shifts of Similar $\eta^1, \eta^4$ -Cycloheptadienyl Complexes .....	70
Figure 2-6. $^1\text{H}$ and $^{13}\text{C}$ Numbering System for Cobalt Vinylcyclohexenyl Cation <b>43</b> .....	71
Figure 2-7. Compounds Possessing $\eta^1, \eta^4$ -Binding Motif .....	73
Figure 2-8. $^1\text{H}$ and $^{13}\text{C}$ Numbering System for Cobalt Cyclohexenyl Silyl Cation <b>47</b> .....	81
Figure 2-9. Perspective View of Cobalt Cyclohexenyl Silyl Cation <b>47</b> .....	83

Figure 2-10. Perspective View of Cobalt Cycloheptadiene Complex <b>51</b> .....	89
Figure 3-1. Perspective View of [( <i>t</i> -Bu <sub>2</sub> C <sub>5</sub> H <sub>3</sub> ) <sub>2</sub> Co] cation <b>63</b> .....	108
Figure 3-2. <sup>1</sup> H and <sup>13</sup> C Numbering System for ( <i>t</i> -Bu <sub>2</sub> C <sub>5</sub> H <sub>3</sub> )Co( $\eta^4$ -C <sub>5</sub> H <sub>6</sub> ) <b>72A</b> .....	120
Figure 3-3. <sup>1</sup> H and <sup>13</sup> C Numbering System for (C <sub>5</sub> H <sub>5</sub> )Co( $\eta^4$ - <i>t</i> -Bu <sub>2</sub> C <sub>5</sub> H <sub>4</sub> ) <b>72B</b> .....	125
Figure 3-4. Perspective View of ( <i>t</i> -Bu <sub>2</sub> C <sub>5</sub> H <sub>3</sub> )Co(2,3-diphenylhepta- 2,4-dien-1-yl) cation <b>77</b> .....	131
Figure 3-5. Perspective View of Spirocycle <b>78</b> .....	133
Figure 3-6. Perspective View of [( <i>t</i> -Bu <sub>2</sub> C <sub>5</sub> H <sub>3</sub> )Co( $\eta^5$ -pentadienyl)] cation <b>81</b> .....	149
Figure 4-1. Metal-Ligand Orbital Interactions .....	156
Figure 4-2. Proposed Carbon-Carbon Bond Activation Mechanism Part 1.....	184
Figure 4-3. Proposed Carbon-Carbon Bond Activation Mechanism Part 2.....	186
Figure 4-4. Examples of Complexes Bearing $\eta^2, \eta^3$ -Vinylcyclohexenyl Organic Fragments.....	187
Figure 4-5. $\eta^2$ -Vinyl and 1-Metalacyclopropene Canonicals .....	188
Figure 4-6. Examples of Half-Sandwich Cobalt Mono-Alkyne Complexes .....	192

Figure 4-7. $^1\text{H}$ Numbering Scheme for Cobalt $\eta^5$ -Cyclohexadienyl Cation <b>110</b> .....	205
Figure 4-8. Potential Targets for the Preparation of Cobalt Mono-Alkyne Complexes .....	214
Figure 4-9. Anionic Tripodal Tris(diphenylphosphinomethyl)borate Complex of Cobalt .....	215

## List of Commonly Used Symbols and Abbreviations

Å	Angstrom
Acac	Acetylacetonato
B	Base
Bu	Butyl group
CHD	cyclohexadiene
COSY	Correlated Spectroscopy
COD	Cyclooctadiene
Cp	$\eta^5$ -Cyclopentadienyl
Cp*	$\eta^5$ -Pentamethylcyclopentadienyl
$\Delta$	Heating
dba	Dibenzylideneacetone
DMAD	Dimethyl acetylenedicarboxylate
Et	Ethyl group
Equiv.	Equivalents
Fp	CpFe(CO) <sub>2</sub>
GCOSY	Gradient COSY
HMBC	Heteronuclear Multiple Bond Coherence
HMQC	Heteronuclear Multiple Quantum Coherence
HOMO	Highest Occupied Molecular Orbital
Hz	Hertz

<i>J</i>	Coupling constant
L	Ligand
LUMO	Lowest Unoccupied Molecular Orbital
M	Metal
Me	Methyl
MO	Molecular Orbital
NMR	Nuclear Magnetic Resonance
Nu	Nucleophile
OAc	Acetate
OTf	Triflate
Ph	Phenyl
Pr	Propyl
psig	pounds per square inch gauge pressure
R	Alkyl group
S	Solvent
<i>t</i> -Bu	<i>tert</i> -Butyl group
THF	Tetrahydrofuran
TMS	Trimethylsilyl
Tol	Toluene
Ts	Tosylate
UV	Ultraviolet
X	Halogen atom or halide ion

$\eta$

Hapticity

$\delta$

Chemical shift

# Chapter 1. Introduction and Background

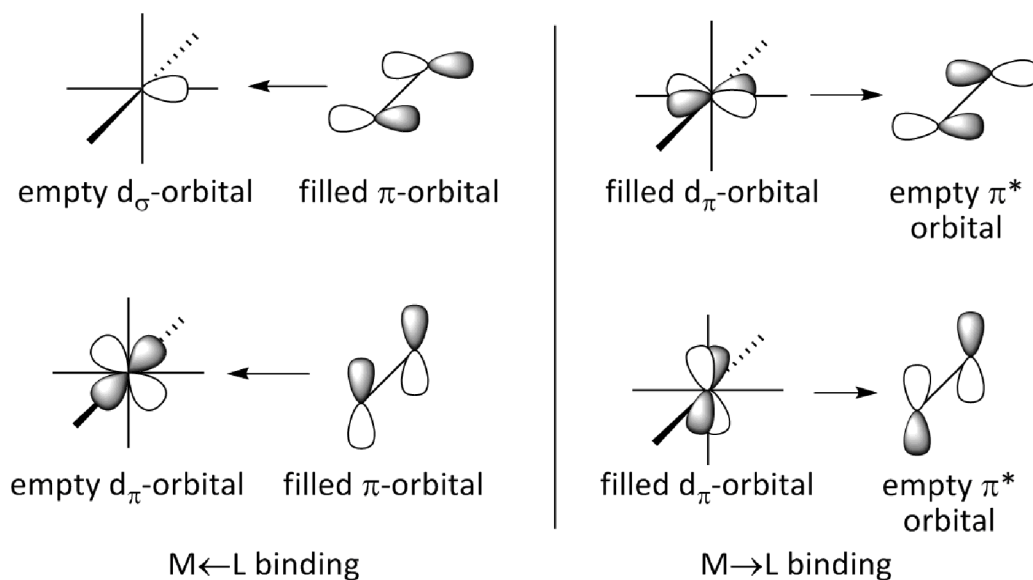
## Section 1. General Introduction

Transition metal-mediated formation of new carbon-carbon bonds is an important process in synthetic organometallic and organic chemistry.<sup>1, 2</sup> Transformations that would have been impossible or demand forcing conditions can now be realized through the use of metal complexes that can alter normal modes of reactivity. One important class of metal-mediated reactions is ring-construction via cycloaddition reactions. Multiple carbon-carbon bond forming reactions can occur in a concerted or step-wise fashion to quickly build complex skeletal arrangements selectively and efficiently.

Among the more ubiquitous substrate classes used for cycloaddition chemistry are the alkynes and numerous reviews have been published on the generality of alkyne cycloaddition reactions to produce both carbocyclic and heterocyclic compounds.<sup>3-5</sup> Metal-alkyne complexes are typically very reactive and can incorporate additional alkynes or other substrates such as carbon monoxide, alkenes, nitriles and ketenes to produce an array of products. Due to the high reactivity of metal-alkyne complexes, it is often difficult to bias a system such that only one product is predominant.<sup>1</sup>

The binding motif of alkynes to metals is similar to olefins and can be best described by the Dewar-Chatt-Duncanson model (Figure 1-1). One of the filled  $\pi$ -molecular orbitals on the alkyne donates electron density to an empty  $\sigma$ -symmetry metal orbital and, in return, a filled  $d_{\pi}$ -molecular orbital donates into the corresponding ligand-based  $\pi^*$ -antibonding orbital.<sup>6-8</sup> Furthermore, there is an orthogonal set of  $\pi/\pi^*$  molecular orbitals that can also interact with the metal centre which can render the alkyne to be either a two or four electron donating ligand. Various examples of this behaviour have been reported.<sup>9</sup>

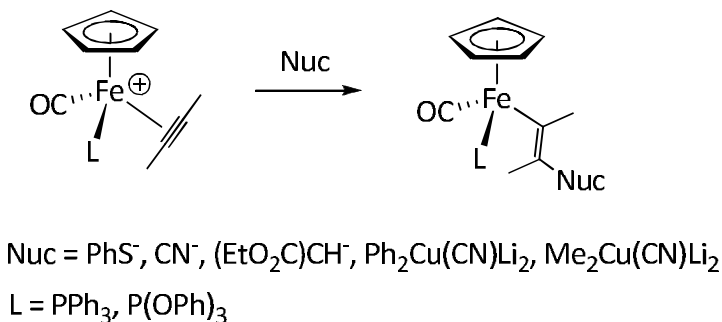
**Figure 1-1:** Dewar-Chatt-Duncanson Description of Metal-Alkyne Bonding



Alkynes that interact with metals via a four-electron binding mode are remarkably inert compared to alkynes that function as two-electron donating

ligands, which are susceptible to electrophilic or nucleophilic attack. An example of this reactivity has been reported by Reger, whereby a variety of nucleophiles add to a bound alkyne to form the corresponding 1-alkenyl complexes (Equation 1-1).<sup>10</sup>

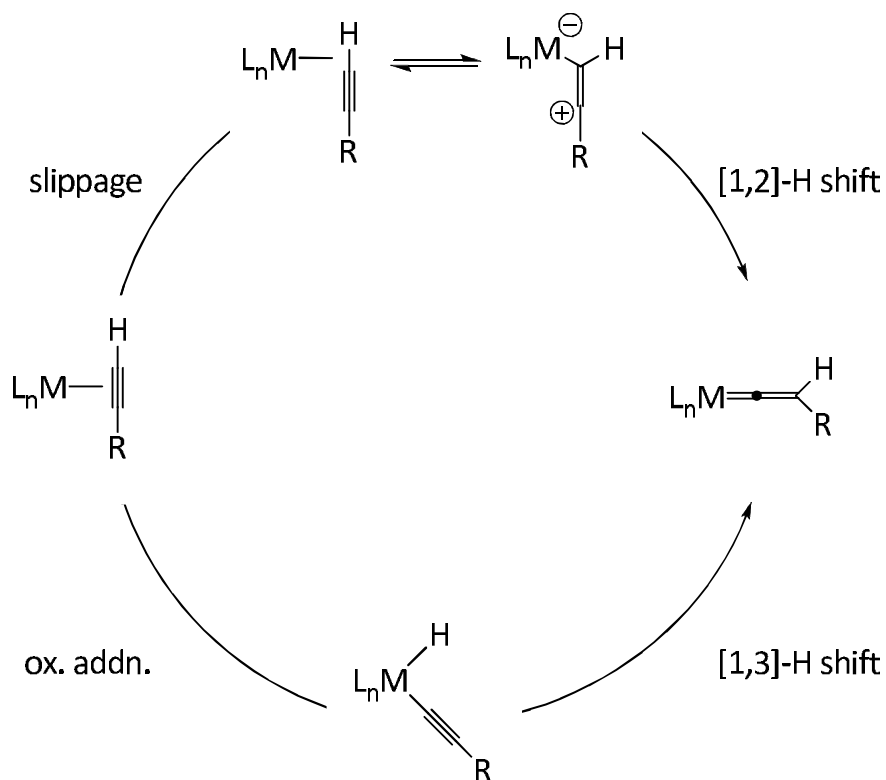
**Equation 1-1**



Metal-alkyne complexes consisting of electron-rich metals and terminal alkynes can also isomerize to metal-vinylidene complexes. Hoffmann has performed extended Huckel calculations that reveal that while the isomerization of free acetylene to free vinylidene is disfavoured, metal-bound  $\eta^2$ -acetylene complexes will readily isomerize to the corresponding metal vinylidene complex.<sup>11, 12</sup> Hoffmann also reports that the mechanism of  $\eta^2$ -alkyne isomerization proceeds via side-on coordination of the alkyne moiety, followed by slippage to an agostic carbon-hydrogen bond and a [1,2]-hydrogen shift (Figure 1-2). Another process that is energetically accessible is  $\sigma$ -donation of the alkyne to the metal to form a zwitterionic intermediate, which can then undergo

a [1,2]-hydrogen shift to afford the metal vinylidene. Hoffman also notes that oxidative addition of the carbon-hydrogen bond followed by a [1,3]-hydrogen shift proposed by Antonova is energetically unfavourable.<sup>13, 14</sup>

**Figure 1-2:** Metal-Alkyne Isomerization to Metal-Vinylidene



Hoffmann suggests that facile isomerization to form the vinylidene arises from the HOMO of the  $\eta^2$ -alkyne complex possessing slight anti-bonding character. On the other hand, the HOMO of the vinylidene complex possesses more non-bonding character.  $\eta^2$ -Alkyne to vinylidene isomerization removes some of the anti-bonding character of the HOMO from the  $\eta^2$ -alkyne complex

and promotes the isomerization to the vinylidene form. Other calculations performed at the MP2 level have confirmed this.<sup>15</sup>

Allyl ligands are another common organic fragment used in cycloaddition reactions. The allyl ligand is coordinated in either the  $\eta^1$ -allyl or  $\eta^3$ -allyl form (Figure 1-3).

**Figure 1-3:**  $\eta^1$ - $\eta^3$  Metal Allyl Isomerization

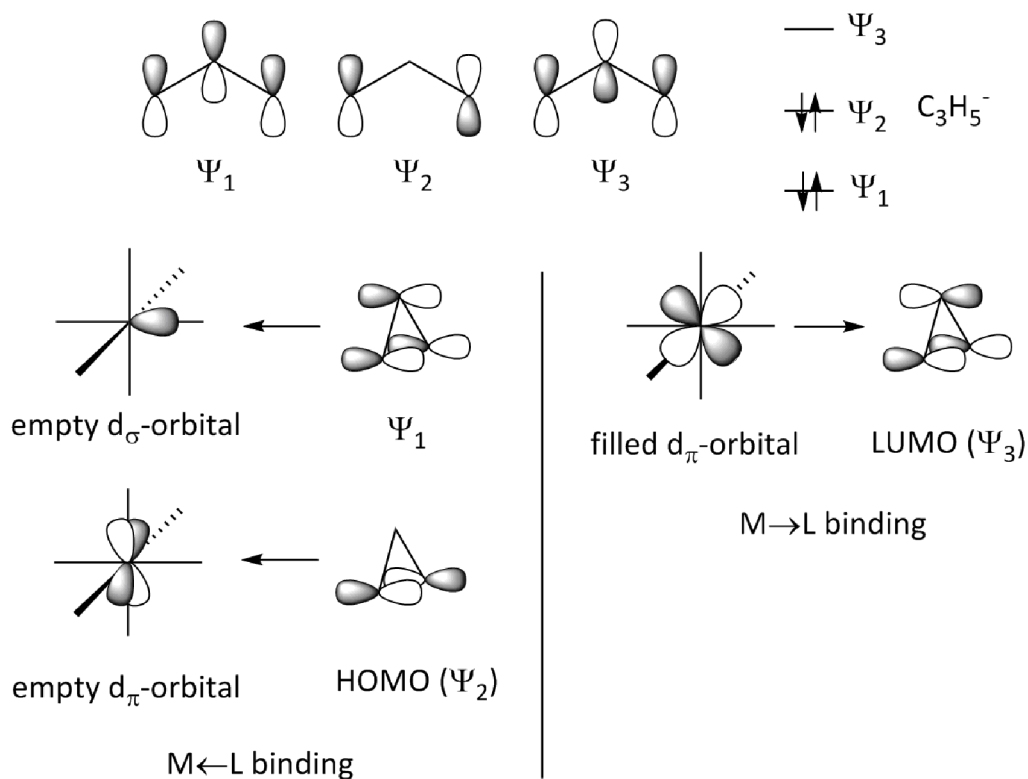


The hapticity is determined by a combination of factors such as the oxidation state of the metal and the availability of a coordination site. The description of  $\eta^3$ -allyl metal bonding can be best described using frontier molecular orbital theory where the allyl anion donates electron density from the  $\pi$ -symmetry HOMO to an empty  $d\pi$ -metal orbital and from the  $\sigma$ -symmetry allyl bonding orbital to an empty  $d\sigma$ -metal orbital (Figure 1-4). In return, the metal donates electron density from a filled  $d\pi$ -orbital into the empty allyl antibonding  $\pi^*$ -molecular orbital.

Metal  $\eta^3$ -allyl complexes can be prepared using a variety of methods.<sup>16-20</sup> Synthetic methodologies to generate metal  $\eta^3$ -allyl complexes include oxidative addition of allylic substrates, transmetallation of main group metal allyl complexes, nucleophilic attack on a 1,3-diene metal complex, insertion of 1,3-dienes into a metal hydride or metal alkyl, acidic cleavage of complexed allylic

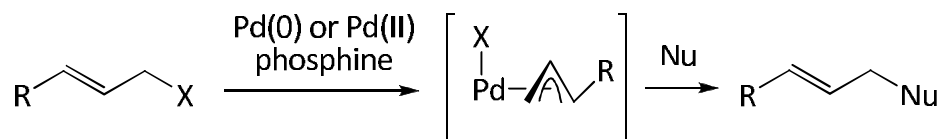
ethers, and allylic proton abstraction from a  $\pi$ -olefin complex either by the metal or an external reagent.<sup>1, 2</sup>

**Figure 1-4:** Frontier Molecular Orbital Description of Metal Allyl Bonding



While many important catalytic processes, including the oligomerization and polymerization of conjugated dienes,<sup>16</sup> involve  $\eta^3$ -allyl complexes as key intermediates, relatively few metal-allyl complexes have been developed as useful reagents in organic synthesis. One notable exception to this is the widespread synthetic application of catalytic palladium for use in nucleophilic substitution or alkylation of allylic substrates in the Tsuji-Trost allylation (Scheme 1-1).<sup>21, 22</sup>

### Scheme 1-1



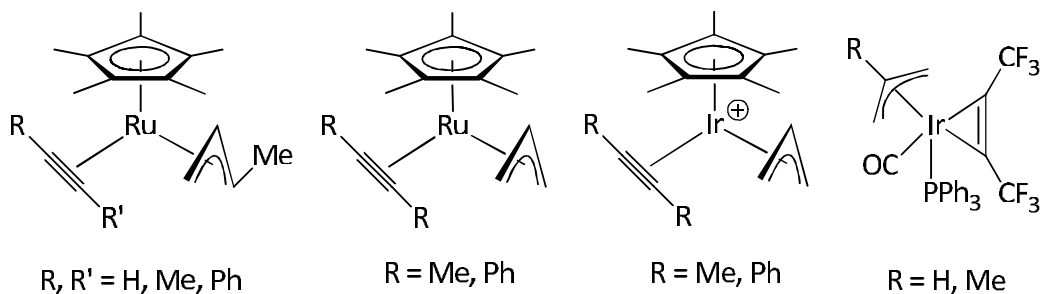
Previous workers in the Stryker group found that allyl-alkyne coupling mediated by iridium, cobalt, and ruthenium complexes could result in the formation of seven-membered carbocycles from the cycloaddition of the allyl moiety with two equivalents of alkyne.<sup>23-25</sup> While this methodology could be of significant utility to synthetic chemists, the use of endocyclic allyl moieties in such cycloaddition reactions has not been explored fully. It is possible that the use of endocyclic allyl ligands would produce bicyclic products and hence increase the complexity of the metal complexes isolated. Such a discovery would benefit the synthetic community and help lower the number of steps used to construct such polycyclic systems using standard organic methodology.

## Section 2. Metal-Mediated Allyl-Alkyne Coupling Reactions

### A. Introduction

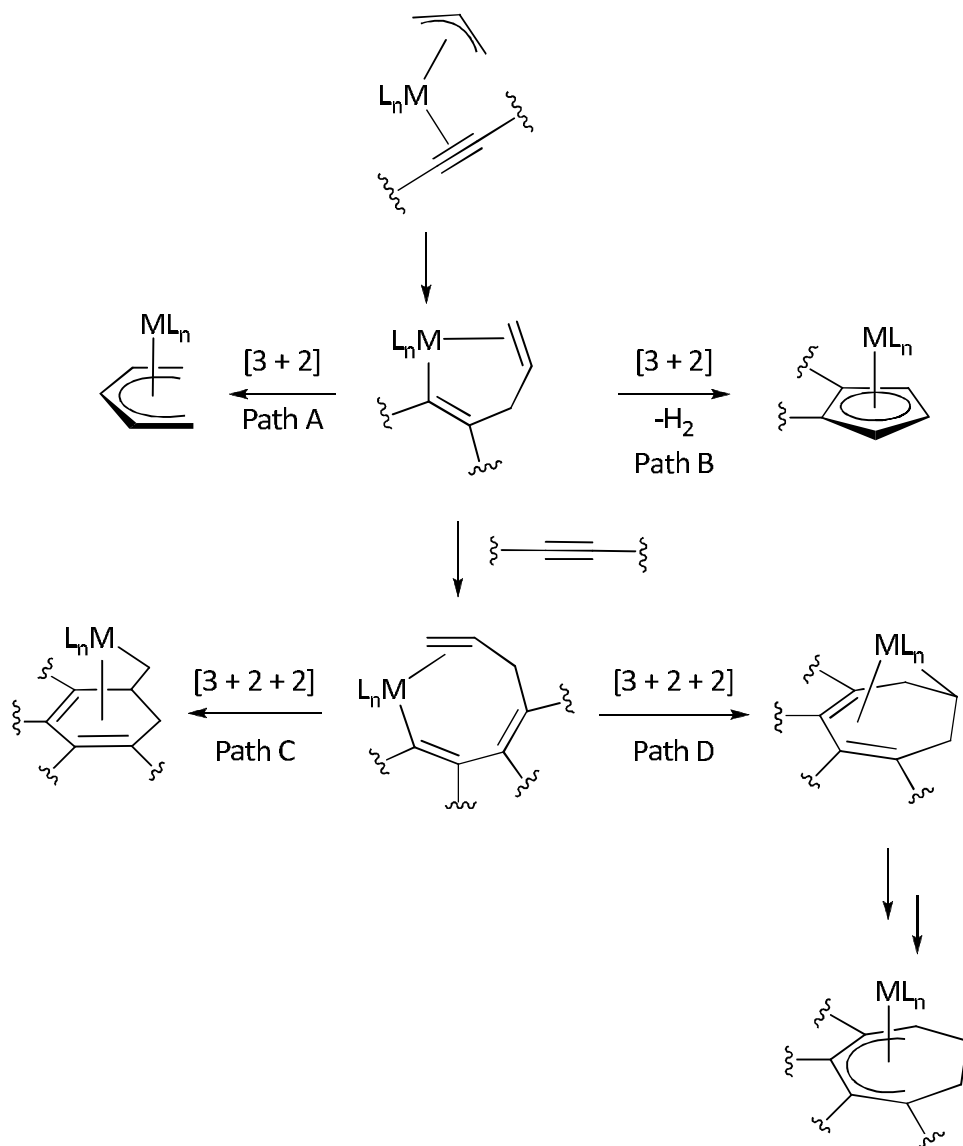
Due to the high reactivity of allyl complexes with alkynes, the intermediate allyl-alkyne metal complex is usually not isolable. Instead, products resulting from migratory insertion reactions are typically observed.<sup>24, 26-28</sup> However, a few examples of isolable allyl-alkyne metal complexes are known in the literature (Figure 1-5).<sup>23, 29-31</sup>

**Figure 1-5:** Examples of Isolable Allyl-Alkyne Metal Complexes



$\eta^3$ -Allyl-alkyne coupling reactions are well known, and are generally presumed to proceed via vinyl-olefin intermediates although this has not been rigorously demonstrated (Scheme 1-2).

Scheme 1-2



Upon incorporation of an equivalent of alkyne, the vinyl-olefin intermediate can (i) be trapped by the addition of Lewis bases,<sup>23, 31</sup> (ii) cyclize with concomitant loss of dihydrogen (Rubezhov cyclization, Path B),<sup>32-36</sup> or undergo allylic activation to form the acyclic  $\eta^5$ -pentadienyl complex (Path A).<sup>30</sup>

<sup>37-40</sup> Upon binding and incorporation of a second equivalent of alkyne, insertion

leads to an extended polyenyl metal intermediate<sup>41-43</sup> which can be trapped through the addition of Lewis bases or undergo ring closure by migratory insertion.<sup>23, 24, 30</sup> Closure on the interior olefinic carbon results in the formation of a methylenecyclohexadiene complex (Path C), whereas closure on the terminal olefinic carbon produces an  $\eta^1, \eta^4$ -cycloheptadienyl complex (Path D), which may or may not isomerize to the fully conjugated form. The polyenyl intermediate could also, in turn, react further with other small unsaturated molecules (e.g. carbon monoxide, nitriles, or olefins) to generate molecules of higher complexity.

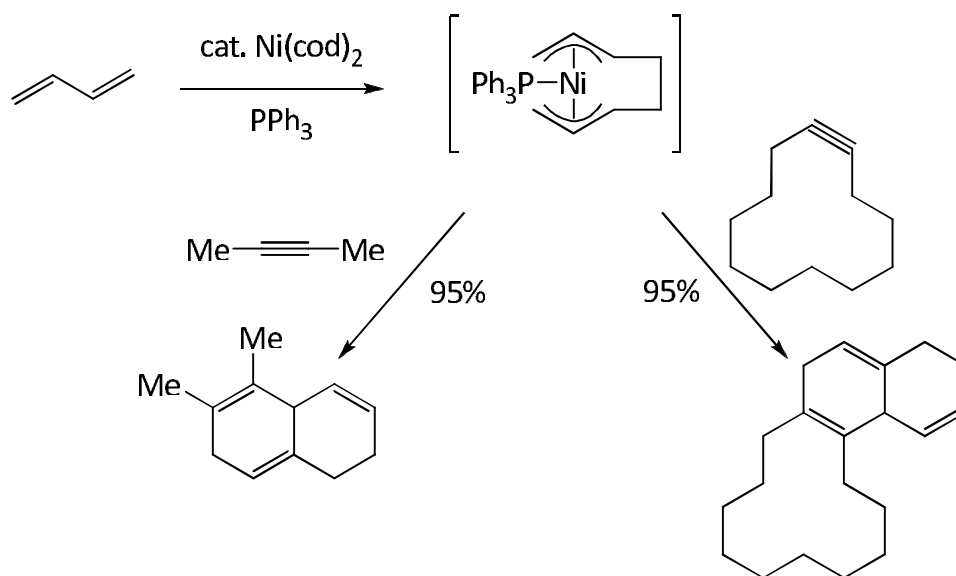
These types of allyl-alkyne coupling reactions can be classified as catalytic allyl-alkyne coupling reactions, stoichiometric allyl-alkyne coupling reactions, multiple allyl-alkyne coupling reactions, [3 + 2] allyl-alkyne cycloaddition reactions, and [3 + 2 + 2] allyl-alkyne cycloaddition reactions. A brief summary of the pertinent literature follows.

## **B. Catalytic Allyl-Alkyne Coupling Processes**

Allyl-alkyne coupling is most often performed using *in situ* generated metal-allyl complexes as part of a catalytic cycle. The organic product obtained from the coupling process is the desired product and therefore intermediates generated during the reaction are typically not identified.

Heimbach reported one of the earliest examples of a catalytic metal allyl-alkyne coupling reaction. Nickel was used to catalyze the oligomerization of butadienes to create a range of products (Scheme 1-3).<sup>44-48</sup> The addition of butadiene and phosphine to a labile source of nickel(0) generates the highly reactive nickel bis(allyl) phosphine complex.<sup>49</sup> This intermediate can couple with alkynes to generate bicyclic products (in the case of acyclic alkynes) and tricyclic systems (in the case of endocyclic alkynes). Furthermore, the catalyst can be modified to be tolerant towards functional groups on the alkyne.<sup>50, 51</sup> Corey *et al.* have used this process in the synthesis of several natural products.<sup>52-54</sup>

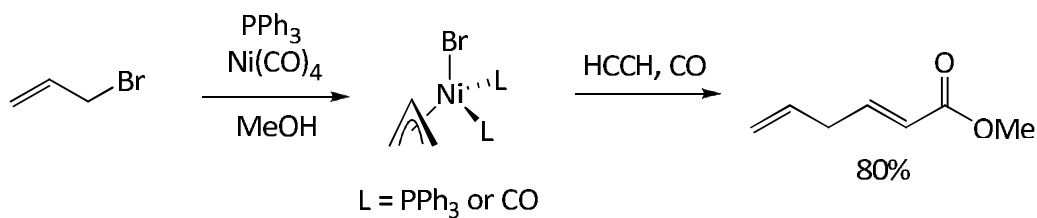
**Scheme 1-3**



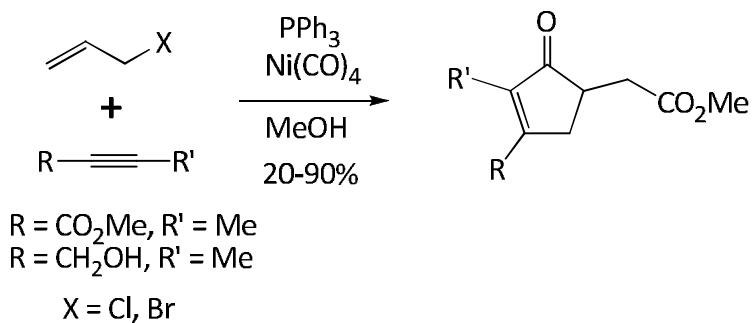
The three-component cycloaddition reaction of alkyne, allyl precursor and carbon monoxide has been reported by Chiusoli *et al.* using a nickel(0)

catalyst (Scheme 1-4).<sup>55</sup> Typically, linear products are obtained but performing the reaction with substituted alkynes can lead to the formation of cyclic products, albeit in variable yields (Equation 1-2).

**Scheme 1-4**



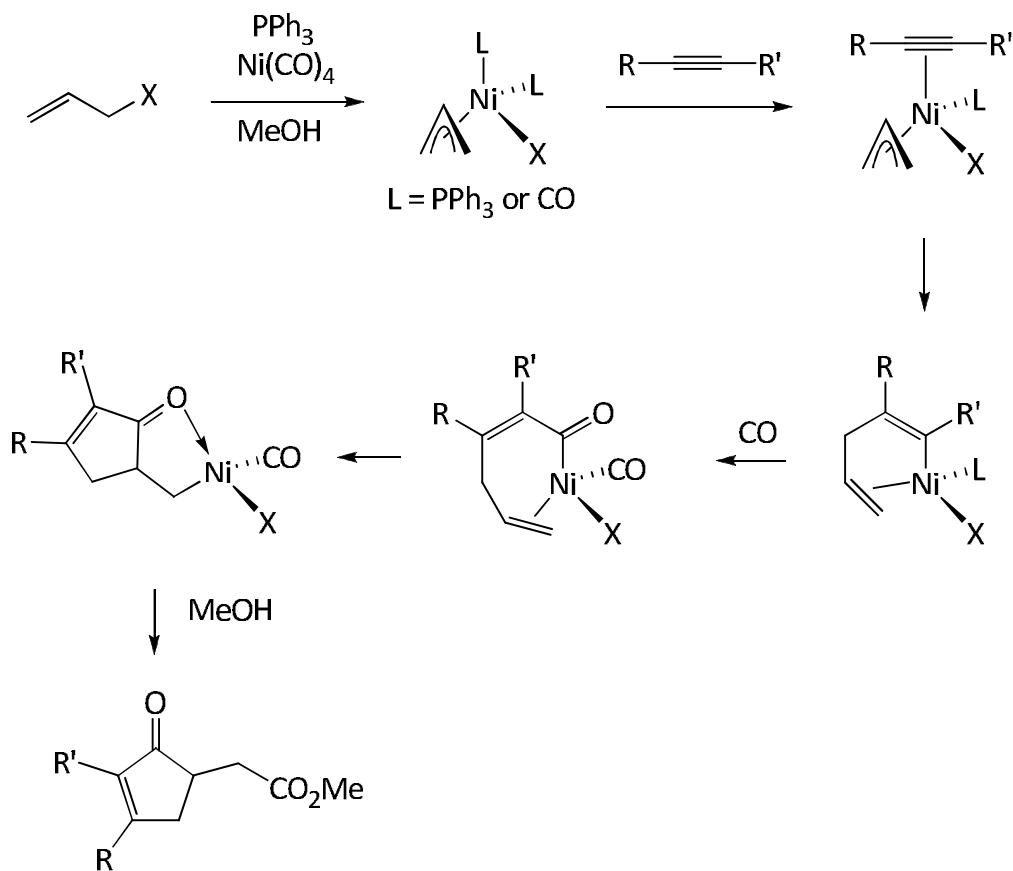
**Equation 1-2**



Both reactions are thought to occur via the initial formation of a nickel  $\eta^3$ -allyl species by oxidative addition to  $\text{Ni}(\text{CO})_4$  or  $\text{Ni}(\text{CO})_3\text{PPh}_3$  (Scheme 1-5). Coordination of the alkyne would then form a  $\pi$ -complex, which rapidly inserts to form a nickel vinyl-olefin complex. Insertion of carbon monoxide and cyclization affords the cyclopentenone complex. Insertion of another equivalent of carbon monoxide and subsequent methanolysis affords the observed product.

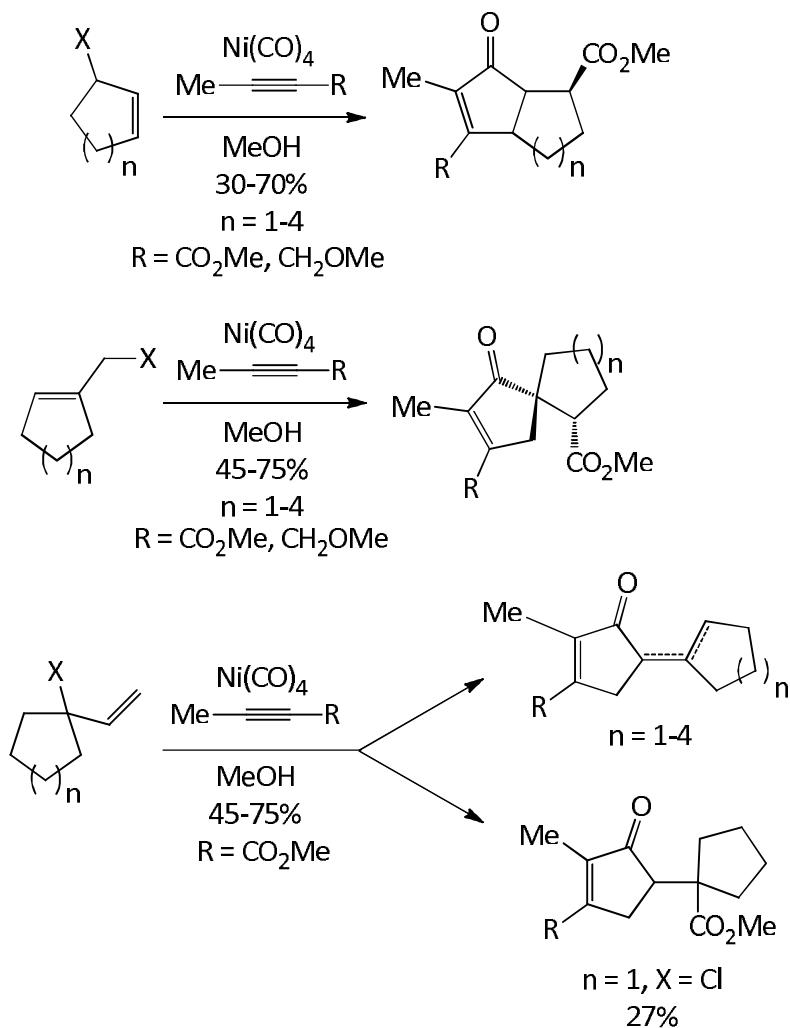
Although ring closure on the terminal olefinic carbon to give the six-membered ring is possible, it is not observed. Additionally, in some cases  $\beta$ -hydride elimination occurs to form the exocyclic double bond.<sup>56</sup>

**Scheme 1-5**



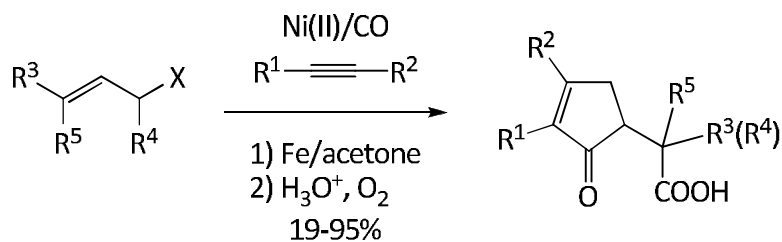
The Chiusoli reaction has also been found to be tolerant to a range of allylic halides, resulting in the formation of fused bicyclic cyclopentenones, spirocyclic compounds and cycloalkylidenecyclopent-2-enones (Scheme 1-6). Several intramolecular examples have also been reported.<sup>55, 57-60</sup>

Scheme 1-6



More recently, Moreto *et al.* have developed the Chiusoli reaction for applications in organic synthesis<sup>61-73</sup> and recently demonstrated that iron metal is required to form a highly active nickel(I) species that is required for catalytic turnover (Equation 1-3).<sup>74</sup>

### Equation 1-3



$\text{R}^1 = \text{Me, Et, Bu, SiMe}_3, \text{Ph, CH}_2\text{OMe}$

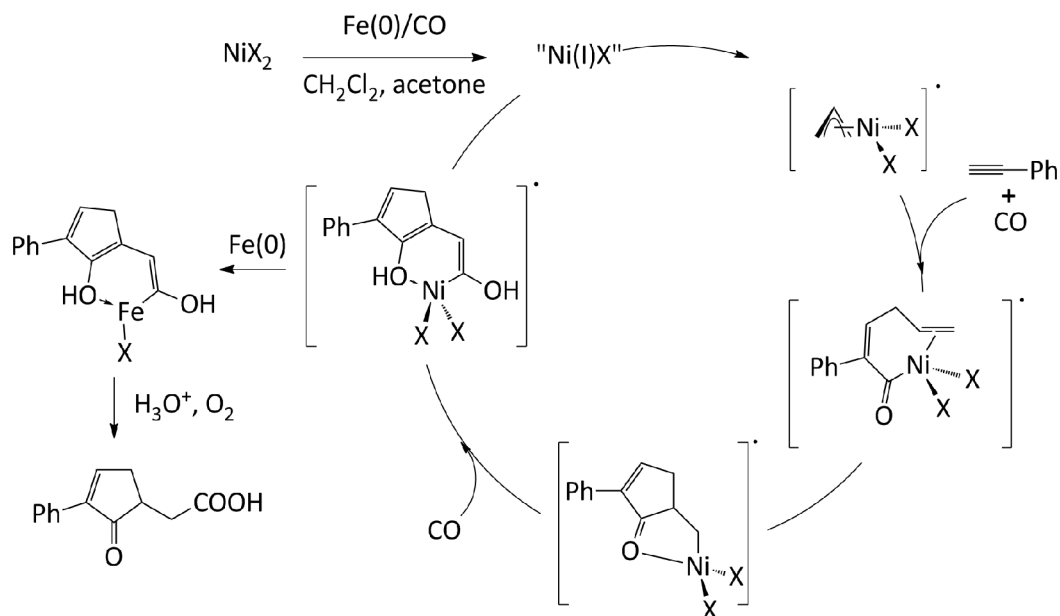
$\text{R}^2 = \text{H, CO}_2\text{Et, CH}_2\text{OMe, Et, SiMe}_3$

$\text{R}^3, \text{R}^5 = \text{H, Me, CO}_2\text{Me}$

$\text{R}^4 = \text{H, Me}$

The addition of sodium ascorbate to this reaction leads to complete reaction inhibition. The authors proposed initially that the addition of sodium ascorbate would reduce any catalytically *inactive* nickel(II) to catalytically *active* nickel(0) and remove HX. Addition of elemental iron powder to the reaction mixture, however, led instead to high turnover. From these two observations, Moreto *et al.* suggested that the iron converts the nickel(II) halide to nickel(I) halide, which subsequently undergoes the same reaction steps as the Chiusoli reaction, albeit within the nickel(I) to nickel(III) manifold (Scheme 1-7). Upon formation of the nickel acyl complex, transmetalation to iron occurs, which is followed by quenching in an aerobic, protic environment to liberate the cyclopentenone product.

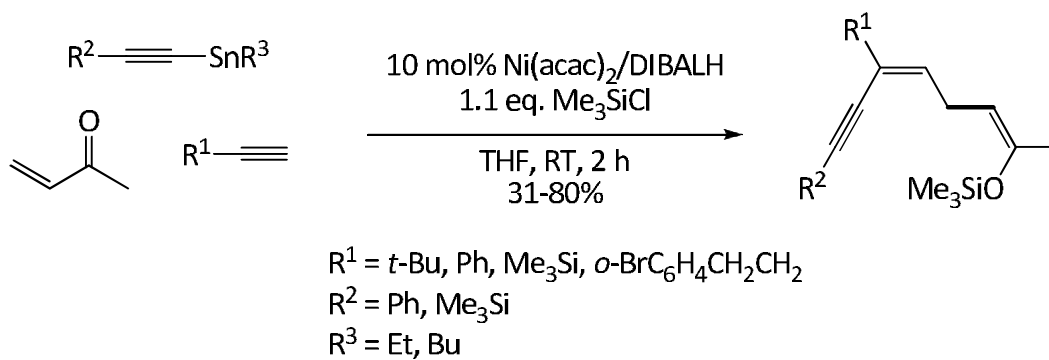
Scheme 1-7



It is possible that the proposed mechanism for the original Chiusoli reaction should be revised to include the generation of nickel(I) and oxidative addition to nickel(III). Generation of nickel(I) without the addition of an oxidant could occur by oxidative addition of an allyl halide to nickel(0), followed by isomerization from  $\eta^3$ -allyl to  $\eta^1$ -allyl, and then bond homolysis to arrive at nickel(I). Even if bond homolysis of an  $\eta^1$ -allyl nickel(II) complex is slow, the generation of a small amount of nickel(I) radical would account for the formation of product.

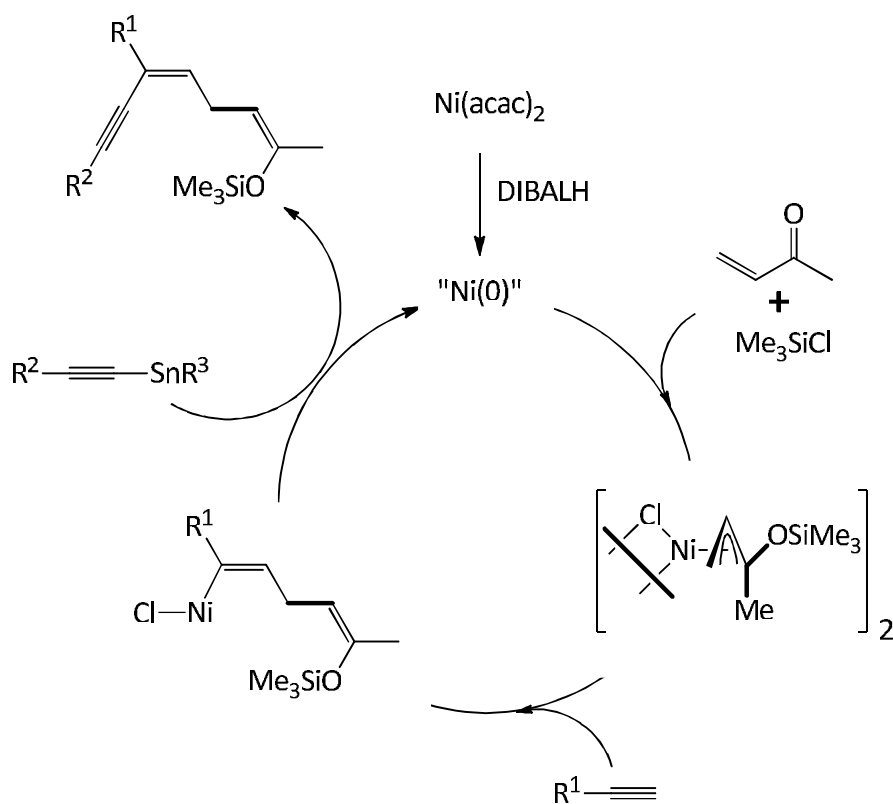
Ikeda *et al.* have demonstrated that allyl halides, terminal alkynes and alkynyl tin reagents can be coupled to produce extended enyne systems (Scheme 1-8).<sup>75-78</sup> This process has also been extended to the use of aluminum and zinc transmetallation reagents, and enones as allyl surrogates.<sup>79</sup>

**Scheme 1-8**



The proposed mechanism for this reaction involves the initial formation of the nickel  $\eta^3$ -allyl complex (Scheme 1-9).

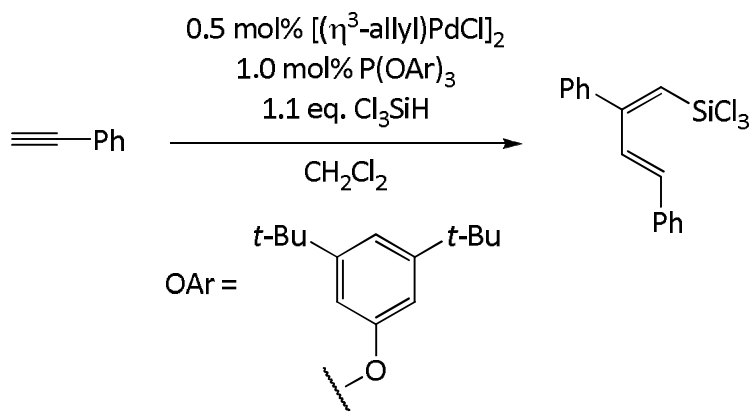
**Scheme 1-9**



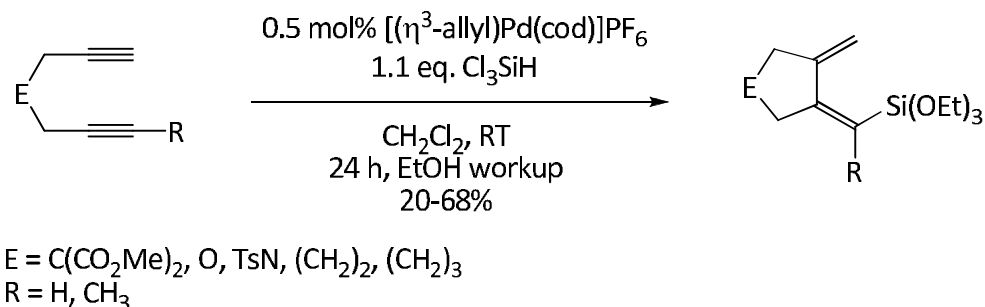
When enones are used in place of allyl halides, it is presumed that there is an initial  $\eta^4$ -coordination of the enone to nickel, followed by nucleophilic attack on TMSCl to produce the alkoxyallyl dimer species. This process can also be viewed as an oxidative addition of TMSCl to nickel(0) followed by migration of the silyl group to the oxygen terminus of the enone. Coordination of the alkyne followed by insertion produces the polyenyl species, which then undergoes transmetalation to arrive at the observed product.

Although much is known about the synthesis and behaviour of palladium allyl complexes and their inherent reactivity (e.g. Tsuji-Trost allylation, *vide supra*), very few catalytic coupling reactions with alkynes have been reported. A prime example of this is the addition of phenylacetylene to a mixture consisting of a catalytic amount of allylchloropalladium dimer, arylphosphite and a stoichiometric amount of trichlorosilane.<sup>80-82</sup> Coupling of the allyl fragment to the alkyne is not observed and the only product isolated from the reaction is the result of head-to-tail dimerization of phenylacetylene (Equation 1-4). When diynes are used, incorporation of the allyl moiety is not detected and only products arising from cyclization are observed (Equation 1-5).

### Equation 1-4

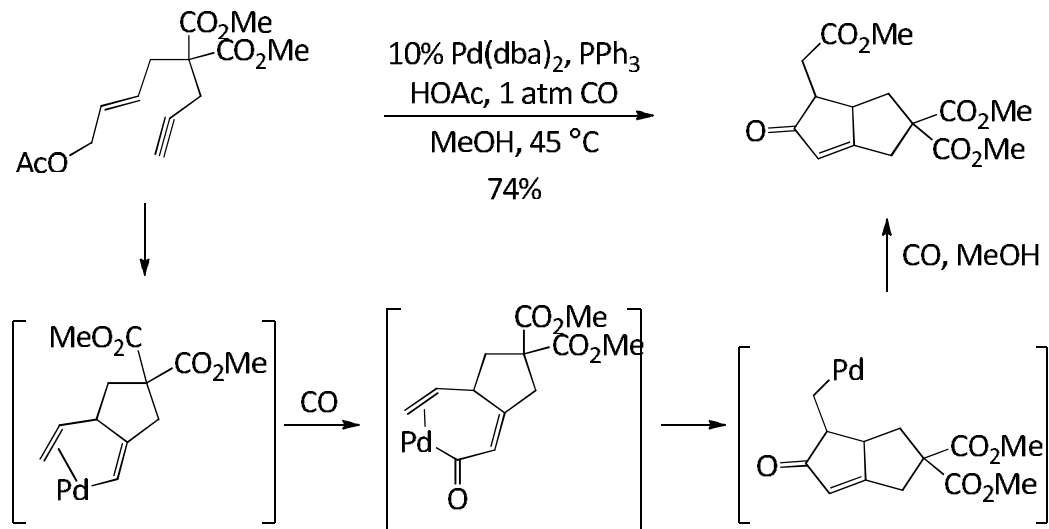


### Equation 1-5



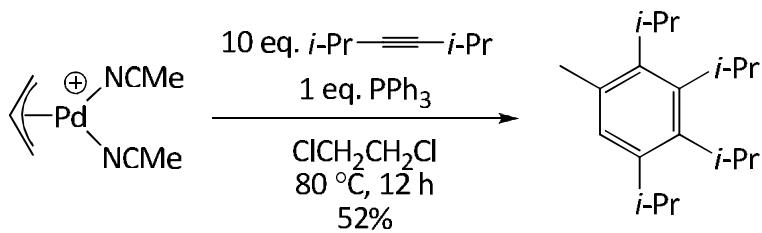
Oppolzer *et al.* have reported the intramolecular coupling of an allylic acetate tethered to a terminal alkyne to produce a fused [5,5]-bicyclic compound (Scheme 1-10).<sup>57</sup> The first step in the reaction is proposed to be oxidative addition of the allyl acetate to palladium(0), which is followed by insertion of the allyl moiety into the alkyne to form the vinyl-olefin complex. Migratory insertion of carbon monoxide and cyclization affords the fused bicyclic system. Incorporation of another equivalent of carbon monoxide and subsequent methanolysis then generates the isolated product.

Scheme 1-10

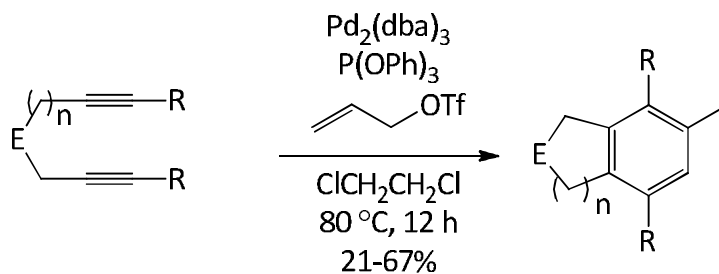


More recently, Tsukada *et al.* have demonstrated that palladium allyl complexes can undergo benzoannulation reactions to form substituted arenes and bicyclic compounds (Equation 1-6 and Equation 1-7).<sup>28, 83</sup> The reaction is tolerant of a range of alkynes and substituted allyl moieties. The use of terminal alkynes, however, leads to multiple regioisomers from the non-biased addition of the alkyne. The use of tethered diynes leads to the formation of bicyclic compounds in variable yields.

Equation 1-6



### Equation 1-7



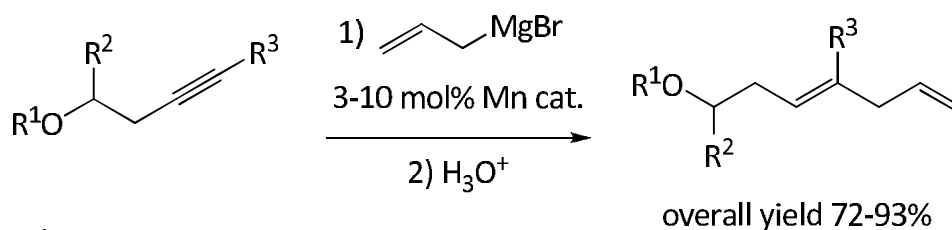
R = Me, Et, Pr, Ph, CO<sub>2</sub>Me

n = 1-3; E = C, O

Conditions: 2.5 mol% Pd, 5 mol% P(OPh)<sub>3</sub>  
5 mol% allyl triflate

Oshima *et al.* have demonstrated that allylic Grignard reagents add to the triple bond of the alkyl ether of homopropargylic alcohols to give monoallylated products with high regio- and stereoselectivities in the presence of a catalytic amount of a manganese compound such as MnI<sub>2</sub>, Mn(acac)<sub>3</sub>, or Mn<sub>2</sub>(CO)<sub>10</sub> (Equation 1-8).<sup>84</sup>

### Equation 1-8



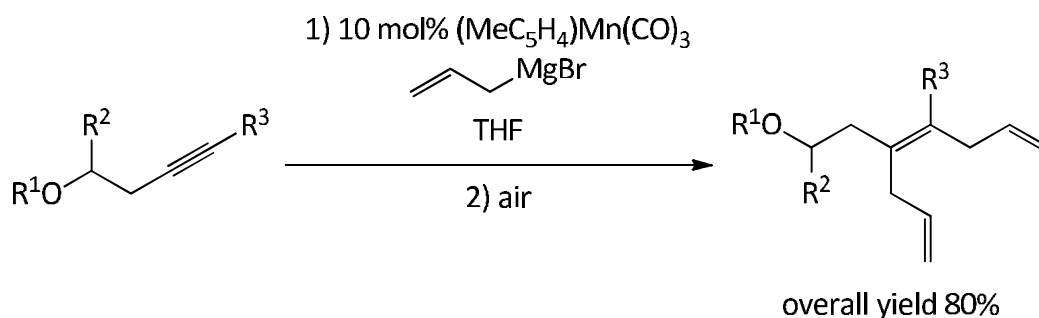
R<sup>1</sup> = Me, PhCH<sub>2</sub>, THP, Me

R<sup>2</sup> = H, Et

R<sup>3</sup> = *n*-Hex, Ph, *n*-Pr

Furthermore, using  $(\text{MeC}_5\text{H}_4)\text{Mn}(\text{CO})_3$  as the catalyst results in double allylation products (Equation 1-9). The addition of allylmagnesium halides to alkynes has also been reported using aluminum,<sup>85, 86</sup> indium,<sup>87</sup> and boron<sup>88, 89</sup> transmetallating reagents.

**Equation 1-9**

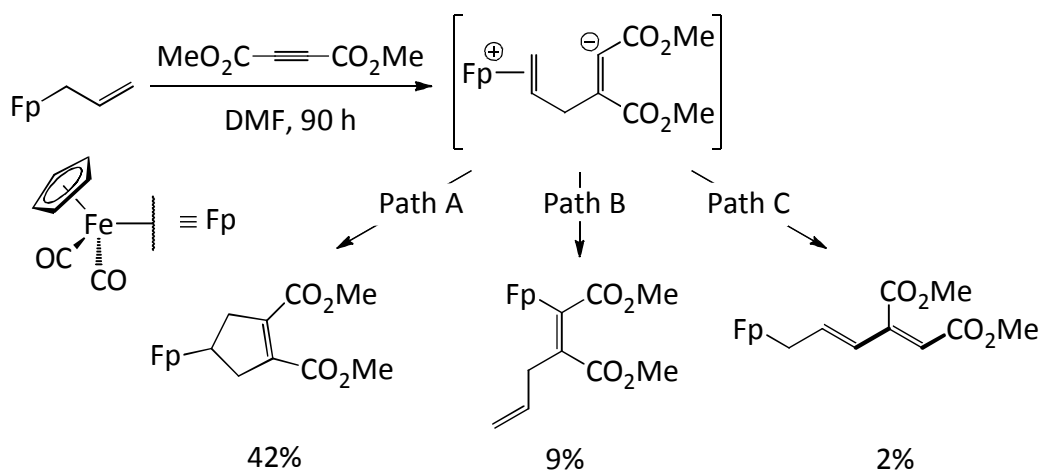


### C. Stoichiometric Allyl-Alkyne Coupling Reactions

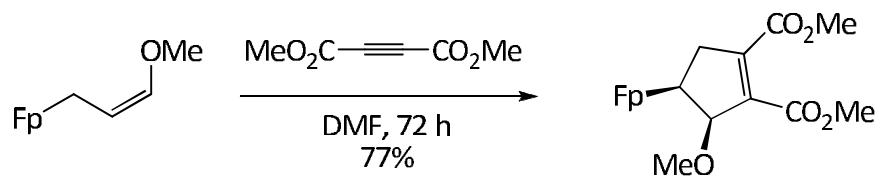
The reaction of  $\text{Fp}(\eta^1\text{-allyl})$  [ $\text{Fp} = (\text{C}_5\text{H}_5)\text{Fe}(\text{CO})_2$ ] complexes with electrophiles has been extensively studied and reviewed,<sup>90-93</sup> though there have been few reports of coupling with alkynes. The iron-bound  $\eta^1\text{-allyl}$  fragment acts as a nucleophile towards the electron-deficient alkyne DMAD to generate three products, arising from a common zwitterionic intermediate (Scheme 1-11). Ring closure accounts for the largest fraction of the three products (Path A), whereas the other two products arise from nucleophilic attack of the vinyl anion to the electrophilic metal centre (Path B) and hydride transfer (Path C). The product

arising from ring closure is the sole product observed when more electron-rich allyl complexes are employed (Equation 1-10).

**Scheme 1-11**

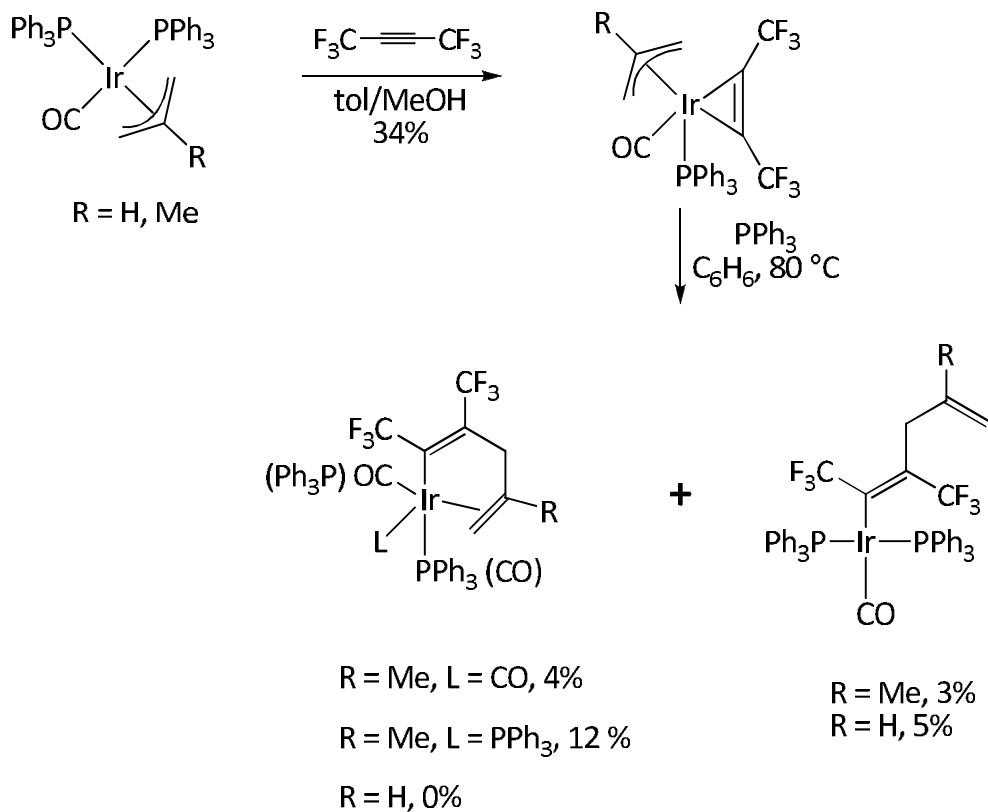


**Equation 1-10**



Typically, isolable adducts formed from allyl-alkyne coupling can be found using third row metals due to the metal's resistance to reductive elimination and the reasonably high activation energy towards insertion processes in general. For example, Green *et al.* have reported the step-wise coordination and insertion of hexafluoro-2-butyne to an iridium allyl complex (Scheme 1-12).<sup>29</sup>

Scheme 1-12

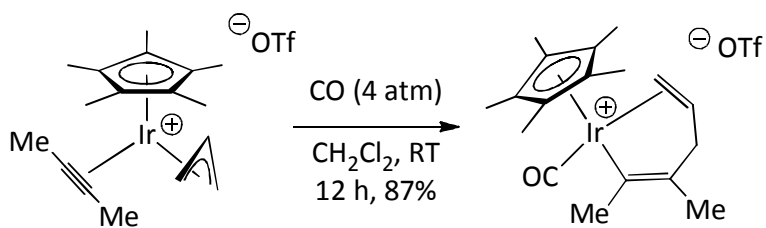


When the substituted acetylene is added, the initial iridacyclopentadiene complex can be isolated. Upon subsequent heating in the presence of triphenylphosphine, two products are produced wherein the orientation of the allyl fragment is either *cis* or *trans* with respect to the iridium centre. The *cis*-arrangement arises from a migratory insertion of the allyl fragment, whereas the *trans*-arrangement most likely arises from dissociation of the alkyne and then nucleophilic attack of the bound allyl ligand to the alkyne.

Schweibert has isolated a carbon monoxide-trapped vinyl-olefin iridium complex in excellent yield (Equation 1-11).<sup>94</sup> Presumably performing the

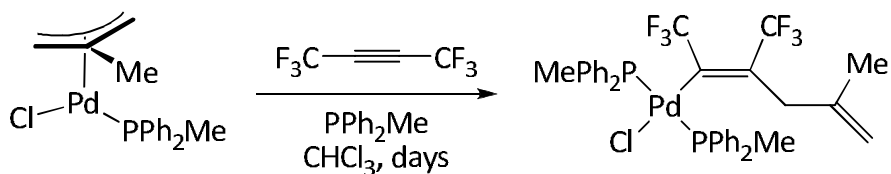
reaction under a carbon monoxide atmosphere traps the intermediate and prevents further reaction of the vinyl-olefin complex.

**Equation 1-11**



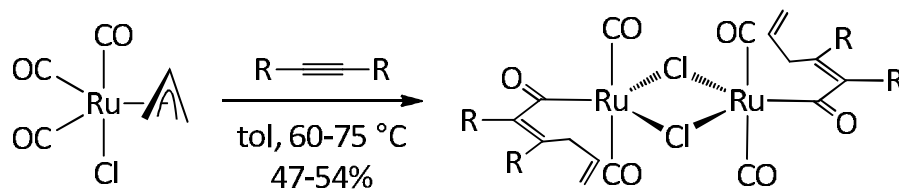
Clark and Puddephatt have also demonstrated single allyl-alkyne insertion on a palladium complex, though the intermediate was not isolated (Equation 1-12).<sup>95</sup> Addition of hexafluoro-2-butyne to a palladium allyl species results in the formation of a vinyl-olefin complex. The pendent olefin functionality remains coordinated to the metal, although in the adduct the addition of an equivalent of phosphine prior to workup displaces the bound olefin.

**Equation 1-12**



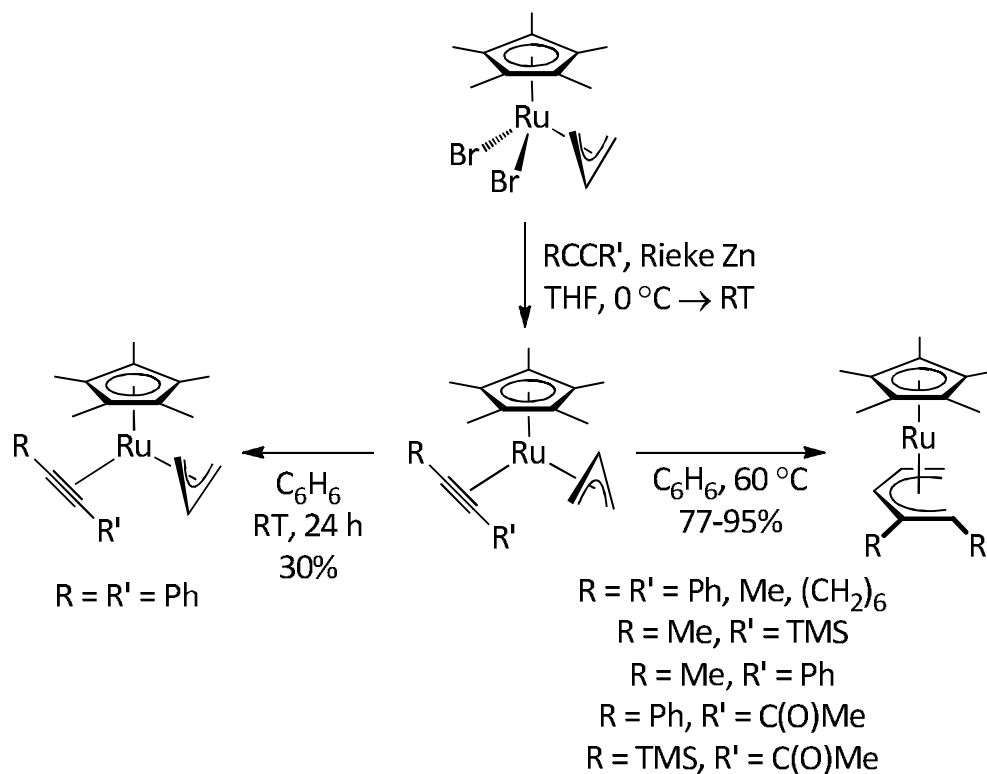
Ruthenium allyl complexes are closely related to both the iridium and palladium systems (Equation 1-13).<sup>96</sup> The addition of alkyne to ruthenium(II) allyl complexes results in step-wise insertion to form the vinyl-olefin complex, which then may or may not incorporate carbon monoxide to form the acyl complex. Symmetric alkynes lead to chloro-bridged dimers, whereas unsymmetrical alkynes lead to inseparable mixtures of products due to lack of regiocontrol of the insertion process.

**Equation 1-13**



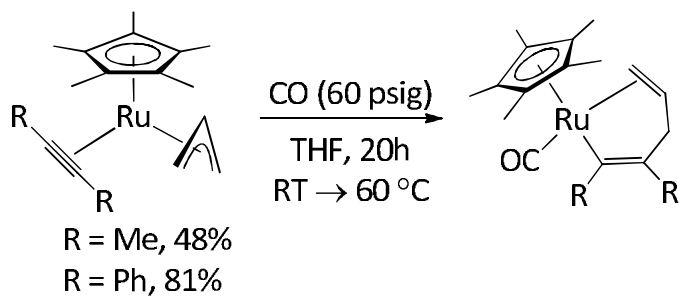
Older found that the reaction of ruthenium(IV)  $\eta^3$ -allyl complexes with Rieke zinc and alkyne forms the corresponding ruthenium(II) allyl-alkyne complexes, analogous to Schweibert's iridium complex. Upon heating, these allyl-alkyne complexes couple to produce acyclic  $\eta^5$ -pentadienyl complexes (Scheme 1-13).<sup>39</sup>

Scheme 1-13



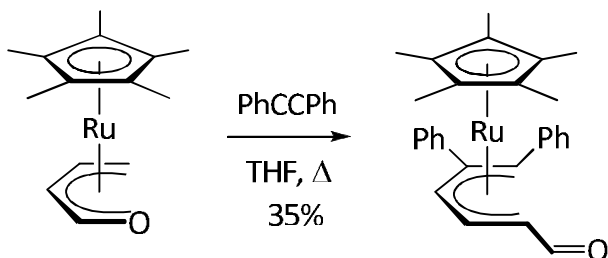
Interestingly, upon standing at ambient temperature in the presence of alkyne, insertion is not observed but rather an *exo* to *endo* conversion. Older has also demonstrated that performing the reaction under an atmosphere of carbon monoxide results in the trapped vinyl-olefin complex (Equation 1-14).<sup>31</sup> The presence of the carbon monoxide-trapped complex suggests that a vinyl-olefin complex is an intermediate in these allyl-alkyne coupling reactions.

### Equation 1-14



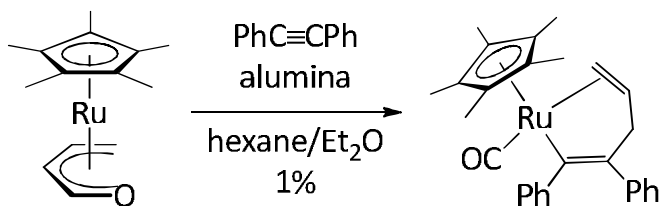
Paz-Sandoval *et al.* have observed the formation of a polyenyl aldehyde by insertion of diphenylacetylene to an acyclic ruthenium(II)  $\eta^5$ -oxadienyl complex (Equation 1-15).<sup>38</sup>

### Equation 1-15



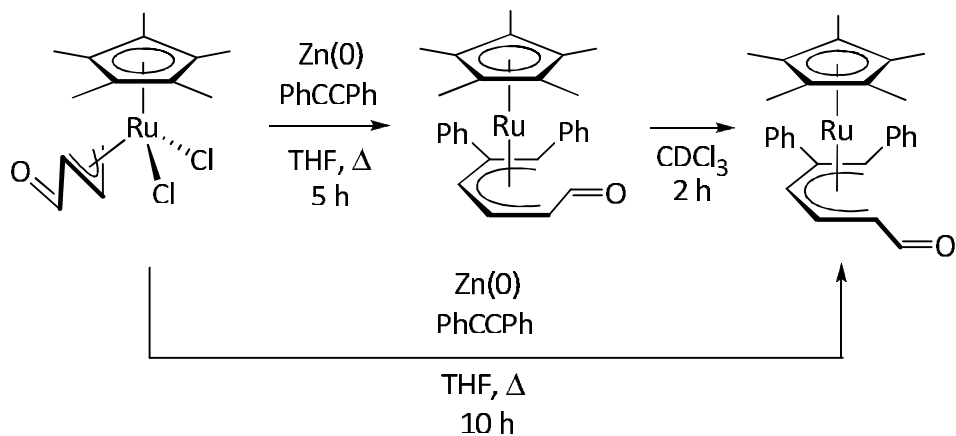
In this reaction, however, the formation of a small amount (~1%) of a rearranged insertion product was observed (Equation 1-16), presumably from the de-insertion of the carbonyl to form a transient ruthenium allyl carbonyl complex as reported by Older, which then reacts with diphenylacetylene to provide the observed byproduct.

Equation 1-16



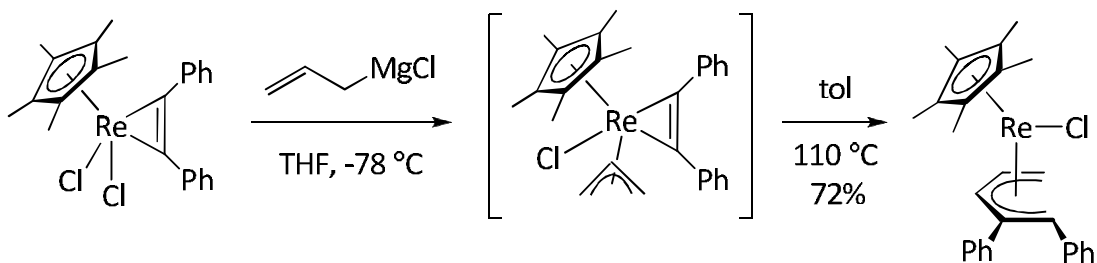
Paz-Sandoval *et al.* have also demonstrated that insertion onto the oxadienyl species also occurs when starting from the analogous ruthenium(IV) complex (Scheme 1-14).<sup>38</sup> The ruthenium(IV)  $\eta^3$ -oxadienyl complex, upon exposure to diphenylacetylene and elemental zinc, initially forms the *endo*- $\eta^5$ -acylpentadienyl product. Upon standing, there is slow conversion to the *exo*-acyl- $\eta^5$ -pentadienyl product, whereas longer reaction times result in the exclusive formation of the *exo*-acyl- $\eta^5$ -pentadienyl product. Presumably after formation of the vinyl-olefin complex, allylic hydrogen activation and transfer occurs, accounting for the isolated product.

Scheme 1-14



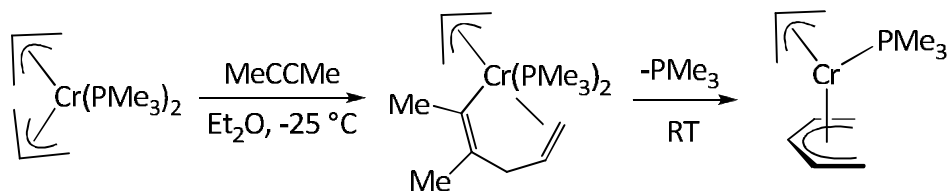
Herrmann *et al.* also observed stoichiometric allyl-alkyne coupling at rhenium (Equation 1-17). It is proposed that coupling of diphenylacetylene and the allyl fragment results from the formation of an allylrhenacyclopropene intermediate. Upon heating, the acyclic  $\eta^5$ -pentadienyl complex is isolated in good yield.<sup>40</sup>

**Equation 1-17**



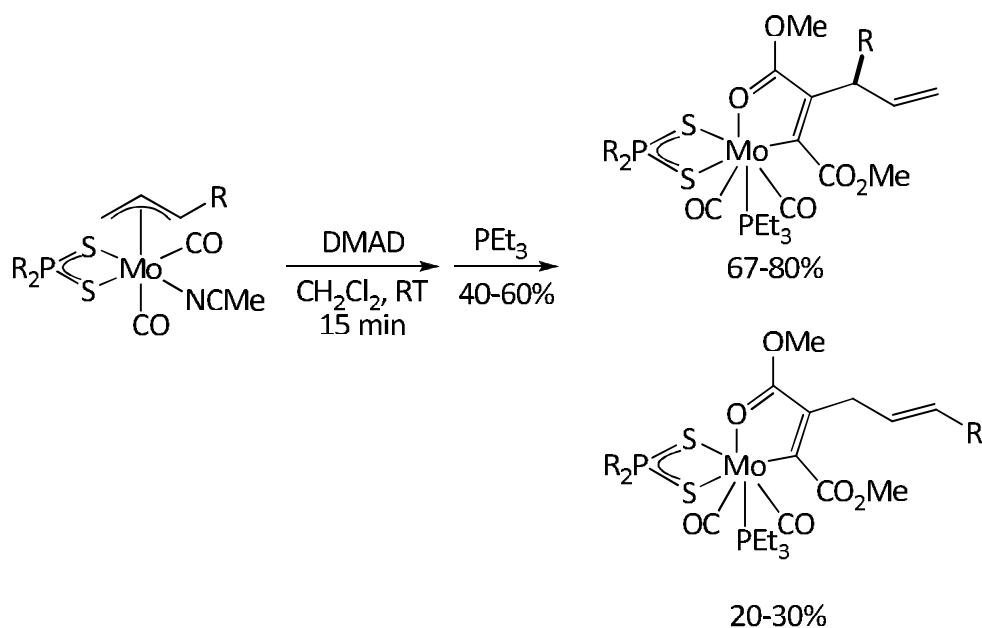
Jolly *et al.* observe a similar acyclic  $\eta^5$ -pentadienyl complex from alkyne addition to bis(allyl) complexes of chromium (Equation 1-18).<sup>37</sup> The allylic activation and formation of the chromium acyclic  $\eta^5$ -pentadienyl complex occurs at a much lower temperature compared to the rhenium example and requires the dissociation of  $\text{PMe}_3$ .

**Equation 1-18**



Molybdenum complexes can also undergo step-wise coupling of an alkyne and the allyl moiety (Scheme 1-15).<sup>97</sup> Insertion of DMAD into the metal-allyl bond produces a vinyl complex intermediate that is stabilized by intramolecular coordination from one of the ester carbonyl groups. The authors argue that the product distribution arises from preferred insertion into the unhindered side of the allyl ligand, followed by an isomerization to give the major product.

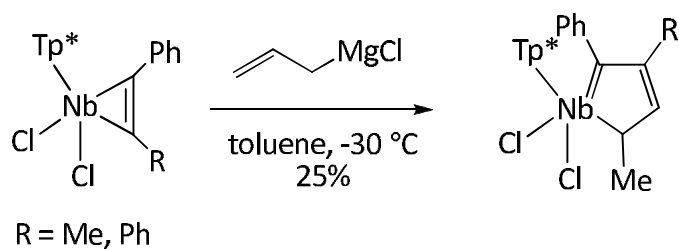
**Scheme 1-15**



A rare case of an isolable allyl-alkyne complex of the early metals has been reported using niobium stabilized by a tripodal tris(pyrazoylborate) ligand (Equation 1-19).<sup>98</sup> The alkyne acts as a 4 e<sup>-</sup> donor and, upon coupling to the allyl

fragment, undergoes an allylic activation to account for the isolated product, which is obtained in low yield.

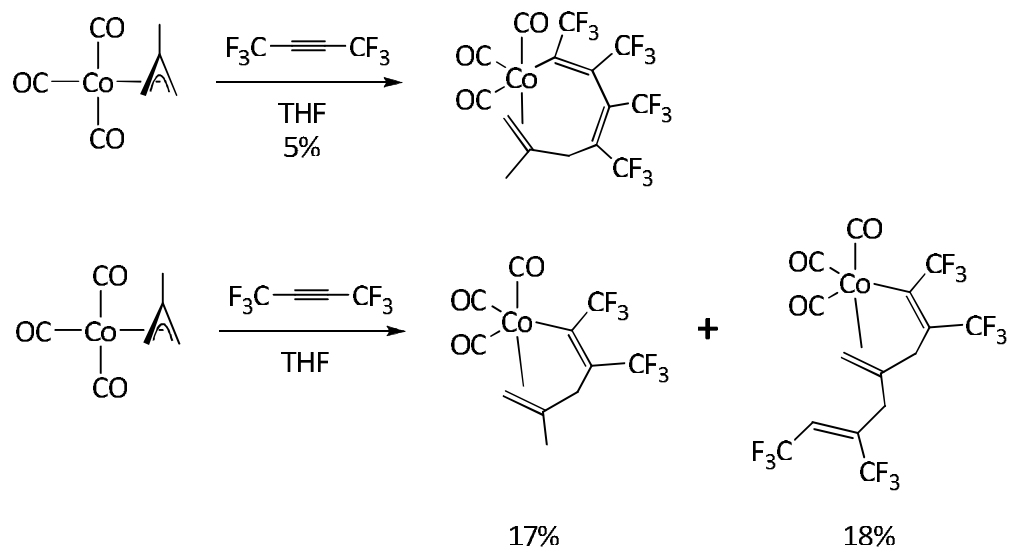
**Equation 1-19**



**D. Multiple Allyl-Alkyne Coupling Reactions**

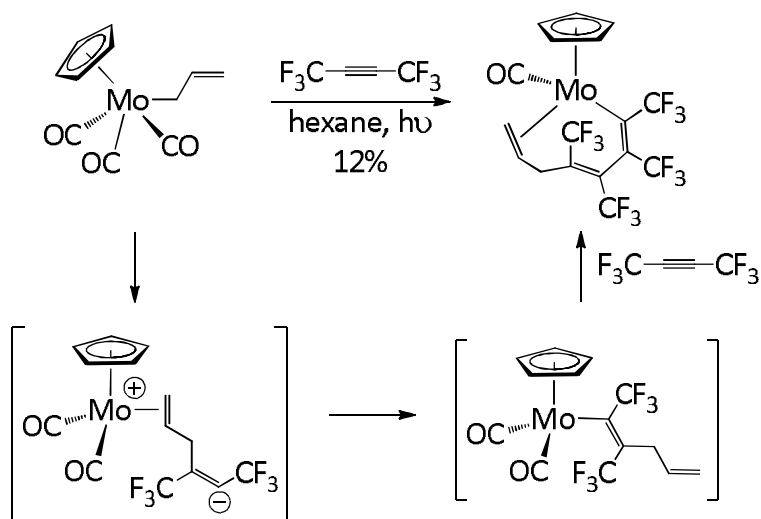
Green,<sup>42</sup> Stone,<sup>41</sup> and respective coworkers independently synthesized a cobalt polyenyl system from the double insertion of hexafluoro-2-butyne to a cobalt  $\eta^3$ -methallyl complex (Scheme 1-16). While Stone's report describes the isolation of a linearly extended polyenyl fragment in miniscule yields, Green's attempt to replicate this reaction resulted in the isolation of two different products, one of which arises from single allyl-alkyne coupling, the other from coupling of one alkyne to each end of the methallyl ligand. The differences in both Green's and Stone's reported data reflect the sensitivity of this reaction to other factors such as temperature, concentration, and reaction time.

**Scheme 1-16**



Stone *et al.* have also reported a molybdenum  $\eta^1$ -allyl complex that incorporates two equivalents of hexafluoro-2-butyne to form a polyenyl complex (Scheme 1-17).<sup>99</sup>

**Scheme 1-17**

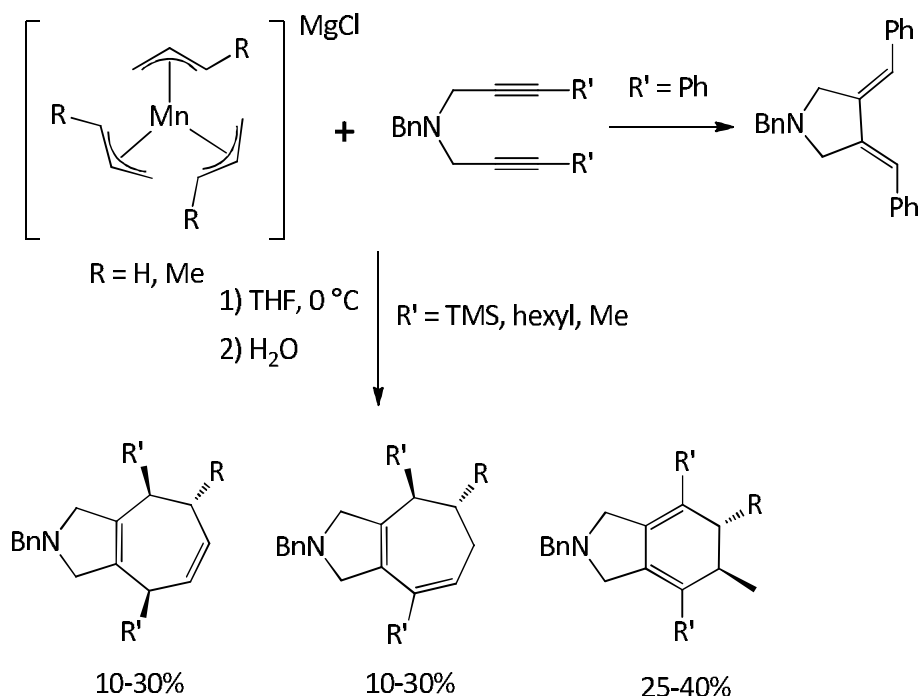


Of particular interest is the *trans*-geometry of the interior olefin, which precludes a “normal” coordinative insertion process for the first equivalent of alkyne. It is likely that the first step in this reaction is the nucleophilic attack of the  $\eta^1$ -allyl moiety on the alkyne, generating a zwitterionic intermediate, similar to the reactions of  $\text{Fp}(\eta^1\text{-allyl})$  complexes (*vide supra*), which accounts for the *trans*-geometry. Rearrangement of the intermediate to a vinyl-olefin complex is then followed by incorporation of a second equivalent of alkyne in a normal *cis*-fashion, resulting in the isolated product. No loss of carbon monoxide and subsequent coordination of the alkyne are observed under photolysis conditions. This reactivity would likely have resulted in migratory insertion of the alkyne to give *cis*-addition and generate an all “*cis*” product.

Oshima *et al.* have observed that in certain cases, double alkyne insertion into a putative anionic manganese-allyl complex results in the formation of seven-membered carbocycles with poor selectivity and in modest yield (Scheme 1-18).<sup>100</sup> The existence of the tris(allyl)manganate anion has not been determined but analogous trialkyl- and triarylmanganate anions have been reported.<sup>101, 102</sup> When phenyl-terminated diynes are used, cyclization without allyl incorporation is observed. Oshima *et al.* rationalize the formation of double insertion products by invoking an initial oxidative cyclization of the diyne, followed by allyl migration to form a manganese vinyl-carbene complex (Scheme 1-19 and Scheme 1-20). The vinyl-carbene complex can now react along divergent pathways to form either six- or seven-membered ring products,

depending on the orientation of the pendent olefin with respect to the metal-carbene.

**Scheme 1-18**

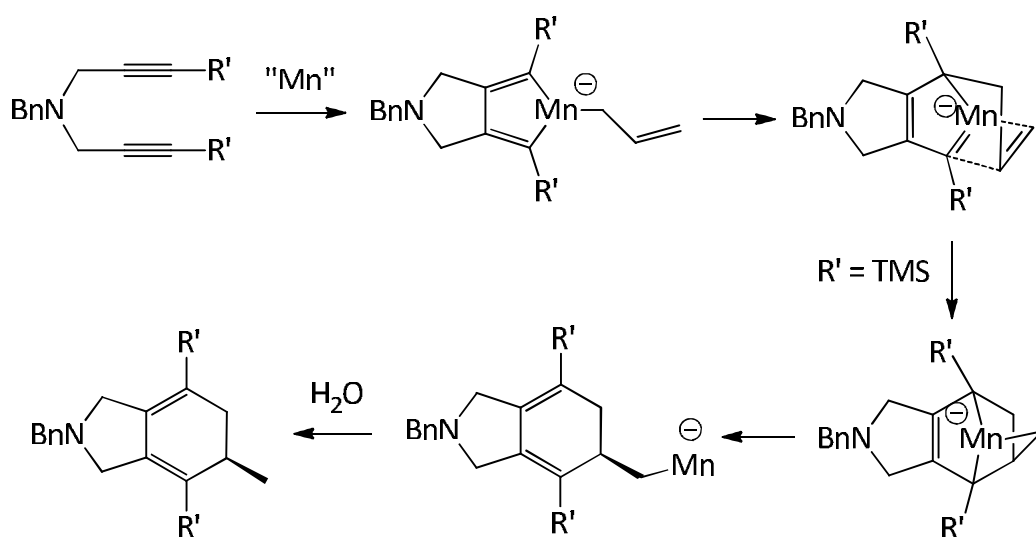


The vinyl-carbene complex can undergo a [2 + 2] cycloaddition reaction to generate a tricyclic manganacyclopentene complex, which can then reductively couple forming the cyclohexadiene framework (Scheme 1-19). The addition of water hydrolyzes the primary manganese-carbon bond resulting in the formation of the six-membered product.

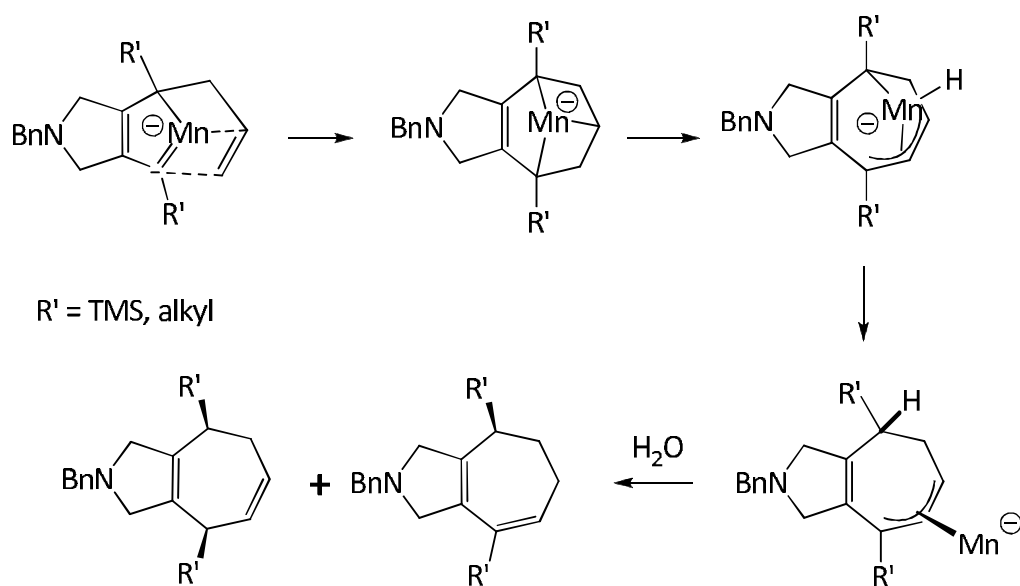
Alternatively, the pendent olefin can rotate and undergo a [2 + 2] cycloaddition reaction with the opposite regiochemistry, generating a tricyclic intermediate (Scheme 1-20). After  $\beta$ -hydride elimination and subsequent

insertion to form the  $\eta^3$ -allyl complex, quenching with water affords an equimolar mixture of seven-membered ring products depending on the location of protonation.

**Scheme 1-19**



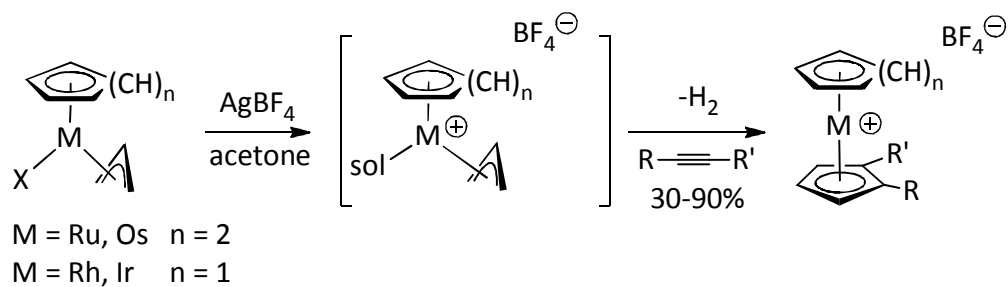
**Scheme 1-20**



## E. [3 + 2] Allyl-Alkyne Cycloaddition Reactions

Perhaps most pertinent to the present investigation, Rubezhov *et al.* have reported many examples of an unusual [3+2] dehydrogenative allyl-alkyne cycloaddition reaction among the heavier Group 8 and 9 metal  $\eta^3$ -allyl complexes (Equation 1-20).<sup>33, 35, 36</sup>

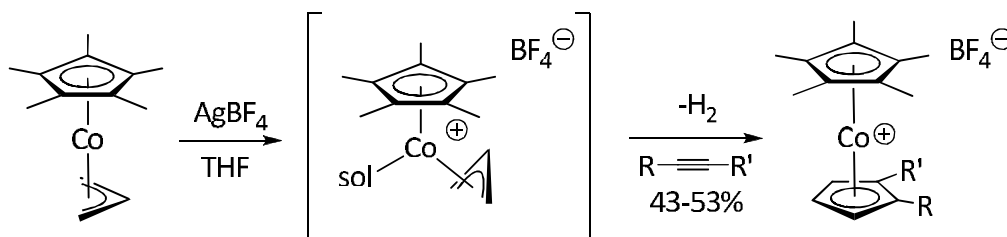
### Equation 1-20



Silver-mediated halide abstraction from cyclopentadienyl-supported Group 9 complexes or arene-supported Group 8 complexes results in the formation of a nominally unsaturated cationic  $\eta^3$ -allyl intermediate. Displacement of the bound solvent molecule and coordination of alkyne is followed by insertion and cyclization. Irreversible extrusion of dihydrogen then affords the cationic sandwich complexes in reasonable to good yields. The mechanism of this reaction has been determined in this group and will be discussed in the following chapter.

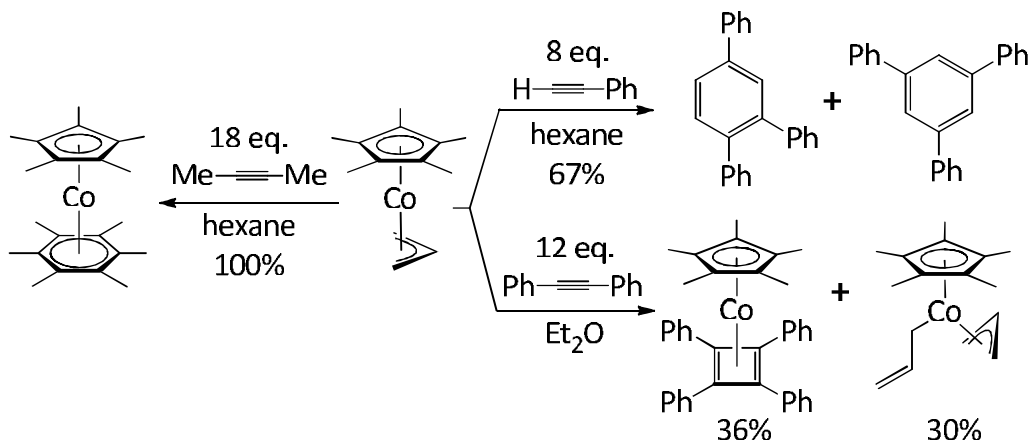
More recently, Nehl reported similar [3 + 2] allyl-alkyne cycloadditions using cobalt (Equation 1-21).<sup>103</sup> The highly reactive neutral  $(C_5Me_5)Co(\eta^3\text{-allyl})$  species undergoes one electron oxidation by  $AgBF_4$  to generate transiently unsaturated cations that are analogous to Rubezhov's putative intermediates. Upon the addition of an alkyne, coordination, insertion, and dihydrogen extrusion occur to give the substituted cobalticenium cations in moderate yields.

**Equation 1-21**



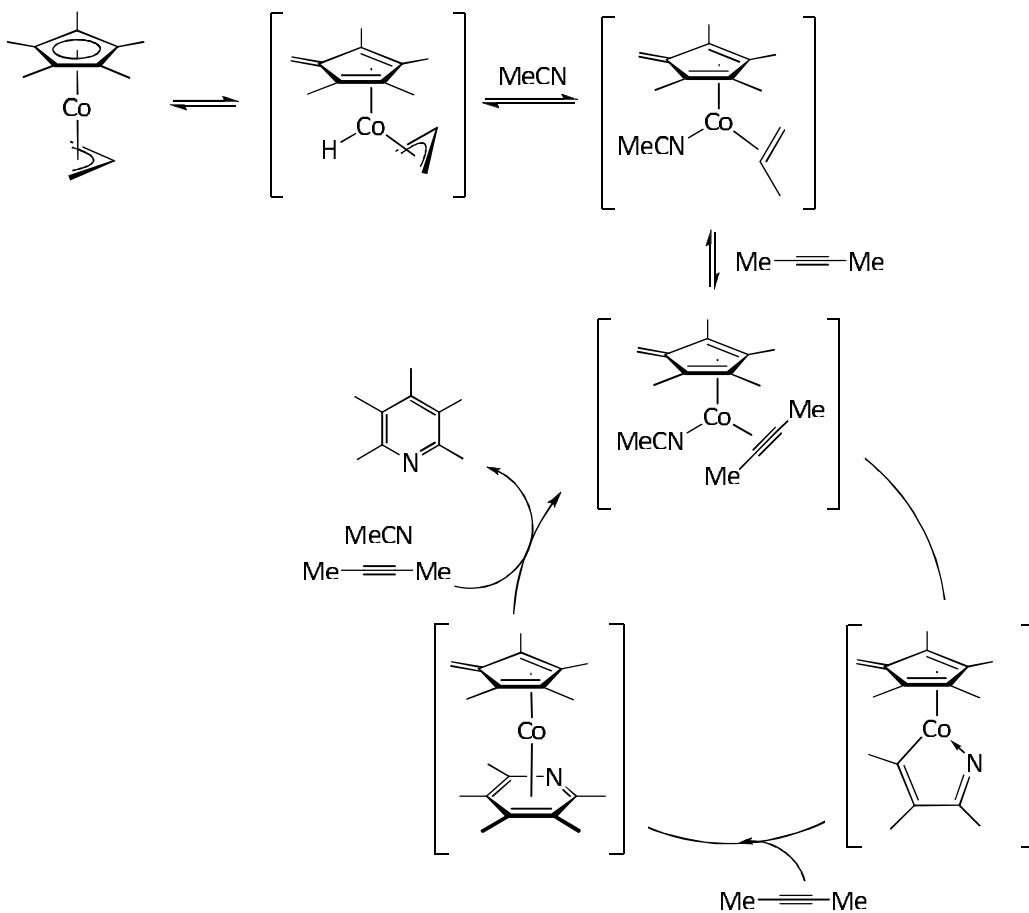
Markedly different reactivity is observed when the reaction is performed in the absence of an oxidizing agent (Scheme 1-21). The cobalt(II) allyl species reacts with alkynes to form products that are a result of catalytic alkyne trimerization. When small alkynes such as 2-butyne are used, complete conversion to hexamethylbenzene is observed, whereas the addition of phenylacetylene leads to both regioisomers of triphenylbenzene. The addition of diphenylacetylene results in the competitive formation of an  $\eta^4$ -tetraphenylcyclobutadiene complex and an  $\eta^3, \eta^1$ -bis(allyl) complex. Nehl has also demonstrated that the cobalt(II) allyl complex is a competent pre-catalyst for the trimerization of pyridines.

Scheme 1-21



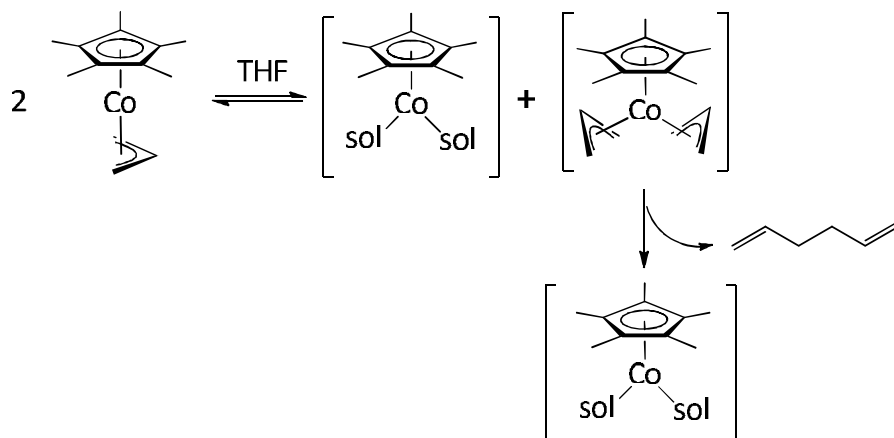
While the fate of allyl ligand during this transformation is unknown, Nehl proposed that during alkyne-nitrile trimerization, carbon-hydrogen bond activation of the pentamethylcyclopentadienyl ligand occurs, affording a cobalt hydrido allyl species (Scheme 1-22).<sup>104</sup> Loss of propene and coordination of alkyne generates a cobalt(0) diene complex which is stabilized by the partially  $\pi$ -acidic nitrile ligands. Migratory insertion of alkyne into the metal-nitrile bond generates a vinyl-imine complex, which coordinates and inserts another equivalent of alkyne to generate a polyenyl intermediate. Migratory ring closure affords the substituted pyridine product which is displaced from the metal coordination sphere by incoming alkyne and nitrile.

Scheme 1-22



A more likely mechanism to account for the allyl moiety would involve disproportionation of the neutral  $(C_5Me_5)Co(\eta^3\text{-allyl})$  complex to form  $(C_5Me_5)Co(\eta^3\text{-allyl})_2$  and  $(C_5Me_5)Co(\text{solvent})$  (Scheme 1-23). Reductive coupling of the  $\eta^3$ -allyl ligands would then generate a cobalt(I) hexadiene complex. The use of cobalt(I) complexes to promote alkyne trimerization and pyridine formation have been well documented.<sup>105-110</sup>

**Scheme 1-23**



## Conclusions

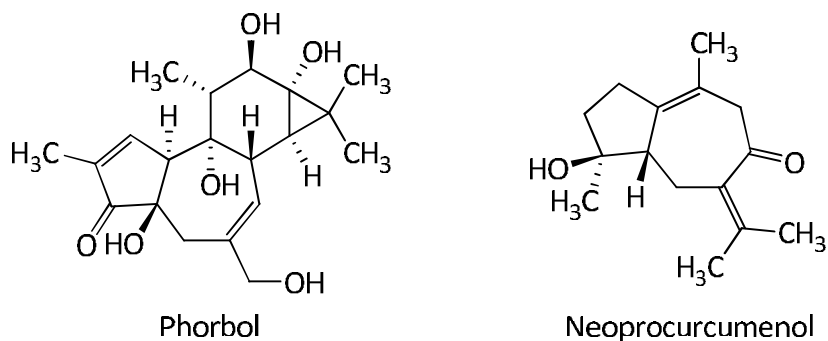
The [3 + 2] coupling of alkynes to  $\eta^3$ -allyl metal complexes is quite general and can be used to assemble cyclic and acyclic products. While the generation of five-membered rings from [3 + 2] cycloaddition reactions is synthetically useful, these cyclic products can be prepared using standard organic methods. However, a more useful application of allyl-alkyne cycloaddition chemistry is the synthesis of seven-membered rings, where few synthetic methodologies exist for the preparation of this ring size. This would necessitate the incorporation of two equivalents of alkyne into an  $\eta^3$ -allyl metal complex. The development of systems capable of accomplishing this double insertion reaction, as well as some recent advances, will be discussed in the following chapter.

## Chapter 2. [3 + 2 + 2] Allyl-Alkyne Cycloaddition Reactions of Agostic Cobalt Cyclohexenyl Complexes

### Section 1. Introduction

Seven-membered frameworks are a common feature in a number of natural products such as phorbol and neoprocucumenol (Figure 2-1). While a host of methodologies exist to prepare five- and six-membered ring systems, comparatively few exist for seven-membered ring systems and are typically limited to specific substrates.<sup>111-113</sup> One such methodology to prepare seven-membered ring systems is through [3 + 2 + 2] allyl-alkyne cycloaddition reactions.<sup>28, 83, 114</sup>

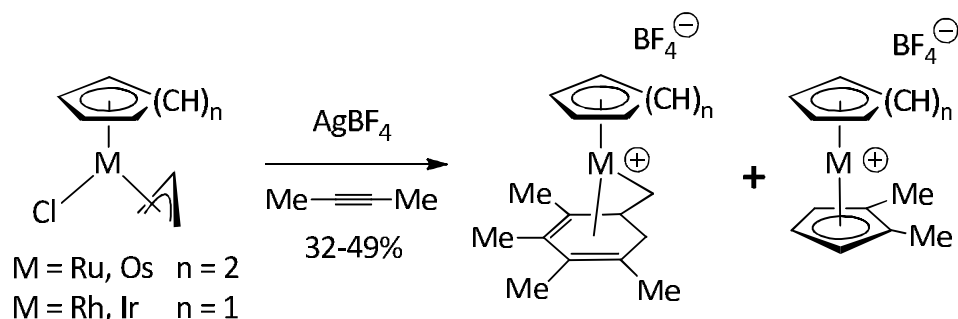
**Figure 2-1:** Examples of Natural Products Containing a Seven-Membered Ring



## A. [3 + 2 + 2] Allyl-Alkyne Cycloaddition Reactions

The first reported examples of [3 + 2 + 2] allyl-alkyne cycloaddition was by Rubezhov, who observed that the reaction of excess 2-butyne with *in situ* generated cationic Group 8 and Group 9  $\eta^3$ -allyl complexes led to products that were the result of allyl-alkyne incorporation (Equation 2-1).<sup>34</sup> Only 2-butyne displayed this type of reactivity whereas other disubstituted alkynes afforded [3 + 2] cycloadducts exclusively.<sup>32, 33, 35, 36</sup> The [3 + 2 + 2] cycloadduct was isolated in modest yield along with the expected [3 + 2] cycloadduct.

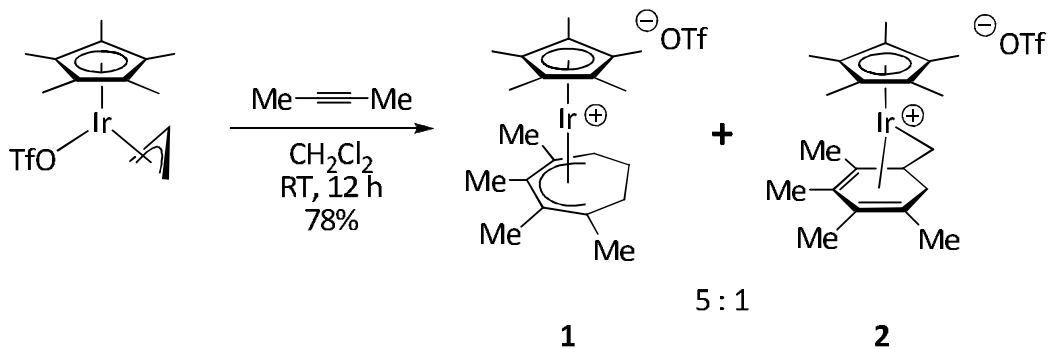
Equation 2-1



In an effort to enhance the selectivity towards double alkyne incorporation and alter the regioselectivity of the cyclization process, Schweibert and Stryker employed a more sterically-hindered  $(C_5Me_5)Ir(III)$  template, obtaining the  $\eta^5$ -cycloheptadienyl complex **1** as the major product of the reaction with 2-butyne (Equation 2-2).<sup>23</sup> The  $\eta^1, \eta^4$ -methylenecyclohexadiene

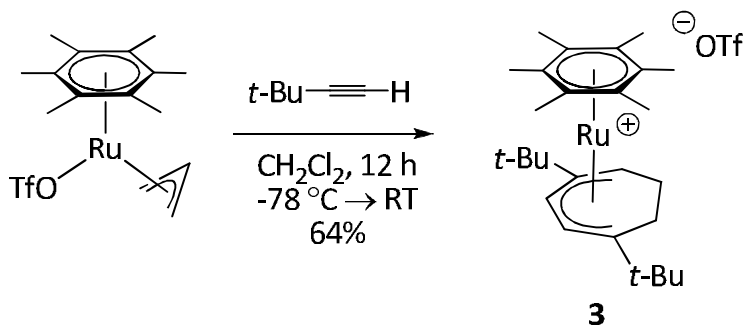
complex **2** was obtained as a minor product and no five-membered ring products were detected.

### Equation 2-2



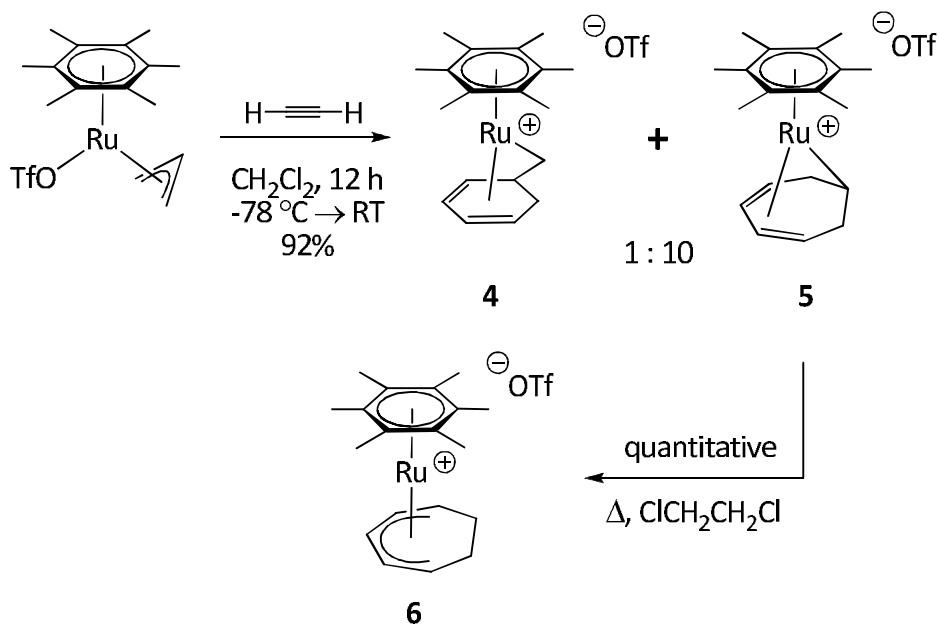
Older and Stryker used the more sterically-hindered  $(\text{C}_6\text{Me}_6)\text{Ru}(\text{II})$  template, preparing the η<sup>5</sup>-cycloheptadienyl complex **3** as the sole product from the reaction with *tert*-butylacetylene (Equation 2-3).<sup>30, 115</sup>

### Equation 2-3



When acetylene was used, both six- and seven-membered ring products (**4** and **5** respectively) were produced in a 1 : 10 ratio (Scheme 2-1). The  $\eta^1, \eta^4$ -cycloheptadienyl product is converted quantitatively to the  $\eta^5$ -cycloheptadienyl isomer **6** by heating in dichloroethane.

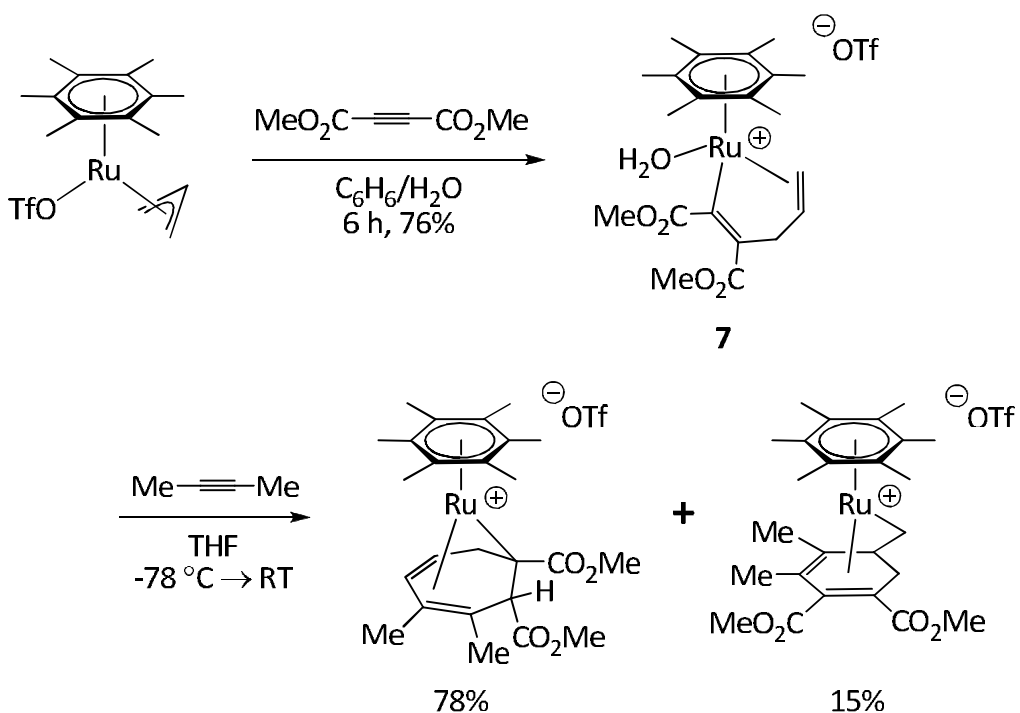
**Scheme 2-1**



Interestingly, Older observed that while treatment of the parent allyl complex with two equivalents of the electron-deficient alkyne dimethylacetylenedicarboxylate (DMAD) resulted in the formation of a seven-membered ring product, treatment with only one equivalent of DMAD resulted in the formation of an isolable vinyl-olefin complex **7**. When 2-butyne was introduced to **7**, formation of both six- and seven-membered ring products was

observed (Scheme 2-2). This finding strongly suggests that the vinyl-olefin complex is an arrested intermediate along the [3 + 2 + 2] pathway.

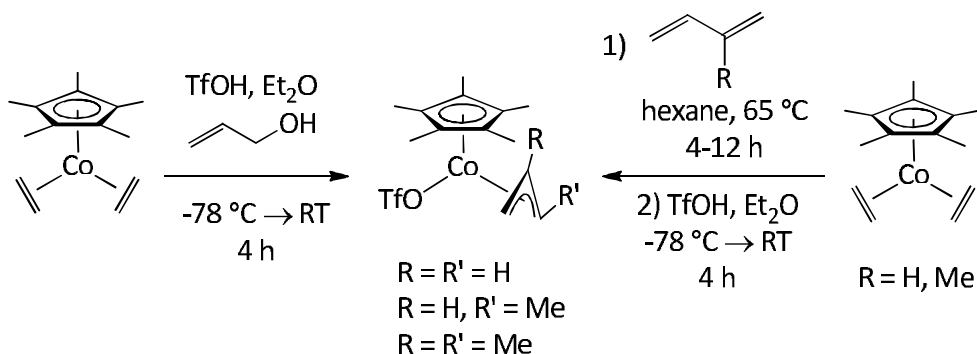
**Scheme 2-2**



Due to the prohibitive cost of employing stoichiometric amounts of iridium and ruthenium, Etkin and Stryker instead focused on the more readily available cobalt analogue and related cobalt-containing templates.<sup>24</sup> Unsubstituted half-sandwich cobalt allyl complexes were generated from the reaction of allyl alcohol with  $(\text{C}_5\text{Me}_5)\text{Co}(\text{C}_2\text{H}_4)_2$ , while substituted cobalt allyl complexes were generated by protonation of the corresponding cobalt

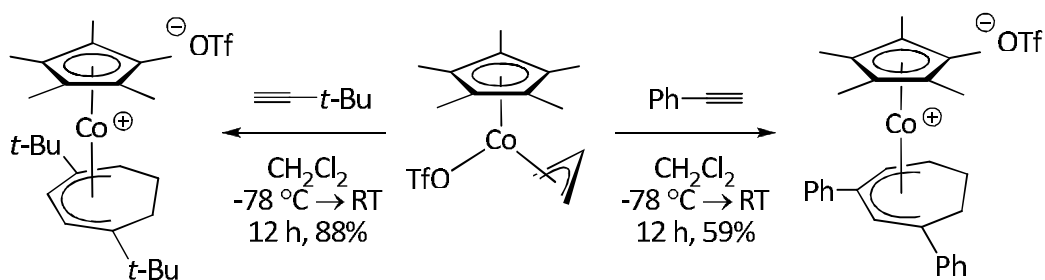
butadiene complexes, which in turn were generated by *in situ* olefin exchange using  $(C_5Me_5)Co(C_2H_4)_2$  (Scheme 2-3).

**Scheme 2-3**



Etkin, and later Dzwiniel, investigated the reactivity of these cobalt(III) allyl complexes.<sup>24, 116</sup> It was noted that while the reaction of the parent  $\eta^3$ -allyl complex with alkynes disubstituted alkynes (4,4-dimethyl-2-pentyne, diphenylacetylene, bis(trimethylsilyl)acetylene) afforded five-membered carbocycles (similar to Rubezhov's [3 + 2] cycloaddition reaction), terminal alkynes (phenylacetylene, *tert*-butylacetylene) afforded seven-membered carbocycles (Scheme 2-4).<sup>24</sup> The location of the substituents on the  $\eta^5$ -cycloheptadienyl fragment is dependent on the nature of the alkyne as well as the series of  $\beta$ -hydride elimination/insertion steps during the post-cyclization valence isomerization.

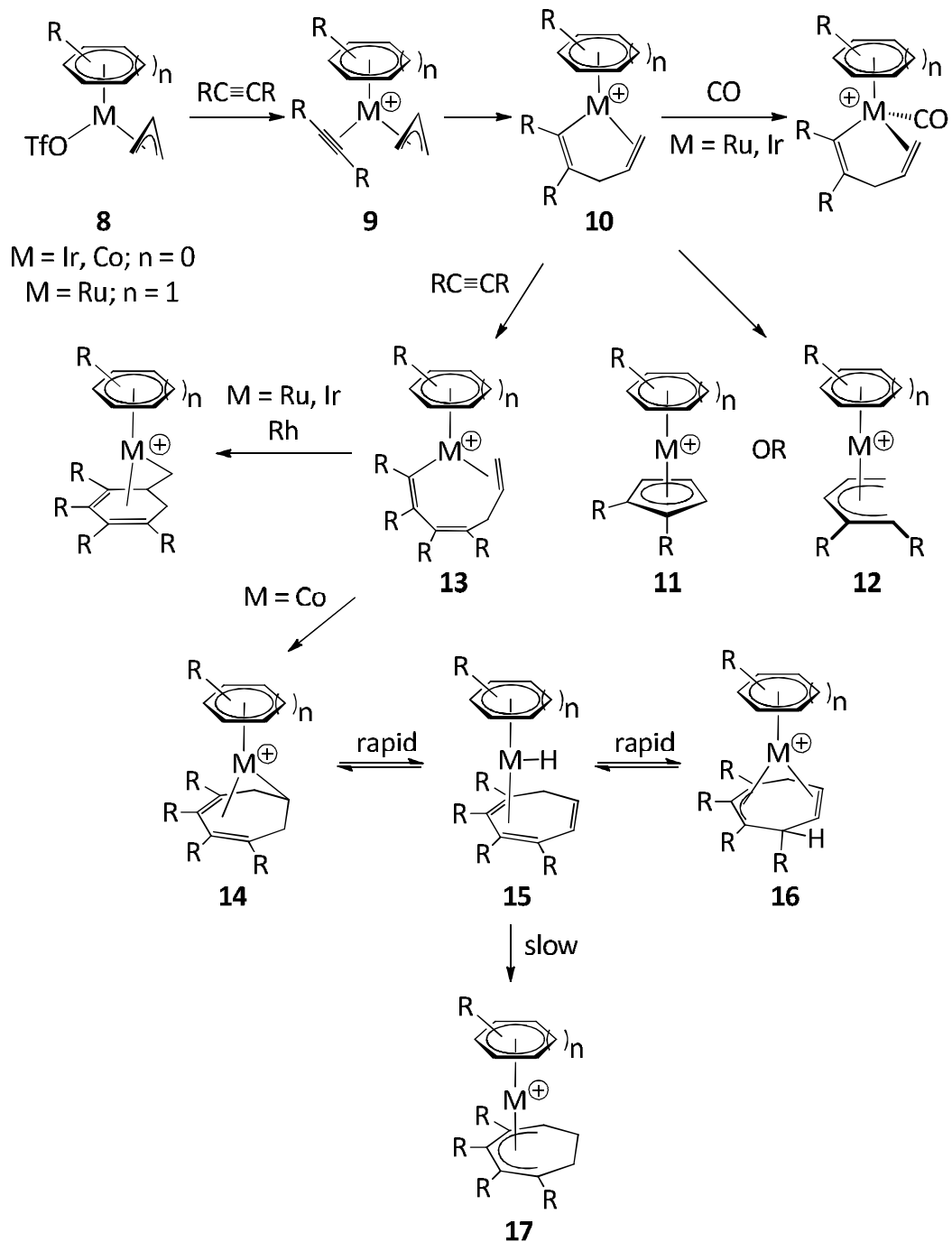
Scheme 2-4



Based on the intermediates and reactivities established using iridium and ruthenium templates, a proposed mechanism has emerged to rationalize the formation of both six- and seven-membered products during the [3 + 2 + 2] allyl-alkyne cycloaddition (Scheme 2-5).<sup>116, 117</sup> A more thorough discussion can be found in Dzwiniel's and Witherell's Ph.D. dissertations and the mechanism is merely summarized here.<sup>116, 117</sup>

In the initial step of the [3 + 2 + 2] allyl-alkyne cycloaddition process, ionization of the weakly coordinated triflate anion is followed by coordination of alkyne to form a cationic allyl-alkyne complex **9**. No such intermediate is observed in the cobalt series, though Schweibert and Older have observed such a complex when iridium and ruthenium templates are used.

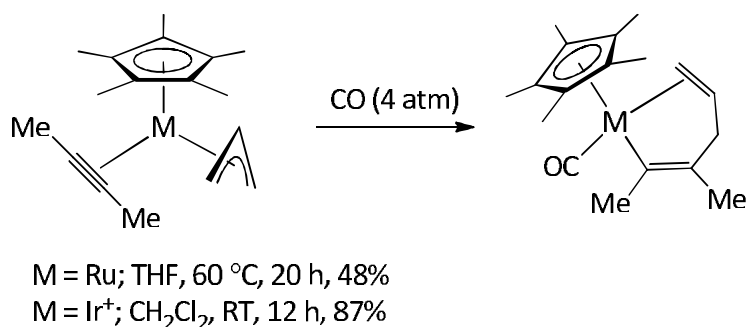
Scheme 2-5



The cationic allyl-alkyne complex undergoes a migratory insertion of the alkyne unit to the allyl ligand to form a vinyl-olefin species **10**. Evidence for this

complex is implied by the isolation of carbonylated iridium and ruthenium analogues by Schweibert and Older (Equation 2-4).<sup>31, 118</sup> No such complex can be trapped using cobalt, as the following reaction steps appear to be faster than the formation of vinyl-olefin complex.

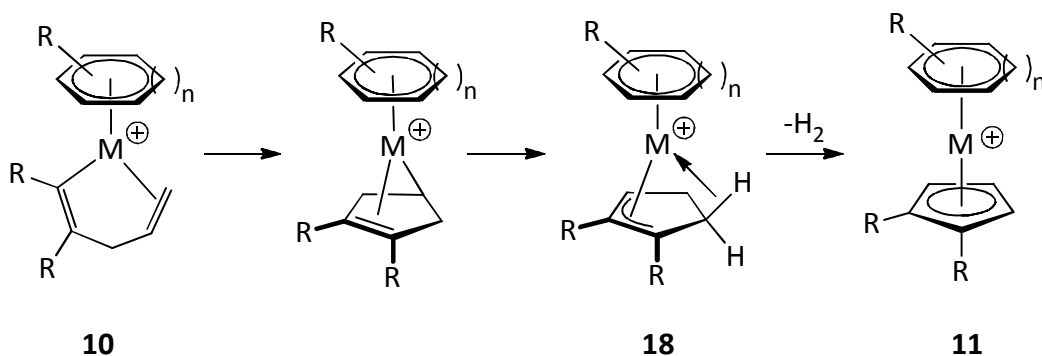
**Equation 2-4**



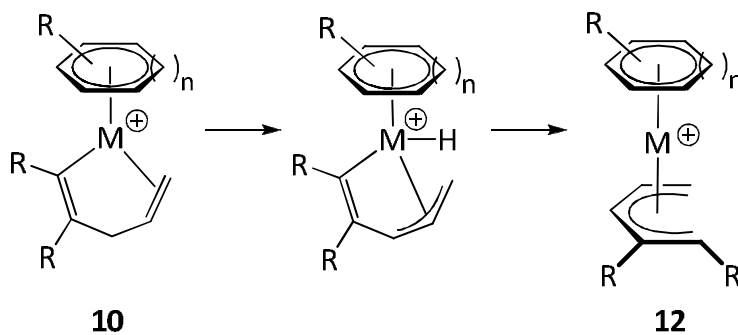
Depending on the conditions, the reaction may proceed down one of two pathways. If the coordination of a second equivalent of alkyne is interrupted as a result of the steric bulk of the alkyne or low concentration in solution, the vinyl-olefin complex **10** can cyclize to give initially a  $\eta^1, \eta^2$ -cyclopentenyl complex, followed by isomerization to afford the agostic  $\eta^3$ -cyclopentenyl complex **18** (Scheme 2-6). Spencer has independently prepared and characterized similar agostic  $\eta^3$ -cyclopentenyl cobalt complexes and reported their rearrangements to give  $\eta^5$ -cyclopentadienyl complexes.<sup>119-121</sup> Alternatively, allylic carbon-hydrogen bond activation of the vinyl-olefin complex **10** provides a vinyl-hydrido-allyl complex, which rearranges by reductive elimination to the acyclic  $\eta^5$ -pentadienyl

complex **12** (Scheme 2-7). The transformation of the agostic cyclopentenyl complex **18** to the  $\eta^5$ -cyclopentadienyl complex **11** is promoted by adventitious water or a Lewis base, which results in the loss of dihydrogen.

**Scheme 2-6**



**Scheme 2-7**



However, in the presence of a second equivalent of alkyne, a second migratory insertion of alkyne can occur to give the polyenyl complex **13** (see Scheme 2-5). No evidence for the existence of this complex exists, but its

identity was deduced from the formation of both six- and seven-membered ring products.

Upon formation of the polyenyl complex **13**, migratory ring closure can occur to either olefinic carbon of the terminal olefin. Closure to the internal olefinic carbon leads to the six-membered ring formation, whereas closure to the remote olefinic carbon leads to seven-membered ring formation. Exclusive seven-membered ring formation is observed when cobalt is used. Some iridium and ruthenium systems that give predominantly seven-membered ring products also give the six-membered ring product in small amounts.

Closure of the polyenyl complex **13** to give the seven-membered ring product proceeds initially to an  $\eta^1, \eta^4$ -cycloheptadienyl complex **14**. Older has isolated several ruthenium complexes exhibiting this hapticity (Scheme 2-1 and Scheme 2-2) from allyl-alkyne insertion. Rearrangement of the  $\eta^1, \eta^4$ -cycloheptadienyl complex **14** to the fully conjugated  $\eta^5$ -cycloheptadienyl complex **17** occurs via a series of rapid and reversible  $\beta$ -hydride elimination/insertion steps.

Dzwiniel has demonstrated through deuterium labeling studies that  $\beta$ -hydride elimination from the  $\eta^1, \eta^4$ -cycloheptadienyl complex **14** forms the hydrido-cycloheptatriene complex **15**. In principle, reinsertion can occur to any of the olefinic carbons. Deuterium labeling studies have demonstrated that the addition and elimination of hydride on carbons two or five of the triene unit

occur rapidly, regenerating and equilibrating among the  $\eta^1,\eta^4$ -cycloheptadienyl isomers.

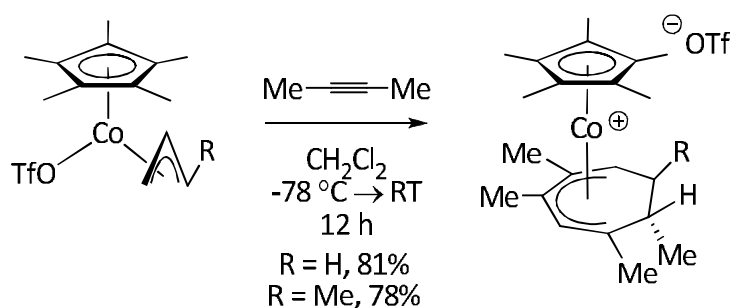
Interestingly, the reinsertion of hydride to carbon three or four of the triene unit would give the  $\eta^2,\eta^3$ -cycloheptadienyl product **16**. While no such products have been isolated during the course of the [3 + 2 + 2] allyl-alkyne cycloaddition reaction, cycloheptadienyl complexes bearing this unusual hapticity have been isolated recently from the analogous [5 + 2] cobalt pentadienyl-alkyne cycloaddition reaction.<sup>122</sup> Bridged bicyclic metal complexes displaying the  $\eta^2,\eta^3$ -cycloheptadienyl hapticity have been reported in iron and ruthenium.<sup>123-130</sup>

Ultimately, the migration of hydride to either terminal carbon of the triene unit results in the formation of the fully conjugated  $\eta^5$ -cycloheptadienyl complex **17**. The addition of hydride to the terminal positions is most likely irreversible considering that the  $\eta^5$ -cycloheptadienyl complex **17** does not isomerize to any of the other seven-membered complexes **14**, **15**, or **16**. Older has demonstrated that ruthenium  $\eta^1,\eta^4$ -cycloheptadienyl complexes will slowly convert to the fully conjugated  $\eta^5$ -cycloheptadienyl complexes upon standing, with the process accelerated upon heating.

## B. Cobalt-Mediated [5+2] Cyclopentenyl-Alkyne Cycloaddition Reactions Involving Carbon-Carbon Bond Activation

During the course of the investigation of cobalt-mediated [3 + 2 + 2] allyl-alkyne cycloaddition reactions, Dzwiniel observed an unusual substitution pattern when  $[(C_5Me_5)Co(\eta^3\text{-allyl})]OTf$  was treated with 2-butyne (Equation 2-5). The isolated  $\eta^5$ -cycloheptadienyl product possessed methyl substituents that were not located on contiguous carbons. The unusual substitution pattern has also been observed when the cobalt crotyl complex is used.

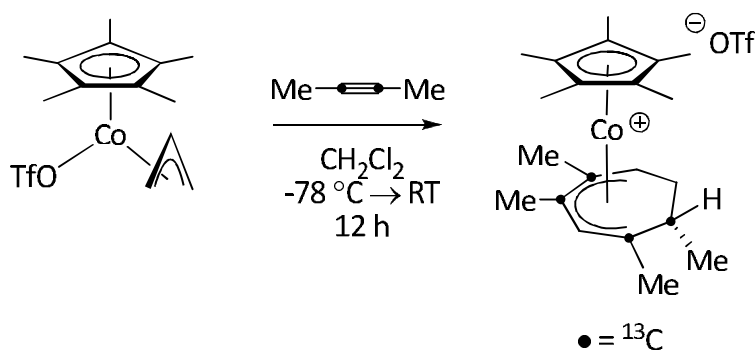
### Equation 2-5



In order to determine whether a skeletal rearrangement or methyl migration accounts for the observed products, Etkin and Dzwiniel treated the parent allyl complex with doubly  $^{13}C$ -labeled 2-butyne, and isolated a product that was quadruply labeled (Equation 2-6). Each labeled carbon remained attached to a methyl group, strongly suggesting that methyl migration was not occurring and that a skeletal rearrangement must occur before ring closure. In

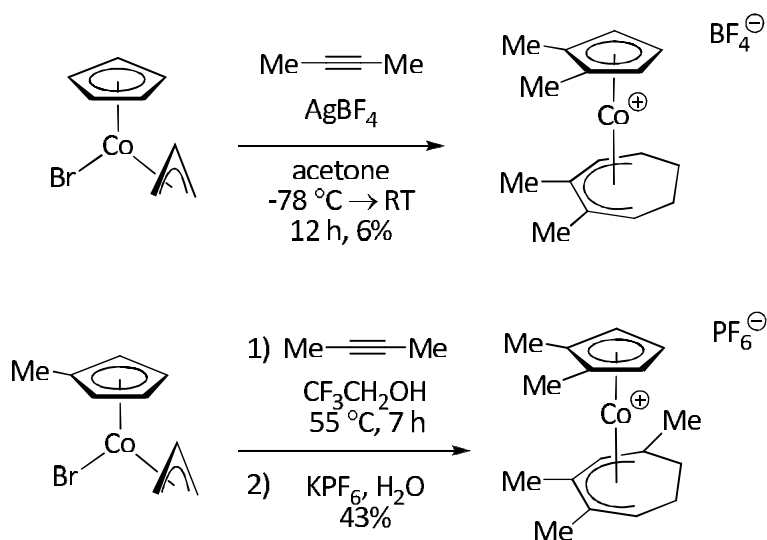
order to rationalize a skeletal rearrangement, Etkin and Dzwiniel invoked a carbon-carbon bond activation process. A more thorough discussion of the details and putative mechanism of carbon-carbon bond activation as it relates to cobalt-mediated seven-membered carbocycle synthesis is presented in Chapter 4.

**Equation 2-6**



Dzwiniel has further explored the scope of this unusual reaction, extending it to mono-substituted cyclopentadienyl ancillary ligands.<sup>25</sup> However, in some cases carbon-carbon bond activation of the ancillary cyclopentadienyl occurs, resulting in a very unusual two-carbon ring-expansion of the cyclopentadienyl ligand to form the  $\eta^5$ -cycloheptadienyl product (Scheme 2-8).

Scheme 2-8

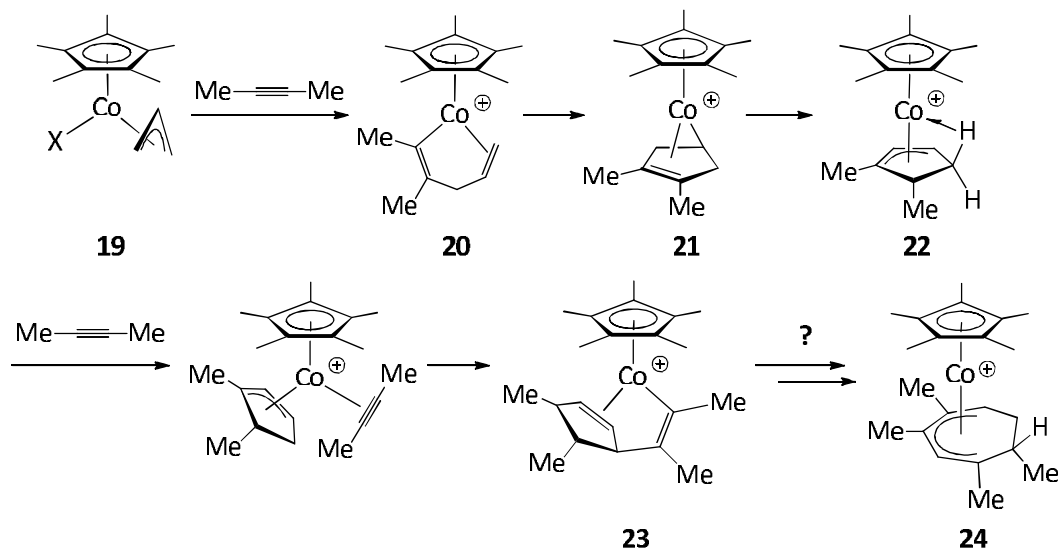


One early mechanistic proposal to account for the rearrangement product and the unusual two-carbon ring-expansion of the cyclopentadienyl ligand presented in Equation 2-5, Equation 2-6, and Scheme 2-8 proceeds through an agostic  $\eta^3$ -cyclopentenyl intermediate formed from ring closure after the first insertion of alkyne (Scheme 2-9).

Beginning with the cobalt allyl complex **19**, treatment with 2-butyne forms the cationic vinyl olefin complex **20**. Subsequent migratory insertion and ring closure forms the  $\eta^1, \eta^2$ -cyclopentenyl complex **21**, which can isomerize through allylic carbon-hydrogen bond activation to form the agostic  $\eta^3$ -cyclopentenyl complex **22**. The coordination and insertion of a second equivalent of alkyne, followed by migratory insertion into the metal-cyclopentenyl bond forms the proposed cationic vinyl-cyclopentene intermediate **23**. The final series of steps, whereby the  $\eta^5$ -cycloheptadienyl

product **24** is formed, is unknown but several proposals for this last series of reactions will be discussed in Chapter 4.

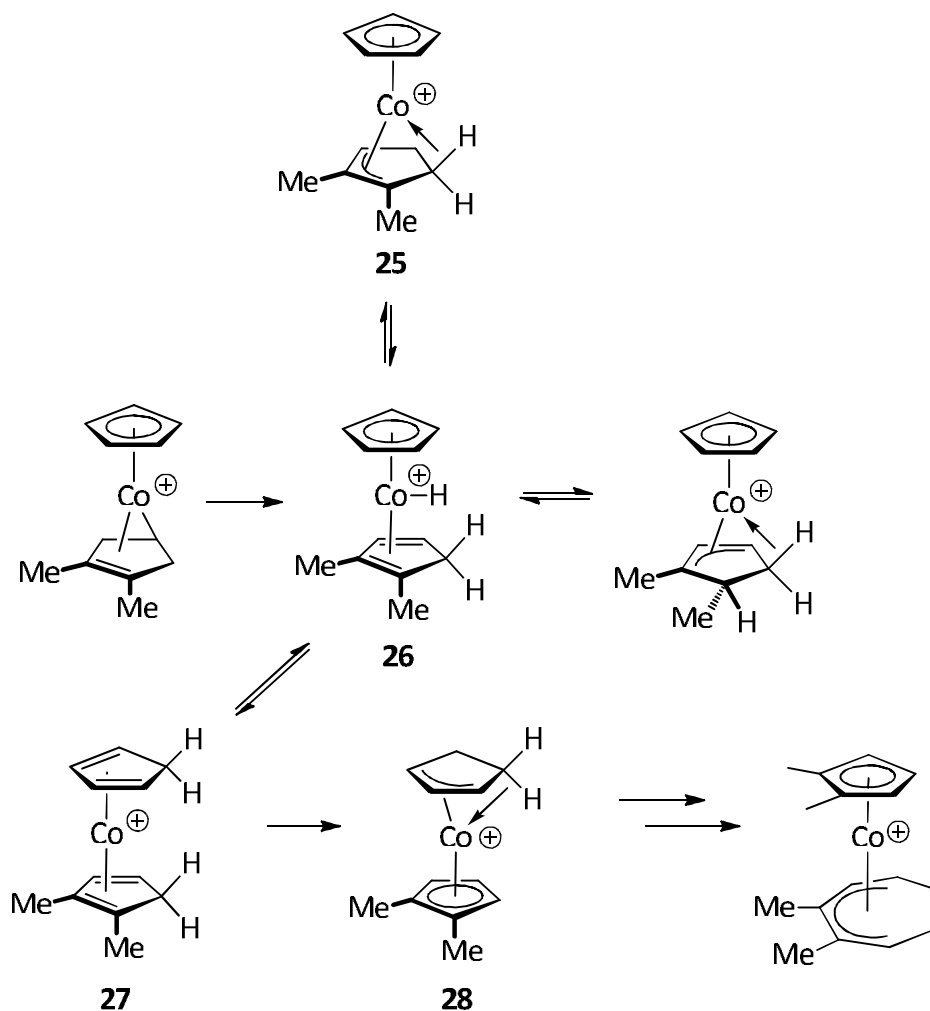
**Scheme 2-9**



To account for the two-carbon expansion of the cyclopentadienyl ligand illustrated in Scheme 2-8, Stryker has proposed a hydride transfer pathway (Scheme 2-10). Upon formation of the cationic  $\eta^1, \eta^2$ -cyclopentenyl complex **25** by cyclization of the corresponding vinyl-olefin complex,  $\beta$ -hydride elimination leads to a classical hydrido diene complex **26**. Hydride migration back onto the dimethylcyclopentadiene ligand results in the formation of two possible isomers. It is very likely that these isomers rapidly interconvert, but neither of these two isomers lead to the product observed. Instead, hydride migration to the cyclopentadienyl ring results in the formation of an unsaturated cationic cobalt

bis(cyclopentadiene) complex **27**, which is followed by another hydride migration to arrive at the (dimethylcyclopentadienyl)cobalt complex **28**.

**Scheme 2-10**

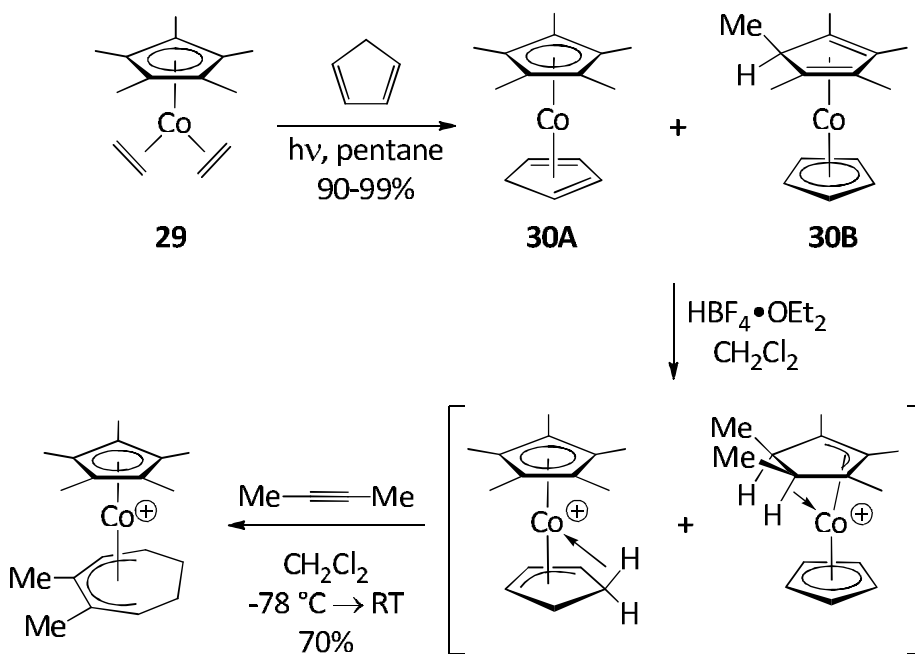


The key intermediates in both of the early mechanistic proposals are the agostic cobalt  $\eta^3$ -cyclopentenyl complexes **22** and **28**. Spencer has prepared several more stable analogues of these agostic  $\eta^3$ -cyclopentenyl complexes and has studied their behaviour in solution.<sup>119-121</sup> A surprising conclusion from this

mechanistic proposal is that the independent protonation of a cobalt  $\eta^4$ -cyclopentadiene complex, followed by treatment with alkyne, should result in the two-carbon ring-expansion of the cyclopentadienyl ligand. This would represent an unusual [5 + 2] cyclopentenyl-alkyne cycloaddition reaction. Dzwiniel has successfully demonstrated this strategy in the synthesis of seven-membered products by protonation of cobalt(I) cyclopentadiene complexes in the presence of alkynes.<sup>116, 131</sup>

In a representative example of the [5 + 2] cyclopentenyl-alkyne cycloaddition reaction, photochemical irradiation of  $(C_5Me_5)Co(C_2H_4)_2$  **29** in the presence of cyclopentadiene produces a mixture of diene isomers **30A** and **30B** (Scheme 2-11).<sup>131</sup>

**Scheme 2-11**

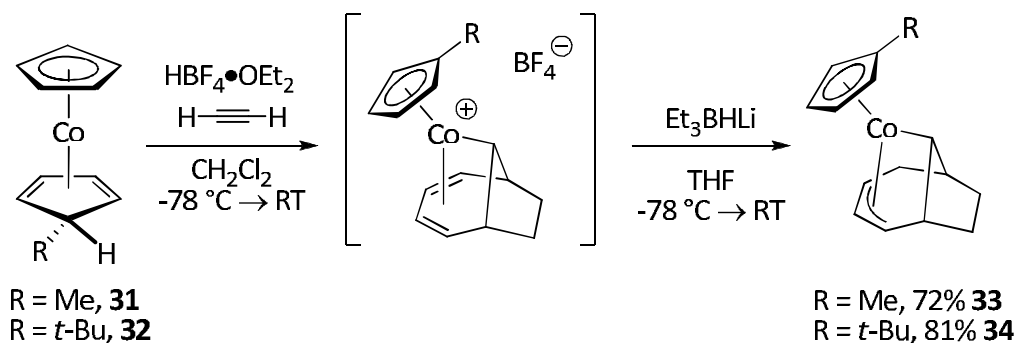


The ratio of the two isomers is dependent on the duration of irradiation and the product mixture cannot be separated. Protonation of the entire mixture followed by treatment with 2-butyne results in the formation of a single  $\eta^5$ -cycloheptadienyl product, implying that protonation of the isomeric mixture leads to a single product, confirming the proposed hydride migrations from the cyclopentadiene ligand to the cyclopentadienyl ligand.

### C. Cobalt-Mediated Cyclopentenyl-Acetylene Cycloaddition Reactions

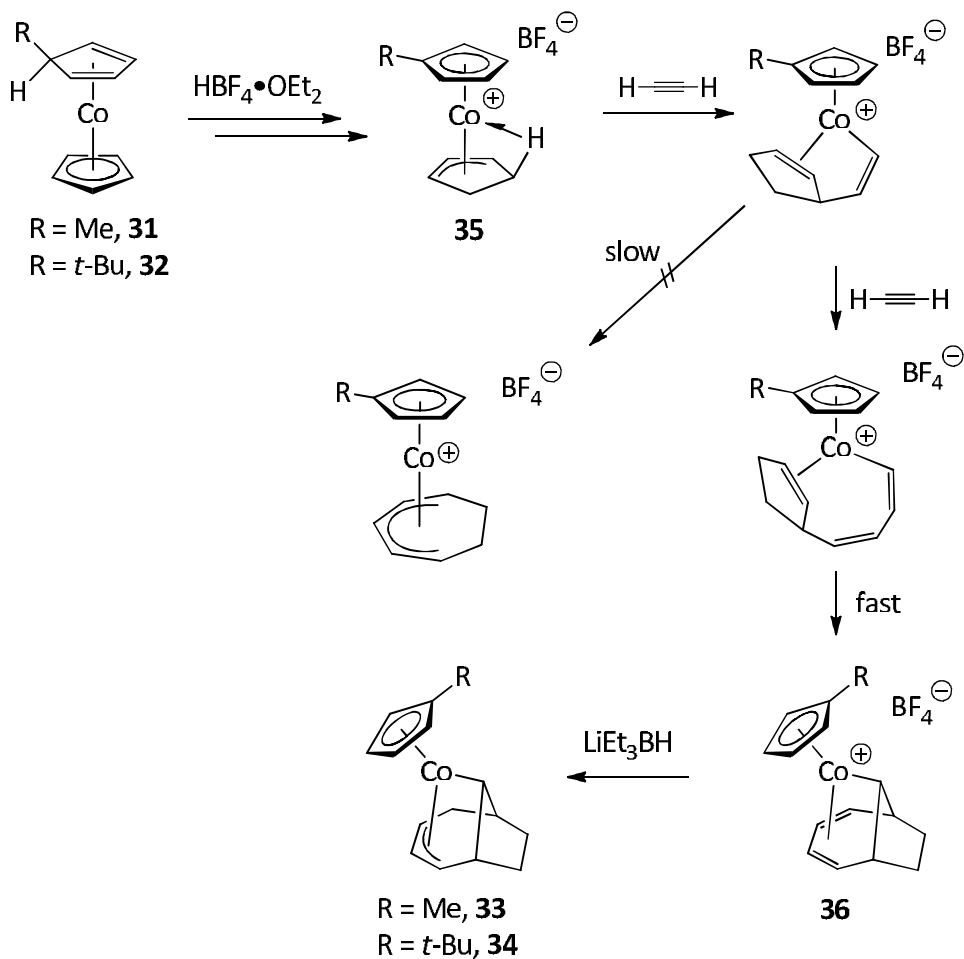
While treatment of  $\text{Cp}'\text{Co}(\eta^4\text{-cyclopentadiene})$  (where  $\text{Cp}' = \text{C}_5\text{Me}_5, \text{MeCp}, t\text{-BuCp}$ ) with most alkynes results in the two-carbon expansion of the less-substituted cyclopentadiene unit, the same cannot be said when acetylene is used. Dwziniel has observed that protonation of either  $(\text{C}_5\text{H}_5)\text{Co}(\eta^4\text{-MeC}_5\text{H}_5)$  **31** or  $(\text{C}_5\text{H}_5)\text{Co}(\eta^4\text{-}t\text{-BuC}_5\text{H}_5)$  **32** in the presence of excess acetylene instead provides the bridged bicyclic products **33** and **34**, respectively (Equation 2-7).<sup>116</sup> The  $\eta^1, \eta^4$ -coordinated products obtained in either case are not stable enough to be isolated directly without decomposition; *in situ* treatment of the product with  $\text{Et}_3\text{BHLi}$  provides the thermally stable, although air-sensitive, bicyclic products **33** and **34**.

Equation 2-7



The proposed mechanism for this reaction begins with the generation of an agostic  $\eta^3$ -cyclopentenyl cobalt complex **35** via protonation of cyclopentadiene complexes **31/32**, followed by hydride migration from the substituted cyclopentadienyl ligand to the unsubstituted cyclopentadienyl ligand (Scheme 2-12). The sequential coordination and insertion of two equivalents of acetylene followed by migratory cyclization affords the kinetic  $\eta^1, \eta^4$ -bicyclic complex **36**. It is reasonable to assume that the small steric bulk of acetylene (as compared to 2-butyne) lowers the kinetic barrier to the second coordination and insertion, intercepting the vinyl olefin intermediate prior to ring-expansion.

Scheme 2-12

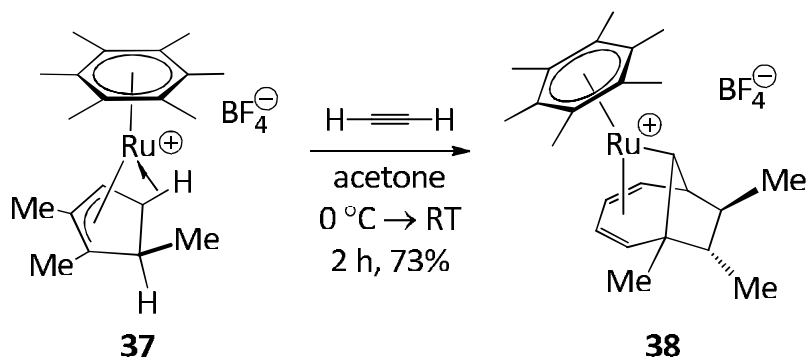


Similar to other examples of cobalt [3 + 2 + 2] allyl-alkyne cycloaddition reactions (*vide supra*), the migratory closure of the polyene fragment can occur on either olefinic carbon. Preferential closure to the remote olefinic carbon to give the bicyclic seven-membered product is consistent with the [3 + 2 + 2] cycloaddition reactions of acyclic  $\eta^3$ -allyl complexes of cobalt, iridium, and ruthenium.<sup>24, 31</sup> Interestingly, isomerization of the  $\eta^1, \eta^4$ -bicyclic complex **36** to the fully conjugated  $\eta^5$ -cycloheptadienyl product is not observed. The

constrained bicyclic framework clearly inhibits isomerization, which must occur via  $\beta$ -hydride elimination of the bridgehead carbon-hydrogen bond.

Similar double insertion bicyclic products have been observed in the related  $\eta^6$ -arene ruthenium series. Older has found that the agostic  $\eta^3$ -trimethylcyclopentenyl complex **37** reacts with acetylene to afford the bridged  $\eta^1, \eta^4$ -bicyclic product **38** that is relatively stable towards decomposition compared to the previously discussed cobalt example (Equation 2-8).<sup>39</sup>

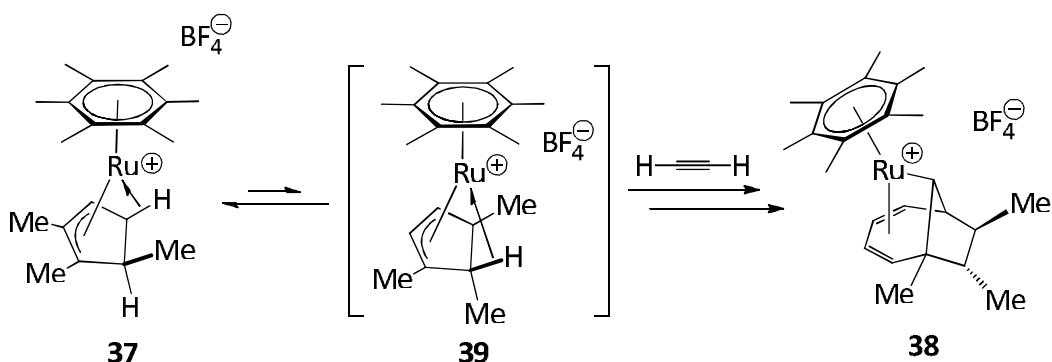
#### Equation 2-8



To rationalize the product obtained in this case, it is presumed there is rapid equilibration of the agostic  $\eta^3$ -cyclopentenyl complex **37** to the more reactive agostic  $\eta^3$ -cyclopentenyl complex **39** before the insertion of the first equivalent of acetylene (Scheme 2-13). The alkyne inserts into the allyl ligand to form a vinylcyclopentene intermediate and is followed by rapid insertion of a second equivalent of acetylene. Although insertion principally occurs on the less substituted terminus of the  $\eta^3$ -cyclopentenyl ligand, it is possible that the

insertion occurs at the more substituted site, however no evidence for the formation of the bicyclic product arising from insertion to the more hindered side of the cyclopentenyl ligand was found.

### Scheme 2-13



### D. Project Goals

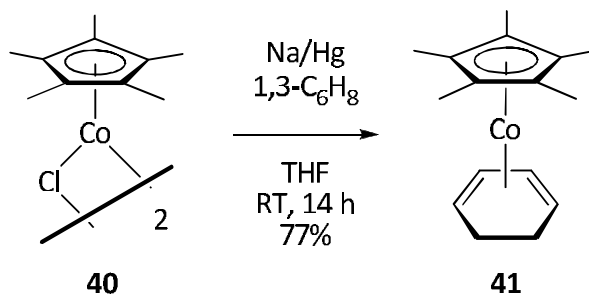
While Dzwiniel has extensively studied the [5 + 2] cyclopentenyl-alkyne cycloaddition reaction and has documented many examples of the two-carbon expansion of five-membered rings to form the corresponding seven-membered ring products, the two-carbon expansion of larger cyclic dienes such as cyclohexadiene, cycloheptadiene, and cyclooctadiene, has not been investigated. The two-carbon expansion of six-, seven-, and possibly eight-membered rings would be of tremendous interest to the synthetic community.

## Section 2. Results and Discussion

### A. Cobalt $\eta^3$ -Cyclohexenyl-Acetylene Cycloaddition Reactions

The success of the  $\eta^4$ -cyclopentadiene template for two-carbon ring-expansion reactions led us to investigate the analogous  $\eta^4$ -cyclohexadiene template. The starting material, (C<sub>5</sub>Me<sub>5</sub>)Co( $\eta^4$ -cyclohexadiene) **41**, was prepared by sodium amalgam reduction of the cobalt(II) chloro-dimer [(C<sub>5</sub>Me<sub>5</sub>)CoCl]<sub>2</sub> **40** in the presence of 1,3-cyclohexadiene (Equation 2-9).<sup>132</sup>

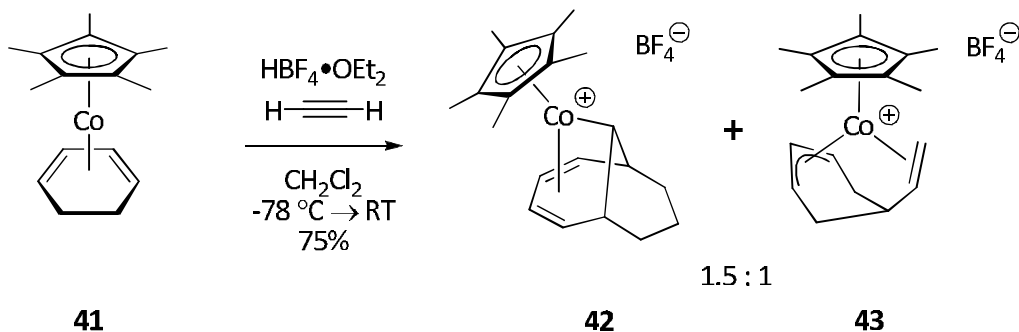
Equation 2-9



Protonation of diene complex **41** with HBF<sub>4</sub>•OEt<sub>2</sub> in acetylene-saturated dichloromethane at low temperature produced a mixture of two products, bridged  $\eta^1, \eta^4$ -bicyclic complex **42** and  $\eta^2, \eta^3$ -vinylcyclohexenyl complex **43**, in a 1.5 : 1 ratio (Equation 2-10). The product mixture was purified by flash chromatography on the bench followed by recrystallization from a dichloromethane/diethyl ether mixture. However, fractional crystallization could

not separate the  $\eta^2, \eta^3$ -vinylcyclohexenyl complex **43** from the bicyclic complex **42**.

**Equation 2-10**



Crystals suitable for X-ray diffraction analysis were grown by layering diethyl ether on top of a dichloromethane solution of the purified product mixture. Two distinct crystal morphologies were isolated and their X-ray structure determinations confirm the structures proposed for **42** and **43** on the basis of spectra data (Figure 2-2 and Figure 2-3).

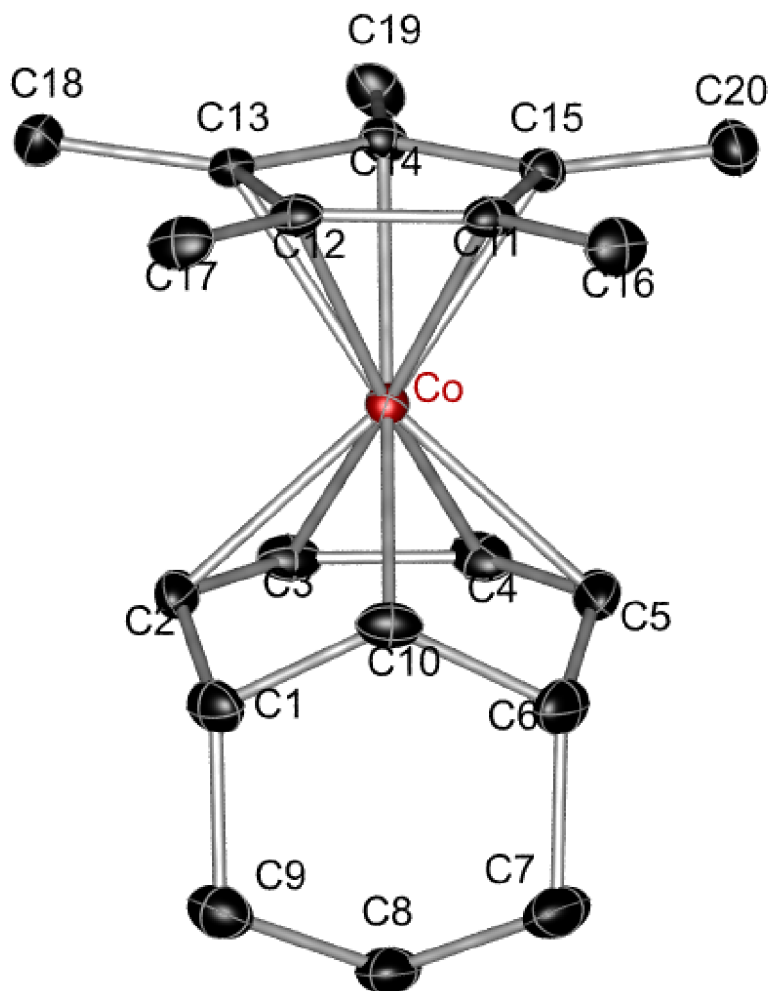


**Figure 2-2:** Perspective view of  $[(C_5Me_5)Co(\eta^4, \eta^1\text{-bicyclo[4.3.1]deca-2,4-dien-10-ide})]$  cation **42**. Final residuals:  $R_1 = 0.0323$ ;  $wR_2 = 0.0724$ . Data collected at  $-80\text{ }^\circ\text{C}$ . Non-hydrogen atoms are represented by Gaussian ellipsoids at the 20% probability level. Hydrogen atoms have been omitted. Selected bond distances ( $\text{\AA}$ ): Co-C2, 2.140(2); Co-C3, 2.039(2); Co-C4, 2.039(2); Co-C5, 2.145(2); Co-C10, 2.048(2); C1-C2, 1.497(3); C1-C9, 1.542(3); C1-C10, 1.495(3); C2-C3, 1.383(3); C3-C4, 1.414(4); C4-C5, 1.394(4); C5-C6, 1.486(4); C6-C7, 1.542(4); C6-C10, 1.495(4); C7-C8, 1.508(4); C8-C9, 1.520(4). The dihedral angle between the planes defined by C2-C5 and C11-C15:  $14.10(7)^\circ$

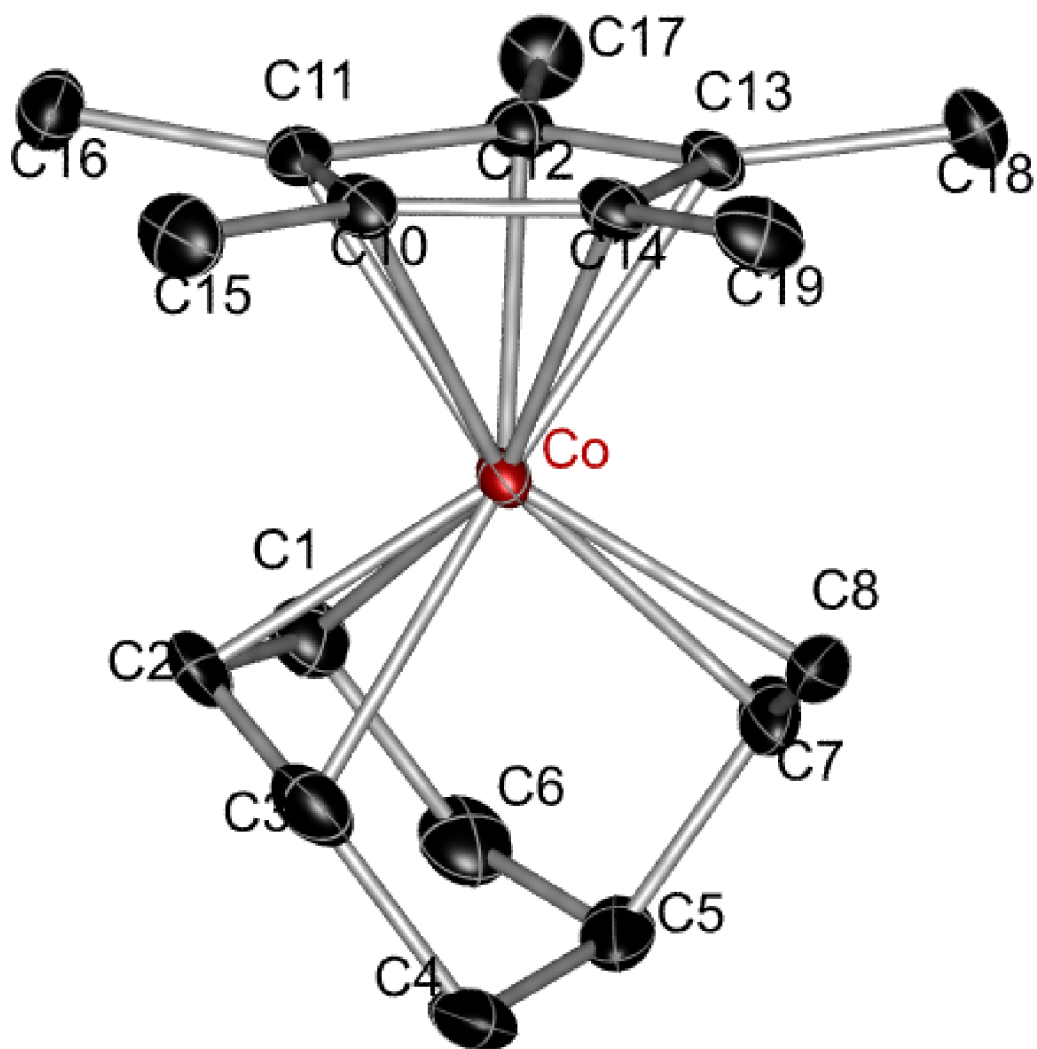


**Figure 2-3:** Perspective view of the  $[(C_5Me_5)Co(\eta^3, \eta^2\text{-5-vinylcyclohex-2-en-1-yl})]$  cation **43**. Final residuals:  $R_1 = 0.0602$ ;  $wR_2 = 0.1677$ . Data collected at  $-80\text{ }^\circ\text{C}$ . Non-hydrogen atoms are represented by Gaussian ellipsoids at the 20% probability level. Hydrogen atoms have been omitted. Selected bond distances ( $\text{\AA}$ ): C1-C2, 1.406(7); C1-C6, 1.520(7); C2-C3, 1.352(8); C3-C4, 1.531(7); C4-C5, 1.561(9); C5-C6, 1.459(9); C5-C7, 1.520(6); C7-C8, 1.356(8); Co-C1, 2.159(5); Co-C2, 2.016(4); Co-C3, 2.153(5); Co-C7, 2.088(4); Co-C8, 2.109(4). The dihedral angle between the planes defined by C1-C3 and C10-C14:  $30.1(4)^\circ$ .

Relevant  $^1\text{H}$  and  $^{13}\text{C}$  NMR spectroscopic information of the bicyclic cation

**42** are summarized in Figure 2-2 and Table 2-1.

**Figure 2-4:**  $^1\text{H}$  and  $^{13}\text{C}$  Numbering System for Bicyclic Cobalt Cation **42**

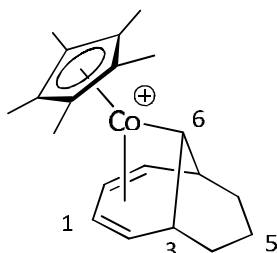
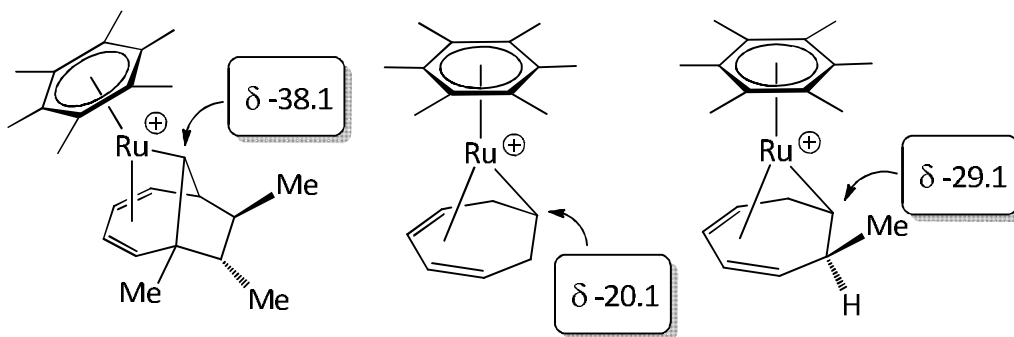


**Table 2-1:** NMR Spectroscopic Data for Bicyclic Cobalt Cation **42**

Position	$\delta$ $^1\text{H}$	$\delta$ $^{13}\text{C}$
1	5.78 (m, 2 <sup>nd</sup> order)	99.9
2	3.80 (m, 2 <sup>nd</sup> order)	61.9
3	2.83 (m, 2 <sup>nd</sup> order)	32.9
4	0.9-1.1 (m, overlapping resonances)	30.4
5	0.5 (m, overlapping resonances)	14.7
6	1.34 (t, $J = 8.5$ Hz)	-16.1
$\text{C}_5(\text{CH}_3)_5$	1.81 (s)	9.56
$\text{C}_5(\text{CH}_3)_5$		100.6

Due to the plane of symmetry bisecting bicyclic complex **42**, the internal and terminal diene protons are chemically equivalent but magnetically inequivalent and display a 2<sup>nd</sup> order appearance in the <sup>1</sup>H NMR spectrum. The bridge proton H<sub>6</sub> couples strongly to both bridgehead protons H<sub>3</sub> and H<sub>3'</sub> (<sup>3</sup>J = 8.5 Hz). The chemical shift of the bridgehead carbon is located upfield at δ -16.1 ppm, which is comparable with the carbon chemical shift in the related ruthenium bridged (δ -38.1 ppm) and unbridged (δ -20.1 and -29.1) η<sup>1</sup>,η<sup>4</sup>-complexes (Figure 2-5).<sup>39</sup>

**Figure 2-5:** Selected <sup>13</sup>C Chemical Shifts of Similar η<sup>1</sup>,η<sup>4</sup>-Cycloheptadienyl Complexes



Relevant <sup>1</sup>H and <sup>13</sup>C NMR spectroscopic information of the vinylcyclohexenyl complex **43** are summarized in Figure 2-6 and in Table 2-2.

**Figure 2-6:**  $^1\text{H}$  and  $^{13}\text{C}$  Numbering System for Cobalt Vinylcyclohexenyl Cation **43**

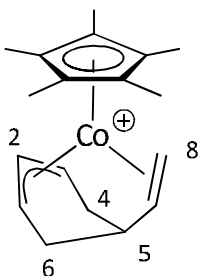


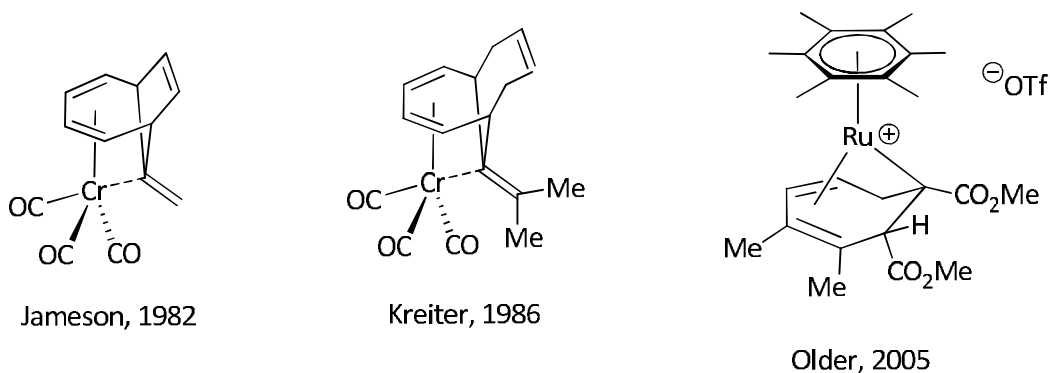
**Table 2-2:** NMR Spectroscopic Data for Cobalt Vinylcyclohexenyl Cation **43**

Position	$\delta ^1\text{H}$	$\delta ^{13}\text{C}$
1	4.83 (t, $J = 7.0$ Hz)	85.9
2	4.30 (t, $J = 7.0$ Hz)	90.0
3	5.32 (dt, $J = 7.0, 1.6$ Hz)	83.2
4	H <sub>4a</sub> : 2.22 (dt, $J = 14.5, 3.5$ Hz) H <sub>4b</sub> : 1.56 (d, $J = 14.5$ Hz)	37.6
5	1.88 (m, partially obscured)	36.4
6	H <sub>6a</sub> : 1.20 (dt, $J = 16.0, 3.5$ Hz) H <sub>6b</sub> : 0.57 (d, $J = 15.5$ Hz)	24.0
7	4.64 (dd, $J = 14.0, 8.0$ Hz)	100.6
8	H <sub>8a</sub> : 4.54 (d, $J = 14.0$ Hz) H <sub>8b</sub> : 3.97 (d, $J = 8.0$ Hz)	75.0
$\text{C}_5(\text{CH}_3)_5$	1.68 (s)	9.7
$\text{C}_5(\text{CH}_3)_5$		99.9

The complex does not possess a plane of symmetry due to the orientation of the pendant alkene, which is tilted with respect to the allyl moiety. Additionally, the orientation of the cyclohexenyl fragment is fixed and the pendant olefin does not dissociate on the NMR timescale, which renders all of the protons chemically inequivalent. The chemical shifts of the olefinic carbons display a large difference of 25 ppm. This is reflected in the crystal structure where the bond distance between the cobalt and the terminal olefinic carbon is  $\sim 0.1$  Å longer than the distance between cobalt and the interior olefinic carbon (2.109 Å compared to 2.088 Å). This is unusual in that the less substituted terminal olefinic carbon would be expected to bind more strongly to the cobalt centre and possess a shorter bond distance. The introduction of coordination strain to the molecule likely prevents this from occurring.

The crystal structure of the bicyclic complex **42** (Figure 2-2) displays an unusual  $\eta^1, \eta^4$ -bonding mode that is not commonly found in the literature. While Older has found the same bonding motif in several unbridged  $\eta^6$ -arene ruthenium complexes, only one such compound has been structurally characterized by X-ray crystallography (Figure 2-7).<sup>115</sup> Both Jameson<sup>133</sup> and Kreiter<sup>134</sup> have independently reported similar crystal structures of a bridged chromium  $\eta^1, \eta^4$ -triene complex that have the  $\eta^1$ -carbon as part of an alkene unit. The chromium complexes possess a very unsymmetrically bonded alkene unit, rendering the terminal alkene carbon essentially unbound.

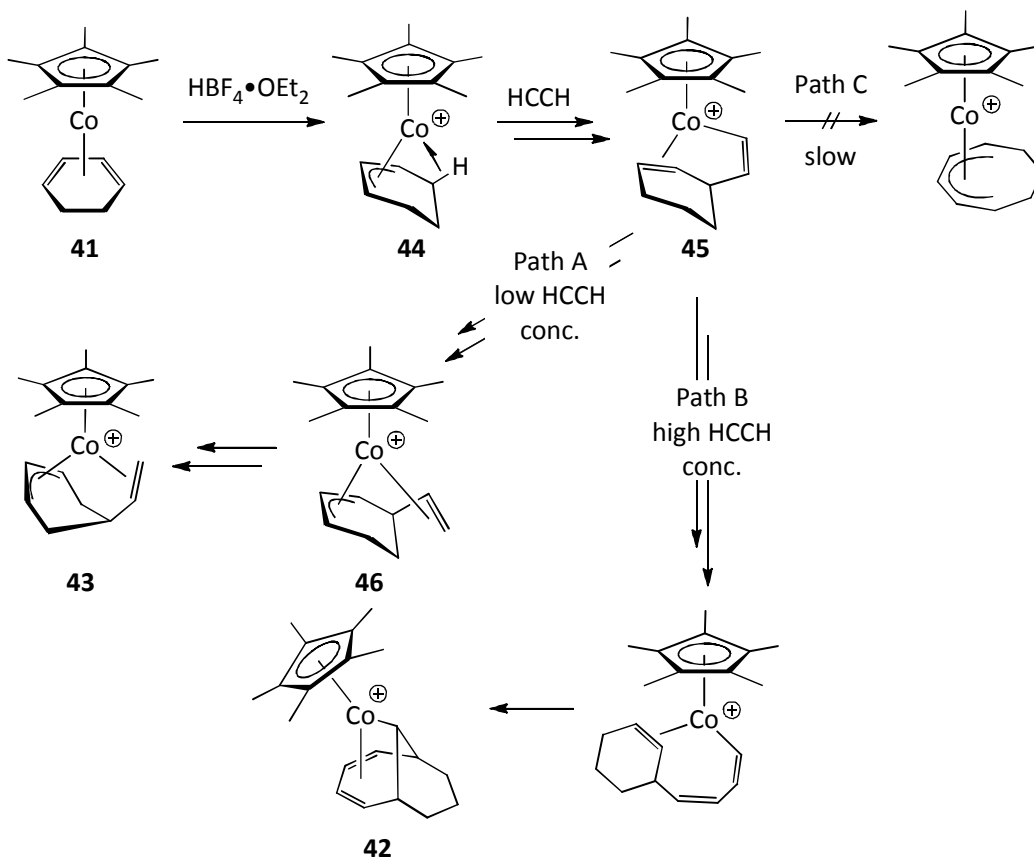
**Figure 2-7:** Compounds Possessing  $\eta^1, \eta^4$ -Binding Motif



The bonding motif displayed in the crystal structure of the  $\eta^2, \eta^3$ -vinylcyclohexenyl cation **43** is also uncommon. While cobalt compounds exhibiting the  $\eta^2, \eta^3$ -coordination mode, where the coordinating carbon fragments bind as isolated allyl and olefin units within a single ring, is known for seven- and eight-membered rings, no crystal structures have been reported for this acyclic version.<sup>122, 135-137</sup>

The proposed mechanism for the formation of both bicyclic product **42** and the vinylcyclohexenyl complex **43** is consistent with that proposed for Dzwiniel's [3 + 2 + 2] cyclopentenyl-acetylene cycloaddition reaction (Scheme 2-14). Protonation of  $(C_5Me_5)Co(\eta^4\text{-cyclohexadiene})$  **41** with  $HBF_4 \cdot OEt_2$  presumably affords the known  $\eta^3$ -cyclohexenyl complex **44**; Salzer and coworkers have observed the formation of the agostic  $(C_5Me_5)Co(\eta^3\text{-cyclohexenyl})$  cation **44** by low temperature  $^1H$  NMR spectroscopy.<sup>132</sup>

Scheme 2-14

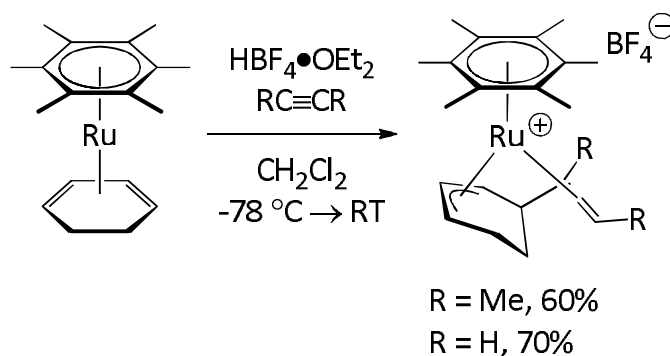


Upon formation of the  $\eta^3$ -cyclohexenyl complex **44**, acetylene coordinates to the vacant site on the cobalt centre and undergoes a migratory insertion to form the vinyl-cyclohexene complex **45**. Depending on the reaction conditions, the reaction may proceed down two of three reasonable pathways. If the coordination of a second equivalent of acetylene is inhibited by the low concentration in solution, the vinyl-cyclohexene complex **45** can undergo an allylic carbon-hydrogen activation and rearrange to the  $\eta^2, \eta^3$ -vinylcyclohexenyl complex **46**. A further allylic isomerization of this complex occurs to afford the observed product **43**. It is possible that the strained coordination geometry

present in vinylcyclohexenyl complex **46** leads to rapid rearrangement under the reaction conditions to the isolated product **43**.

The single insertion of acetylene and quick allylic carbon-hydrogen bond activation to form the initial  $\eta^2, \eta^3$ -vinylcyclohexenyl complex **46** has been similarly observed by Older in the reaction of a ruthenium cyclohexenyl cation with acetylene and 2-butyne (Equation 2-11).<sup>39</sup>

**Equation 2-11**



Coupling of a ruthenium  $\eta^3$ -cyclohexenyl system with either acetylene or 2-butyne produces the  $\eta^2, \eta^3$ -vinylcyclohexenyl product with a different substitution pattern than what is observed for cobalt. The analogous cobalt congener **46** of the ruthenium  $\eta^2, \eta^3$ -vinylcyclohexenyl complex is thus very likely to be an intermediate on the pathway to the observed cobalt  $\eta^2, \eta^3$ -vinylcyclohexenyl product **43**.

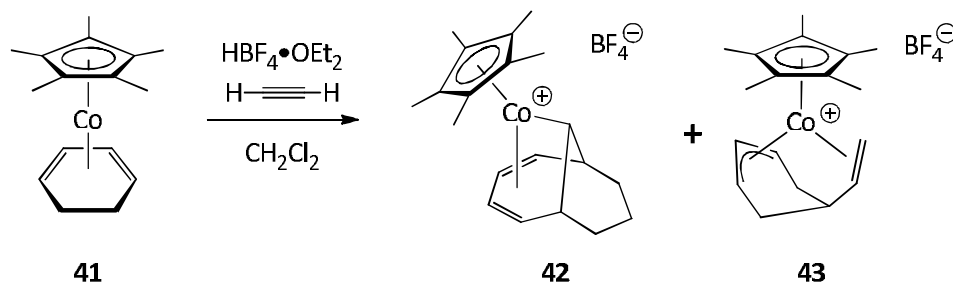
However, upon binding a second equivalent of acetylene, a second migratory insertion to the initial alkyne insertion product **45** can occur to give a polyenyl complex (Path B, Scheme 2-14). No evidence for the existence of the polyenyl complex has been obtained, but its identity is consistent with the proposed mechanism for the [3 + 2 + 2] allyl-alkyne cycloaddition reaction. A regioselective migratory cyclization to the remote cyclohexene carbon affords the observed  $\eta^1, \eta^4$ -bicyclic product **42**. In contrast to the bicyclic complexes **33** and **34** isolated by Dzwiniel, the pentamethylcyclopentadienyl analogue **42** is air- and moisture stable and can be chromatographed on silica gel on the bench.

Alternatively, a third pathway is hypothetically possible from the vinyl-cyclohexene complex **45** (Path C, Scheme 2-14). Products arising from the two-carbon ring-expansion of the  $\eta^3$ -cyclohexenyl species, however, are not observed under any reactions conditions. This is consistent with Dzwiniel's observation that the treatment of the  $(C_5Me_5)Co(\eta^3\text{-cyclopentenyl})$  cation with acetylene also undergoes a very rapid insertion of the second alkyne and thus does not undergo cycloexpansion.

When the reaction is performed using acetylene-saturated dichloromethane and warmed from  $-78\text{ }^\circ\text{C}$  to ambient temperature overnight, the product ratio is approximately 1.5 : 1 in favour of the bicyclic product **42**. If, however, the reaction is warmed to ambient temperature more slowly in stages over several days, the bicyclic complex **42** is preferentially formed in a 10 : 1 ratio (Scheme 2-15). Conversely, when the reaction is performed using

dichloromethane that had been quickly sparged with acetylene, the  $\eta^2, \eta^3$ -vinylcyclohexenyl complex **43** is preferentially formed in a 10 : 1 ratio (Scheme 2-15). These observations establish that coordination and insertion of the second equivalent of acetylene is kinetically competitive with cyclization.

**Scheme 2-15**



Conditions	Ratio (42 : 43)	Yields
-78 °C, 24 h		
-78 °C → -50 °C, 48 h	10 : 1	64%
-50 °C → -30 °C, 4 h		
-78 °C → RT, 3 h	1 : 10	94%

Bicyclic [4.3.1]  $\eta^1, \eta^4$ -cycloheptadienyl complex **42** is markedly more stable at ambient temperature, compared to the bicyclic [4.2.1] product **36** formed from the reaction of  $(\text{C}_5\text{Me}_5)\text{Co}(\eta^3\text{-cyclopentenyl})$  cation with acetylene observed by Dzwiniel. The reactivity of the latter is thus due to the more constrained bicyclic framework imposed by the two-carbon linkage. The addition of an extra methylene unit to this linkage in **42** decreases the ring strain

in the bicyclic complex as compared to **36**. Both  $\eta^1, \eta^4$ -bicyclic products **36** and **42** possess bridgehead hydrogens that are not amenable to  $\beta$ -hydride elimination, preventing isomerization to a fully conjugated bicyclic  $\eta^5$ -cycloheptadienyl product.

The presence of the endocyclic  $\eta^3$ -allyl moiety in the  $\eta^2, \eta^3$ -vinylcyclohexenyl complex **43** suggested that further incorporation of acetylene might be possible, depending on the lability of the bound  $\eta^2$ -olefin moiety. Treatment of the  $\eta^2, \eta^3$ -vinylcyclohexenyl complex **43** with acetylene in refluxing dichloromethane in a sealed reaction bomb resulted in no observable change. Heating the mixture at a higher temperature in dichloroethane resulted in a slight darkening of the solution mixture, but  $^1\text{H}$  NMR analysis of the residue indicated only broadened resonances from the starting material, strongly suggesting decomposition of the  $\eta^2, \eta^3$ -vinylcyclohexenyl complex **43** rather than alkyne insertion. However, ultraviolet irradiation of a solution of vinylcyclohexenyl complex **43** and acetylene resulted in the quick decomposition of the starting material to a paramagnetic residue. These observations strongly suggest that the  $\eta^2$ -olefin is bound very tightly to the cobalt centre and resists dissociation under forcing thermal conditions. Most likely the chelating nature and rigidity of the bound  $\eta^2$ -olefin moiety allows for efficient re-coordination after dissociation. Under ultraviolet irradiation, however, the rapid decomposition of the starting material to an unknown paramagnetic residue suggests the formation of a paramagnetic cobalt(II) complex. A reasonable route

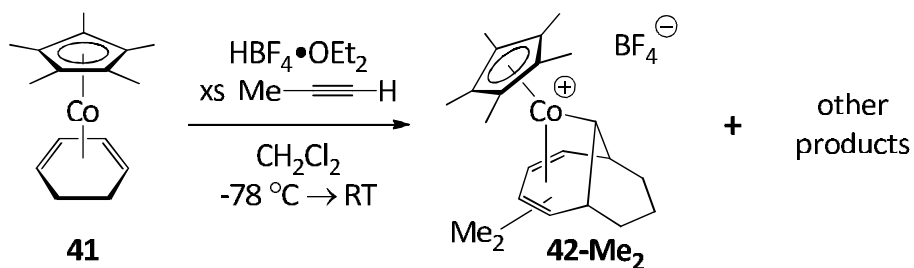
to a paramagnetic cobalt(II) complex would occur via isomerization of the bound  $\eta^3$ -cyclohexenyl unit to an unsaturated  $\eta^1$ -cyclohexenyl moiety, followed by metal-carbon bond homolysis to arrive at a paramagnetic  $17e^-$  cobalt(II) complex, though no evidence exists for such a mechanism.

While the addition of acetylene to the cobalt  $\eta^3$ -cyclohexenyl cation **44** resulted in single and double insertion products, the addition of 2-butyne to the cobalt  $\eta^3$ -cyclohexenyl complex **44** afforded only an intractable paramagnetic residue. This result is surprising since the treatment of the related  $(C_5Me_5)Co(cyclopentenyl)$  cation with 2-butyne leads to a two-carbon ring-expansion of the five-membered ring to form the  $\eta^5$ -cycloheptadienyl product (Scheme 2-11).<sup>131</sup> Neither the two-carbon expansion of the  $\eta^3$ -cyclohexenyl unit nor products arising from single and double 2-butyne insertion have been observed.

The  $\eta^3$ -cyclohexenyl cation **44** was also treated with various other mono- and disubstituted alkynes. Treatment of cation **44** with excess propyne resulted in a complex oily mixture consisting of multiple inseparable products as demonstrated by  $^1H$  NMR spectroscopy. Furthermore, broadened resonances in the  $^1H$  NMR spectrum indicate a small amount of a persistent paramagnetic impurity is present. However, an electrospray mass spectrum of the product reveals the formation of at least two cobalt-containing products, one arising from the incorporation of two equivalents of alkyne (**42-Me<sub>2</sub>**), and a second product arising from the incorporation of three equivalents of alkyne (Equation

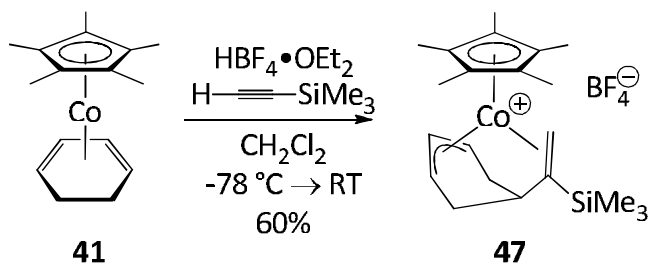
2-12). No evidence for either the single insertion product or ring-expansion was observed.

**Equation 2-12**



In contrast, the reaction of the  $\eta^3$ -cyclohexenyl complex **44**, formed *in situ* by protonation of cyclohexadiene complex **41**, with excess trimethylsilylacetylene at low temperature yielded only one product (**47**) in moderate yield after purification by flash chromatography (Equation 2-13).

**Equation 2-13**



The isolated product contains an  $\eta^2, \eta^3$ -vinylcyclohexenyl moiety similar to cobalt vinylcyclohexenyl complex **43** (*vide supra*), where the trimethylsilyl moiety

resides on the interior olefinic carbon. Relevant  $^1\text{H}$  and  $^{13}\text{C}$  NMR spectroscopic data of the vinylcyclohexenyl silyl cation complex **47** are summarized in Figure 2-8 and Table 2-3.

**Figure 2-8:**  $^1\text{H}$  and  $^{13}\text{C}$  Numbering System for Cobalt Cyclohexenyl Silyl Cation **47**

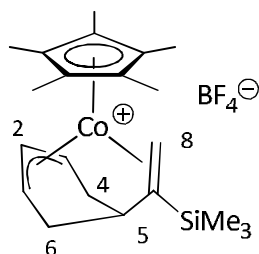


**Table 2-3:** NMR Spectroscopic Data for Cobalt Cyclohexenyl Silyl Cation **47**

Position	$\delta$ $^1\text{H}$	$\delta$ $^{13}\text{C}$
1	5.55 (d, $J = 6.0$ Hz)	82.0
2	4.19 (t, $J = 6.0$ Hz)	90.0
3	4.70 (t, $J = 5.6$ Hz)	83.0
4	H <sub>4a</sub> : 1.18 (d, $J = 16.0$ Hz) H <sub>4b</sub> : 0.4 (d, $J = 16.0$ Hz)	23.8
5	1.60 (obscured by C <sub>5</sub> Me <sub>5</sub> )	40.8
6	H <sub>6a</sub> : 2.37 (dt, $J = 14.4, 3.6$ Hz) H <sub>6b</sub> : 1.51 (d, $J = 14.4$ Hz)	38.8
7		121.7
8	H <sub>8a</sub> : 5.04 (s); H <sub>8b</sub> : 4.09 (s)	82.0
Si(CH <sub>3</sub> ) <sub>3</sub>	0.34 (s)	2.2
C <sub>5</sub> (CH <sub>3</sub> ) <sub>5</sub>	1.66 (s)	10.2
C <sub>5</sub> (CH <sub>3</sub> ) <sub>5</sub>		100.1

Compared to the parent  $\eta^2,\eta^3$ -vinylcyclohexenyl complex **43**, the silyl analogue possesses similar  $^{13}\text{C}$  NMR chemical shifts. The olefinic carbon directly attached to the trimethylsilyl group is shifted downfield 20 ppm compared to the parent system and the difference in chemical shift between the olefinic carbons is increased. Both olefinic carbons are shifted slightly upfield with respect to free vinyltrimethylsilane ( $\delta$  140.3, 130.9 ppm), suggesting limited backbonding from the electrophilic cobalt centre.

Although the spectroscopic data support the structure of **47** and are similar to the data obtained for the parent  $\eta^2,\eta^3$ -vinylcyclohexenyl complex **43**, suitable crystals for X-ray diffraction analysis were grown from a mixture of dichloromethane and diethyl ether (Figure 2-9). Like the parent  $\eta^2,\eta^3$ -vinylcyclohexenyl complex **43**, the bond distance between the cobalt and the terminal olefinic carbon is  $\sim 0.1$  Å longer than the distance between cobalt and the interior olefinic carbon (2.222 Å compared to 2.133 Å).

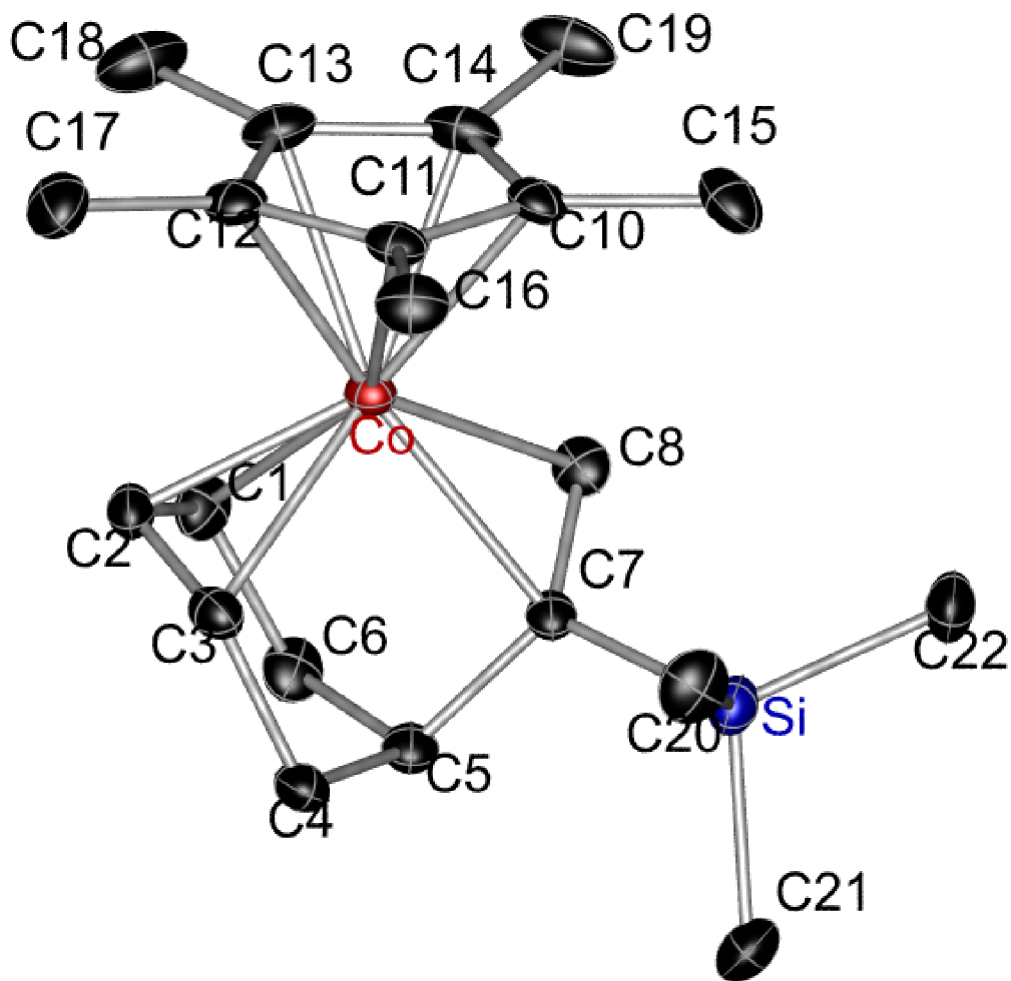
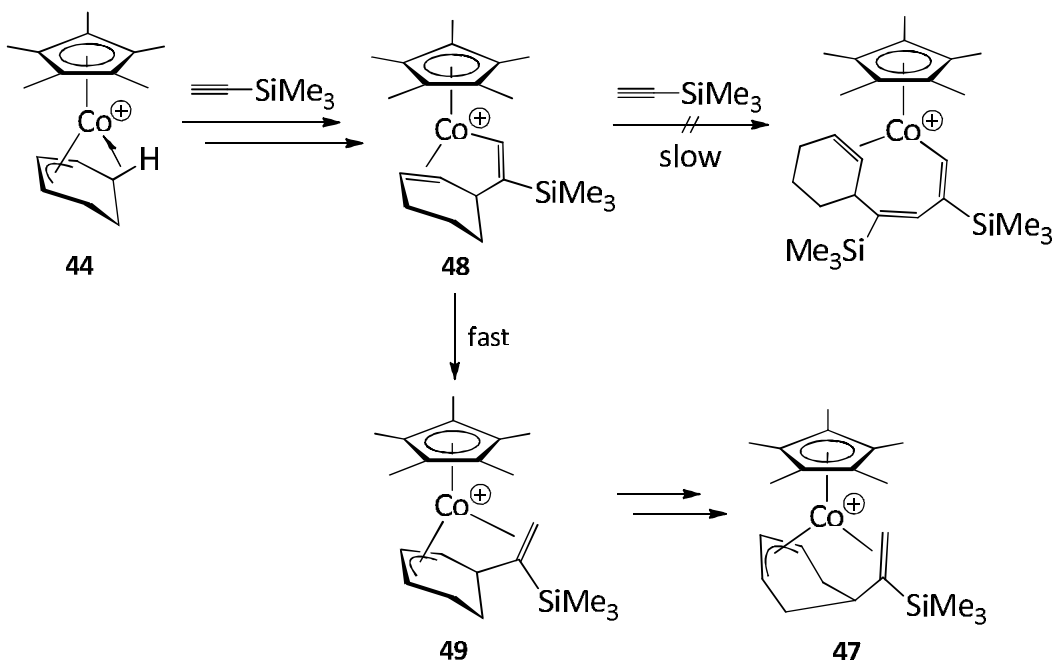


**Figure 2-9:** Perspective view of  $[(C_5Me_5)Co(\eta^3,\eta^2-5-(1-$   
 trimethylsilylvinyl)cyclohex-2-en-1-yl)] cation **47**. Final residuals:  $R_1 = 0.0461$ ;  
 $wR_2 = 0.1267$ . Data collected at  $-80\text{ }^\circ\text{C}$ . Non-hydrogen atoms are represented by  
 Gaussian ellipsoids at the 20% probability level. Hydrogen atoms have been  
 omitted. Selected bond distances ( $\text{\AA}$ ): C1-C2, 1.391(7); C1-C6, 1.494(7); C2-C3,  
 1.404(7); C3-C4, 1.527(6); C4-C5, 1.521(6); C5-C6, 1.535(6); C5-C7, 1.518(6); C7-  
 C8, 1.374(6); Co-C1, 2.168(4); Co-C2, 2.024(4); Co-C3, 2.146(4); Co-C7, 2.222(4);  
 Co-C8, 2.133(4); C7-Si, 1.902(4). The dihedral angle between the planes defined  
 by C1-C3 and C10-C14:  $31.9(3)^\circ$ .

The proposed mechanism for the formation of **47** is consistent with that discussed for the formation of the parent vinylcyclohexenyl complex **43** (Scheme 2-16).

**Scheme 2-16**



The coordination and regioselective migratory insertion of trimethylsilylacetylene to the  $\eta^3$ -cyclohexenyl complex **44** forms the vinylcyclohexene complex **48**. Coordination and irreversible migratory insertion of the trimethylsilylacetylene in an orientation such that the silyl group is located on the  $\alpha$ -vinyl carbon is not observed, possibly due to steric interactions between the trimethylsilyl group and the pentamethylcyclopentadienyl ancillary ligand. Upon formation of the vinylcyclohexene complex **48**, two possible

pathways are available. The formation of a single insertion product suggests that coordination and migratory insertion of a second equivalent of trimethylsilylacetylene to form a polyenyl complex is disfavoured, possibly due to steric interactions between the incoming alkyne and the metal-vinyl moiety. Allylic carbon-hydrogen bond activation and hydride migration to the metal-vinyl moiety affords the  $\eta^2, \eta^3$ -vinylcyclohexenyl complex **49**, which subsequently rearranges to form the observed product **47**.

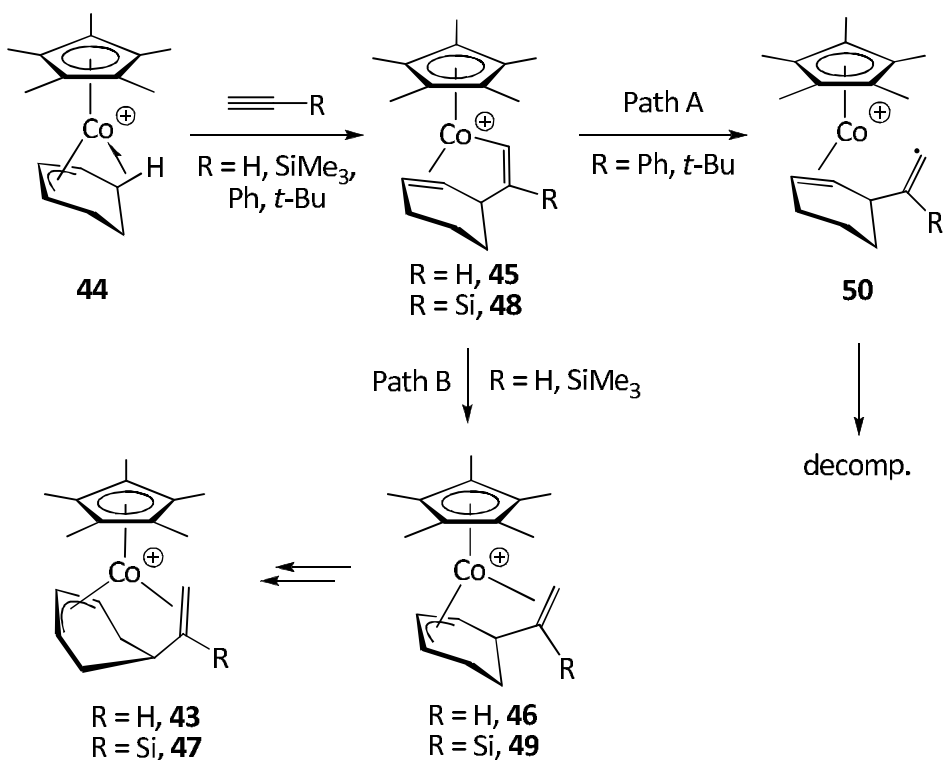
Similar to the parent complex, isomerization of the *endo*-cyclic  $\eta^3$ -allyl moiety to a position one carbon further away from the vinyl group is observed. No evidence for the ring-expansion of the six-membered ring is observed, consistent with results obtained using acetylene.

Other terminally substituted alkynes, when treated with the  $\eta^3$ -cyclohexenyl cation **44**, do not react similarly to either acetylene or trimethylsilylacetylene. Treatment of **44** with either *tert*-butylacetylene or phenylacetylene affords intractable paramagnetic residues. This is quite surprising considering that the impact of the steric bulk of both the *tert*-butyl and phenyl substituents on the alkyne was expected to be comparable to that of the trimethylsilyl substituent.

The formation of paramagnetic residues from the treatment of the agostic  $\eta^3$ -cyclohexenyl complex **44** with larger monosubstituted alkynes may arise from metal-carbon bond homolysis from an intermediate after the initial

coordination and insertion of one equivalent of alkyne, which would produce cobalt(II)-containing complexes (Scheme 2-17).

**Scheme 2-17**



Treatment of the  $\eta^3$ -cyclohexenyl cation **44** with phenylacetylene, *tert*-butylacetylene or trimethylsilylacetylene would be expected to produce a vinyl-cyclohexene complex. At this juncture, two possible pathways exist. Metal-carbon bond homolysis of the vinyl-cyclohexene complex would produce a vinyl radical complex **50** (Path A). Dissociation of the organic radical fragment would, in turn, generate a paramagnetic cobalt(II) complex. However,  $\text{sp}^2$  carbon-metal bonds are generally stronger than  $\text{sp}^3$  carbon-metal bonds by approximately 10

kcal/mol, suggesting that bond homolysis may be promoted by other unknown factors.<sup>138</sup>

Alternatively, allylic carbon-hydrogen bond activation and isomerization would produce the  $\eta^2,\eta^3$ -vinylcyclohexenyl complex which rearranges to the observed product, as in the case when trimethylsilylacetylene and acetylene are used (Path B). Presumably, allylic carbon-hydrogen bond activation is faster than metal-vinyl bond homolysis, which results in the observed  $\eta^2,\eta^3$ -vinylcyclohexenyl product.

The lack of general reactivity displayed by phenylacetylene and *tert*-butylacetylene can be rationalized by the stability of the intermediate vinyl-cyclohexene complex **45** or **48**. Acetylene, due to its small size, reacts quickest with the agostic  $\eta^3$ -cyclohexenyl complex **44** to afford, ultimately, the observed  $\eta^2,\eta^3$ -vinylcyclohexenyl product **43**. When trimethylsilylacetylene is used, the trimethylsilyl group most likely stabilizes the vinyl-cyclohexene intermediate **48** via hyperconjugation of a silicon-carbon  $\sigma$ -bond to the cobalt centre and prevents metal-vinyl bond homolysis. The stabilization of carbocations by the hyperconjugation of adjacent silicon-carbon bonds is well known and has been studied in detail.<sup>139, 140</sup> In contrast, neither the *tert*-butyl nor phenyl substituents can stabilize the intermediate vinyl-cyclohexene and metal-vinyl bond homolysis becomes more favourable and, ultimately, affords paramagnetic decomposition products.

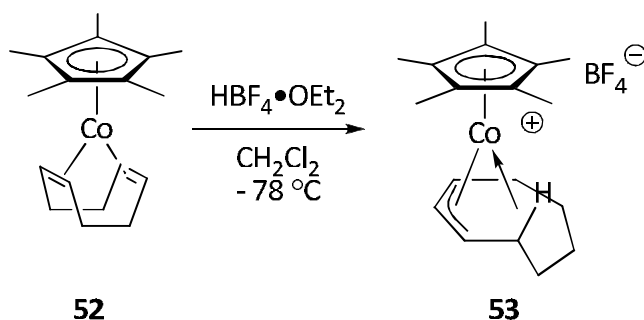
## B. Reactions of (C<sub>5</sub>Me<sub>5</sub>)Cobalt $\eta^3$ -Cycloheptenyl and $\eta^3$ -Cyclooctenyl Complexes with Alkynes

Preparation of (C<sub>5</sub>Me<sub>5</sub>)Co( $\eta^4$ -cycloheptadiene) **51** and (C<sub>5</sub>Me<sub>5</sub>)Co( $\eta^4$ -cyclooctadiene) **52** was done in an analogous fashion to the preparation of (C<sub>5</sub>Me<sub>5</sub>)Co( $\eta^4$ -cyclohexadiene); namely, sodium amalgam reduction of a THF solution of chlorocobalt dimer **40** and diene.<sup>121, 141, 142</sup> Both compounds possess <sup>1</sup>H and <sup>13</sup>C NMR spectra consistent with the published data. Crystals of the  $\eta^4$ -cycloheptadiene complex **51** suitable for X-ray diffraction analysis were obtained by crystallization from a pentane solution (Figure 2-10).



The protonation of the  $\eta^4$ -cyclooctadiene complex **52** furnishes the known agostic  $\eta^3$ -cyclooctenyl complex **53**, which had been extensively characterized by Spencer using low temperature NMR spectroscopy (Equation 2-14).<sup>121</sup> While the protonation of the  $\eta^4$ -cycloheptadiene complex **51** has not been reported, a  $\eta^3$ -cycloheptenyl complex consistent with the  $\eta^3$ -cyclooctenyl congener **53** would be expected.

**Equation 2-14**

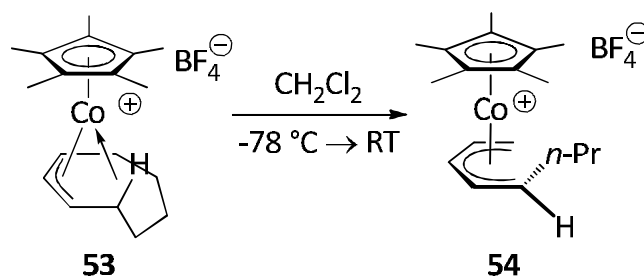


We had envisioned that the addition of alkyne to the agostic  $\eta^3$ -cycloheptenyl or  $\eta^3$ -cyclooctenyl complexes should afford either two-carbon ring-expanded products, as demonstrated with the  $\eta^3$ -cyclopentenyl series (*vide supra*) or single and double alkyne insertion products, as demonstrated with the  $\eta^3$ -cyclohexenyl series (*vide supra*).

However, there are other possible reaction pathways. Spencer has reported that warming of the  $\eta^3$ -cyclooctenyl complex **53** to ambient temperature leads to ring opening of the organic fragment, affording the acyclic

$\eta^5$ -*anti*-1-propylpentadienyl complex **54** (Equation 2-15).<sup>121</sup> Previous work in this group has demonstrated that the addition of a range of alkynes to terminally substituted acyclic  $\eta^5$ -pentadienyl cobalt complexes affords seven-membered ring products from [5 + 2] pentadienyl-alkyne cycloaddition reactions.<sup>122</sup> However, Dzwiniel has demonstrated that the addition of 2-butyne to the  $\eta^5$ -1-*anti*-propylpentadienyl complex **54** yields a mixture of unidentified products, none of which were indicative of  $\eta^5$ -cycloheptadienyl complexes.<sup>116</sup>

#### Equation 2-15



Therefore, the addition of alkyne to either the  $\eta^3$ -cycloheptenyl complex or the  $\eta^3$ -cyclooctenyl complex would be expected to afford i) nine- and ten-membered ring products, respectively, from a two-carbon ring-expansion or ii) single or double alkyne insertion products. With respect to the  $\eta^3$ -cyclooctenyl complex **53**, the reaction could additionally afford i) the  $\eta^5$ -1-propylpentadienyl complex **54** if there is no reaction with alkyne or ii) a seven-membered ring product from the [5 + 2] pentadienyl-alkyne cycloaddition reaction of the  $\eta^5$ -1-propylpentadienyl complex **54** with alkyne.

Unfortunately, treatment of the agostic  $\eta^3$ -cyclooctenyl complex **53** with acetylene or 2-butyne afforded an uncharacterizable paramagnetic residue. Similarly, treatment of the agostic  $\eta^3$ -cycloheptenyl complex with acetylene or 2-butyne also affords an uncharacterizable paramagnetic residue. These two findings suggest that decomposition to a paramagnetic residue is more favourable than either ring-expansion or alkyne insertion.

### C. Conclusions

While the reactions of mono- and disubstituted alkynes with the  $(C_5Me_5)Co(\eta^3\text{-cyclopentenyl})$  cation furnish  $\eta^5$ -cycloheptadienyl products via a two-carbon ring-expansion process, the same results are not obtained for reactions of larger endocyclic cobalt  $\eta^3$ -allyl complexes.

The addition of acetylene to the  $(C_5Me_5)Co(\eta^3\text{-cyclohexenyl})$  cation results in a mixture of two products: an  $\eta^1,\eta^4$ -bicyclic complex from the insertion of two equivalents of acetylene, and an  $\eta^2,\eta^3$ -vinylcyclohexenyl complex from the insertion of one equivalent of acetylene. The mechanism for the formation of both products is consistent with the previously proposed mechanism for [3 + 2] allyl-alkyne cycloaddition. When the  $\eta^3$ -cyclohexenyl cation is treated with substituted terminal alkynes, such as propyne, a mixture of regioisomers is observed in both single and double insertion manifolds. Larger terminally

substituted alkynes such as phenylacetylene and *tert*-butylacetylene fail to give characterizable products when treated with the  $\eta^3$ -cyclohexenyl cation whereas trimethylsilylacetylene does, giving a single  $\eta^2, \eta^3$ -vinylcyclohexenyl complex. Furthermore, disubstituted alkynes, such as 2-butyne, failed to give tractable products. In all cases where alkynes does react with the  $\eta^3$ -cyclohexenyl cation to produce isolable complexes, products arising from a two-carbon ring-expansion are, unfortunately, not observed.

Larger cyclic diene complexes of cobalt were prepared and protonated, affording the corresponding cationic endocyclic  $\eta^3$ -allyl intermediates. However, once the resulting  $\eta^3$ -cycloheptenyl and  $\eta^3$ -cyclooctenyl complexes were treated with alkyne, intractable paramagnetic mixtures were obtained.

The unusual two-carbon ring-expansion observed in the  $C_5Me_5$ -supported  $\eta^3$ -cyclopentenyl series is not observed when the larger  $\eta^3$ -cyclohexenyl,  $\eta^3$ -cycloheptenyl, and  $\eta^3$ -cyclooctenyl complexes are used. This suggests that the structure and conformation of the cyclic organic moiety is of paramount importance to mediate ring-expansion. The smaller five-membered ring template supports both cycloaddition and cycloexpansion reactions, compared to the six-membered template which only undergoes alkyne cycloaddition reactions. Neither the seven- nor eight-membered templates react in either fashion and, instead, produce paramagnetic residues. It is possible that the modest degree of ring strain inherent in the  $\eta^3$ -cyclopentenyl species is requisite

for cycloexpansion reactions, whereas the larger endocyclic  $\eta^3$ -allyl systems adopt more relaxed conformations and less conducive to cycloexpansion.

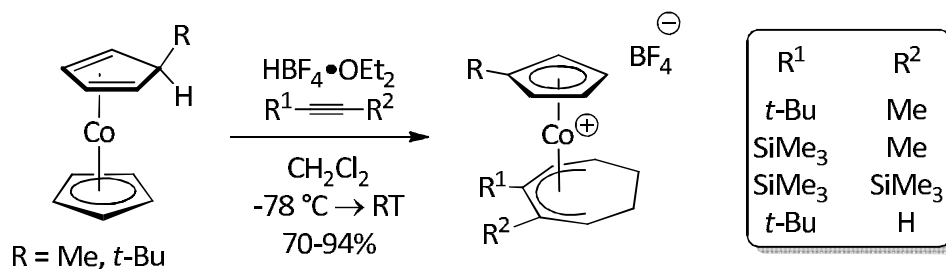
It is possible that the lack of coherent reactivity of the larger cycloalkenyl systems with alkynes is due to the large steric profile of the pentamethylcyclopentadienyl ligand. A more detailed discussion of an alternative substituted cyclopentadienyl ancillary ligand is found in Chapter 3. A more detailed study of this cycloexpansion process via carbon-carbon bond activation is discussed in Chapter 4.

## Chapter 3. 1,3-Di-*tert*-butylcyclopentadienyl Cobalt Complexes

### Section 1. Introduction

As discussed in the previous chapter, Dzwiniel extensively studied the two-carbon ring-expansion of cationic agostic  $(C_5Me_5)Co(\eta^3\text{-cyclopentenyl})$  complexes with mono- and disubstituted alkynes.<sup>131</sup> However, treatment of cobalt  $\eta^3\text{-cyclopentenyl}$  complexes with larger disubstituted alkynes afforded ring-expanded products only in poor to moderate yields. Dzwiniel has shown, however, that smaller cyclopentadienyl systems, such as the methylcyclopentadienyl and *tert*-butylcyclopentadienyl templates, can promote the two-carbon cycloexpansion of the  $\eta^3\text{-cyclopentenyl}$  ligand using larger disubstituted alkynes which would not normally proceed when using the pentamethylcyclopentadienyl ancillary ligand (Equation 3-1).

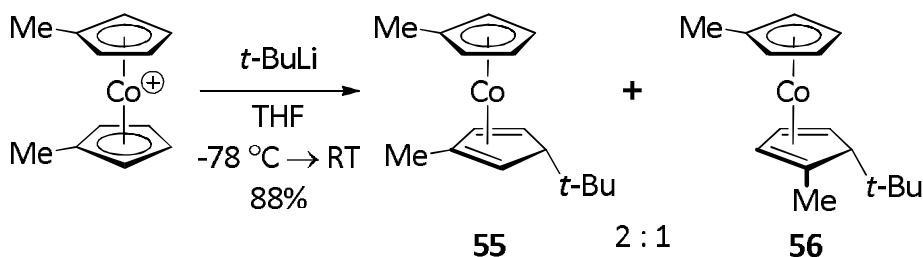
Equation 3-1



The two-carbon ring-expansion of  $\eta^3$ -cyclopentenyl complexes has also been studied by Dzwiniel using the disubstituted *tert*-butyl-methylcyclopentadienyl template. The synthesis of mixtures of the two regioisomeric (*tert*-butyl-methyl)cyclopentadienyl cobalt complexes was accomplished by two different methods: treatment of the  $(\text{MeC}_5\text{H}_4)_2\text{Co}$  cation with *tert*-butyllithium, and treatment of the  $(t\text{-BuC}_5\text{H}_4)_2\text{Co}$  cation with methylithium.<sup>143</sup>

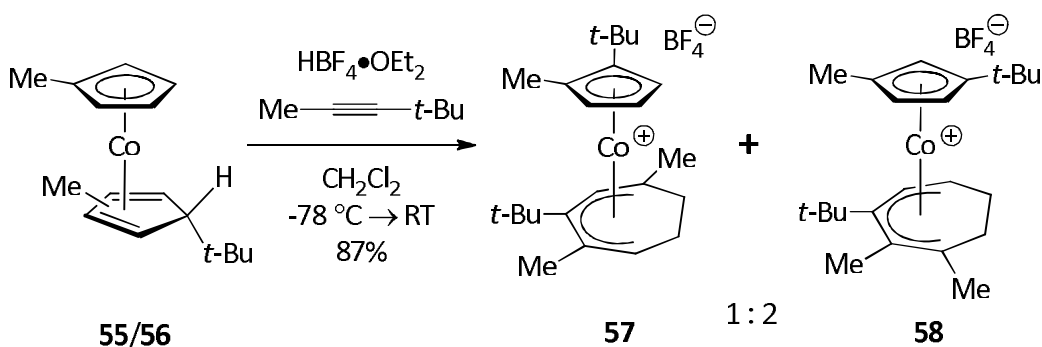
Treatment of  $[(\text{MeC}_5\text{H}_4)_2\text{Co}]\text{PF}_6$ <sup>144, 145</sup> with *tert*-butyllithium produces both the 1,3- (**55**) and 1,2-disubstituted (**56**) cobalt complexes in a 2 : 1 ratio favouring the 1,3-substitution pattern (Equation 3-2). This ratio suggests that the methyl group does not sufficiently block the sites adjacent to it during the addition of the *tert*-butyl anion to control the site of nucleophilic addition. The separation and isolation of the pure compounds proved difficult; the entire mixture was used during a preliminary investigation of subsequent ring-expansion reactions.

**Equation 3-2**



Despite the mixture, Dzwiniel demonstrated that the *tert*-butyl-methylcyclopentadienyl template shows a wider tolerance of functional groups on alkynes than the  $C_5Me_5$  analogue. Typically when the mixture of methylcyclopentadienyl complexes **55** and **56** are used, both templates react independently with alkyne to produce isomeric  $\eta^5$ -cycloheptadienyl products from activation of the monosubstituted ring. A representative example of this divergent pathway is the treatment of a mixture of **55** and **56** with  $HBF_4 \cdot OEt_2$  and 4,4-dimethyl-2-pentyne, which yields two  $\eta^5$ -cycloheptadienyl products (Equation 3-3).

**Equation 3-3**

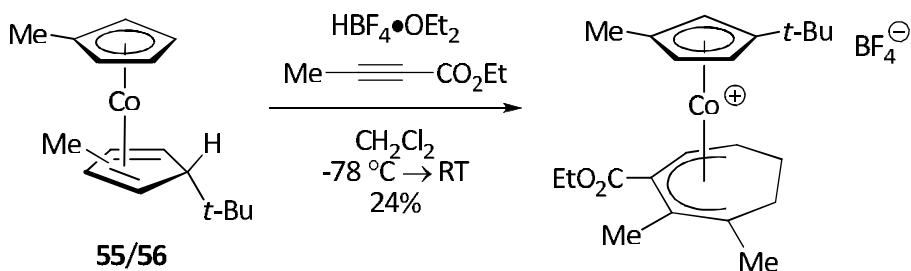


The 1,2-disubstituted template appears to react with the pentyne to form only the 1,3,4-trisubstituted  $\eta^5$ -cycloheptadienyl product **57**, whereas the 1,3-disubstituted template reacts with the pentyne to form only the 3,4,5-trisubstituted  $\eta^5$ -cycloheptadienyl product **58**, as assigned by NMR spectroscopic analysis. The 1,3-disubstituted cyclopentadienyl-containing compound is the

major product in this reaction; the ratio of products reflects the ratio of the starting material.

Electron deficient alkynes are surprisingly tolerated in the ring-expansion. Ethyl 2-butynoate, when treated with a mixture of **55** and **56** and strong acid, leads to a single product in poor yield (Equation 3-4).

**Equation 3-4**



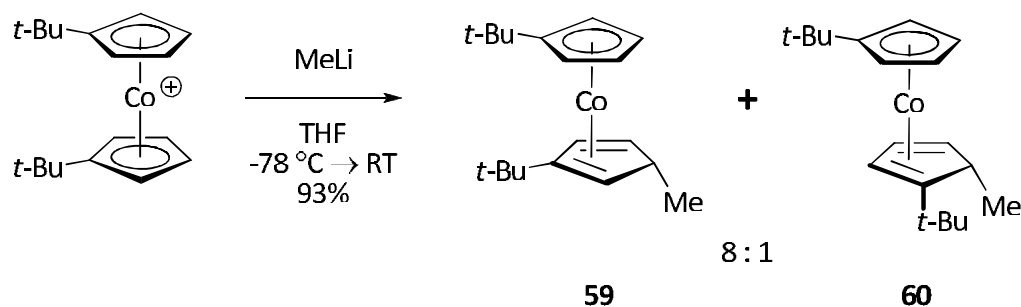
In contrast, electron-deficient alkynes do not react at all with the agostic  $(C_5Me_5)Co(\eta^3\text{-cyclopentenyl})$  cation to afford ring-expanded products. Furthermore, the isolated product possesses the 1,3-disubstituted cyclopentadienyl template; no evidence for any 1,2-disubstituted cyclopentadienyl product was found.

In all cases where the mixture of **55** and **56** were treated with  $HBF_4 \cdot OEt_2$  and alkynes, the least-substituted five-membered ring undergoes cycloexpansion; no evidence for ring expansion of the 1,2- or 1,3-disubstituted cyclopentadienyl ligand is observed in this series. This is consistent with

Dzwiniel's earlier findings in mixed cobaltocene systems, where the least substituted  $\eta^3$ -cyclopentenyl ligand preferentially undergoes cycloexpansion.

Other unsymmetrical cobaltocenes can also be prepared in a similar manner. The addition of methyllithium to  $[(t\text{-BuC}_5\text{H}_4)_2\text{Co}]\text{PF}_6$ <sup>144, 145</sup> generates two products (**59** and **60**), with the 1,3-disubstituted compound again being the major product (Equation 3-5).

**Equation 3-5**



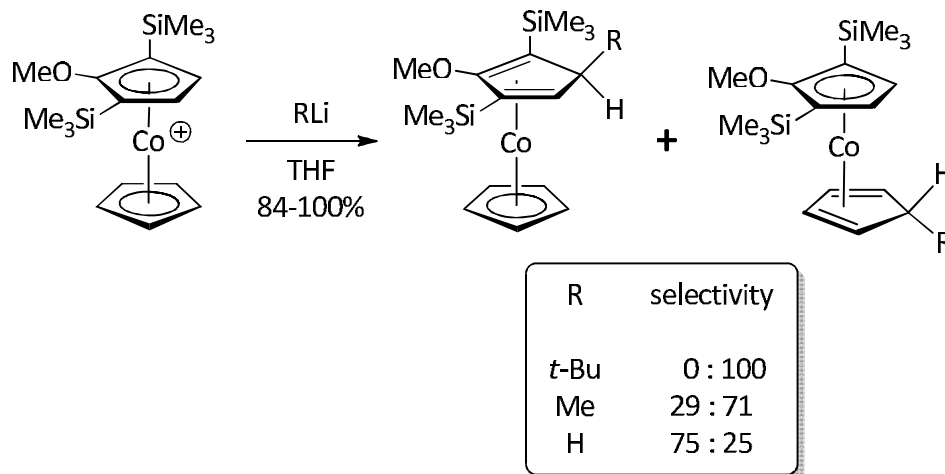
The steric bulk of the *tert*-butyl group forces the addition of the methyl anion away from the *tert*-butyl group and results in an 8 : 1 ratio favouring the 1,3-substitution pattern. Again, the separation of the two products proved difficult and the entire mixture was used in subsequent reactions.

However, treatment of this mixture with strong acid and alkyne yields inseparable mixtures of isomeric seven-membered ring products. The full assignment of the signals in the <sup>1</sup>H NMR spectrum proved difficult and the complexes remain largely uncharacterized. While the identity of the product mixture remains unknown, the most likely assessment is that the two major

products are substitutional isomers of a  $\eta^5$ -*tert*-butylcycloheptadienyl organic fragment. Furthermore, the possibility of products arising from ring opening of both mono- and disubstituted cyclopentadiene ligands cannot be excluded. Additionally, the minor components in the reaction mixture can be attributed to the reaction of the minor isomer with strong acid and alkyne. This suggests that the reaction of **59** and **60** with strong acid and alkyne is neither selective for the least substituted cyclopentadiene ring, nor is it regioselective in the orientation of the alkyne.

Based upon the promising results obtained by Dzwiniel pertaining to the (1-*tert*-butyl-3-methyl)cyclopentadienyl template, further investigation into the use of disubstituted cyclopentadienyl templates was proposed. However, several limitations are inherent to the procedures that Dzwiniel employed. The addition of *tert*-butyllithium or methyllithium to a 1,1'-disubstituted cobalticenium cation produces both 1,2- and 1,3-disubstituted cyclopentadienyl cobalt complexes in varying ratios. Vollhardt has extensively studied the various steric and electronic effects on the addition of alkyllithium reagents to substituted cobalticenium complexes (Equation 3-6).<sup>146</sup> Except in situations where a large steric barrier to the addition exists, mixtures of isomeric addition products are always obtained.<sup>147-151</sup>

### Equation 3-6



Another limitation to this procedure lies in the target cyclopentadiene ligand: mixed cobaltocene complexes possessing an unsubstituted cyclopentadiene ligand cannot be prepared by the addition of alkyllithium reagents to 1,1'-disubstituted cobalticenium salts.

An alternative strategy to overcome these proposed limitations consists of an independently generated cyclopentadienide anion, followed by treatment with a suitable electrophilic cobalt precursor already bearing one cyclopentadienyl ligand. This strategy should allow a library of mixed cobaltocenium complexes to be prepared in a highly selective manner, raising the possibility of conducting a comprehensive optimization and generalization of the ring-expansion process.

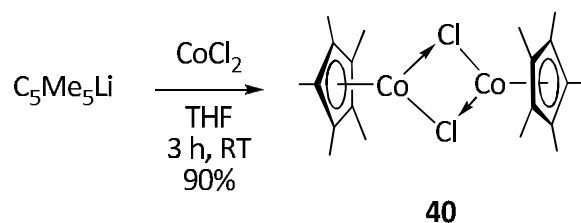
Of the possible choices for a disubstituted cyclopentadienyl ligand, the 1,3-di-*tert*-butylcyclopentadienyl ligand was selected due to its relatively facile

preparation and steric bulk, which would be slightly larger than the (1-*tert*-butyl-3-methyl)cyclopentadienyl moiety discussed earlier. We envisioned that the reactivity of the 1,3-di-*tert*-butylcyclopentadienyl cobalt template would be similar to that of the (1-*tert*-butyl-3-methyl)cyclopentadienyl. The independent preparation of the 1,3-di-*tert*-butylcyclopentadienide anion, followed by treatment with an electrophilic cobalt precursor, should provide an easy entry to the 1,3-di-*tert*-butylcyclopentadienyl cobalt series.

#### A. Synthetic Routes to Cobaltocene Complexes

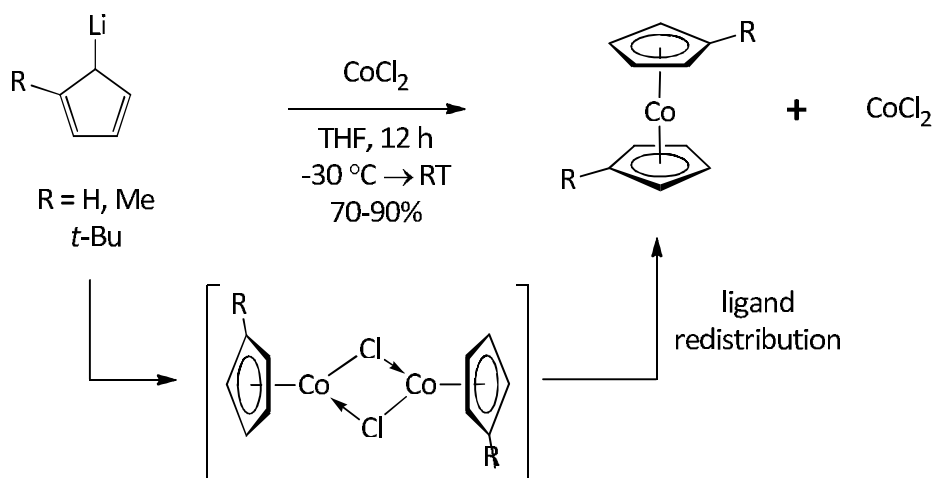
Surprisingly few methods exist for the synthesis of unsymmetrically disubstituted cobaltocene or cobalticinium complexes. Symmetrical cobaltocene complexes are prepared in a straightforward manner by the addition of two equivalents of a cyclopentadienide anion to an electrophilic cobalt precursor, such as cobalt(II) chloride. However, this method is inadequate when preparing unsymmetrical cobaltocene and cobalticinium complexes. The addition of a sterically bulky cyclopentadienide anion, such as  $C_5Me_5Li$ <sup>152-156</sup> or 1,3,4-tri-*tert*-butylcyclopentadienide,<sup>157-159</sup> to cobalt(II) chloride affords the desired half-sandwich cobalt halide complex in excellent yield (Equation 3-7).

### Equation 3-7



However, treatment of an unsubstituted or monosubstituted cyclopentadienide anion, such as  $MeC_5H_4Li$  or  $t-BuC_5H_4Li$ , with cobalt(II) chloride does not furnish the analogous dimeric species.<sup>143, 152</sup> The intermediate monosubstituted cyclopentadienyl cobalt chloride dimer is highly unstable and quickly undergoes ligand disproportionation to form the symmetrical cobaltocene and cobalt(II) chloride (Scheme 3-1).

### Scheme 3-1



Another synthetic strategy is ligand exchange of a disubstituted cyclopentadiene on a labile cyclopentadienyl cobalt complex such as  $(C_5H_5)Co(C_2H_4)_2$ . The required labile cyclopentadienyl cobalt precursor is not easily prepared, requiring sodium-mercury amalgam reduction in the case of  $[(C_5Me_5)CoCl]_2$ <sup>152</sup>, and potassium sand reduction in the case of  $(C_5H_5)_2Co$ .<sup>160-163</sup> Other than  $(C_5H_5)Co(C_2H_4)_2$  and  $(C_5Me_5)Co(C_2H_4)_2$ , no other isolable half-sandwich bis(ethylene) complexes of cobalt have been reported;  $(\eta^5\text{-indenyl})Co(C_2H_4)_2$  decomposes above  $-30\text{ }^\circ\text{C}$ .<sup>164</sup> Furthermore, the exchange of ethylene for added cyclopentadiene is not clean; Dzwiniel has demonstrated that in the  $C_5Me_5$  series, cyclopentadiene exchange does not proceed well thermally and affords a mixture of products photochemically.<sup>116</sup>

## B. Project Goals

While Dzwiniel has extensively studied the ring-expansion of substituted cyclopentadienes using the (1-*tert*-butyl-3-methyl)cyclopentadienyl cobalt template, the analogous unsubstituted cyclopentadiene ring-expansion has not been studied due to the paucity of synthetic methods necessary to prepare the corresponding starting materials. The independent preparation of the 1,3-di-*tert*-butylcyclopentadienide anion, followed by its ligation to cobalt, would allow

the preparation of a more diverse pool of unsymmetrical cobaltocene complexes and allow a better understanding of the scope of the ring-expansion process.

Furthermore, the reaction of 1,3-di-*tert*-butylcyclopentadienyl cobalt complexes possessing six-, seven-, and eight-membered cycloalkadiene rings can also be investigated. While none of the C<sub>5</sub>Me<sub>5</sub>-supported cobalt complexes possessing six-, seven- and eight-membered rings undergo the two-carbon ring-expansion with alkyne, it is hoped that this new cyclopentadienyl cobalt template might address this problem, or, at the very least, provide new insight into why the ring-expansion of larger cyclic dienes is problematic.

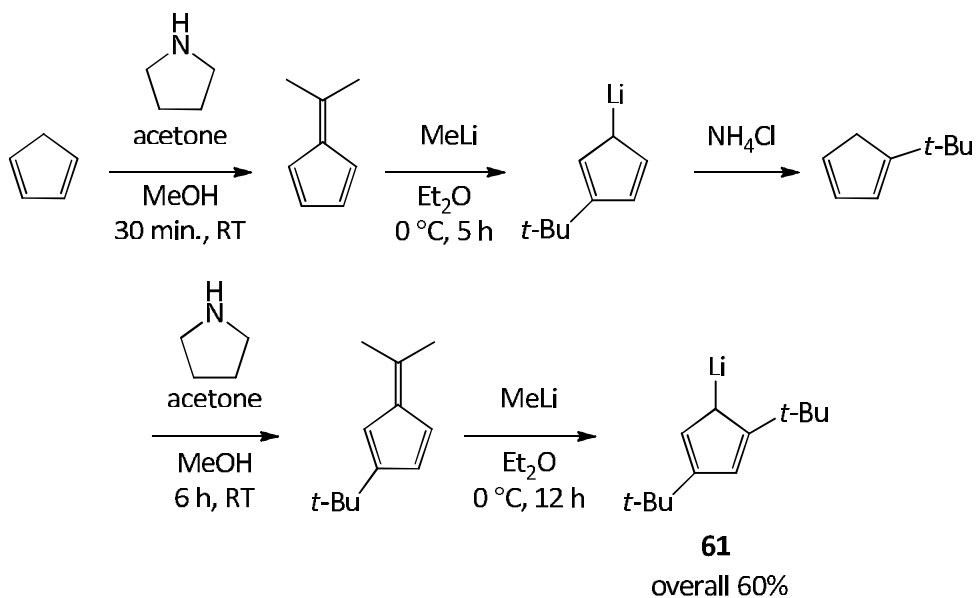
## Section 2. Results and Discussion

### A. Preparation of 1,3-Di-*tert*-butylcyclopentadienyl Cobalt Templates

#### 1,3-Di-*tert*-butylcyclopentadienyl Cobalt Precursors

The synthesis of the 1,3-di-*tert*-butylcyclopentadienide anion was performed according to literature procedures and in overall good yields (Scheme 3-2).<sup>165-167</sup>

Scheme 3-2

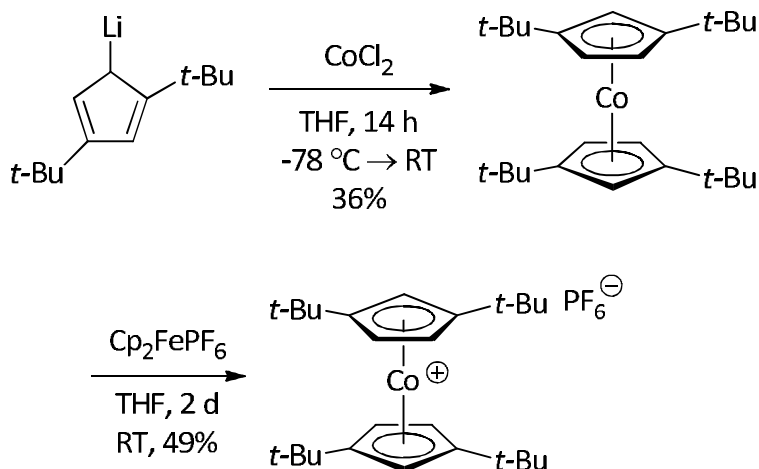


Monomeric cyclopentadiene was treated with acetone and pyrrolidine in methanol to afford 6,6-dimethylfulvene. The intense yellow liquid was subsequently treated with methyllithium to afford lithium *tert*-

butylcyclopentadienide, which was quenched with saturated ammonium chloride solution. This series of reactions was repeated to give lithium 1,3-di-*tert*-butylcyclopentadienide **61**.

With the desired cyclopentadienide anion in hand, the addition to a cobalt precursor was investigated. Treatment of one equivalent of 1,3-di-*tert*-butylcyclopentadienide anion **61** to cobalt(II) chloride at low temperature does not afford the dimeric  $[(t\text{-Bu}_2\text{C}_5\text{H}_3)\text{CoCl}]_2$ , but the symmetrical cobaltocene ( $t\text{-Bu}_2\text{C}_5\text{H}_3$ )<sub>2</sub>Co **62** (Scheme 3-3). The symmetrical cobaltocene **62** was detected by mass spectrometry, but isolated as the cationic cobalt(III) derivative **63** by treatment with ferrocenium hexafluorophosphate and characterized by <sup>1</sup>H NMR spectroscopy and X-ray crystallographic analysis (Figure 3-1). Cobalticinium complex **63** exists as a single rotamer in solution, as demonstrated by NMR spectroscopy, despite the large *tert*-butyl substituents which might hinder rotation.

**Scheme 3-3**



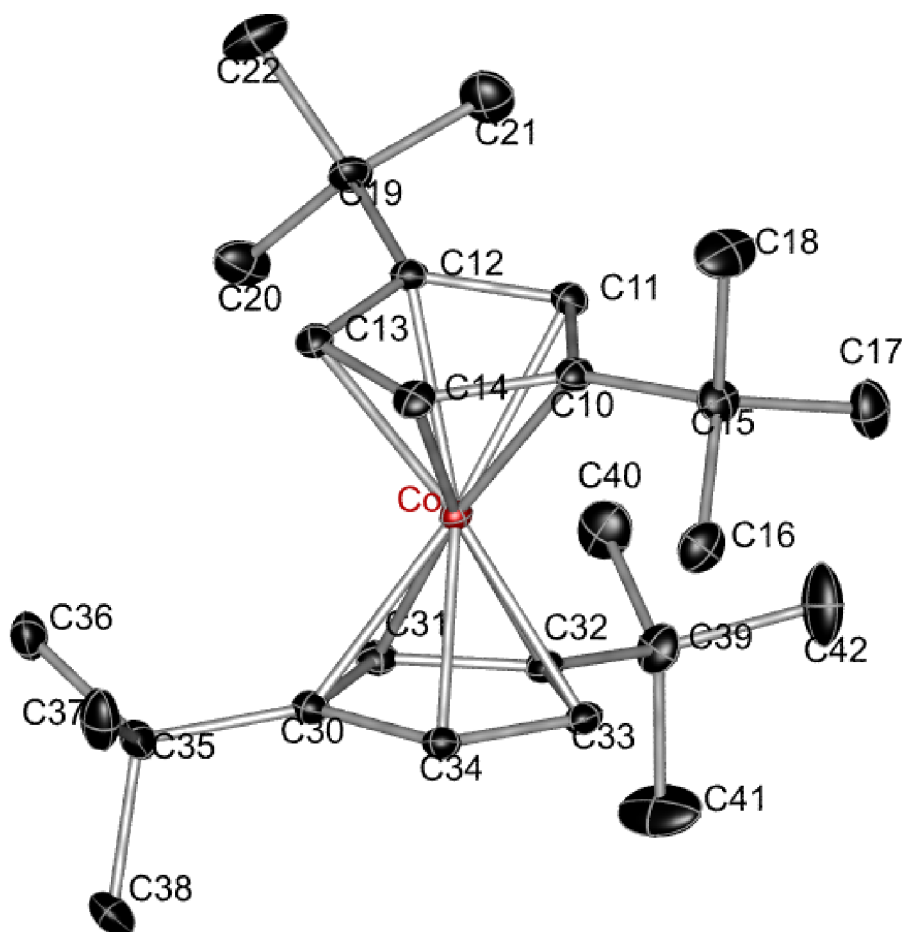
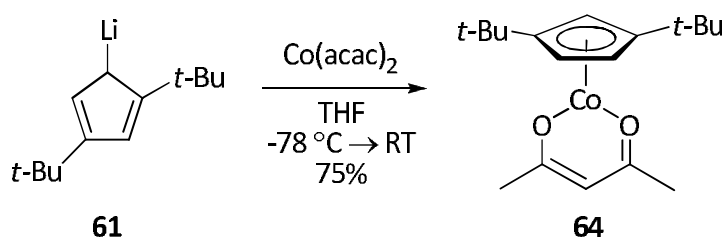


**Figure 3-1:** Perspective view of the  $[(t\text{-Bu}_2\text{C}_5\text{H}_3)_2\text{Co}]$  cation **63**. Final residuals:  $R_1 = 0.0320$ ;  $wR_2 = 0.0846$ . Data collected at  $-100\text{ }^\circ\text{C}$ . Non-hydrogen atoms are represented by Gaussian ellipsoids at the 20% probability level. Hydrogen atoms have been omitted. Selected bond distances ( $\text{\AA}$ ): C10-C11, 1.432(3); C11-C12, 1.423(3); C12-C13, 1.425(3); C13-C14, 1.415(3); C10-C14, 1.422(3); C30-C31, 1.419(3); C31-C32, 1.421(3); C32-C33, 1.424(3); C33-C34, 1.415(3); C30-C34, 1.435(4); Co-C10, 2.065(2); Co-C11, 2.064(2); Co-C12, 2.091(2); Co-C13, 2.033(2); Co-C14, 2.029(2); Co-C30, 2.061(2); Co-C31, 2.064(2); Co-C32, 2.086(2); Co-C33, 2.037(2); Co-C34, 2.016(2). The dihedral angle between the planes defined by C10-C14 and C30-C34 =  $8.65(14)^\circ$ .

The formation of the symmetrical cobaltocene product **62** was unexpected as it was anticipated the steric bulk of the 1,3-di-*tert*-butylcyclopentadienyl ligand would be sufficient to prevent ligand redistribution, particularly when the reaction was maintained at low temperature.

Based on the formation of disproportionation products, other cobalt precursors were examined. Bunel,<sup>168</sup> Andersen,<sup>169</sup> and Carmichael<sup>170</sup> have each independently reported the preparation of half-sandwich cobalt complexes using cobalt(II) acetylacetonate as a precursor. Thus, treatment of 1,3-di-*tert*-butylcyclopentadienide anion **61** with cobalt(II) acetylacetonate at low temperature afforded the desired half-sandwich cobalt complex **64** in good yield with no evidence for the symmetrical cobaltocene as demonstrated by high resolution mass spectrometry and elemental analysis (Equation 3-8).

### Equation 3-8



### *Preparation of (1,3-Di-*tert*-butylcyclopentadienyl)cobalt Bis(alkene) Complexes*

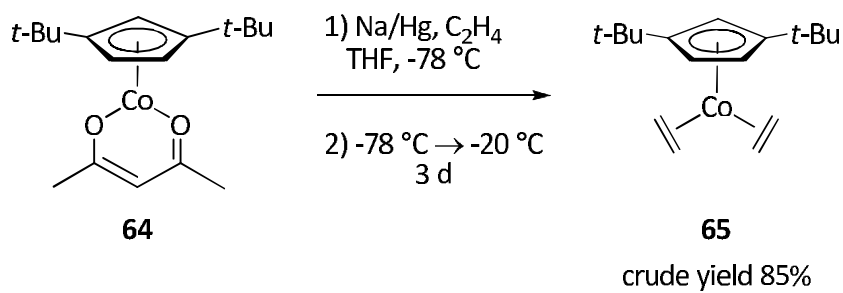
Cyclopentadienyl cobalt diene complexes are typically prepared via one of two methods: thermal or photochemical exchange of labile ligands for the

diene or direct reduction of suitable cobalt precursors in the presence of the diene. Typically, cyclopentadienyl cobalt bis(ethylene) is chosen as the precursor for exchange reactions due to the lability of the ethylene ligands at ambient temperatures. The cobalt bis(ethylene) complex is in turn generated via one of two methods: sodium amalgam reduction of a cyclopentadienyl cobalt halo-precursor in the presence of ethylene<sup>152, 171, 172</sup> or potassium sand reduction of the corresponding cobaltocene in the presence of ethylene.<sup>160-163, 173</sup> The synthesis of  $(C_5Me_5)Co(C_2H_4)_2$  is usually performed using the former method due to the availability of the chloro-bridged dimer  $[(C_5Me_5)CoCl]_2$ , whereas the synthesis of  $(RC_5H_4)Co(C_2H_4)_2$  (where R = hydrocarbyl) is performed using the latter, since the corresponding chloro-bridged dimer is unavailable. However, potassium reductions of cobaltocene complexes are prone to over-reduction, forming anionic cobaltate complexes such as  $[Co(cod)_4]^-$ ,  $[Co(C_2H_4)_4]^-$ , and  $[Co(cod)(C_2H_4)]^-$ .<sup>173</sup>

Our attempts to synthesize  $(t-Bu_2C_5H_3)Co(C_2H_4)_2$  via one of these methods met with moderate success. Treatment of symmetrical cobaltocene complex **62** with one equivalent of potassium sand under an ethylene atmosphere at 0 °C led to an intractable residue, presumably due to the lability of the ethylene ligands.<sup>160-163</sup> However, reduction of acetylacetonate complex **64** with sodium amalgam under an ethylene atmosphere affords the bis(ethylene) complex **65** in moderate yield (Equation 3-9). The reaction yield is improved if

the mixture is warmed from -78 °C to -20 °C slowly in several stages and is handled above 0 °C only for short durations during isolation.

**Equation 3-9**

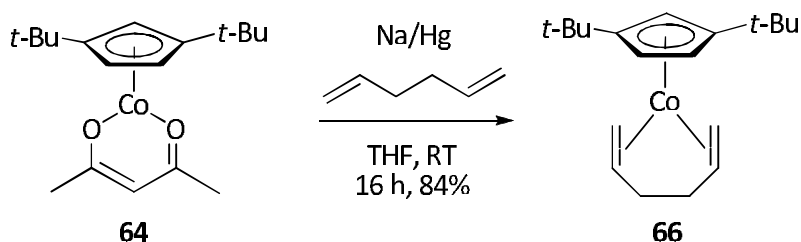


As expected in the <sup>1</sup>H NMR spectrum, the chemical shifts of the ethylene protons are located at 0.6 ppm and 2.6 ppm, upfield from free ethylene due to strong π-backbonding from the metal centre (Table 3-1). Both ethylene proton resonances display a complex 2<sup>nd</sup> order AA'BB' splitting pattern and indicate ethylene rotation is slow compared to the NMR experiment timescale. Cobalt bis(ethylene) complex **65** is a dark red oil at ambient temperature and attempts to crystallize it have been unsuccessful, largely due to thermal sensitivity at ambient temperature.<sup>171, 172</sup> Upon prolonged standing at ambient temperature, NMR analysis of the complex displayed progressive broadening of the peaks, attributed to paramagnetic decomposition products. To avoid decomposition, isolation and purification of this compound was done as rapidly as possible and the solvent was not completely removed *in vacuo* before storing at -35 °C. Because of this sensitivity, a clean <sup>13</sup>C NMR spectrum could not be collected.

**Table 3-1:**  $^1\text{H}$  NMR Spectroscopic Data for  $(t\text{-Bu}_2\text{C}_5\text{H}_3)\text{Co}(\text{C}_2\text{H}_4)_2$  **65**

Position	$\delta$ $^1\text{H}$
CH-CH	3.77 (d, $J = 2.5$ Hz)
CH	3.44 (t, $J = 2.4$ Hz)
C(CH <sub>3</sub> )	1.40 (s)
C <sub>2</sub> H <sub>4</sub>	2.61 (m, 2 <sup>nd</sup> order, AA'BB') 0.67 (m, 2 <sup>nd</sup> order, AA'BB')

Seeking a less labile alternative, the synthesis of  $(t\text{-Bu}_2\text{C}_5\text{H}_3)\text{Co}(1,5\text{-hexadiene})$  **66**, was considered. The chelating nature of the 1,5-hexadiene ligand was expected to confer a greater degree of kinetic stability compared to the ethylene ligand. Correspondingly, sodium amalgam reduction of cobalt acetylacetonate precursor **64** in the presence of excess 1,5-hexadiene gives high yields of 1,5-hexadiene adduct **66**, which was isolated as a dark red oil (Equation 3-10).

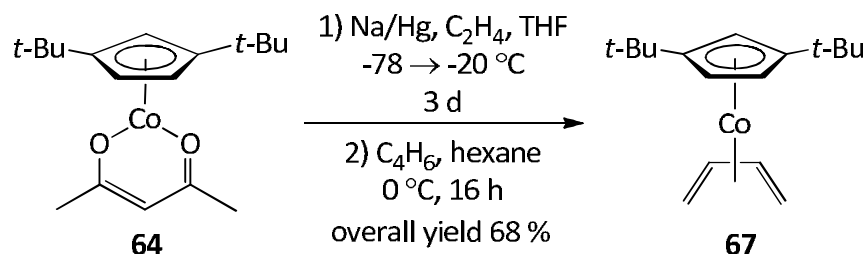
**Equation 3-10**

The product solidifies upon standing at  $-35$  °C, but failed to recrystallize under a range of conditions. The complex was thus used without further

purification. Although 1,5-hexadiene adduct **66** can be handled at ambient temperature with less decomposition than bis(ethylene) adduct **65**, prolonged standing at ambient temperature eventually leads to substantial decomposition, as evidenced by broadened resonances in the  $^1\text{H}$  NMR spectrum.

While both cobalt bis(alkene) complexes **65** and **66** can be prepared by alkali metal reduction, the same cannot be said for butadiene adduct **67**, due to competing anionic polymerization induced by the reductant. However, stirring a solution of cobalt bis(ethylene) complex **65** at 0 °C in butadiene-saturated hexane affords cobalt butadiene adduct **67** in moderate isolated yield (Equation 3-11).

#### Equation 3-11



Similar to the  $^1\text{H}$  NMR spectrum of the bis(ethylene) complex **65**, the terminal vinyl protons of **67** exhibit an upfield shift compared to the normal chemical shift of free butadiene. Both the terminal and the interior vinyl protons display 2<sup>nd</sup> order multiplicity. As expected, the chemical shift of the interior vinyl

protons is downfield from the terminal vinyl protons by virtue of the metalacyclopentene canonical.

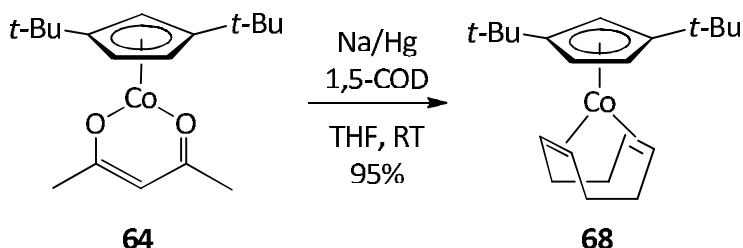
### ***Preparation of (1,3-Di-tert-butylcyclopentadienyl)Cobalt $\eta^4$ -Cycloalkadiene***

#### ***Complexes***

Cobalt complexes of cyclic dienes can be prepared in an analogous fashion, using sodium amalgam reduction of cobalt acetylacetonate complex **64** in the presence of the cyclic diene. Dienes used in this reaction include 1,5-cyclooctadiene, 1,3-cyclohexadiene and 1,4-cyclohexadiene.

The 1,5-cyclooctadiene adduct was prepared following a similar procedure for the pentamethylcyclopentadienyl congener **52**.<sup>121</sup> Treatment of a THF solution of cobalt acetylacetonate complex **64** and 1,5-cyclooctadiene with sodium amalgam at ambient temperature afforded in excellent yield ( $t\text{-Bu}_2\text{C}_5\text{H}_3$ )Co(1,5-cod) (**68**, Equation 3-12).

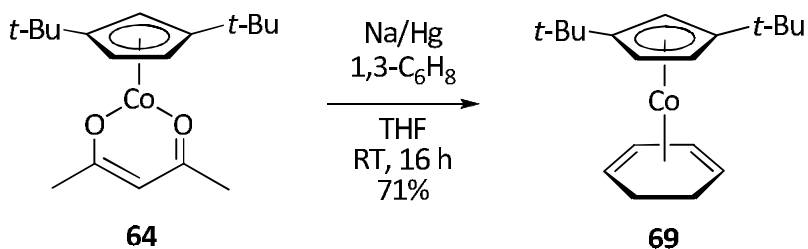
#### **Equation 3-12**



The compound is obtained as a stable, dark red oil and is the sole product observed in the  $^1\text{H}$  NMR spectrum. The purity of this compound was confirmed by spectroscopic and elemental analysis. Upon standing at  $-35\text{ }^\circ\text{C}$  over 12 hours, the oil solidifies, but further attempts to recrystallize the resulting solid from pentane were unsuccessful.

The 1,3-cyclohexadiene adduct was prepared similarly, analogous to the pentamethylcyclopentadienyl congener.<sup>132</sup> Treatment of a THF solution of cobalt acetylacetonate complex **64** with 1,3-cyclohexadiene and sodium amalgam at ambient temperature afforded in good yield ( $t\text{-Bu}_2\text{C}_5\text{H}_3$ )Co( $\eta^4$ -cyclohexadiene) **69** as a red oil (Equation 3-13). Similar to cyclooctadiene adduct **68**, cyclohexadiene adduct **69** solidifies upon standing at  $-35\text{ }^\circ\text{C}$ , but further attempts to recrystallize the product were unsuccessful. The  $^1\text{H}$  NMR spectrum of the oil revealed the formation of a single product which was confirmed by elemental analysis.

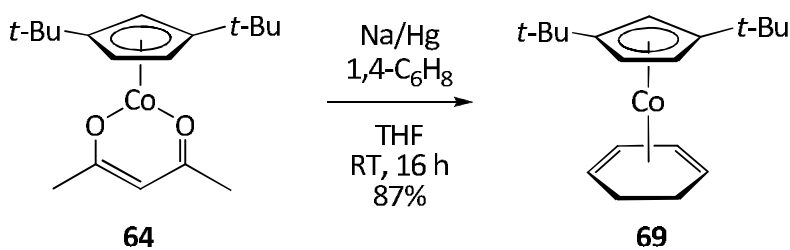
Equation 3-13



Interestingly, reduction of cobalt acetylacetonate complex **64** in the presence of 1,4-cyclohexadiene proceeds cleanly to the same product obtained

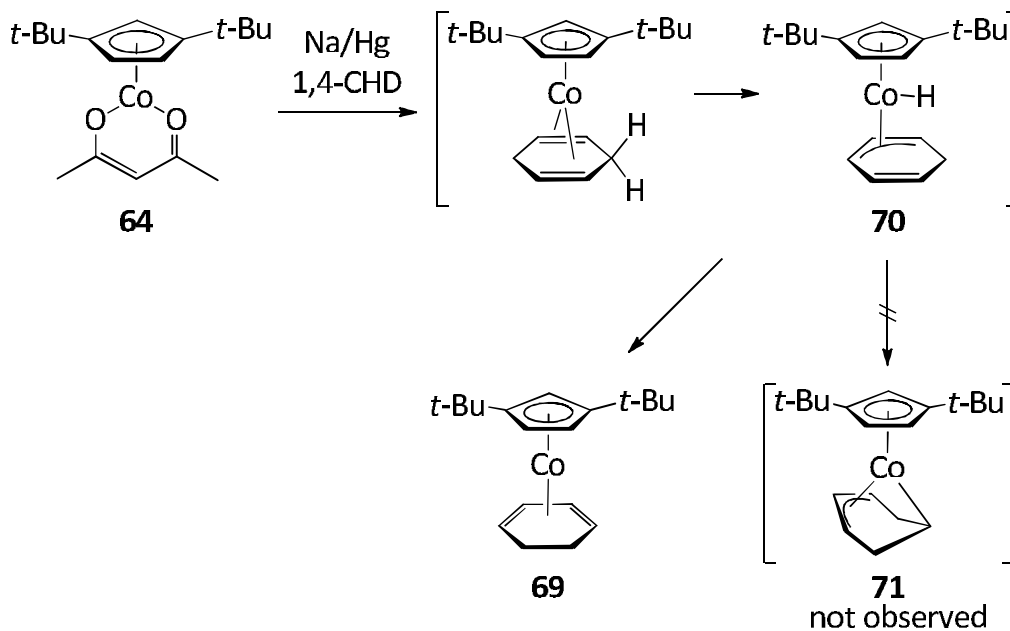
from 1,3-cyclohexadiene (Equation 3-14). In this case, a single product is formed, as evidenced by  $^1\text{H}$  NMR spectroscopy, and the reaction proceeds in higher yield compared to the addition of 1,3-cyclohexadiene.

**Equation 3-14**



Presumably, the reaction proceeds by initial formation of the 1,4-cyclohexadiene adduct, followed by allylic carbon-hydrogen bond activation of one of two *endo*-hydrogen atoms to form cobalt  $\eta^5$ -cyclohexadienyl hydrido intermediate **70** (Scheme 3-4). Migration of the metal-bound hydride then proceeds to either terminal olefinic carbon of the  $\eta^5$ -cyclohexadienyl system, producing the 1,3-cyclohexadiene adduct. Interestingly, hydride migration to the 2- or 4-position of the cyclohexadienyl moiety would produce an  $\eta^1, \eta^3$ -cyclohexadiene complex **71**, similar to the bridged bicyclic complexes prepared by Dzwiniel (Complexes **34** and **35**, Equation 2-7). Such a complex has not been observed during the course of the reaction and most likely is a thermodynamically disfavoured geometry.

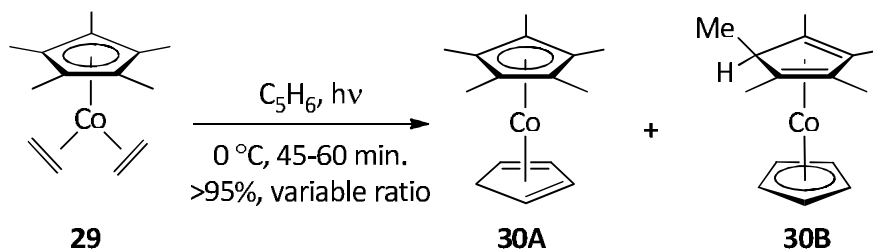
Scheme 3-4



**Preparation of (1,3-Di-tert-butylcyclopentadienyl)cobalt( $\eta^4$ -cyclopentadiene)**

Preparation of (1,3- $t\text{-Bu}_2\text{C}_5\text{H}_3$ )Co( $\eta^4$ -cyclopentadiene) from either the bis(ethylene) adduct **65** or the 1,5-hexadiene adduct **66** was envisioned to occur via photochemical or thermal ligand exchange in the presence of monomeric cyclopentadiene. Dzwiniel demonstrated that the *in situ* exchange of ethylene for cyclopentadiene in  $(\text{C}_5\text{Me}_5)\text{Co}(\text{C}_2\text{H}_4)_2$  proceeds ideally under photochemical conditions, affording a mixture of two cyclopentadiene compounds depending on the duration of irradiation (Equation 3-15).<sup>131</sup> The thermal exchange reaction led to an intractable residue.

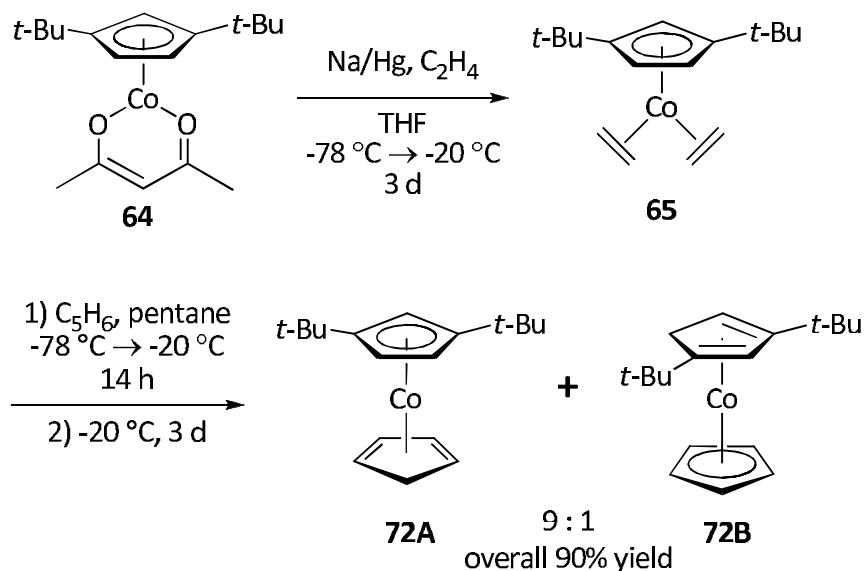
### Equation 3-15



Both thermal and photochemical exchange reactions with cyclopentadiene were investigated starting from bis(ethylene) complex **65**. Upon exposure of complex **65** to excess cyclopentadiene in hexane at ambient temperature, a slight darkening of colour was observed. The  $^1\text{H}$  NMR spectrum of the residue displayed resonances characteristic of the expected product, but due to an unknown paramagnetic impurity, significant broadening of the resonances was observed from competitive decomposition of bis(ethylene) complex **65** upon prolonged standing at ambient temperature.

However, initiating the thermal exchange reaction at  $-78\text{ }^{\circ}\text{C}$  and holding the temperature at  $-20\text{ }^{\circ}\text{C}$  over several days affords a 9 : 1 mixture of the expected cobalt  $\eta^4$ -cyclopentadiene product **72A** and  $\eta^4$ -1,3-di-*tert*-butylcyclopentadiene tautomer **72B** in excellent overall yield from the starting cobalt acetylacetonate complex **64**. (Scheme 3-5). This greatly contrasts with the reactions of the pentamethylcyclopentadienyl congener, where thermal exchange of ethylene for cyclopentadiene was not successful.

**Scheme 3-5**



The minor product presumably arises from facile hydride transfer from the less substituted cyclopentadiene ring to the more substituted cyclopentadienyl ligand mechanistically similar to the isomerization of cyclohexadiene isomers previously discussed (Scheme 3-4). The NMR data for minor product **72B**, as well as an independent synthesis of this complex, will be discussed at a later point.

The  $^1\text{H}$  NMR data for the major product **72A** are summarized in Figure 3-2 and Table 3-2. Complex **72A** exhibits a single *tert*-butyl resonance along with a mutually coupled doublet at 4.48 ppm and triplet at 4.14 ppm ( $^4J_{\text{HH}} = 1.6\text{ Hz}$ ), consistent with the 1,3-di-*tert*-butylcyclopentadienyl ligand. The resonances attributed to the  $\eta^4$ -cyclopentadiene moiety are located downfield at 5.27 ppm and 4.48 ppm, corresponding to the inner and outer olefinic protons

respectively. Also present are two doublet of triplets from the diastereotopic methylene protons at 2.10 ppm and 2.75 ppm. Each multiplet possesses a large geminal coupling constant ( $^2J_{\text{HH}} = 13.4$  Hz), and smaller vicinal and allylic coupling constants ( $^3J_{\text{HH}} = 2.0$  Hz).

**Figure 3-2:**  $^1\text{H}$  Numbering System for  $(t\text{-Bu}_2\text{C}_5\text{H}_3)\text{Co}(\eta^4\text{-C}_5\text{H}_6)$  **72A**

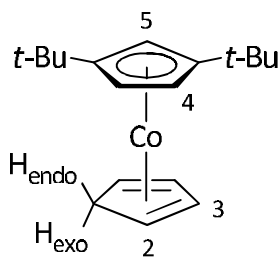
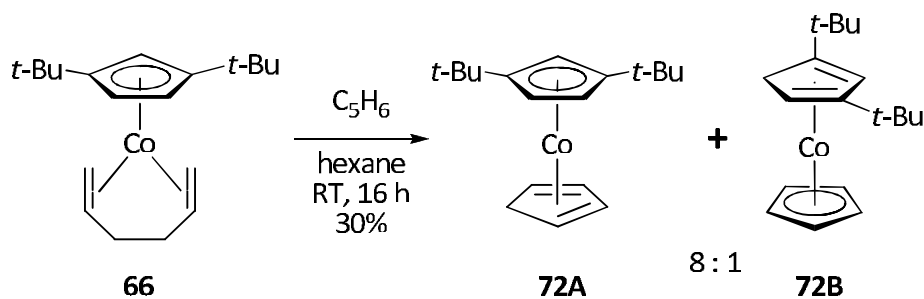


**Table 3-2:**  $^1\text{H}$  NMR Spectroscopic Data for  $(t\text{-Bu}_2\text{C}_5\text{H}_3)\text{Co}(\eta^4\text{-C}_5\text{H}_6)$  **72A**

Position	$\delta$ $^1\text{H}$
1	$\text{H}_{\text{endo}}$ : 2.75 (dt, $J = 13.6, 2.0$ Hz) $\text{H}_{\text{exo}}$ : 2.09 (dt, $J = 13.6, 1.7$ Hz)
2	2.42 (br. s)
3	5.27 (m, 2 <sup>nd</sup> order)
4	4.48 (d, $J = 1.6$ Hz)
5	4.14 (t, $J = 1.6$ Hz)
$\text{C}(\text{CH}_3)_3$	1.16 (s)

To address whether the reversal of thermal and photochemical trends is unique to the bis(ethylene) complex **65**, the corresponding acyclic hexadiene adduct **66** was also treated with cyclopentadiene under thermal and photochemical exchange conditions. Similar to bis(ethylene) complex **65**, thermal exchange affords an 8 : 1 mixture of cyclopentadiene complexes **72A** and **72B**, albeit in much lower yield (Equation 3-16). The photochemical reaction again affords an intractable paramagnetic residue, establishing that, in contrast to the pentamethylcyclopentadienyl congener, the 1,3-di-*tert*-butylcyclopentadienyl template does not support photochemical exchange reactions.

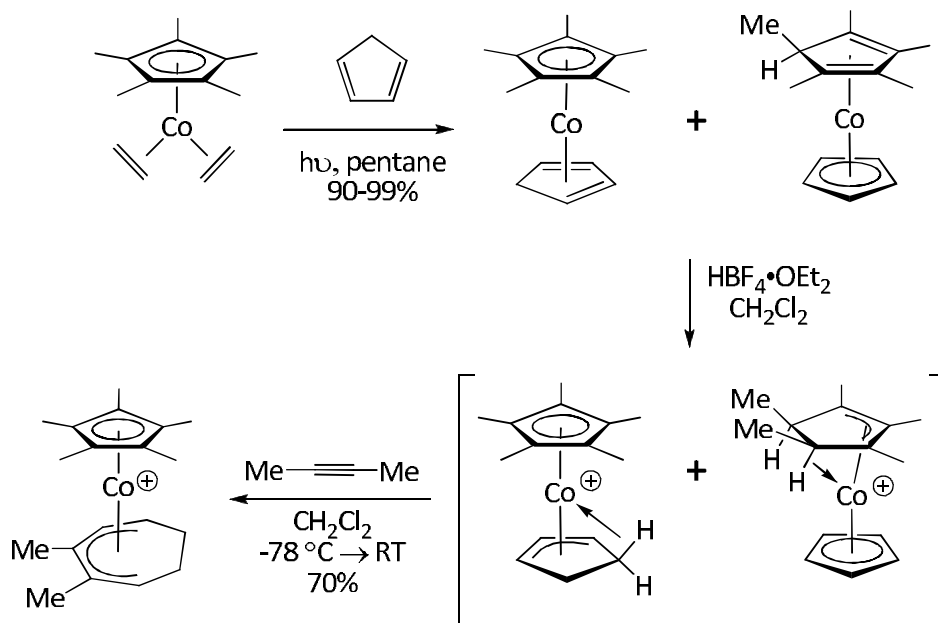
**Equation 3-16**



The temperature sensitivity of bis(ethylene) complex **65** renders this synthetic strategy inconvenient on a larger scale. An alternative method was thus devised to prepare complexes **72A** and **72B**. Dzwiniel previously demonstrated that the photochemical reaction of  $(\text{C}_5\text{Me}_5)\text{Co}(\text{C}_2\text{H}_4)_2$  with cyclopentadiene produces analogous isomeric mixtures and that protonation of

the mixture in the presence of 2-butyne results in the formation of only one  $\eta^5$ -cycloheptadienyl product (Scheme 3-6).<sup>24, 25, 131</sup> This observation implies that a targeted synthesis of  $\eta^4$ -1,3-di-*tert*-butylcyclopentadiene complex **72B** could be developed, avoiding the use of bis(ethylene) complex **65** completely, since protonation of complex **72B** followed by treatment with alkyne should converge to the  $\eta^5$ -cycloheptadienyl product from rapid hydride transfer to the less substituted cyclopentadiene ligand.

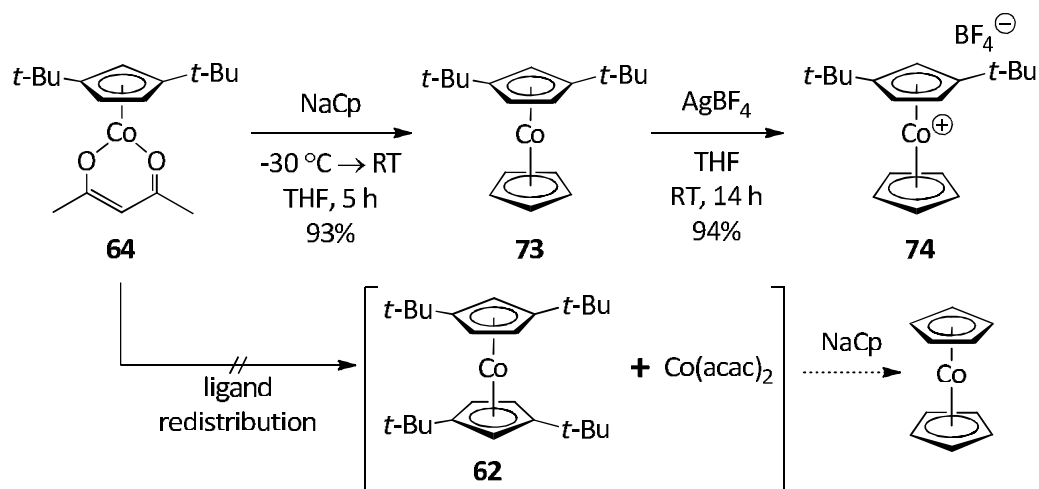
**Scheme 3-6**



To address this issue experimentally, nucleophilic hydride addition to the  $[(1,3-t\text{-Bu}_2\text{C}_5\text{H}_3)\text{Co}(\text{C}_5\text{H}_5)]\text{BF}_4$  salt **74** was investigated. The corresponding unsubstituted cyclopentadiene complex,  $(\text{C}_5\text{H}_5)\text{Co}(\eta^4\text{-C}_5\text{H}_6)$ , was prepared in 1959 by sodium borohydride reduction of the cobalticenium complex.<sup>174</sup>

The cobalticenium complex  $[(1,3-t\text{-Bu}_2\text{C}_5\text{H}_3)\text{Co}(\text{C}_5\text{H}_5)]\text{BF}_4$  **74** was prepared by the addition of one equivalent of sodium cyclopentadienide to acetylacetonate complex **64** at low temperature, to afford the neutral cobaltocene complex  $(1,3-t\text{-Bu}_2\text{C}_5\text{H}_3)\text{Co}(\text{C}_5\text{H}_5)$  **73**. Subsequent oxidation with silver tetrafluoroborate afforded the unsymmetrical cobalticenium salt **74** (Scheme 3-7).

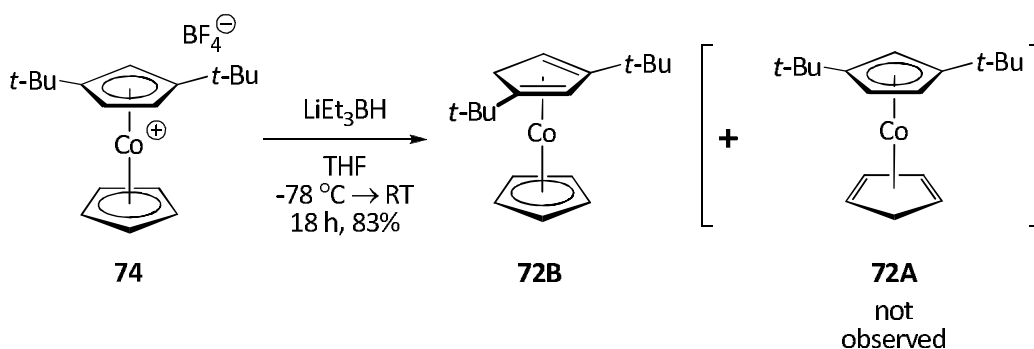
**Scheme 3-7**



No evidence for the formation of the unsubstituted cobaltocene, via prior ligand redistribution of complex **64** to form disubstituted cobaltocene complex **62** and cobalt(II) acetylacetonate, was observed. These results demonstrate the utility of using cobalt(II) acetylacetonate as a source of electrophilic cobalt to prepare half-sandwich cobalt complexes.

Treatment of **74** with  $\text{LiEt}_3\text{BH}$  in THF afforded a deep red oil which was determined spectroscopically to be  $(\text{C}_5\text{H}_5)\text{Co}(\eta^4\text{-1,3-}t\text{-Bu}_2\text{C}_5\text{H}_4)$  **72B** (Equation 3-17). No evidence for the formation of the tautomer **72A** was observed.

**Equation 3-17**



The  $^1\text{H}$  NMR data for complex **72B** are summarized in Table 3-3 with the numbering scheme given in Figure 3-3. The complex possesses a diagnostic  $\text{C}_5\text{H}_5$  resonance at 4.64 ppm. On the 1,3-di-*tert*-butylcyclopentadienyl ring, the diastereotopic methylene protons are mutually coupled and also couple the vicinal vinyl proton. The presence of a doublet ( $^4J_{\text{HH}} = 1.8$  Hz), attributed to  $\text{H}_3$ , and both diastereotopic methylene protons establish that the cyclopentadiene isomer obtained has both *tert*-butyl groups residing at olefinic positions.

**Figure 3-3:**  $^1\text{H}$  and  $^{13}\text{C}$  Numbering System of  $(\text{C}_5\text{H}_5)\text{Co}(\eta^4\text{-}t\text{-Bu}_2\text{C}_5\text{H}_4)$  **72B**

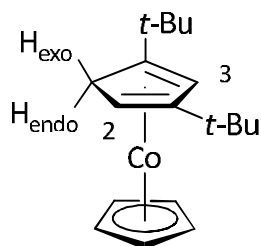


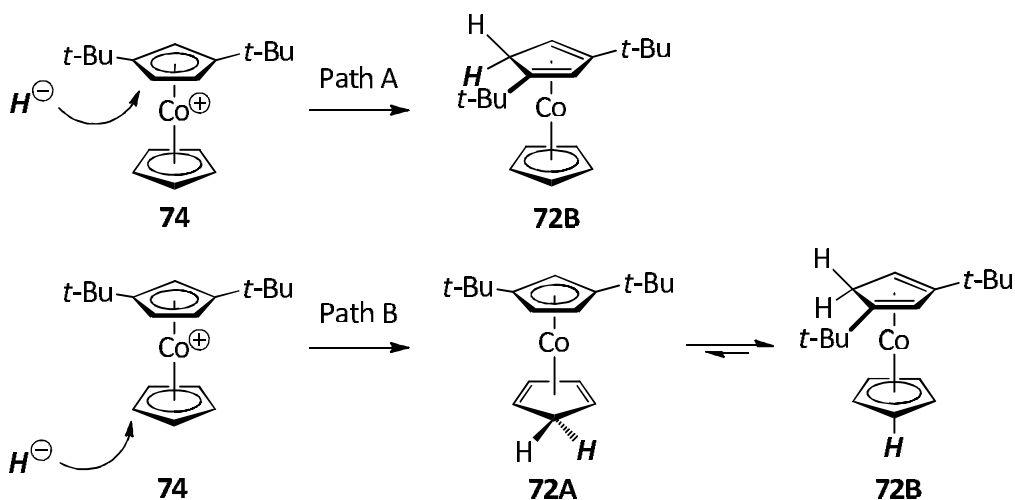
**Table 3-3:**  $^1\text{H}$  NMR Spectroscopic Data for  $(\text{C}_5\text{H}_5)\text{Co}(\eta^4\text{-}t\text{-Bu}_2\text{C}_5\text{H}_4)$  **72B**

Position	$\delta$ $^1\text{H}$
1	H <sub>exo</sub> : 2.13 (dd, $J = 13.2, 2.0$ Hz) H <sub>endo</sub> : 2.57 (dd, $J = 13.4, 2.5$ Hz)
2	2.43 (apparent dt, $J = 2.3, 1.8$ Hz)
3	5.05 (d, $J = 1.8$ Hz)
C <sub>5</sub> H <sub>5</sub>	4.64 (s)
C(CH <sub>3</sub> ) <sub>3</sub>	1.26 (s)
C(CH <sub>3</sub> ) <sub>3</sub>	0.92 (s)

The selective addition of nucleophiles to the more substituted cyclopentadienyl ring in similar mixed cobalticene complexes has also been observed by Dzwiniel.<sup>116</sup> The cyclopentadienyl complex **72B** can, in principle, be obtained in one of two ways: 1) *exo*-hydride attack at the most substituted ring, giving the observed product in one step (Path A, Scheme 3-8), or 2) *exo*-hydride

attack at the least substituted ring, followed by equilibrium hydride transfer to the opposite cyclopentadienyl ligand (Path B, Scheme 3-8).

**Scheme 3-8**

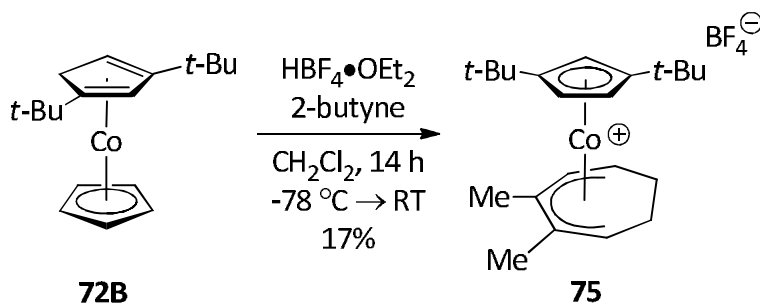


Hydride addition to the metal followed by transfer to the more substituted ring is disfavoured by the absence of empty orbitals on the 18 e<sup>-</sup> cobalt centre. *Exo*-hydride addition to the isolated unsubstituted carbon of the 1,3-di-*tert*-butylcyclopentadienyl ligand is reasonable, but this reaction is presumably inhibited sterically. *Exo*-hydride addition to either of the *tert*-butyl substituted carbons, followed by isomerization to the observed product, could also occur but is even more disfavoured due to steric crowding of the *tert*-butyl groups. The isolation of complex **72B**, from hydride addition to cobalticene complex **74**, with no evidence of **72A**, establishes that *exo*-hydride addition to the more substituted cyclopentadienyl ligand occurs.

Proton NMR analysis of a sample of **72B** over a period of several days revealed the growth of resonances characteristic of **72A**, implying that **72A** and **72B** are in thermal equilibrium. Again, this starkly contrasts the reactivity of the pentamethylcyclopentadienyl congener, where isomerization between **30A** and **30B** requires photochemical irradiation. However, upon warming a sample of **72B** to ascertain the equilibrium ratio between **72A** and **72B**, significant broadening of the resonances in the  $^1\text{H}$  NMR spectrum was observed, demonstrating the temperature sensitivity of these complexes upon prolonged standing at ambient temperature.

#### **B. Ring-Expansion Reactions of the (1,3-Di-*tert*-butylcyclopentadienyl)cobalt( $\eta^3$ -cyclopentenyl) Complex With Alkyne**

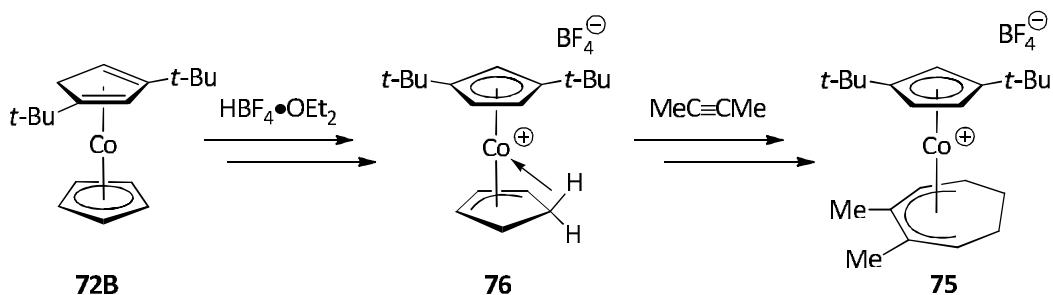
Treatment of cobalt 1,3-di-*tert*-butylcyclopentadiene complex **72B** with  $\text{HBF}_4 \cdot \text{OEt}_2$  and excess 2-butyne in dichloromethane at low temperature afforded the corresponding seven-membered carbocyclic complex **75**, albeit in low yield (Equation 3-18). This is surprising, considering that the same reaction using the pentamethylcyclopentadienyl template proceeds in high yield.

**Equation 3-18**

Moreover, the  $^1\text{H}$  NMR spectrum of the crude product mixture reveals the formation of a complex mixture, as indicated by multiple *tert*-butyl resonances. However, the  $^1\text{H}$  NMR spectrum showed signals that were indicative of the same  $\eta^5$ -cycloheptadienyl ring system seen in the  $\text{C}_5\text{Me}_5$  series. Flash chromatography of the crude mixture provided a fraction possessing characteristic resonances for the product, but significantly broadened, indicating the co-elution of a minor paramagnetic impurity. The identity of the paramagnetic impurity is not known and it is debatable whether it was formed during the course of the reaction or upon chromatography. The reaction gave a similarly low yield ( $\sim 16\%$ ) when three equivalents of 2-butyne were used.

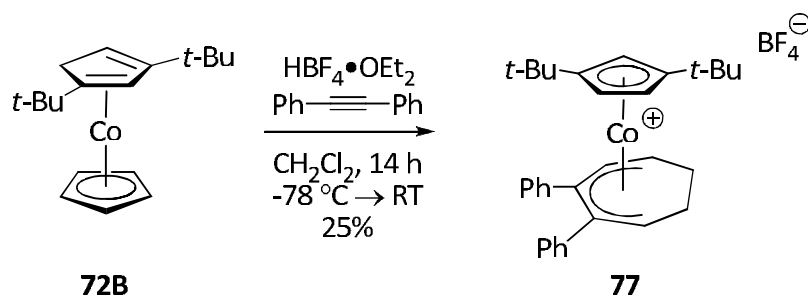
The proposed mechanism for this reaction is similar to the pentamethylcyclopentadienyl, methylcyclopentadienyl, and *tert*-butylcyclopentadienyl congeners (Scheme 3-9).<sup>175</sup> Treatment of the starting material **72B** with strong acid presumably forms the  $\eta^3$ -cyclopentenyl complex **76**, which undergoes ring-expansion to afford the observed seven-membered ring product.

### Scheme 3-9



Other disubstituted alkynes were also added to the intermediate  $\eta^3$ -cyclopentenylium complex **76**. Treatment of the 1,3-di-*tert*-butylcyclopentadiene complex **72B** with  $\text{HBF}_4 \cdot \text{OEt}_2$  and three equivalents of diphenylacetylene in dichloromethane at low temperature affords the ring-expanded product **77**, again in low yield (Equation 3-19).

### Equation 3-19



This product also exhibited significant line broadening in the  $^1\text{H}$  NMR spectrum. Upon subsequent flash chromatography and recrystallization from dichloromethane/diethyl ether mixture, the purified product still showed

broadened  $^1\text{H}$  NMR resonances, suggesting either slow decomposition while in solution at ambient temperature or during chromatography. The identity of one of the product components was provided by single crystal X-ray crystallography (Figure 3-4). The bond angles and lengths exhibited by the  $\eta^5$ -cycloheptadienyl complex **77** are consistent with other cobalt  $\eta^5$ -cycloheptadienyl examples previously obtained in this group.<sup>122, 131</sup> The crystals used for X-ray diffraction were dissolved in  $\text{CDCl}_3$  and the  $^1\text{H}$  NMR spectrum exhibited broadened resonances, suggesting that the crystal morphologies of the paramagnetic impurity and complex **77** were similar.

The 1,3-di-*tert*-butylcyclopentadienyl system thus reacts similarly to the pentamethylcyclopentadienyl and (1-*tert*-butyl-3-methyl)cyclopentadienyl systems towards disubstituted alkynes, but affords  $\eta^5$ -cycloheptadienyl products in overall lower yields.

The ring-expansion of  $\eta^3$ -cyclopentenyl complex **76** was also examined using unsymmetrical alkynes. In contrast to symmetrical alkynes, ring expansion with unsymmetrical alkynes can potentially lead to the formation of multiple regioisomers as a result of the orientation of the alkyne during incorporation. However, Dzwiniel has observed that typically only one  $\eta^5$ -cycloheptadienyl product is isolated from the reaction mixture.<sup>131</sup> When terminal alkynes, such as *tert*-butylacetylene are used, the alkyl substituent resides on the central carbon of the resulting  $\eta^5$ -cycloheptadienyl product.

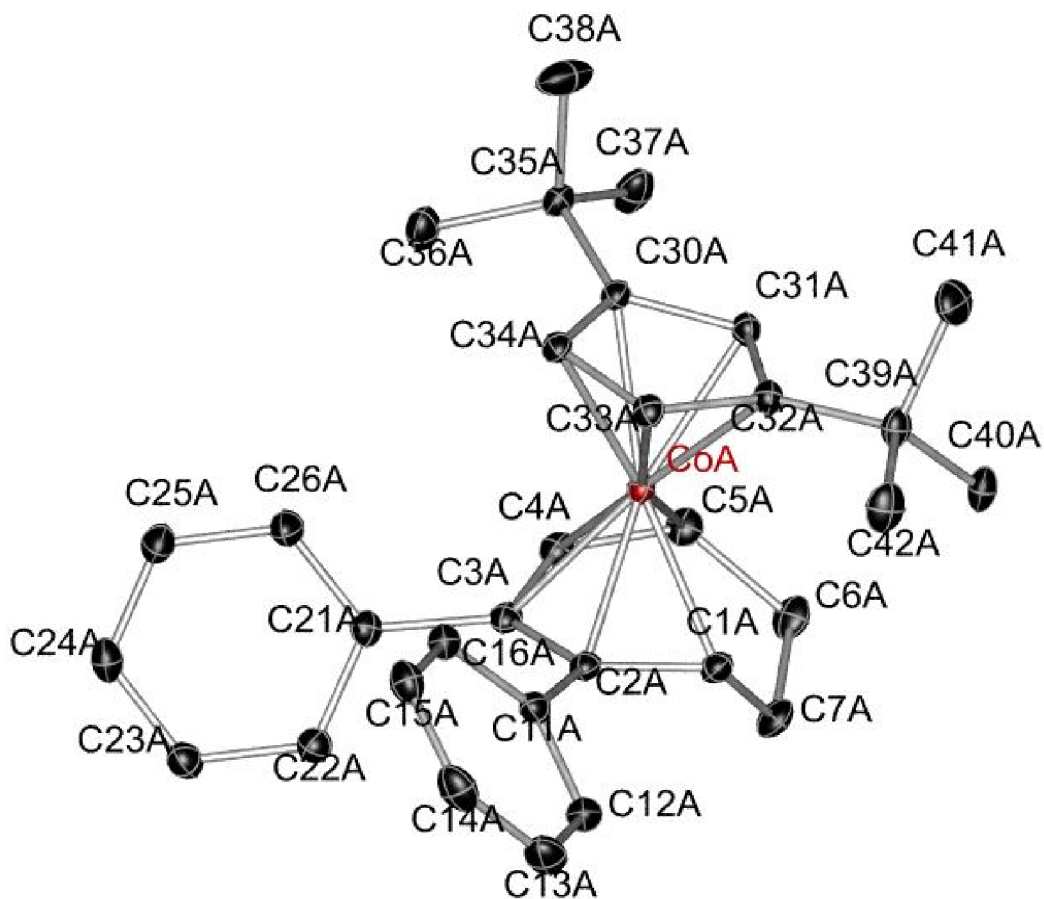
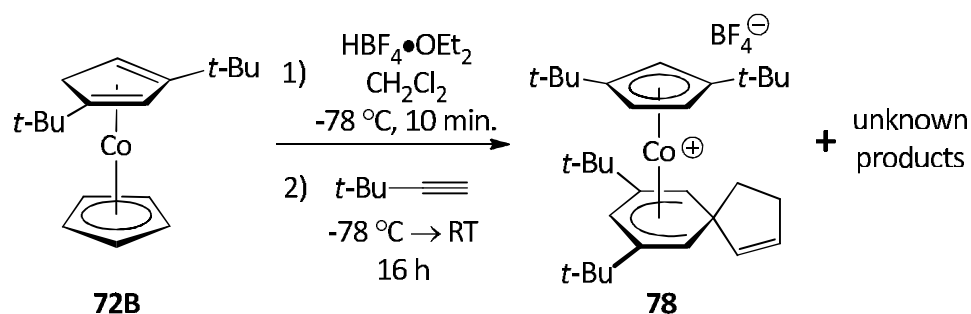


**Figure 3-4:** Perspective view of one of two crystallographically independent [(*t*-Bu<sub>2</sub>C<sub>5</sub>H<sub>3</sub>)Co(2,3-diphenylhepta-2,4-dien-1-yl)] cations **77**. Final residuals:  $R_1 = 0.0481$ ;  $wR_2 = 0.1351$ . Data collected at -100 °C. Non-hydrogen atoms are represented by Gaussian ellipsoids at the 20% probability level. Hydrogen atoms have been omitted. Selected bond distances (Å): C1A-C2A, 1.421(4); C2A-C3A, 1.434(4); C3A-C4A, 1.435(4); C4A-C5A, 1.409(4); C5A-C6A, 1.506(4); C6A-C7A, 1.504(5); C1A-C7A, 1.513(4); Co-C1A, 2.112(3); Co-C2A, 2.060(3); Co-C3A, 2.096(3); Co-C4A, 2.023(3); Co-C5A, 2.088(3). The dihedral angle between the planes defined by C1A-C5A and C30A-C34A: 10.42(17)°

Cyclopentadiene complex **72B** was thus treated with strong acid and excess *tert*-butylacetylene in dichloromethane at low temperature (Equation 3-20). Subsequent  $^1\text{H}$  NMR analysis of the product residue displayed two sets of *tert*-butyl resonances which were initially ascribed to the two regioisomers arising from different orientations of the alkyne during the addition step. After flash chromatography and subsequent recrystallization from a dichloromethane/diethyl ether mixture,  $^1\text{H}$  NMR spectroscopy of the product showed broadened resonances, indicative of a persistent paramagnetic impurity.

Equation 3-20



Crystals suitable for X-ray crystallography were isolated from a diethyl ether/dichloromethane mixture and the crystal structure obtained (Figure 3-5). What was initially thought to be two  $\eta^5$ -cycloheptadienyl products was revealed instead to be an unusual  $\eta^5$ -cyclohexadienyl complex with an incorporated spirocyclic cyclopentene. The assignment of spirocycle **78** was based solely on the X-ray crystallographic data.

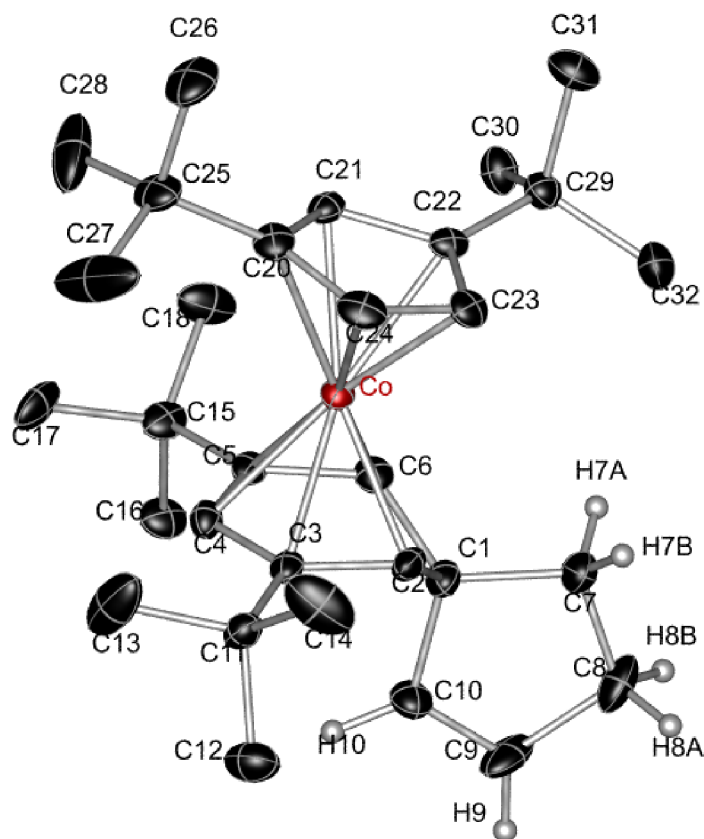


**Figure 3-5:** Perspective view of the  $[(t\text{-Bu}_2\text{C}_5\text{H}_3)\text{Co}(7,9\text{-di-tert-butylspiro}[4.5]\text{deca-1,6,9-trien-8-yl})]$  cation **78**. Final residuals:  $R_1 = 0.0681$ ,  $wR_2 = 0.2162$ . Data collected at  $-100\text{ }^\circ\text{C}$ . Non-hydrogen atoms are represented by Gaussian ellipsoids at the 20% probability level. Hydrogen atoms have been omitted except on C7 to C10, where H7A/7B, H8A/8B, H9 and H10 have been located. Selected bond distances ( $\text{\AA}$ ): C1-C2, 1.496(8); C1-C6, 1.514(8); C1-C7, 1.547(8); C1-C10, 1.521(8); C2-C3, 1.412(7); C3-C4, 1.417(8); C4-C5, 1.421(8); C5-C6, 1.409(7); C7-C8, 1.430(9); C8-C9, 1.507(10); C9-C10, 1.338(9). Selected bond angles (deg): C1-C7-C8, 108.8(5); C7-C8-C9, 106.8(5); C8-C9-C10, 109.8(6); C1-C10-C9, 112.1(6). The dihedral angle between the planes defined by C2-C6 and C20-C24 = 12.1(4) $^\circ$ . The torsional angle defined by C7-C10 = 7.3(9) $^\circ$ .

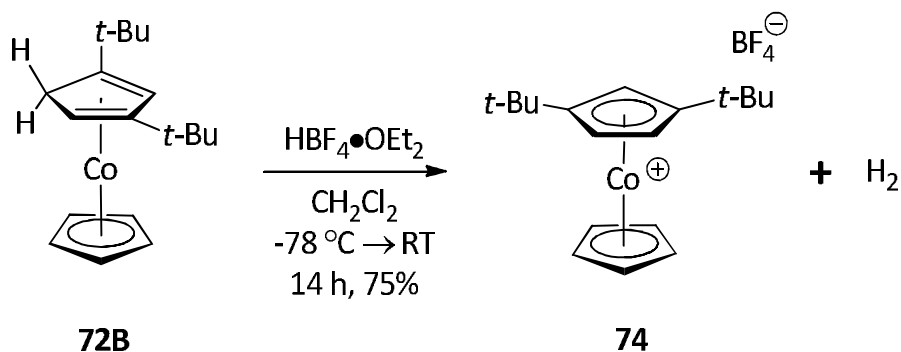
The crystal structure for spirocycle complex **78** displays several noteworthy elements. The presence of the  $\eta^5$ -cyclohexadienyl ring system is of particular interest in that the straightforward incorporation of two equivalents of *tert*-butylacetylene cannot explain the formation of a *six*-membered ring. The incorporation of one equivalent of *tert*-butylacetylene in a ring-expansion process would result in the formation of an  $\eta^5$ -cycloheptadienyl product, which is not observed. The presence of the  $\eta^5$ -cyclohexadienyl moiety suggests that transfer of one ancillary 1,3-di-*tert*-butylcyclopentadienyl ring to another intermediate  $\eta^3$ -cyclopentenyl complex, followed by ring-opening, might account for the formation of the unusual  $\eta^5$ -cyclohexadienyl framework (*vide infra*). No alkyne is, apparently, incorporated in this reaction.

Another noteworthy element displayed by the crystal structure of spirocycle complex **78** is the presence of the single cyclopentene unit. The cyclopentene sub-unit was confirmed by locating and refining the hydrogen atoms attached to the  $sp^2$ -carbons of the cyclopentene moiety. The two  $sp^3$ -carbons (C7-C8) have a bond distance of 1.430(9) Å, whereas the separation between the  $sp^3$ - $sp^2$  carbons (C8-C9) is 1.507(10) Å and the  $sp^2$ - $sp^2$  carbons (C9-C10) 1.338(9) Å. The bond length between C7 and C8 is unusually short for a  $sp^3$ - $sp^3$  carbon single bond, compared to the  $sp^3$ - $sp^2$  single bond length between C8 and C9. However, the large standard deviation of all carbon-carbon bond distances of the cyclopentene unit suggests that a small amount of the regioisomer, where the olefin is on the opposite side of the spirocyclopentene

moiety, is also present in the crystal. Furthermore, the X-ray diffraction data were weak, which accounts for the large  $R_1$  and  $wR_2$  values.

In the absence of alkyne, protonation of **72B** with  $\text{HBF}_4 \cdot \text{OEt}_2$  in dichloromethane at low temperature, followed by chromatography and recrystallization from a dichloromethane/diethyl ether mixture, furnishes the bis(1,3-di-*tert*-butylcyclopentadienyl)cobalticenium salt **74** in good yield as a single product with no evidence for decomposition by cyclopentadienyl ligand transfer (Equation 3-21).

Equation 3-21

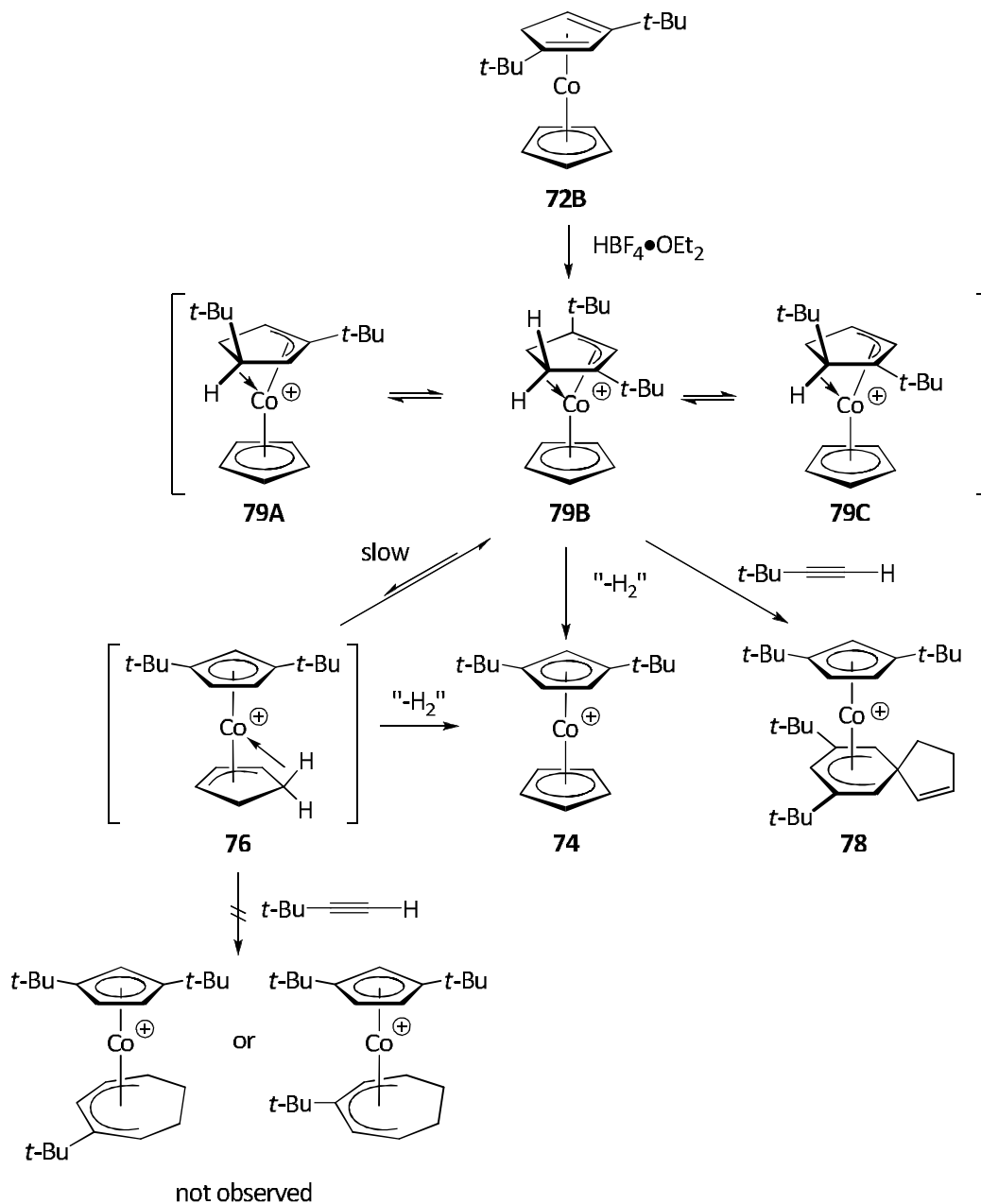


Formation of the unsymmetrical cobalticenium salt arises directly from dehydrogenation of the intermediate agostic  $\eta^3$ -cyclopentenyl complex. This implies that at least one equivalent of alkyne must react with the unsaturated cobalt intermediate prior to any redistribution of the ancillary ligand, yet no alkyne is incorporated into the observed product.

One proposed mechanism for the formation of spirocycle **78** begins with protonation of the 1,3-di-*tert*-butylcyclopentadiene complex **72B** at low temperature, presumably forming an equilibrium mixture of agostic  $\eta^3$ -cyclopentenyl complexes **79A**, **79B**, and **79C** (Scheme 3-10). The absence of any isolable seven-membered ring products after *tert*-butylacetylene addition implies that hydride transfer from the more substituted five-membered ring of agostic complexes **79A/79B/79C** to the unsubstituted ring to form intermediate **76** is either kinetically slow, thermodynamically unfavourable, or a combination of the two factors. In the absence of alkyne, tautomers **79A**, **79B**, or **79C** undergo dehydrogenation to arrive at the unsymmetrical cobalticene complex **74**. The formation of **74** could also occur via dehydrogenation of the agostic  $\eta^3$ -cyclopentenyl complex **76** (Scheme 3-10).

The unusual organic framework of spirocycle **78** strongly suggests that the ten carbon moiety comes from the coupling of the 1,3-di-*tert*-butylcyclopentadienyl ligand with the unsubstituted cyclopentadienyl ligand, followed by extensive rearrangement. Based on the observation that protonation of **72B** in the absence of alkyne does not lead to redistribution of the ancillary ligands, coupling of the two cyclopentadienyl fragments must be preceded by alkyne coordination.

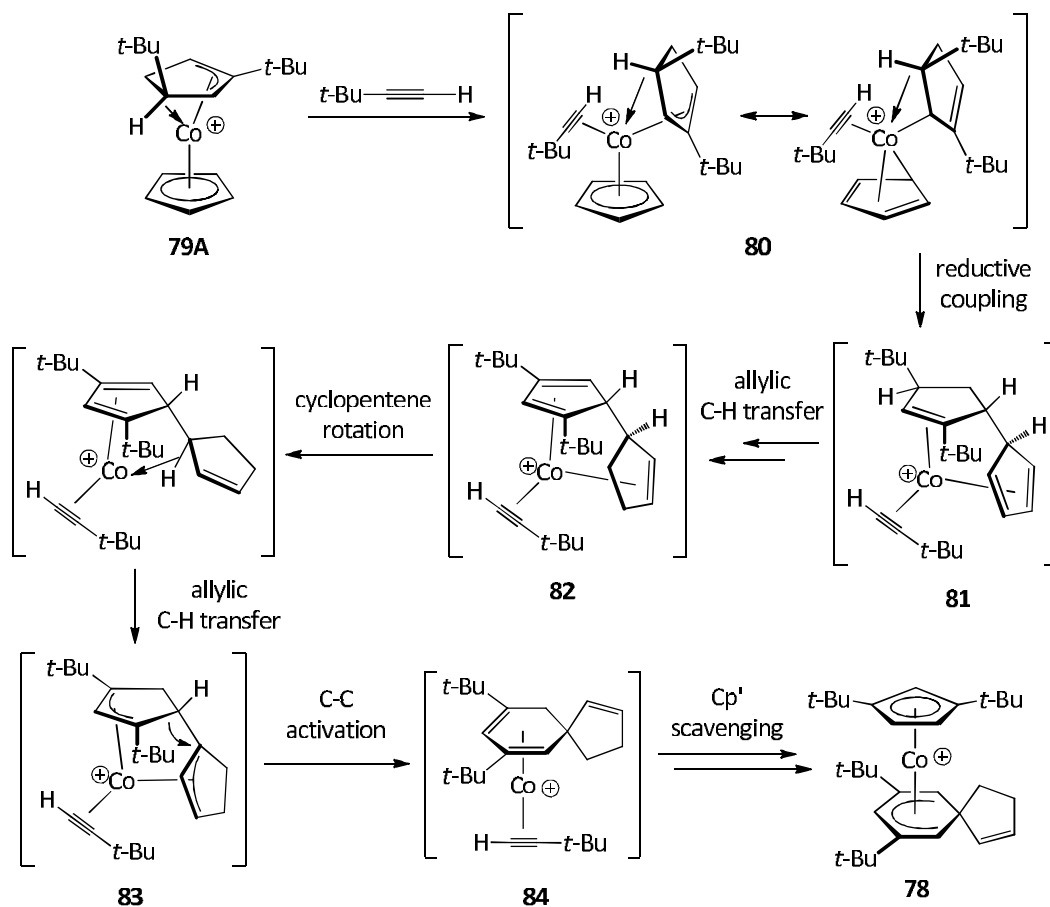
Scheme 3-10



In theory, any of the agostic  $\eta^3$ -cyclopentenyl tautomers **79A**, **79B** or **79C** could react with alkyne to form the mono-alkyne adduct (Scheme 3-11). Due to the steric bulk of the *tert*-butyl substituents on the cyclopentenyl and alkyne

moieties, cyclopentenyl-alkyne coupling does not occur and, instead, the constrained geometry imposed by alkyne coordination may bring both five-membered rings into close proximity, facilitating reductive coupling of the rings, forming cyclopentene-cyclopentadiene intermediate **81** (Scheme 3-11). Equally possible is the *intermolecular* coupling of two equivalents of **80** in order to produce a bimetallic variant of complex **81**.

**Scheme 3-11**



A series of allylic carbon-hydrogen transfers from the cyclopentene ring to the cyclopentadiene ring furnishes tautomer **82**, which undergoes cyclopentene rotation and subsequent allylic carbon-hydrogen transfer to afford the bis(cyclopentenyl) complex **83**. A [1,2]-migration of the carbon-carbon bond in complex **83** from the substituted cyclopentenyl unit to the terminus of the unsubstituted cyclopentenyl unit leads to spirocycle **84**. Further transformations, such as cyclohexadiene-to-cyclohexadienyl isomerization and scavenging of the 1,3-di-*tert*-butylcyclopentadienyl ligand from another agostic intermediate, are needed to furnish the observed spirocyclic product.

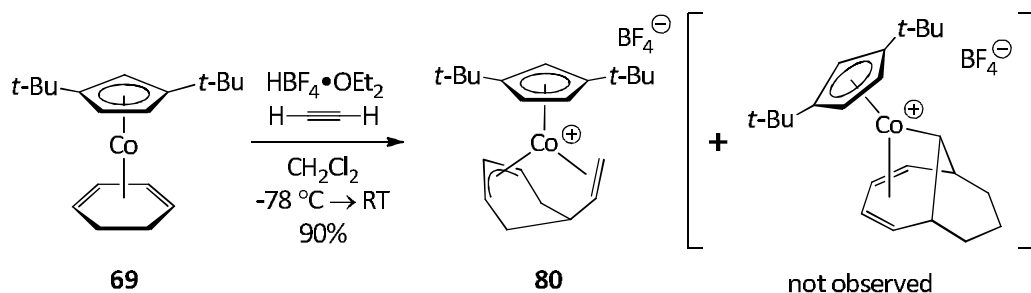
### C. Reactions of (1,3-Di-*tert*-butylcyclopentadienyl)cobalt $\eta^3$ -Cyclohexenyl, $\eta^3$ -Cycloheptenyl, and $\eta^3$ -Cyclooctenyl Complexes With Alkynes

One of the limitations of the pentamethylcyclopentadienyl template is the unwillingness to activate larger cyclic dienes towards ring-expansion. Treatment of the  $(C_5Me_5)Co(\eta^3\text{-cyclohexenyl})$  cation, obtained by protonation of the corresponding cyclohexadiene adduct **41** at low temperature, with terminal alkynes such as acetylene, propyne, or trimethylsilylacetylene, affords products arising from both single and double insertion of alkyne (Chapter 2). However, treatment of the  $(C_5Me_5)Co(\eta^3\text{-cyclohexenyl})$  cation with 2-butyne and larger terminal alkynes affords an intractable paramagnetic residue. Larger ring

endocyclic  $\eta^3$ -allyl complexes, such as  $[(C_5Me_5)Co(\eta^3\text{-cycloheptenyl})]BF_4$  and  $[(C_5Me_5)Co(\eta^3\text{-cyclooctenyl})]BF_4$ , also return paramagnetic residues when treated with excess acetylene and 2-butyne. Given these limitations in the pentamethylcyclopentadienyl template, the 1,3-di-*tert*-butylcyclopentadienyl template was evaluated for potential two-carbon ring-expansion reactions of larger endocyclic allyl systems.

Treatment of the  $(t\text{-Bu}_2C_5H_3)Co(\eta^4\text{-C}_6H_8)$  **69** with  $HBF_4 \cdot OEt_2$  and excess acetylene in dichloromethane at low temperature, followed by chromatography and recrystallization from a mixture of dichloromethane/diethyl ether, affords the  $\eta^2, \eta^3$ -vinylcyclohexenyl complex **80** as the sole product in excellent yield (Equation 3-22). The detection and isolation of the  $\eta^2, \eta^3$ -vinylcyclohexenyl product **80** parallels the results obtained from the pentamethylcyclopentadienyl template. However, there is no evidence for the competitive formation of the  $\eta^1, \eta^4$ -bicyclic product. Both the  $^1H$  and  $^{13}C$  NMR spectra of the vinyl-cyclohexenyl complex **80** are analogous to the  $C_5Me_5$  congener (Chapter 2).

Equation 3-22



The formation of the  $\eta^1,\eta^4$ -bicyclic product in the pentamethylcyclopentadienyl series was attributed to the competitive coordination and insertion of a second equivalent of acetylene versus isomerization to the  $\eta^2,\eta^3$ -vinylcyclohexenyl adduct. Treatment of the  $(C_5Me_5)Co(\eta^3\text{-cyclohexenyl})$  cation with excess acetylene under un-optimized conditions resulted in a 1.5 : 1 ratio of  $\eta^1,\eta^4$ -bicyclic product to  $\eta^2,\eta^3$ -vinylcyclohexenyl complex (Equation 2-10). However, in the case of the 1,3-di-*tert*-butylcyclopentadienyl congener, only the  $\eta^2,\eta^3$ -vinylcyclohexenyl complex **80** is observed, suggesting that the intermediate vinyl-cyclohexene complex adopts a geometry such that isomerization to the  $\eta^2,\eta^3$ -vinylcyclohexenyl complex **80** is much faster or much more favourable than coordination and insertion of a second equivalent of acetylene. The steric bulk of the *tert*-butyl substituents could hinder the approach of a second equivalent of acetylene, allowing isomerization to be the dominant pathway.

Similar to the  $\eta^2,\eta^3$ -vinylcyclohexenyl products **43** and **47** obtained from the pentamethylcyclopentadienyl congener, cobalt vinylcyclohexenyl complex **80** has undergone an allylic carbon-hydrogen bond activation and isomerization to arrive at the isolated product. However, unlike the pentamethylcyclopentadienyl congener, compound **80** does not display a comparable robustness towards air and moisture. Attempted purification via column chromatography on silica gel resulted in formation of a green paramagnetic residue that has not been identified. The markedly different

stabilities to air and moisture displayed by the pentamethylcyclopentadienyl complexes **43** and **47** and 1,3-di-*tert*-butylcyclopentadienyl complex **80** are not well understood, but this suggests that the large *tert*-butyl substituents induce greater coordination strain in the organic fragment. The coordination strain predisposes the vinyl-cyclohexenyl fragment to isomerize to an  $\eta^1$ -allyl, which could be followed by metal-carbon bond homolysis, protonolysis on silica gel, or reaction with dioxygen.

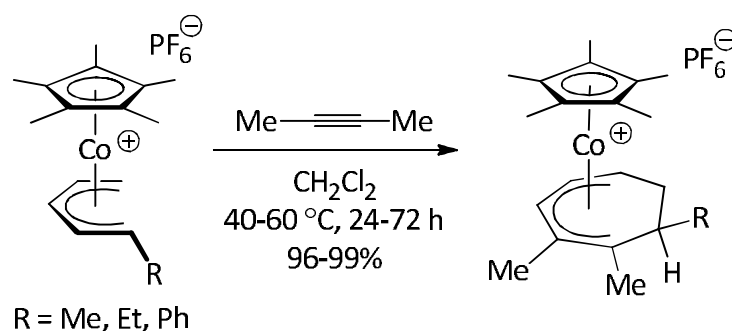
Treatment of  $(t\text{-Bu}_2\text{C}_5\text{H}_3)\text{Co}(1,5\text{-cod})$  **68** with  $\text{HBF}_4 \cdot \text{OEt}_2$  in dichloromethane at low temperature, followed by either excess acetylene or 2-butyne, afforded a paramagnetic residue unlike the analogous reaction of cyclohexadiene adduct **69** with strong acid and alkyne (Equation 3-22). Furthermore, warming of the protonated reaction mixture to ambient temperature in the absence of alkyne does not furnish the acyclic  $\eta^5$ -*anti*-1-propylpentadienyl complex, as Spencer reported for the pentamethylcyclopentadienyl congener, but instead leads to the formation of a paramagnetic residue.

These observations establish that the two-carbon ring-expansion remains limited to five-membered ring substrates and presumably cannot be extended to larger ring systems using substituted cyclopentadienyl ancillary ligands.

## D. Synthesis of Acyclic $\eta^5$ -Pentadienyl Complexes of Cobalt

Previously, Witherell and Ylijoki in this group prepared a library of substituted acyclic  $\eta^5$ -pentadienyl complexes of cobalt and discovered the first efficient [5 + 2] alkyne-pentadienyl cycloaddition reaction (Equation 3-23).<sup>122, 176</sup>

**Equation 3-23**

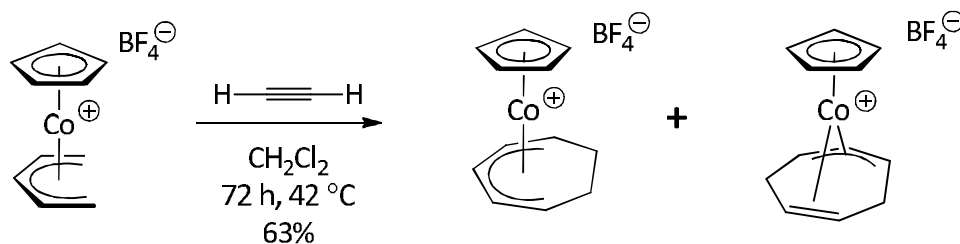


A range of alkynes can be incorporated, but only a limited set of substitution patterns on the acyclic  $\eta^5$ -pentadienyl fragment are tolerated. Specifically, alkyl or aryl substitution at either terminus of the  $\eta^5$ -pentadienyl moiety is required to promote reactivity towards alkynes, whereas substitution at either the 2- or 3-positions inhibits reactivity. The unsubstituted  $\eta^5$ -pentadienyl moiety is unreactive towards alkyne as well.

More recently, Kirk in this group reported that substituted pentadienyl complexes of the form  $[(C_5H_5)Co(\eta^5\text{-pentadienyl})]BF_4$  also incorporate a range of alkynes to form the corresponding seven-membered ring products, albeit in

variable yield.<sup>177</sup> Interestingly, Kirk found that the unsubstituted  $\eta^5$ -pentadienyl complex reacts with excess acetylene to form two isomeric seven-membered ring products in moderate yield differing by the ligand coordination mode (Equation 3-24).

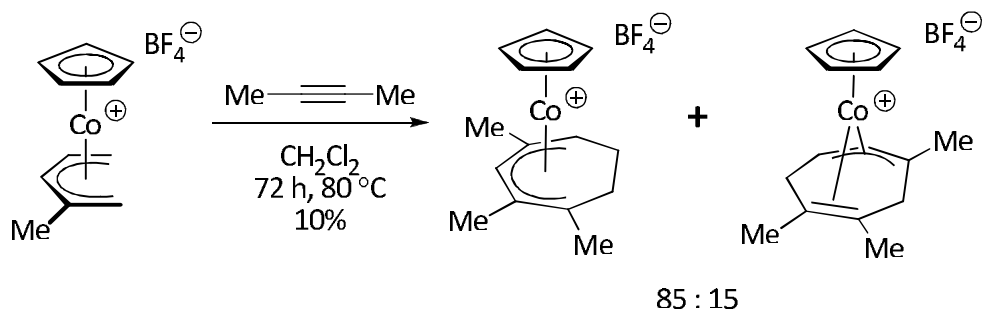
**Equation 3-24**



76 : 24

More surprisingly, 2-substituted  $\eta^5$ -pentadienyl complexes, which are unreactive towards alkynes in the  $C_5Me_5$  series, slowly incorporate 2-butyne to form seven-membered ring products, albeit only at elevated temperature and in low yield (Equation 3-25). No reaction is observed when 3-substituted pentadienyl complexes are used.

**Equation 3-25**



The incorporation of alkyne into acyclic  $\eta^5$ -pentadienyl complexes of cobalt is initiated by  $\eta^5$ - to  $\eta^3$ -pentadienyl isomerization, which is unusually facile for 1-substituted pentadienyl complexes. Subsequent alkyne coordination, insertion, and cyclization is fully consistent with the mechanism for [3 + 2 + 2] allyl-alkyne cycloaddition discussed in Chapter 2 (Scheme 2-5).

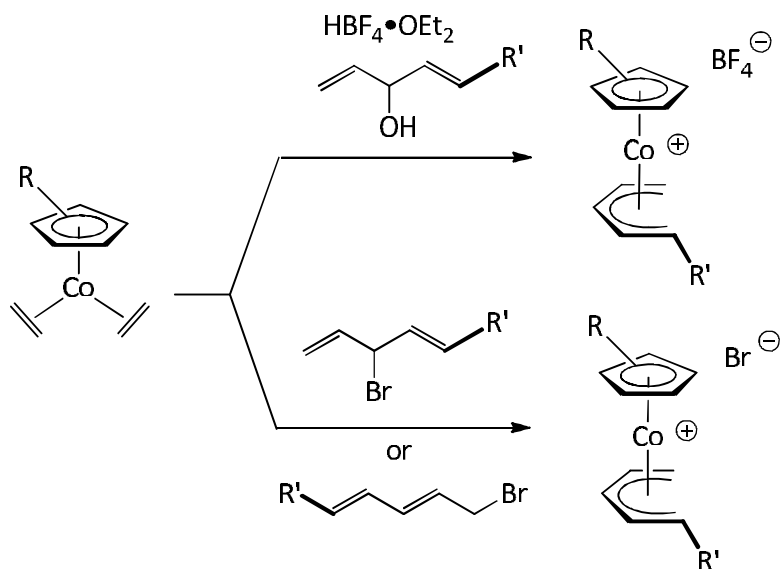
Compared to the  $\text{C}_5\text{Me}_5$  series, the more electron-deficient  $\text{C}_5\text{H}_5$  series modestly promotes [5 + 2] cycloaddition of unsubstituted and 2-substituted pentadienyl frameworks. The difference in reactivity between the  $\text{C}_5\text{Me}_5$  and  $\text{C}_5\text{H}_5$  series can be attributed to the relative degree of backbonding experienced by the pentadienyl framework. Compared to the  $\text{C}_5\text{H}_5$  ancillary ligand, the more electron-rich  $\text{C}_5\text{Me}_5$  ligand donates more electron density to the cobalt centre, which in turn increases the degree of back-bonding to the pentadienyl moiety. Stronger back-bonding favours  $\eta^5$ -hapticity, inhibiting the  $\eta^5$ - to  $\eta^3$ -isomerization required for alkyne coordination. Using less strongly donating cyclopentadienyl ancillary ligands should thus decrease the degree of back-bonding and encourage  $\eta^5$ - to  $\eta^3$ -isomerization of the pentadienyl ligand. This line of reasoning is

supported by the thermal stability of the pentadienyl complexes:  $\eta^5$ -pentadienyl complexes in the  $C_5Me_5$  series are both air and moisture stable while those in the  $C_5H_5$  series are susceptible to decomposition in the air.

The 1,3-di-*tert*-butylcyclopentadienyl ancillary ligand should be less electron-rich than the  $C_5Me_5$  ligand; thus, the  $\eta^5$ -pentadienyl fragment should be more amenable toward dissociation to  $\eta^3$ -hapticity, freeing a coordination site for incoming alkyne. No other substituted cyclopentadienyl ancillary ligand has been investigated for [5 + 2] pentadienyl-alkyne cycloaddition reactivity; thus, a quick study using the available 1,3-di-*tert*-butylcyclopentadienyl cobalt system was undertaken.

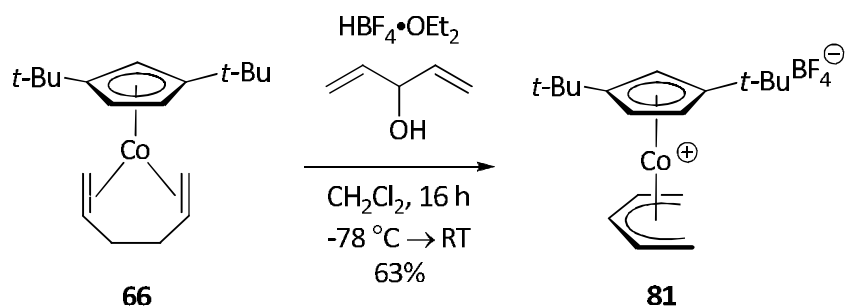
Two efficient and facile entries into acyclic  $\eta^5$ -pentadienyl complexes of cobalt are ligand exchange/protonolysis of substituted dienols, such as 2,4-pentadien-3-ol, and oxidative addition of substituted brominated dienes, such as 1-bromo-2,4-pentadiene and 3-bromo-1,5-pentadiene (Scheme 3-12).<sup>122</sup>

Scheme 3-12



The availability of cobalt 1,5-hexadiene complex **66** and the temperature sensitivity of bis(ethylene) complex **65** led us to probe the synthesis of (1,3-di-*tert*-butylcyclopentadienyl)cobalt( $\eta^5$ -pentadienyl) complexes starting from 1,5-hexadiene complex **66**. Treatment of cobalt 1,5-hexadiene complex **66** with strong acid in dichloromethane at low temperature, followed by 1,4-pentadien-3-ol, afforded the acyclic  $\eta^5$ -pentadienyl complex **81** in moderate yield (Equation 3-26). The product was purified by column chromatography and recrystallized from a dichloromethane/diethyl ether mixture.

### Equation 3-26



Crystals suitable for X-ray diffraction analysis were obtained from a dichloromethane/diethyl ether mixture (Figure 3-6). The bond distances and angles of  $\eta^5$ -pentadienyl complex **81** are consistent with related examples previously characterized in this group.<sup>176</sup> Similar to other cationic cobalt(III)  $\eta^5$ -pentadienyl complexes,  $\eta^5$ -pentadienyl complex **81** is air and moisture stable and can be purified on the bench by column chromatography.

Our proposed mechanism for the formation of the  $\eta^5$ -pentadienyl complex begins with protonation of 1,5-hexadiene complex **66**, initially forming an  $\eta^1, \eta^2$ -hexenyl complex **82** (Scheme 3-13).

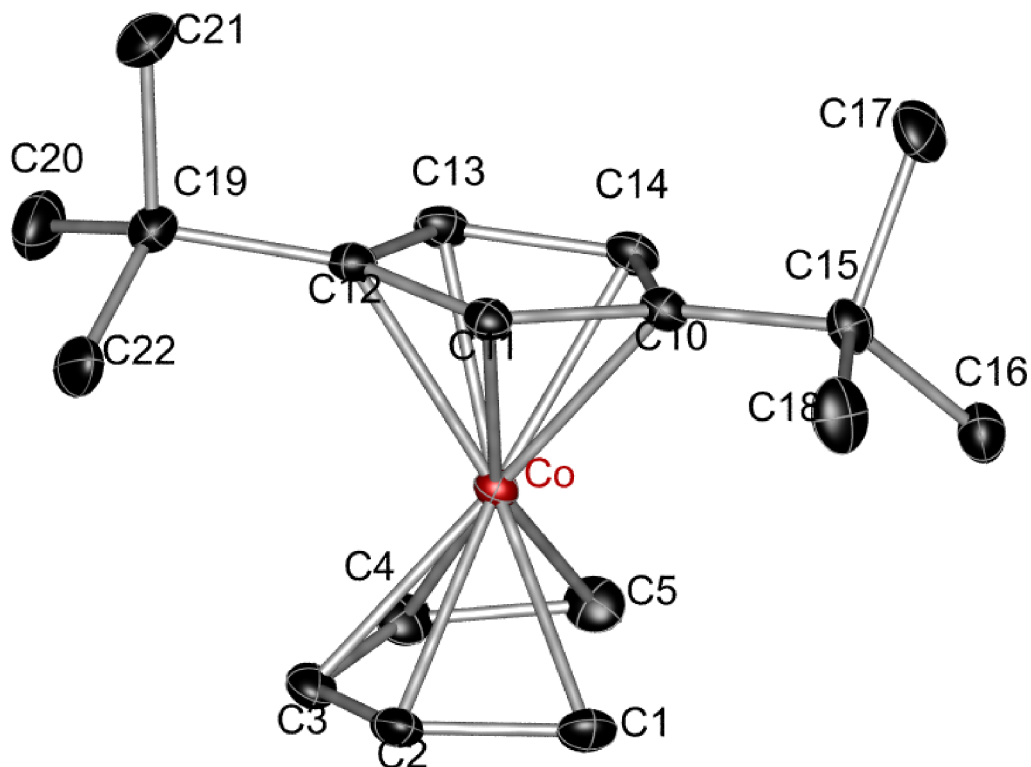
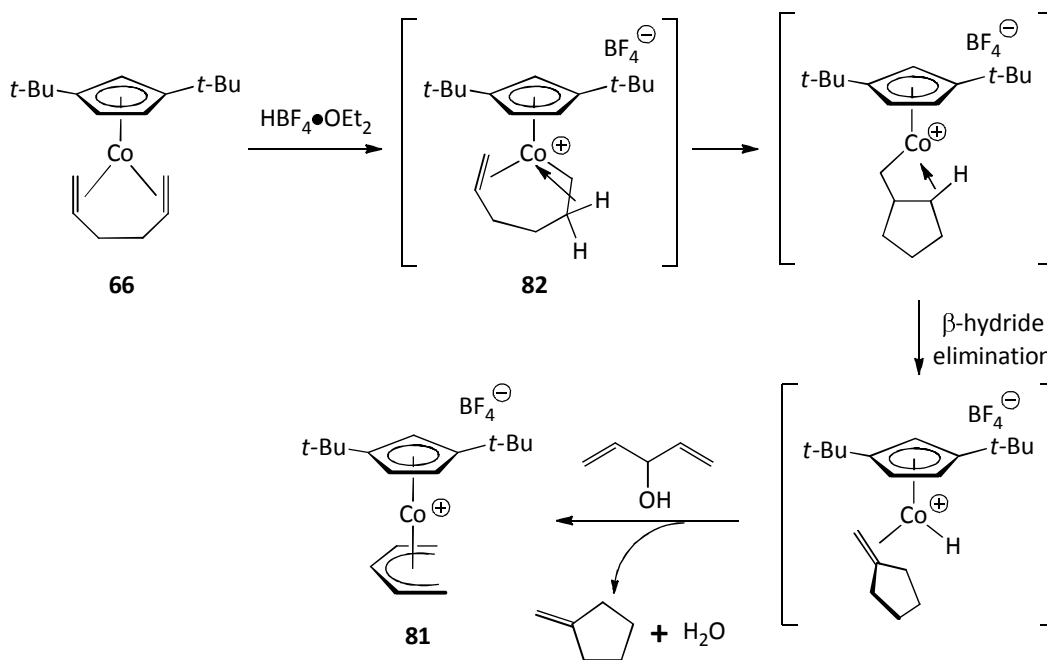


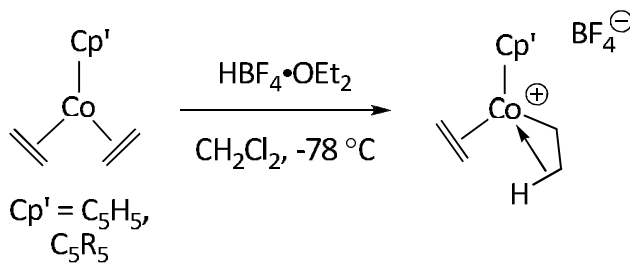
**Figure 3-6:** Perspective view of the  $[(t\text{-Bu}_2\text{C}_5\text{H}_3)\text{Co}(\eta^5\text{-pentadienyl})]$  cation **81**. Final residuals:  $R_1 = 0.0454$ ,  $wR_2 = 0.1377$ . Data collected at  $-100\text{ }^\circ\text{C}$ . Non-hydrogen atoms are represented by Gaussian ellipsoids at the 20% probability level. Selected bond distances ( $\text{\AA}$ ): C1-C2, 1.406(5); C2-C3, 1.411(5); C3-C4, 1.418(5); C4-C5, 1.408(5); Co-C1, 2.109(3); Co-C2, 2.042(3); Co-C3, 2.064(3); Co-C4, 2.037(3); Co-C5, 2.093(3). The dihedral angle between the planes defined by C1 to C5 and C11 to C14 =  $9.97(16)^\circ$ . The torsional angle defined by C1 to C4 =  $-8.9(5)^\circ$  and by C2 to C5 =  $7.2(5)^\circ$ .

**Scheme 3-13**



While no evidence for compound **82** exists, both Spencer<sup>178, 179</sup> and Brookhart<sup>180-183</sup> have reported the addition of strong acid to the bis(alkene) complex  $(\text{C}_5\text{R}_5)\text{Co}(\text{C}_2\text{H}_4)_2$  ( $\text{R} = \text{H}, \text{Me}$ ) at low temperature yields the cationic agostic ethyl complex (Equation 3-27).

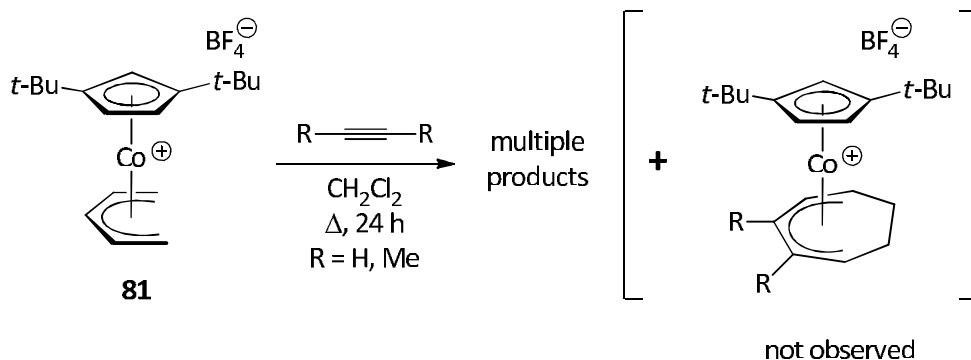
**Equation 3-27**



It is possible that complex **82** does not undergo direct ligand exchange but, instead, undergoes quick migratory cyclization followed by  $\beta$ -hydride elimination to afford a cobalt hydrido olefin complex. Displacement of the bound olefin by incoming pentadienol is followed by loss of water, affording the isolated acyclic pentadienyl complex **81**. However, no attempt to analyze the volatile fraction to confirm the loss of olefin was made.

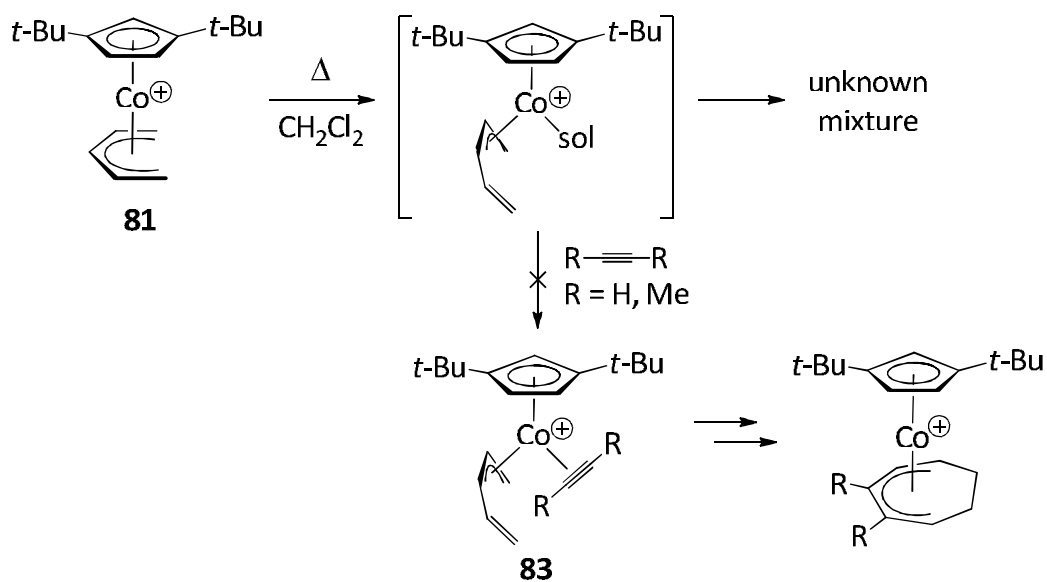
The reactivity of acyclic pentadienyl complex **81** towards alkyne was probed by treating a solution of complex **81** in dichloromethane with excess acetylene at ambient temperature (Equation 3-28). After 24 hours, however, no reaction had occurred, as evidenced by  $^1\text{H}$  NMR spectroscopy. Performing the reaction at elevated temperatures resulted in complete consumption of the starting material. However, the product mixture was spectroscopically complex and contained a multitude of unidentified products. The reaction was repeated with 2-butyne, but again, no incorporation of alkyne was observed at ambient temperature and an intractable residue was obtained at elevated temperature.

**Equation 3-28**



One reasonable interpretation of these data is that isomerization of the  $\eta^5$ -pentadienyl fragment to the  $\eta^3$ -hapticity is disfavoured at ambient temperature. At elevated temperature, complete consumption of the starting material suggests that the intermediate  $\eta^3$ -pentadienyl complex decomposes competitively with alkyne coordination (Scheme 3-14).

**Scheme 3-14**



This is plausible since the expected pentadienyl-alkyne complex **83**, once formed, should readily convert to the seven-membered ring product. The steric bulk of the *tert*-butyl substituents on the disubstituted ancillary ligand most likely inhibits alkyne coordination. In the absence of a strongly coordinating ligand, the cobalt complex could further isomerize to  $\eta^1$ -hapticity, followed by cobalt-carbon bond homolysis and loss of the pentadienyl fragment.

Alternatively, the pentadienyl ligand could couple intramolecularly with the cyclopentadienyl ligand, similar to the proposed mechanism for the formation of complex **78**.

## E. Conclusions

The initial goal of developing the chemistry of the 1,3-di-*tert*-butylcyclopentadienyl cobalt fragment was to address the limitations of the pentamethylcyclopentadienyl system; namely, the poor-to-moderate yields obtained using disubstituted alkynes during [5 + 2] cyclopenteny-alkyne cycloexpansion reactions and the generally limited scope of the two-carbon ring expansion process.

Unfortunately, the isolated yields of seven-membered products using the 1,3-di-*tert*-butylcyclopentadienyl system with alkyne have been universally low, in contrast to the (1-*tert*-butyl-3-methyl)cyclopentadienyl or pentamethylcyclopentadienyl systems. The large difference in reactivity observed when a methyl substituent is exchanged for a *tert*-butyl substituent in the disubstituted cyclopentadienyl systems is surprising. Furthermore, the seven-membered ring products are isolated as one component of complex product mixtures, indicating that the cationic agostic intermediates are not selective for ring-expansion. Further purification of the ring-expanded products

by simple chromatography is impossible as the carbocyclic products are prone to decomposition on silica gel, unlike the  $C_5Me_5$  congeners.

Although the [5 + 2] cyclopentenyl-alkyne ring-expansion reaction has been studied in detail by Dzwiniel, the cycloexpansion of larger ring systems remains elusive. While the cyclohexenyl system selectively undergoes alkyne insertion instead of cycloexpansion, the cycloheptenyl and cyclooctenyl systems afford intractable product mixtures. It is reasonable to conclude that an entirely new ancillary ligand design is required in order to expand the scope of the ring-expansion process.

The detailed mechanism of the ring-expansion process is not well understood. Several mechanisms have been proposed, but recent computational investigation has offered new mechanistic insight.<sup>175</sup> This and related chemistry will be discussed in the following chapter.

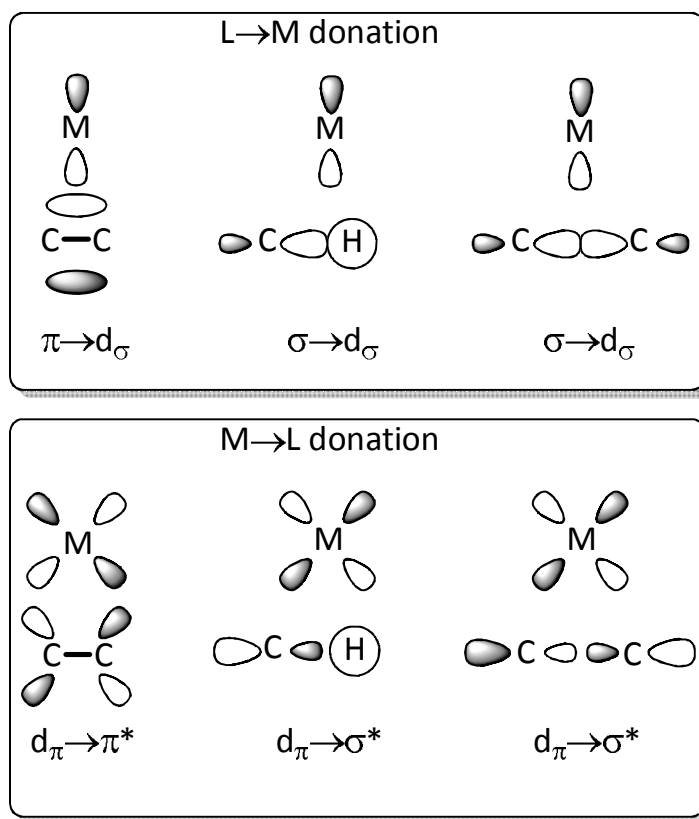
## Chapter 4. Mechanism and Intermediates in the Cyclopentenyl/Alkyne Carbon-Carbon Bond Activation Process

### Section 1. Introduction

Carbon-carbon  $\sigma$ -bond activation has received a tremendous amount of scientific and technological interest due to the abundance and poor reactivity of relatively inert alkanes. Industry has largely used heterogeneous catalysts or naked metal ions to activate alkanes.<sup>184</sup> Furthermore, skeletal rearrangements of alkanes using platinum oxide catalysts have been reported.<sup>185, 186</sup> However, homogeneous activation of carbon-carbon  $\sigma$ -bonds under ambient conditions is not a routine process.

In most heterogeneous and homogeneous systems, carbon-hydrogen bond activation is much more prevalent than carbon-carbon  $\sigma$ -bond activation. Due to the directionality of the carbon-carbon single bond, the corresponding anti-bonding orbitals required for oxidative cleavage are less accessible, whereas carbon-hydrogen anti-bonding orbitals are located on the periphery of the substrate and hence are more easily accessible (Figure 4-1). In most cases where carbon-carbon  $\sigma$ -bond activation does occur, rapid and reversible carbon-hydrogen bond activation has occurred.<sup>187</sup>

**Figure 4-1: Metal-Ligand Orbital Interactions**



Carbon-hydrogen bond activation is also more prevalent than carbon-carbon  $\sigma$ -bond activation due to thermodynamic factors. The carbon-carbon single bond has a dissociation energy of approximately 356 kJ/mol (85 kcal/mol) whereas a typical metal-carbon bond has a dissociation energy of 146 kJ/mol (35 kcal/mol),<sup>20, 188</sup> making the overall process endothermic. However, the strength of the carbon-hydrogen bond in methane is approximately 435 kJ/mol (104 kcal/mol), whereas the strength of a metal-hydride bond is approximately 251 kJ/mol (60 kcal/mol),<sup>189-191</sup> making the overall process less energy intensive than carbon-carbon  $\sigma$ -bond activation.

Due to this combination of thermodynamic and kinetic factors, other processes, such as carbon-hydrogen bond activation, are typically faster and more favourable than carbon-carbon  $\sigma$ -bond activation. Consequently, various strategies have been demonstrated to enhance the likelihood of carbon-carbon bond activation over carbon-hydrogen bond activation, often including a combination of ring strain, intramolecular  $\beta$ -carbon activation, activating functional groups, and proximity effects.<sup>192-194</sup>

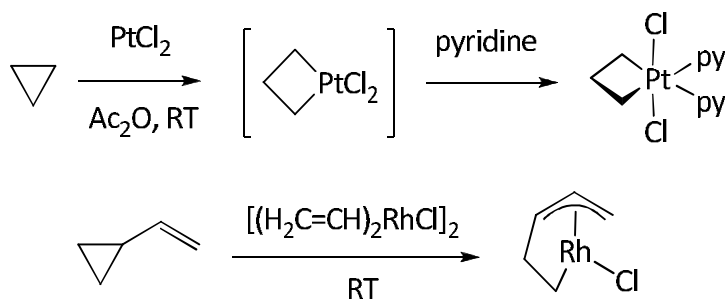
#### **A. Activation of Carbon-Carbon $\sigma$ -Bonds In Strained Ring Systems**

Due to the endothermic nature of carbon-carbon  $\sigma$ -bond activation, an external driving force is generally used to induce the reaction to proceed. The use of cyclopropanes and cyclobutanes is particularly advantageous due to the energy associated with ring strain, weakening the  $\sigma$ -bond, so that the formation of the metal-activated product overcomes the endothermic nature of unstrained carbon-carbon  $\sigma$ -bond activation.

The use of cyclopropanes as substrates for metal-mediated carbon-carbon bond activation has been known at least since 1955 when Tipper reported the insertion of platinum into the carbon-carbon bond (Scheme 4-1).<sup>195</sup> Jun,<sup>196</sup> Wender,<sup>197-202</sup> and others<sup>203-213</sup> have independently reported the ring-opening of vinylcyclopropane moieties in cycloaddition reactions used for natural product synthesis. The insertion into cyclopropane is driven by both the ring

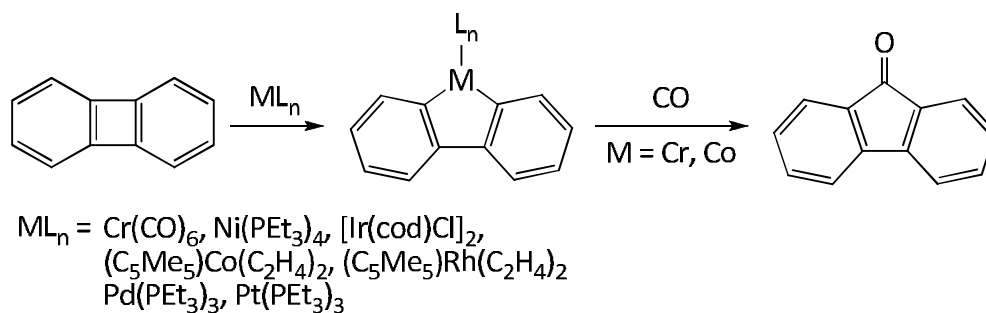
strain of the substrate as well as the improved directionality of the anti-bonding orbitals.

#### Scheme 4-1



The cyclobutadiene ring-opening of biphenylene has been reported using chromium,<sup>214</sup> iridium,<sup>215</sup> nickel,<sup>216</sup> rhodium,<sup>217, 218</sup> cobalt,<sup>217, 218</sup> platinum<sup>219</sup> and palladium (Scheme 4-2).<sup>219</sup> In most cases, the metal inserts into the cyclobutadiene moiety to produce the metalacyclopentadiene, whereas when chromium or cobalt are used, carbonyl insertion and formation of 9-fluorenone is observed.

#### Scheme 4-2

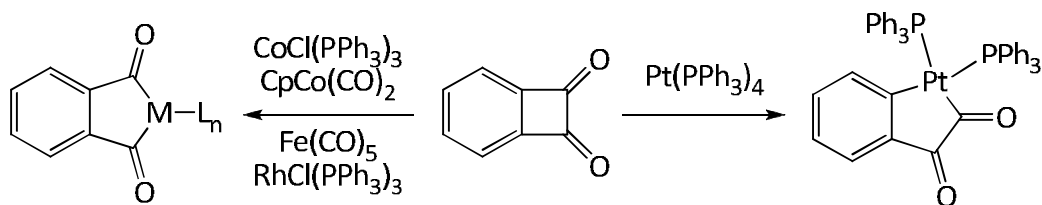


## B. Carbonyl Group Activation of Carbon-Carbon $\sigma$ -Bonds

Carbon-carbon single bonds between the carbonyl carbon and the  $\alpha$ -carbon are activated compared to other carbon-carbon single bonds and thus are more amenable to metal insertion. The bond dissociation energy of the carbon-carbon bond in ethane is 368 kJ/mol (88 kcal/mol) while the dissociation energy in acetone is 343 kJ/mol (82 kcal/mol).<sup>220</sup> Furthermore, initial coordination of the metal fragment to the carbonyl oxygen brings the adjacent carbon-carbon bond into close proximity to the metal centre, increasing the likelihood carbon-carbon  $\sigma$ -bond activation.

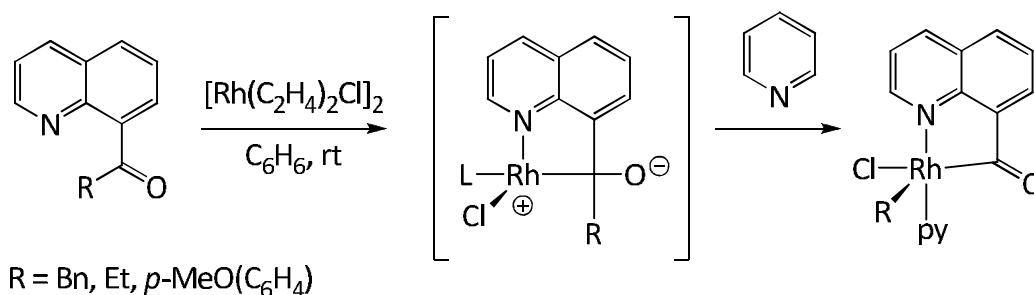
Liebeskind demonstrated that treatment of benzocyclobutane-1,2-dione with a platinum(0) source results in unsymmetrical cleavage of the four-membered ring, whereas other low-valent late metal sources result in symmetrical activation to afford phthaloyl metal complexes (Scheme 4-3).<sup>221, 222</sup> Both unsymmetrical and symmetrical cleavage of these bicyclic diones can be attributed to the activation of the carbon-carbon bond adjacent to the functionality and the strain energy contained in the cyclobutane moiety.

**Scheme 4-3**



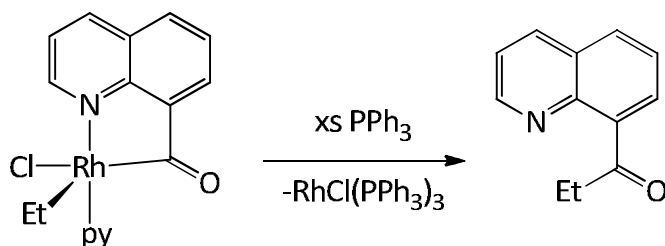
Suggs has used both the activating ability of the carbonyl functionality and proximity effects to promote the cleavage of 8-quinolyl alkyl ketones (Scheme 4-4). Upon coordination of the quinoline nitrogen to rhodium, direct nucleophilic attack of the rhodium on the carbonyl functionality forms the tetrahedral intermediate. Reformation of the ketone is concomitant with hydrocarbyl migration to the rhodium centre, which is trapped as the pyridine adduct.<sup>223, 224</sup> Transfer of the hydrocarbyl moiety may occur in a concerted or step-wise fashion analogous to a semi-pinacol rearrangement.

**Scheme 4-4**



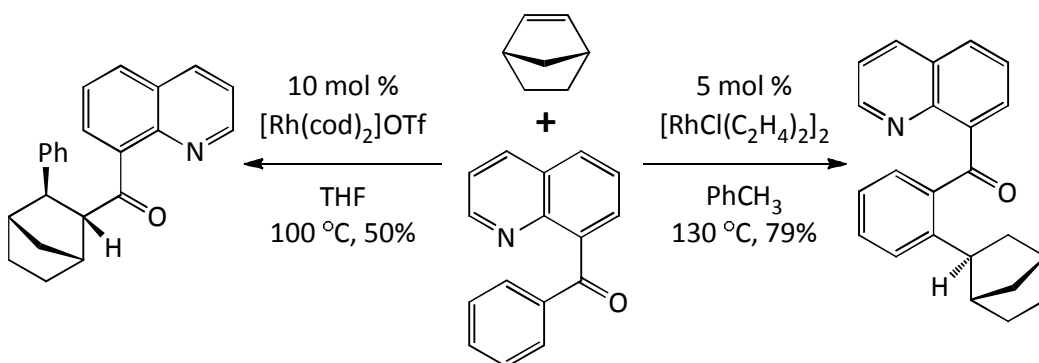
The addition of a softer Lewis base such as triphenylphosphine initiates reductive coupling to regenerate the starting quinoline derivative, demonstrating that carbon-carbon bond activation is a reversible process (Equation 4-1).

#### Equation 4-1



Douglas has recently reported that competitive *ortho*-carbon-hydrogen bond activation and carbon-carbon bond activation of 8-quinolyl alkyl ketones can be controlled under the appropriate catalyst and solvent conditions (Scheme 4-5).<sup>225</sup>

#### Scheme 4-5



### C. Nitrile Group Activation of Carbon-Carbon $\sigma$ -Bonds

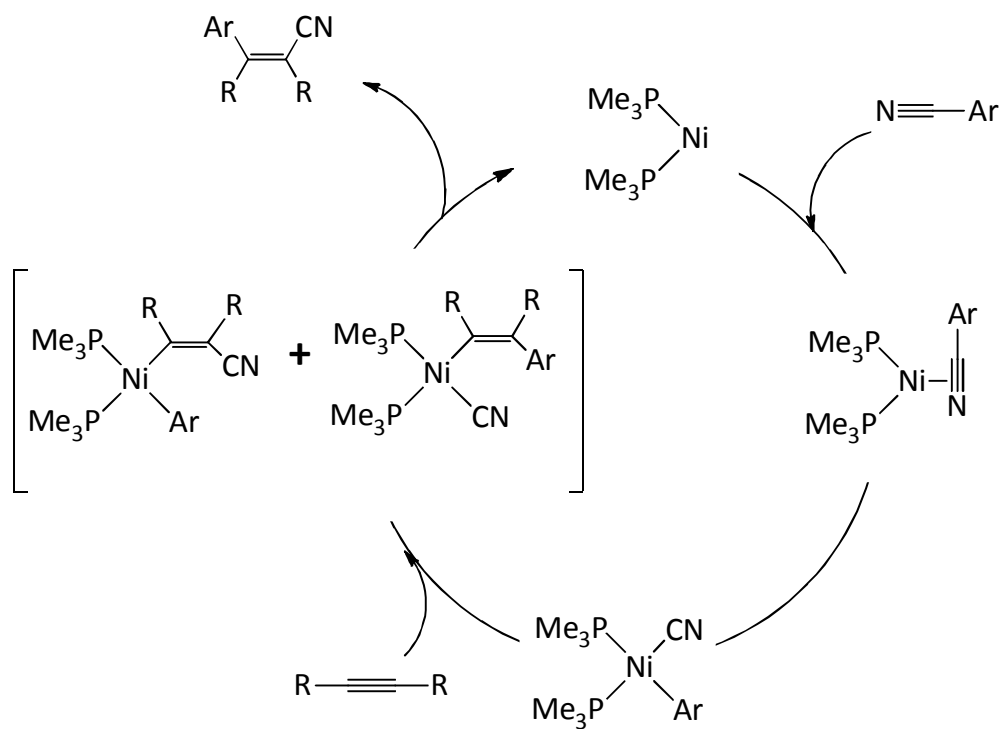
The scission of carbon-carbon  $\sigma$ -bond in nitriles has also been reported. Early reports on the activation of nitriles were performed using nickel,<sup>226-229</sup> and

platinum.<sup>230</sup> Activations using cobalt<sup>231</sup> and molybdenum<sup>232</sup> have also been reported. Activations using rhodium and iron were assisted by trialkyl- and triarylsilyl groups.<sup>233-237</sup>

Computational calculations using benzonitrile as a substrate show that a side-on  $\pi$ -bonding of the nitrile is required for activation of the carbon-carbon  $\sigma$ -bond with phosphine-supported nickel(0) systems.<sup>238, 239</sup>

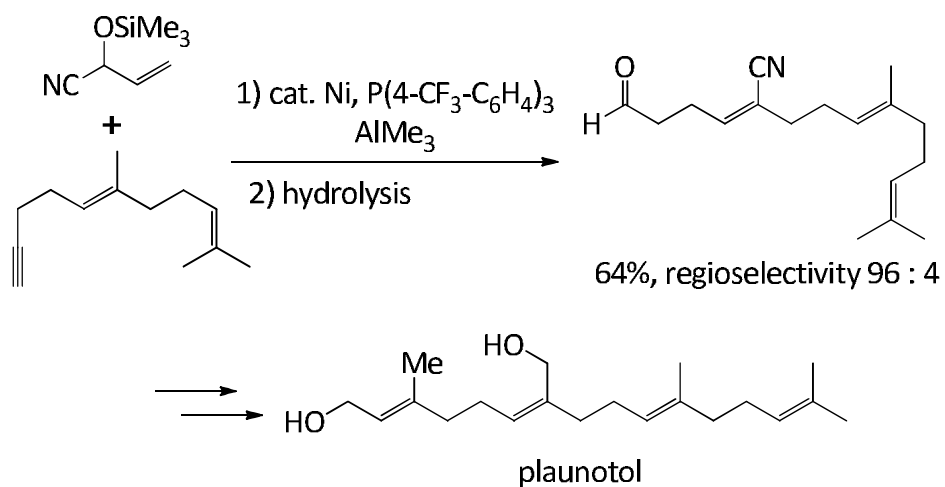
While stoichiometric activation of the carbon-carbon  $\sigma$ -bond in nitriles is well known, catalytic examples are not as common. Hiyama has reported a catalytic nickel(0) arylocyanation of alkynes to produce acrylonitrile derivatives (Scheme 4-6).<sup>240, 241</sup>

**Scheme 4-6**



This process has received considerable attention from the chemical industry due to the potential utility of substituted acrylonitrile derivatives. Side-on coordination of the aryl nitrile and subsequent oxidative cleavage affords the aryl cyano metal complex. Coordination of alkyne can occur and can either insert into the metal cyanide bond or, more commonly, the metal aryl bond. Upon insertion, a reductive elimination step from either intermediate furnishes the product and regenerates the starting nickel(0) bisphosphine complex. More recently, Hiyama has used this methodology to prepare polysubstituted 2,5-hexadienenitriles, which are used as precursors for the total synthesis of plaunotol, an antibacterial natural product active against *Helicobacter pylori* (Scheme 4-7).<sup>242</sup>

**Scheme 4-7**

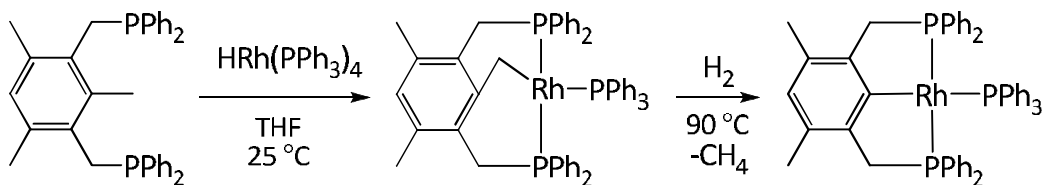


## D. Proximity Effects

The use of proximity effects is one of the principal strategies used to activate carbon-carbon bonds. If a carbon-carbon  $\sigma$ -bond is brought into close proximity to a metal upon substrate coordination, some of the problems associated with weak interactions and steric congestion are alleviated. Milstein has used proximity effects to great effect when employing a pincer-type ligand, where the Lewis basic phosphine or amine arms of the ligand brings the metal close to a carbon-carbon or carbon-hydrogen bond of interest.

Milstein *et al.* have found that the addition of a rhodium(I) source to a diphosphine-pincer type ligand results in coordination initially but, upon subsequent heating in an atmosphere of dihydrogen, transforms to the carbon-carbon activated product and produces methane (Scheme 4-8).<sup>243</sup>

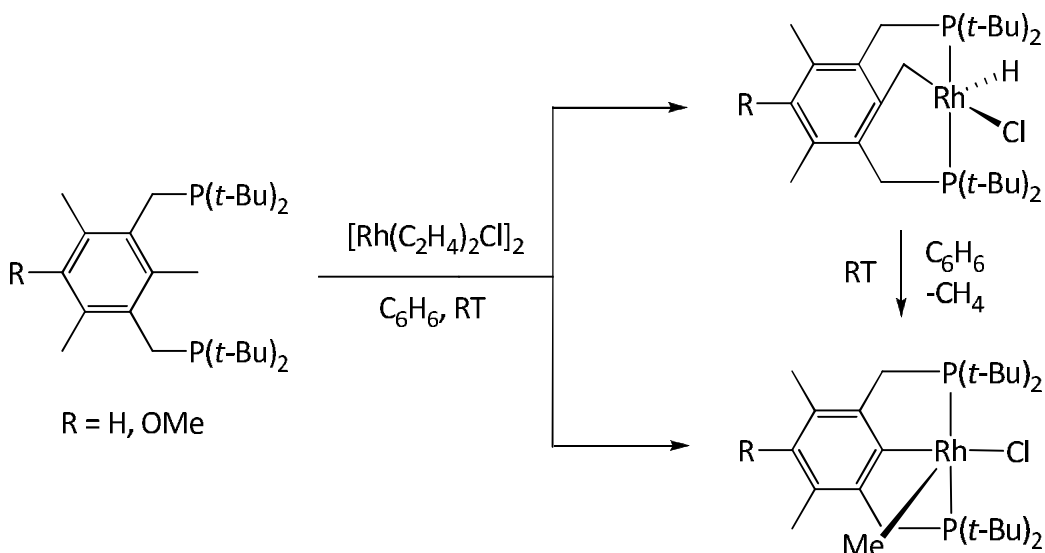
**Scheme 4-8**



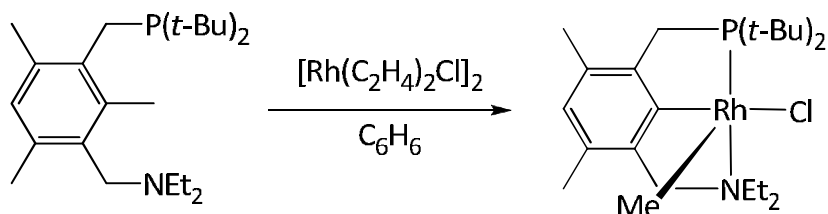
Milstein has also demonstrated in a closely related system that both the carbon-hydrogen bond activated product and the carbon-carbon bond activated product are produced. Under the reaction conditions used, however, carbon-

hydrogen bond activation is reversible while carbon-carbon bond activation is irreversible (Scheme 4-9).<sup>187</sup> When a mixed phosphine-amine pincer ligand is used, carbon-hydrogen activation is not observed even at -50 °C, and the only product isolated was from carbon-carbon activation (Equation 4-2).<sup>244</sup>

**Scheme 4-9**



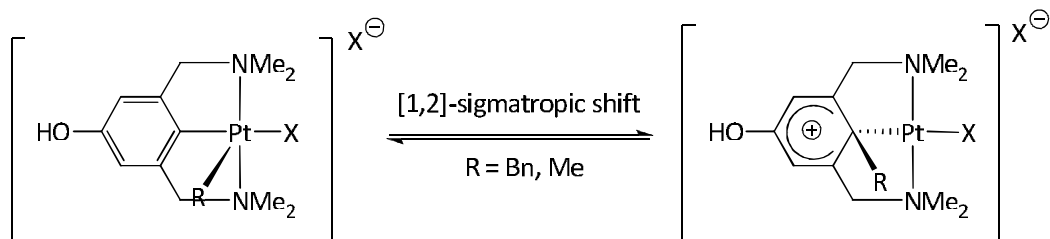
**Equation 4-2**



Van Koten *et al.* have reported a similar carbon-carbon  $\sigma$ -bond scission using a pincer ligand supported platinum complex (Equation 4-3).<sup>245, 246</sup> In contrast to Milstein's mechanistic proposal, van Koten proposes an electrophilic

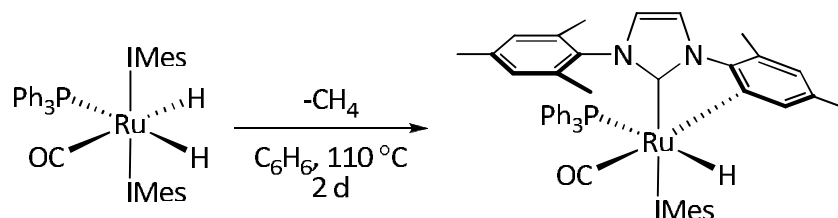
aromatic substitution-type mechanism to rationalize the hydrocarbyl migration. The addition of methyl or benzyl halide to a platinum(II) pincer complex generates the platinum(IV) hydrocarbyl halide cation. A [1,2]-sigmatropic shift of the hydrocarbyl group to the arene generates a platinum arenium complex. The coupled organic product can be released by the addition of cyanide anion. The microscopic reverse of the [1,2]-sigmatropic shift is a carbon-carbon  $\sigma$ -bond activation.

**Equation 4-3**



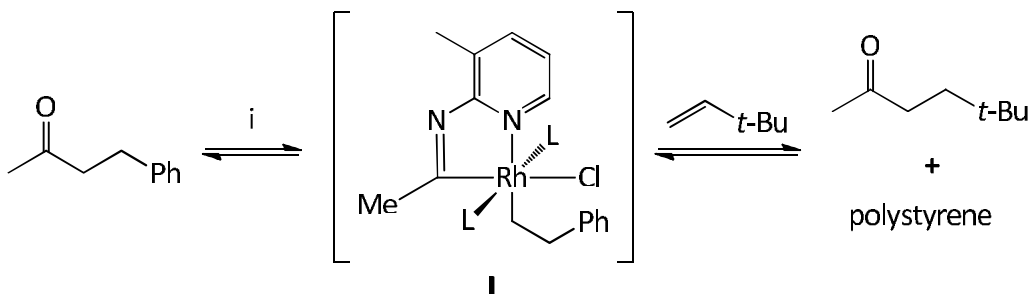
Whittlesey *et al.* have observed another example of proximity-driven carbon-carbon  $\sigma$ -bond activation. They found that heating of a ruthenium N-heterocyclic carbene complex over two days results in the activation of a mesityl group and subsequent elimination of methane (Equation 4-4).<sup>247</sup>

#### Equation 4-4



Recently, Jun has reported the use of metal-organic cooperative catalysis (MOCC) as an avenue to cleave carbon-carbon  $\sigma$ -bonds (Scheme 4-10).<sup>248</sup>

#### Scheme 4-10

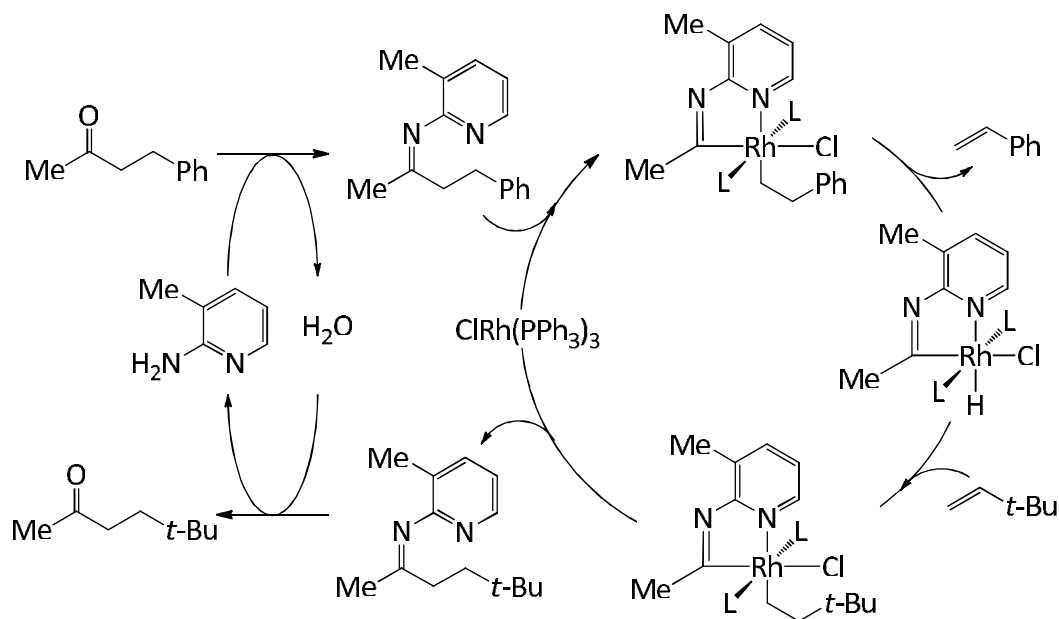


i)  $\text{RhCl}(\text{PPh}_3)_3$  (5 mol%), 2-amino-3-picoline (100 mol%)  
toluene, 150 °C, 48 h, 84%

Benzylacetone will react with 2-amino-3-picoline to afford the corresponding imine, which more readily undergoes carbon-carbon  $\sigma$ -bond scission (Scheme 4-11). Upon coordination of the imine to the rhodium(I) complex, the carbon-carbon bond adjacent to the imine functionality is cleaved to generate an (iminoacyl)rhodium(III) complex I, which subsequently undergoes  $\beta$ -hydride elimination to afford the (iminoacyl)rhodium(III) hydride complex and

styrene. Coordination of 3,3-dimethyl-1-butene to the rhodium(III) complex is followed by sequential migratory insertion into the rhodium-hydride bond and reductive elimination to afford the imine product. An aqueous work-up furnishes the corresponding ketone. These reactions are at thermodynamic equilibrium and are driven to completion using either excess alkene or by the formation of a more thermodynamically stable byproduct.

**Scheme 4-11**

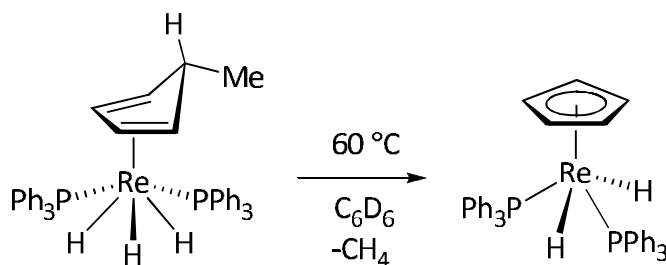


### E. $\beta$ -Carbon Elimination and Aromatization

Ligand aromatization forms a small subset of general  $\beta$ -alkyl elimination reactions, whereby substituted  $\eta^4$ -cyclopentadiene and  $\eta^5$ -cyclohexadienyl

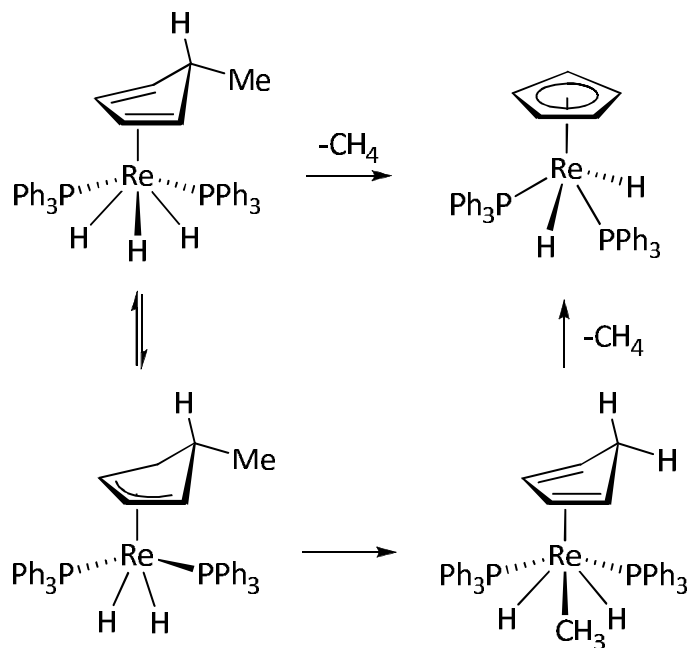
ligands are activated to produce the corresponding dealkylated aromatic  $\eta^5$ -cyclopentadienyl and  $\eta^6$ -arene moieties. These transformations typically require an open coordination site, and are driven by the large stabilization in free energy associated with aromaticity. Green reported an early example of this using molybdenum,<sup>249</sup> but similar types of activations have been reported with various metals including iron,<sup>250</sup> manganese,<sup>251</sup> and rhenium (Equation 4-5).<sup>252</sup>

**Equation 4-5**



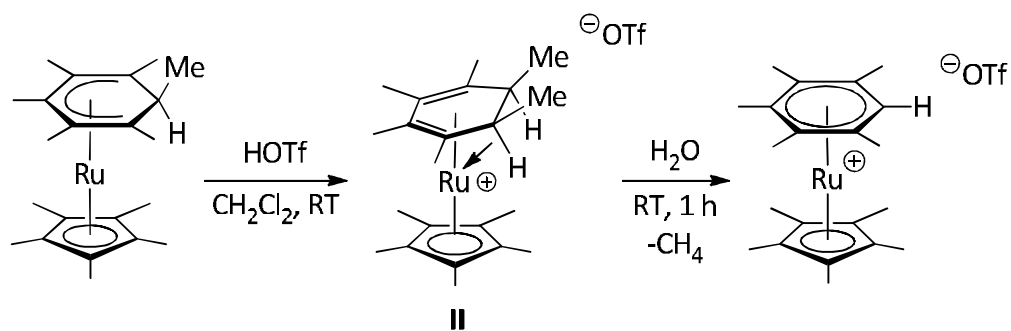
Jones' example using rhenium is of particular interest because only the *endo*-substituent on the cyclopentadiene ring is cleaved (Scheme 4-12).<sup>252</sup> When the *exo*-methylcyclopentadiene ligand is used, dihydrogen production is observed and the corresponding methylcyclopentadienyl ligand is formed. The mechanism has been probed using labeling studies and is consistent with the proposal that hydride migration to the ring forms the cyclopentenyl system which then can either reversibly transfer hydride to the metal, or irreversibly transfer the methyl group. Subsequent reductive elimination affords either methane or dihydrogen as the observed product.

Scheme 4-12



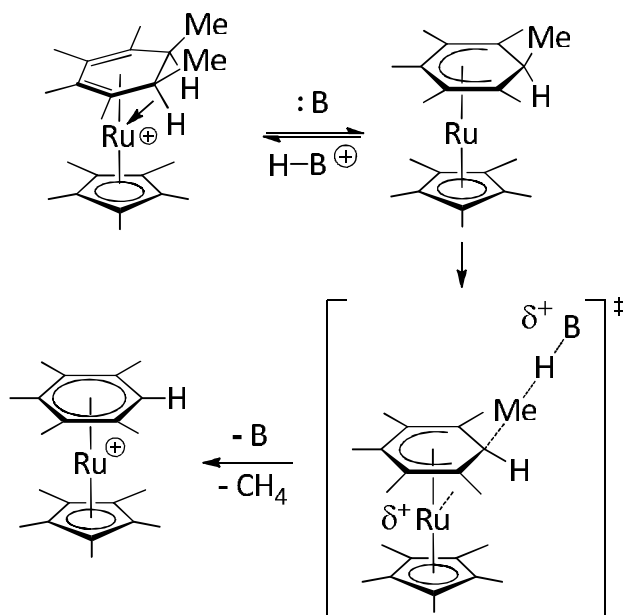
Stryker has reported a  $\beta$ -alkyl elimination and aromatization of 6-methylcyclohexadienyl ruthenium complexes by an unusual protolytic dealkylation process.<sup>253, 254</sup> Interestingly, protonation of the *exo*-methylcyclohexadienyl complex leads to the loss of methane; protonation of the *endo*-methylcyclohexadienyl complex instead results in selective dehydrogenation (Scheme 4-13).

**Scheme 4-13**



The mechanism of this unusual  $\beta$ -alkyl elimination reaction has been probed using deuterium labeling studies and is consistent with dissociation of acid from the agostic cyclohexadiene cation **II** by reaction with a weak base, typically adventitious water or the weakly coordinating anion, followed by protolytic activation of the alkyl group (Scheme 4-14).

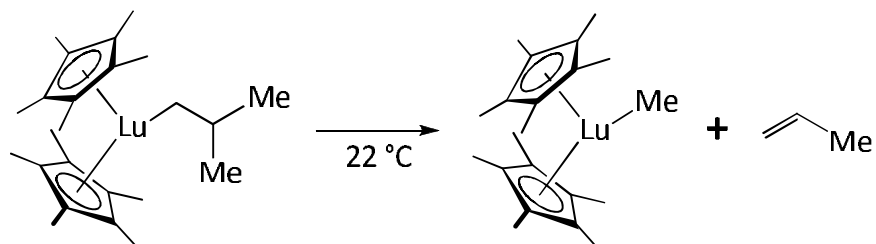
**Scheme 4-14**



The loss of the alkyl group is assisted by the metal, which stabilizes the transition state by donation of a filled metal-centred orbital to the  $\sigma^*$ -orbital of the activated carbon-carbon bond.

$\beta$ -Alkyl elimination has also been observed in chain transfer reactions in various Ziegler-Natta olefin catalysts and lanthanide complexes.<sup>255-257</sup> Watson *et al.* have observed  $\beta$ -methyl elimination from a lutetium(III) isobutyl complex; the authors propose a four-centered transition state to rationalize the formation of the lutetium methyl complex and propylene (Equation 4-6).<sup>258</sup>

**Equation 4-6**



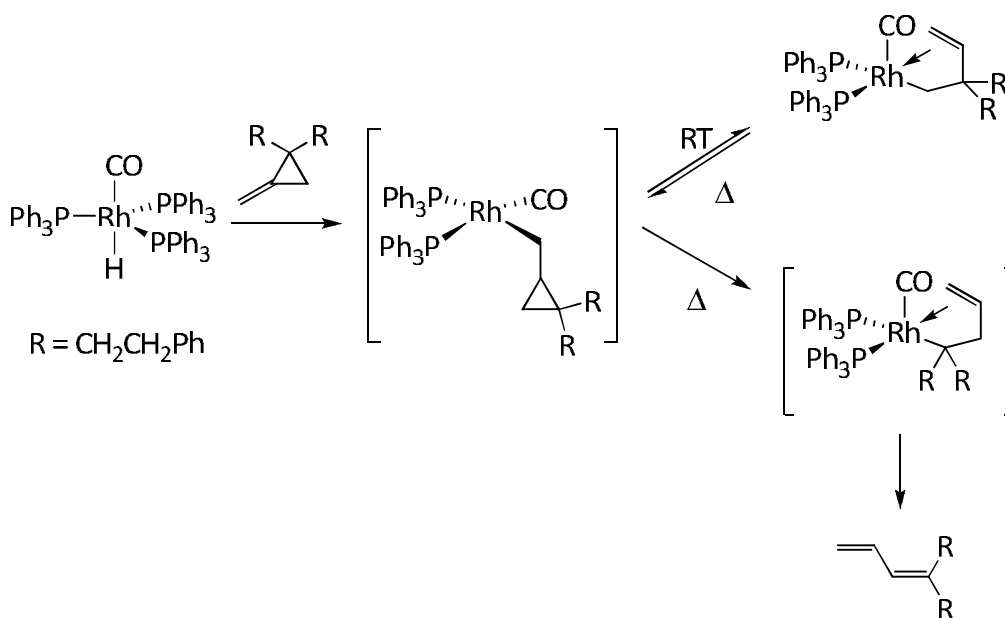
While there are many examples of  $\beta$ -alkyl elimination occurring on early metal and lanthanide complexes, there have been fewer reports of reactions using late metals.  $\beta$ -Alkyl elimination has, however, been demonstrated using ruthenium,<sup>259, 260</sup> platinum,<sup>261</sup> iridium,<sup>262</sup> palladium<sup>263, 264</sup> and platinum.<sup>261, 265</sup>

Bergman *et al.* observed an intermediate along the pathway of  $\beta$ -alkyl elimination (Equation 4-7).<sup>266</sup> Upon thermolysis of the ruthenacyclobutane,  $\text{PMe}_3$  dissociates and  $\beta$ -methyl transfer occurs to form both the *endo*- and *exo*-



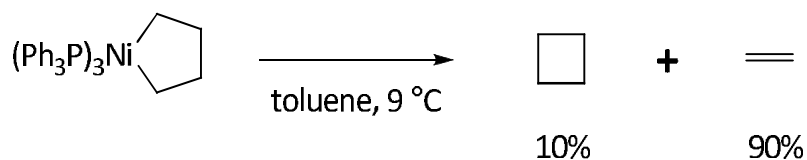
methylenecyclopropane moiety and subsequent  $\beta$ -alkyl elimination on the opposite side of the cyclopropane ring.

**Scheme 4-15**



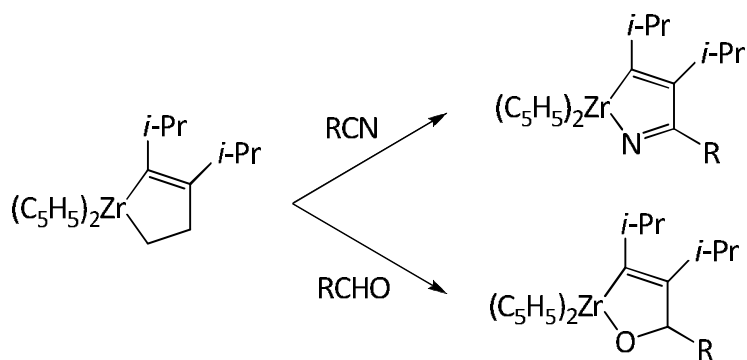
Another common form of  $\beta$ -alkyl elimination is the reverse of oxidative cyclization. Typically, the addition of two olefins to a low-valent metal centre results in the formation of a metalacyclopentane or, in the case of two alkynes, metalacyclopentadiene. Grubbs has reported that the oxidative coupling of olefins is reversible and has observed the formation of cyclobutane and ethylene from a tris(triphenylphosphine)nickelacyclopentane, which decomposes below ambient temperature (Equation 4-8).<sup>268-272</sup>

### Equation 4-8



Similar cycloreversion and subsequent scrambling has also been observed in metalacyclopentane complexes of zirconium and hafnium.<sup>273, 274</sup> Negishi has demonstrated a useful adaptation of this phenomenon, using zirconacyclopentenes that can reductively cleave to form a transient zirconium alkyne alkene complex. Upon exchange of the alkene for nitriles or aldehydes, new heteroatom-containing metalacyclopentadienes or metalacyclopentenes can be prepared, respectively (Scheme 4-16).<sup>275</sup>

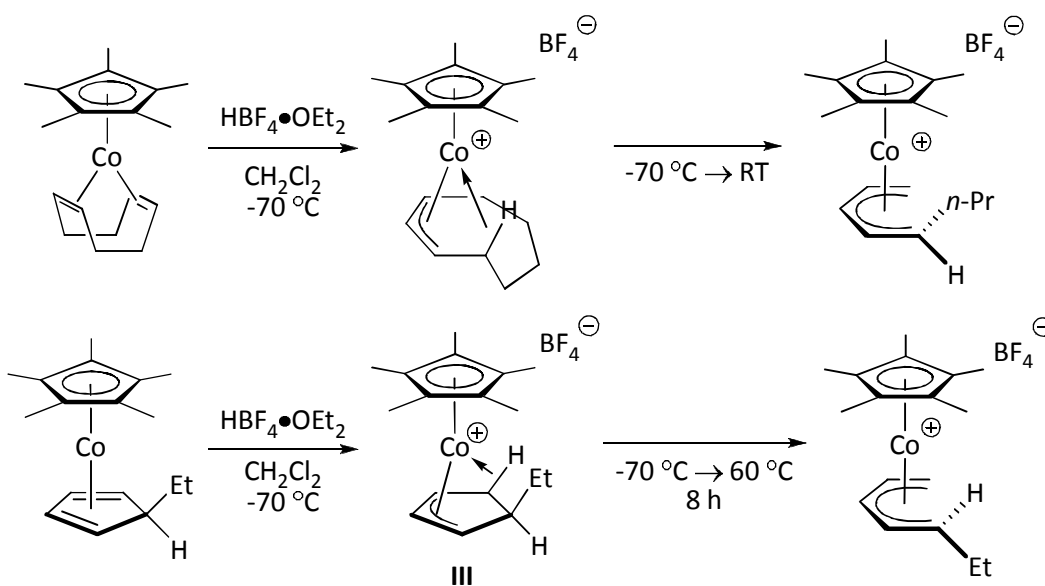
### Scheme 4-16



## F. Activation by Electrophilic Cobalt Complexes

Spencer *et al.* have found that electrophilic agostic cobalt complexes can undergo  $\beta$ -carbon-carbon bond scission.<sup>119-121</sup> Protonation of both  $(C_5Me_5)Co(1,5-cod)$  and  $(C_5Me_5)Co(endo-\eta^4-EtC_5H_5)$  results in the isolation of the corresponding acyclic  $\eta^5$ -pentadienyl complex, where carbon-carbon  $\sigma$ -bond activation of the cycloalkyl intermediate has occurred (Scheme 4-17). The key intermediate during the latter transformation is the agostic cyclopentenyl complex **III**, which Spencer has characterized via  $^1J_{CH}$  measurements of the agostic carbon. Interestingly, carbon-carbon bond activation of both the 1,5-cyclooctadiene and ethylcyclopentadiene moieties results in the stereospecific formation of the *anti*- and *syn*-substituted pentadienyl complexes, respectively.

Scheme 4-17



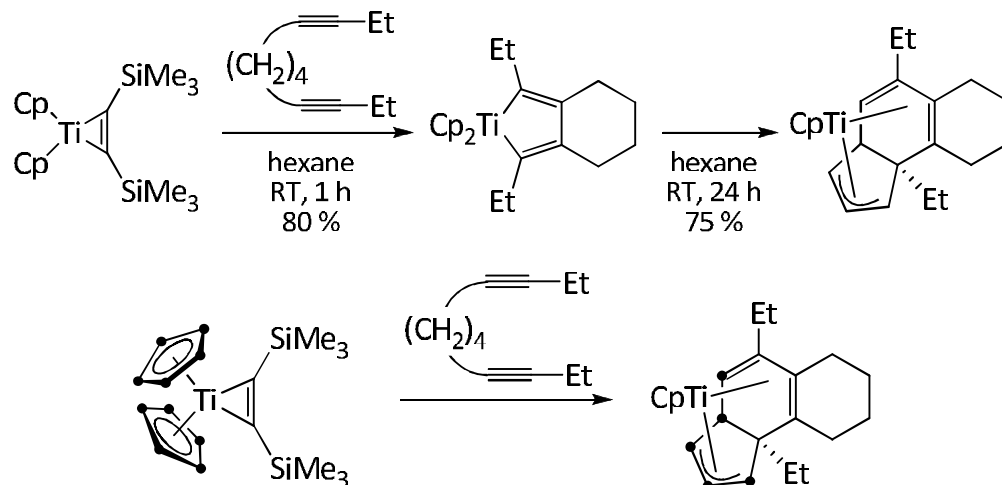
Stryker has reported a more general carbon-carbon bond activation using electrophilic cobalt complexes.<sup>24, 25, 131</sup> A brief introduction of cobalt-mediated carbon-carbon bond activation can be found in Chapter 2, Part B. The mechanism will be discussed shortly (*vide infra*).

### G. Activation by Electrophilic Titanium Complexes

While the activation of carbon-carbon  $\sigma$ -bonds has been well-studied, the corresponding activation of cyclopentadienyl ligands is rare. There are few reports of cyclopentadienyl activation; Rosenthal<sup>276</sup> and Takahashi<sup>277-280</sup> have each independently reported examples of cyclopentadienyl activation using titanium and as has Stryker using cobalt.<sup>25, 131</sup>

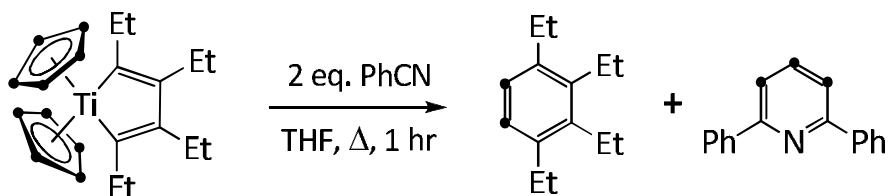
Rosenthal *et al.* have found that treatment of  $\text{Cp}_2\text{Ti}(\text{Me}_3\text{SiCCSiMe}_3)$  with a series of disubstituted diynes affords bicyclic titanacyclopentadienes via ligand exchange and oxidative cyclization.<sup>276</sup> However, in one specific example, the resulting bicyclic titanacyclopentadiene rearranges at ambient temperature to form a stable tricyclic dihydroindenyltitanium complex by cyclopentadienyl cleavage and intramolecular carbon-carbon coupling (Scheme 4-18). Interestingly, when  $^{13}\text{C}$ -labeled cyclopentadienyl ligands are used, the arrangement of the labeled carbons suggests that carbon-carbon bond activation of the cyclopentadienyl unit has occurred and clearly indicates that cyclopentadienyl migration is not involved in this reaction.

Scheme 4-18



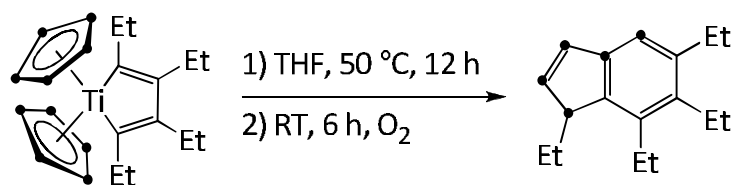
Takahashi *et al.* have reported a titanium-mediated cleavage of the cyclopentadienyl ligand and the incorporation of the fragments to form arene and pyridine products upon addition of nitriles to a titanacyclopentadiene complex.<sup>277</sup> While the mechanism is unknown, Takahashi has found through labeling studies that two of the cyclopentadienyl carbons are transferred to the arene, while the remaining three are incorporated into the pyridine (Equation 4-9).

Equation 4-9

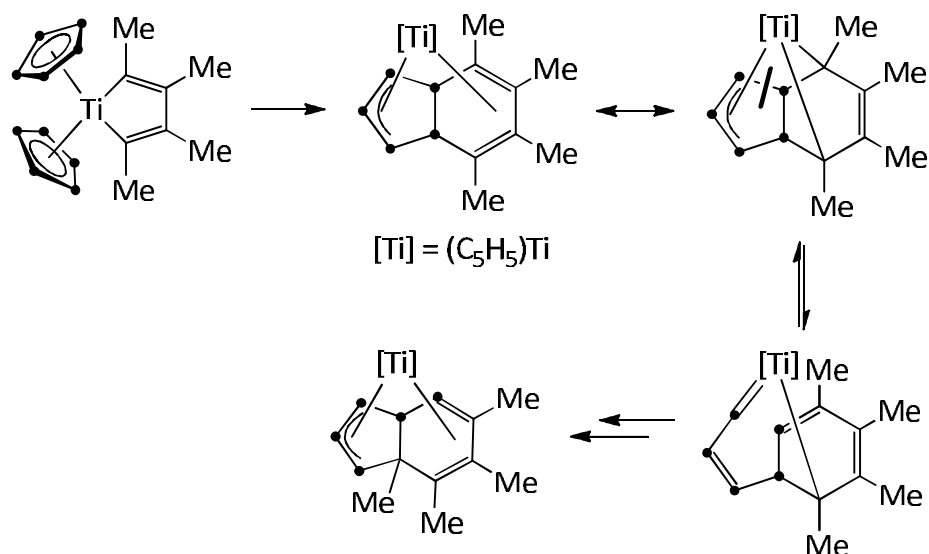


In the absence of nitrile, cyclopentadienyl incorporation into the titanacyclopentadiene unit is observed under mild thermolysis and a tetra-substituted indene is isolated (Equation 4-10).<sup>278-280</sup> When <sup>13</sup>C-labelled cyclopentadienyl ligands are used, <sup>13</sup>C-incorporation is observed in the product in similar indenyl positions as Rosenthal's dihydroindenyltitanium complex. The key step in the proposed mechanism is the formation of a titanacyclobutane moiety and its subsequent conversion to a titanium carbene and olefin by a metathesis-like cycloreversion (Scheme 4-19).

Equation 4-10



Scheme 4-19

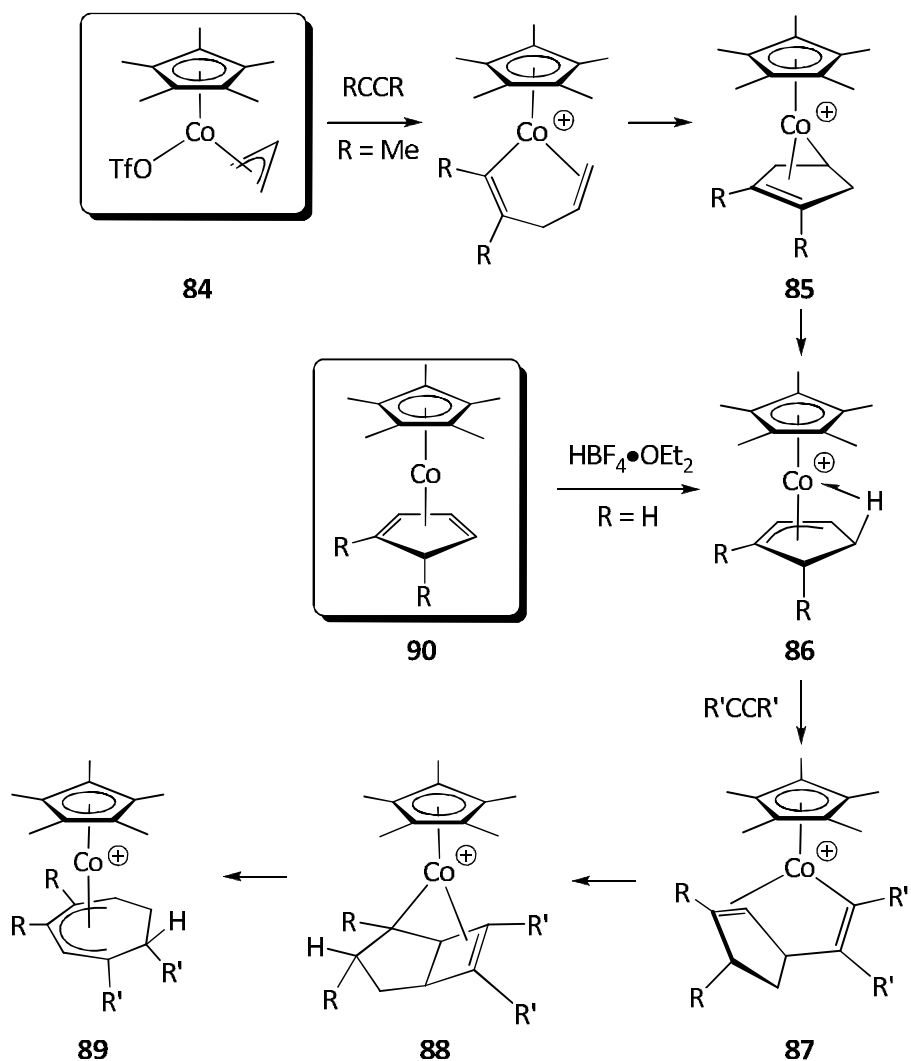


## H. Mechanistic Proposals for the [5 + 2] $\eta^3$ -Cyclopentenyl-Alkyne Cycloaddition/Carbon-Carbon Bond Activation Process

As discussed in Chapter 2, Part B, an early mechanism proposed by Dzwiniel to account for the products arising from the “anomalous [3 + 2 + 2]” allyl-alkyne cycloaddition and the [5 + 2] cyclopentenyl-alkyne ring-expansion reactions invokes the formation of an agostic cyclopentenyl intermediate. Spencer demonstrated the intermediacy of this agostic cyclopentenyl cation upon protonation of cobalt cycloalkadiene complexes at low temperature (Scheme 4-17).<sup>119-121</sup> Dzwiniel noted that in the case of the “anomalous [3 + 2 + 2]” reaction, the substitution pattern of the various products implied that a [3 + 2] cycloaddition reaction to form a five-membered ring must occur before a subsequent carbon-carbon bond activation leads to ring-expansion.

In the Dzwiniel proposal, the addition of alkyne to cobalt allyl triflate complex **84** results in initial migratory insertion and cyclization to afford the  $\eta^1, \eta^2$ -cyclopentenyl complex **85**, which subsequently isomerizes to the  $\eta^3$ -cyclopentenyl complex **86** (Scheme 4-20). Coordination of a second equivalent of alkyne and migratory insertion results in the formation of vinyl-cyclopentene intermediate **87**. Migration of the vinyl ligand to the interior olefin position forms the strained cyclobutene complex **88**, which is followed by a [2 + 2] cycloreversion.

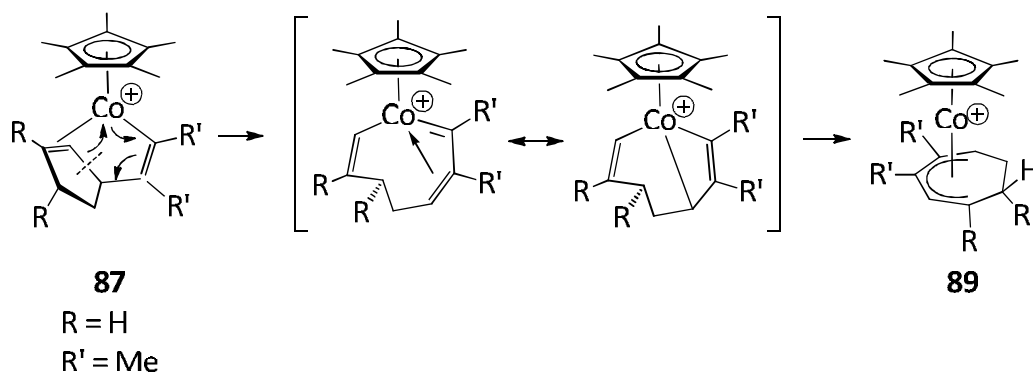
Scheme 4-20



The proposed mechanism for the [5 + 2] cyclopentenyln-alkyne ring-expansion is also accounted for in this mechanism: protonation of  $(C_5Me_5)Co(\eta^4-C_5H_6)$  derivatives **90** would produce an agostic  $\eta^3$ -cyclopentenyln complex analogous to complex **86**, which upon incorporation of alkyne would lead to  $\eta^5$ -cycloheptadienyln products.

The transient formation of the bicyclic cyclobutene complex **88** (Scheme 4-20) appears to be a high-energy process and alternative mechanisms have been proposed that circumvent cyclobutene formation. Vinyl-cyclopentene intermediate **87** can undergo direct carbon-carbon bond activation of the bond adjacent to the coordinated olefin (Scheme 4-21). This would generate a bicyclic cobalt(V) intermediate, which may be better represented as the corresponding cobalt(III) vinyl-carbene canonical structure. 1,2-Migration of the vinyl group to the carbene would produce the  $\eta^5$ -cycloheptadienyl product.<sup>281, 282</sup> High valent cobalt(V) complexes, though unusual, are not rare and various groups have synthesized such electron-deficient species.<sup>283-286</sup>

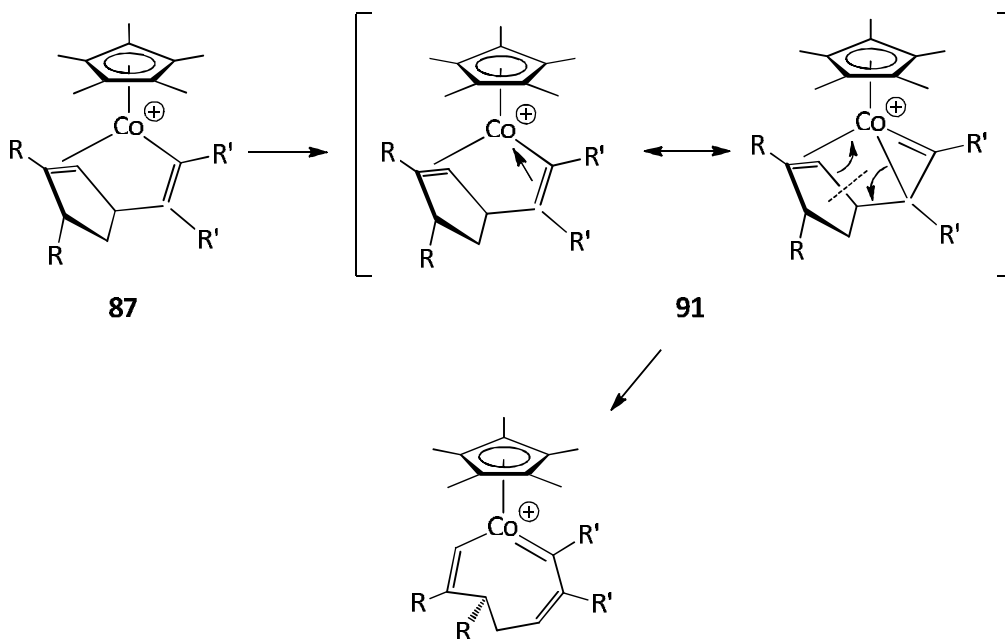
**Scheme 4-21**



Another viable mechanistic proposal to rationalize the carbon-carbon  $\sigma$ -bond scission invokes the formation of metalacyclopropene intermediate **91** upon insertion of the first equivalent of alkyne (Scheme 4-22). After formation

of the metalacyclopropene,  $\beta$ -carbon elimination forms the extended vinyl-carbene complex, which rearranges to afford the  $\eta^5$ -cycloheptadienyl product.

**Scheme 4-22**



While these proposals all involve the formation of an agostic  $\eta^3$ -cyclopentenyl intermediate to rationalize both the “anomalous [3 + 2 + 2]” and [5 + 2] ring-expansion reactions, recent computational work from Stryker, Nakamura, and Ammal suggest that protonation of the cobalt cyclopentadiene complex is reversible and not the key step in the transformation (Figure 4-2).<sup>175</sup>

The orientation of the cyclopentadiene ligand during the tandem [2 + 2]/retro-[2 + 2] process leads to two different pathways. While in principle both orientations of the cyclopentadiene ligand are possible during the initial [2 + 2]

cycloaddition step, only one orientation leads to seven-membered product formation. Formation of **93A** is presumed to be lower in energy compared to **93B** due to stabilization from an adjacent agostic carbon-hydrogen bond which is not present in **93B**.

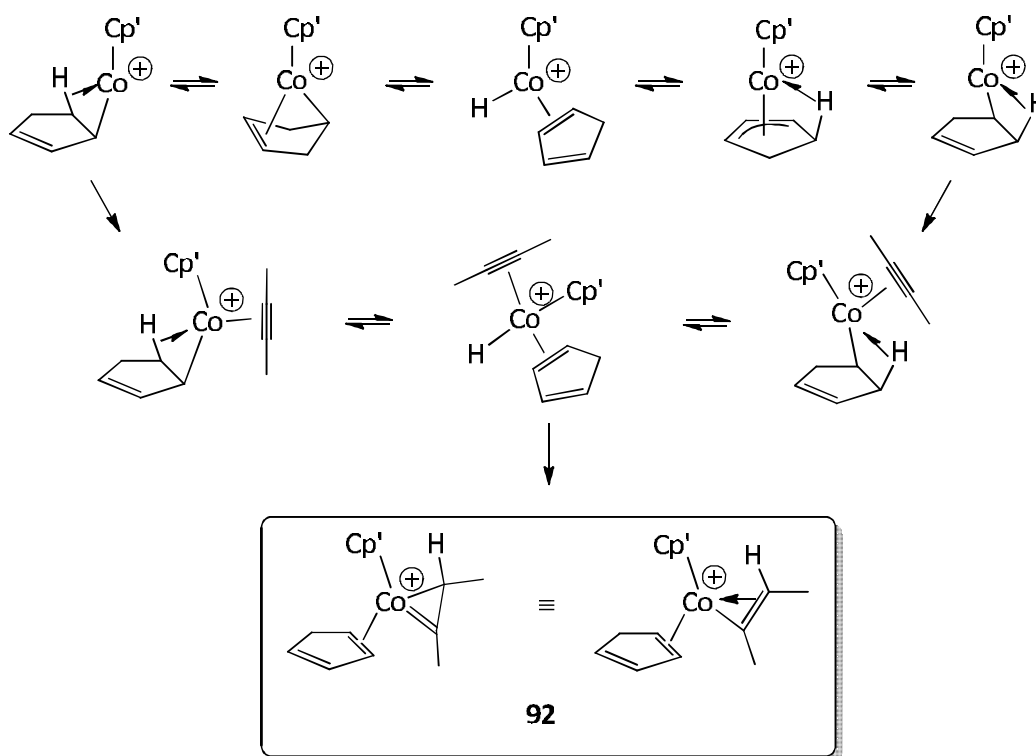


**Figure 4-2:** Proposed Carbon-Carbon Bond Activation Mechanism Part 1 - DFT calculations were performed using Gaussian 98 at the B3LYP level. [Co: Stuttgart/Dresden ECP (SDD); remaining atoms: 6-31G(D)]<sup>175</sup>

In this mechanism, treatment of the agostic  $\eta^3$ -cyclopentenyl complex with alkyne results in the transfer of the proton to the bound alkyne unit, forming a cobalt  $\eta^2$ -vinyl intermediate **92**. An alternative canonical view of the

$\eta^2$ -vinyl species **92** is as the 1-metalacyclopropene complex. In any case, this complex subsequently reacts with  $\eta^2$ -bound cyclopentadiene in a tandem [2 + 2]/retro-[2 + 2] fashion to form the allyl-carbene complex **94** (Figure 4-3). The vinyl moiety inserts into the metal-allyl bond forming the seven-membered ring complex **95**, followed by a series of  $\beta$ -hydride eliminations and reinsertions which results in the observed product **89**.

Interestingly, **93B** can isomerize readily to the  $\eta^2,\eta^3$ -vinylcyclopentenyl complex **96**. While complexes bearing this hapticity have not been isolated in the cyclopentenyl series, they are the predominant products formed in the cyclohexenyl series (Figure 4-4). These mechanistic calculations suggest that, in the cyclopentenyl series, the stabilization obtained from the agostic interaction in **93A** is greater than the corresponding agostic interaction in the cyclohexenyl series. It is this lack of stabilization that leads to the formation and isolation of alkyne insertion products in the cyclohexenyl series, instead of ring-expansion products (Scheme 4-23).

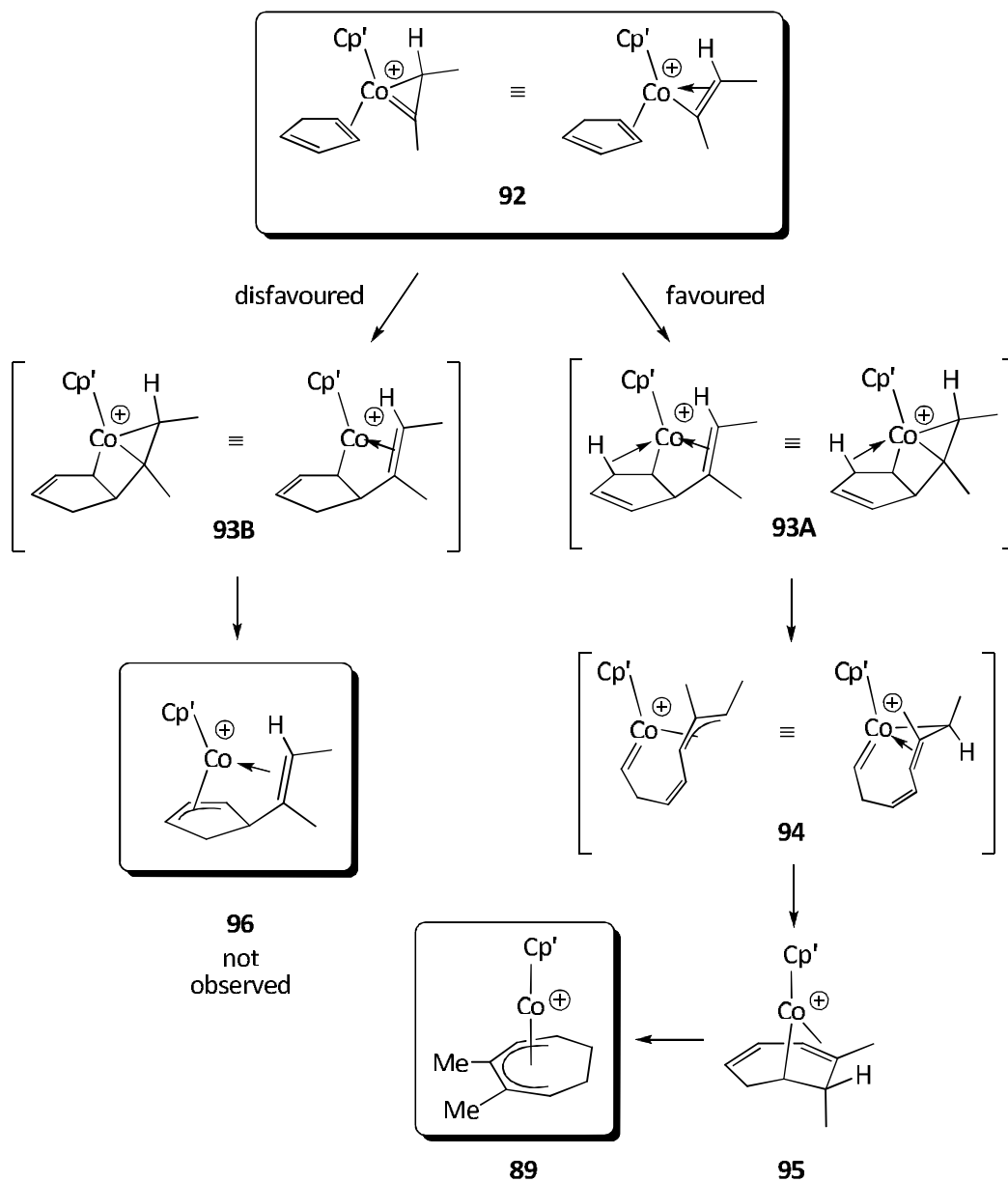
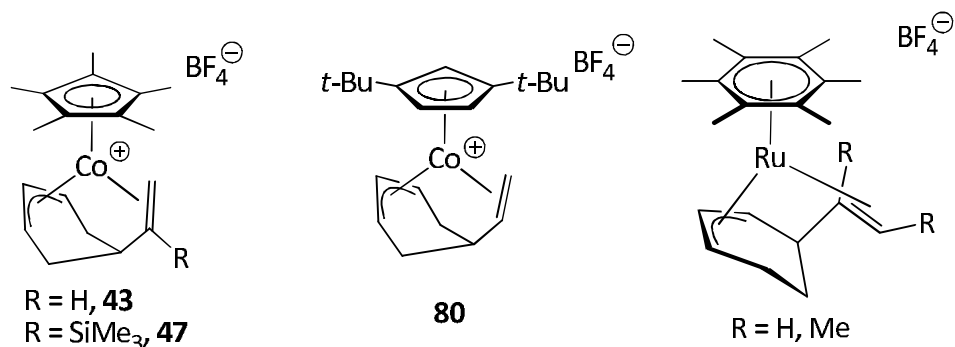
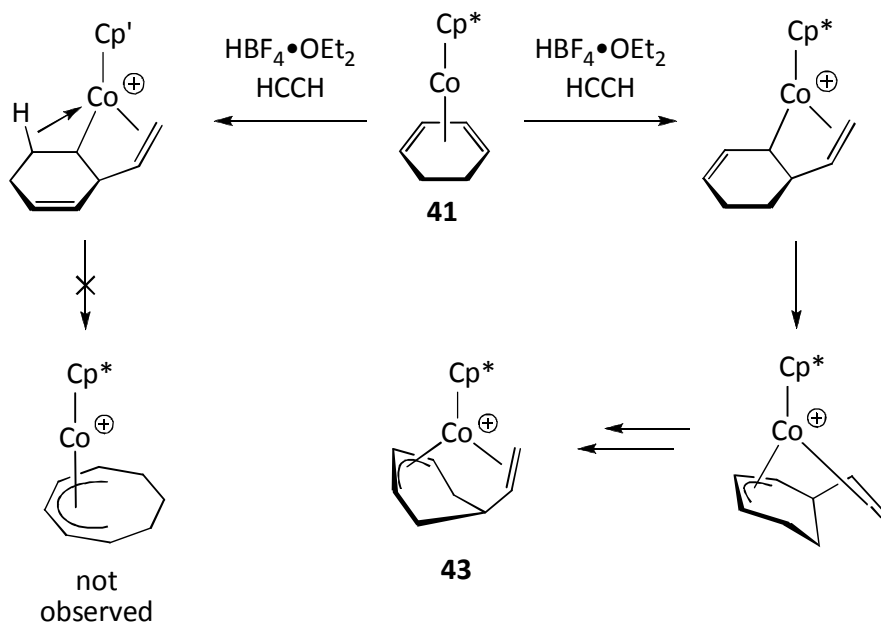


**Figure 4-3:** Proposed Carbon-Carbon Bond Activation Mechanism Part 2 - DFT calculations were performed using Gaussian 98 at the B3LYP level. [Co: Stuttgart/Dresden ECP (SDD); remaining atoms: 6-31G(D)]<sup>175</sup>

**Figure 4-4:** Examples of Complexes Bearing  $\eta^2, \eta^3$ -Vinylcyclohexenyl Organic Fragments



**Scheme 4-23**



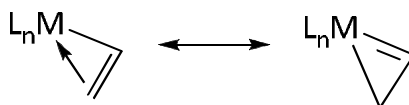
If these computational results are correct, then the independent synthesis of a cationic cobalt  $\eta^2$ -vinyl complex and treatment with cyclopentadiene should induce carbon-carbon activation and ring-expansion.

Furthermore, other cyclic dienes or even simple cyclic alkenes could be used. Ring-expansion of medium sized rings would be invaluable to synthetic chemists.

### I. General Formation of $\eta^2$ -Vinyl/1-Metalacyclopropene Complexes

Metal complexes possessing four-electron donor vinyl ligands are alternatively described as  $\eta^2$ -vinyl complexes or 1-metalacyclopropene complexes (Figure 4-5). Historically classified as  $\eta^2$ -vinyl complexes, Casey proposed that the metalacyclopropene nomenclature should be used because of physical properties that can be best described by using the metalacyclopropene canonical.<sup>287</sup> While 2<sup>nd</sup> and 3<sup>rd</sup> row metal-vinyl complexes can be certainly viewed as 1-metalacyclopropenes, due to the high electron density on the metal stabilizing the higher oxidation state of the 1-metalacyclopropene canonical, 1<sup>st</sup> row metal-vinyl complexes should not necessarily be labeled as such. Compared to 2<sup>nd</sup> and 3<sup>rd</sup> row transition metals, the 1<sup>st</sup> row metals are less electron-rich and in most cases cannot back-bond to the extent required to reach the 1-metalacyclopropene structure.

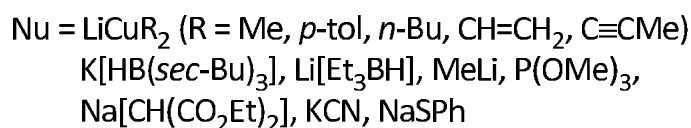
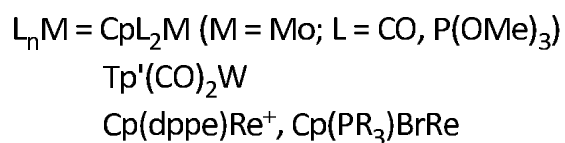
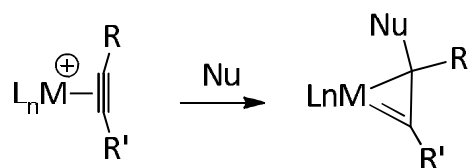
**Figure 4-5:**  $\eta^2$ -Vinyl and 1-Metalacyclopropene Canonicals



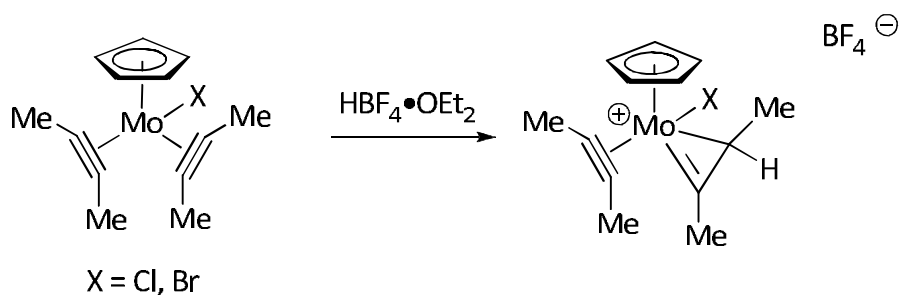
Nucleophilic addition to unsaturated neutral or cationic 2<sup>nd</sup> and 3<sup>rd</sup> row metal-alkyne complexes is generally the most facile way to prepare 1-metalacyclopropene complexes (Equation 4-11).<sup>288-297</sup> The metal-alkyne complexes used typically possess four-electron donating alkyne ligands; nucleophilic addition to metal-alkyne complexes possessing two-electron donating alkyne ligands typically produce  $\eta^1$ -vinyl complexes, at least initially.

Alternatively, treatment of electron-rich metal-alkyne complexes with electrophiles can be used to generate the corresponding 1-metalacyclopropene complex. Treatment of bis(alkyne) molybdenum(II) complex with a strong acid, for example, generates the 1-metalacyclopropene cation (Equation 4-12).<sup>298</sup>

#### Equation 4-11



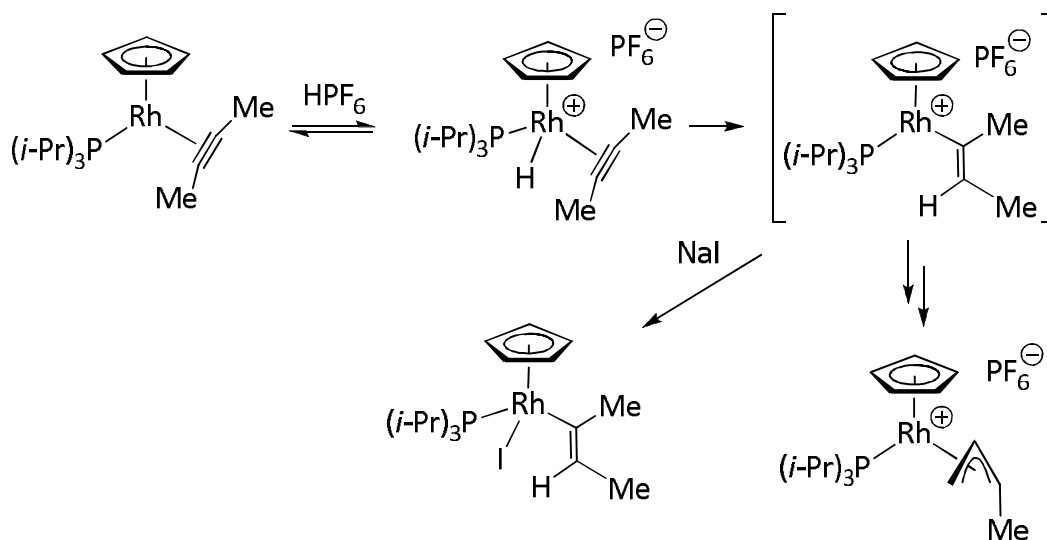
### Equation 4-12



Casey has also observed metalacyclopropene intermediates in the acid-catalyzed rearrangement of alkyne ligands into  $\eta^3$ -allyl and  $\eta^2$ -allene ligands in  $(C_5Me_5)Re(CO)_2(\eta^2\text{-alkyne})$  complexes.<sup>287, 299, 300</sup>

Werner earlier demonstrated that the addition of strong acid to a half-sandwich rhodium(I) alkyne complex affords the corresponding rhodium(III)  $\eta^3$ -*anti*-crotyl complex (Scheme 4-24). To rationalize the formation of the crotyl product, Werner proposes that the mechanism must pass through an intermediate rhodium-vinyl complex. Evidence for the formation of the vinyl complex was provided by performing the reaction in the presence of sodium iodide, which yielded the iodide adduct, confirming the intermediacy of the rhodium-vinyl complex. Although Werner suggests that an  $\eta^1$ -vinyl ligand is present in the hydride insertion product, it could also be described as the 1-metalacyclopropene canonical.

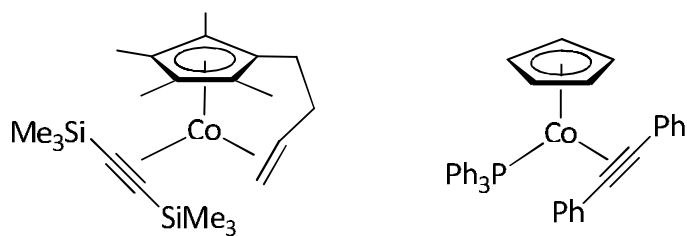
Scheme 4-24



The use of isolable half-sandwich metal alkyne complexes to generate corresponding 1-metalacyclopropene complexes is common among the second and third row transition metals, though not so for cobalt. Typically, small alkynes such as acetylene or 2-butyne react with low-valent cobalt precursors to afford products arising from  $[2 + 2 + 2]$  alkyne cyclotrimerization.<sup>3, 4, 105-107, 112, 301-304</sup> However, bulkier disubstituted alkynes or electron-deficient alkynes are not as prone to cobalt-mediated trimerization and can be isolated as the mono-alkyne adduct.<sup>305-309</sup> Okuda has demonstrated that cyclopentadienyl ligands possessing a pendent olefin can be used to stabilize cobalt mono-alkyne complexes (Figure 4-6).<sup>310</sup> Interestingly, Yamazaki *et al.* have demonstrated that the unsubstituted cyclopentadienyl ligand can also be used, but only when the alkyne is diphenylacetylene (Figure 4-6).<sup>311, 312</sup> Presumably, stronger backbonding into the

electron-deficient alkyne renders the phosphine less labile, preventing disproportionation and resultant alkyne coupling.

**Figure 4-6:** Examples of Half-Sandwich Cobalt Mono-Alkyne Complexes



## Section 2. Results and Discussion

The two most direct synthetic routes to the proposed cationic cyclopentadienyl cobalt vinyl complexes both involve nucleophilic vinylation: i) the addition of vinylmagnesium halide to a cyclopentadienylcobalt(III) precursor followed by conversion to the corresponding cation, and ii) the addition of vinylmagnesium halide to a cyclopentadienylcobalt(II) precursor and subsequent oxidation to the cation. Of the simple cyclopentadienylcobalt(III) precursors that can be easily prepared,  $[(C_5Me_5)CoX_2]_n$ <sup>313-315</sup> (X = Cl, **96**; X = I, **97**),  $(C_5Me_5)Co(CO)I_2$ <sup>313, 314, 316, 317</sup> (**98**), and  $(C_5Me_5)Co(PPh_3)I_2$ <sup>313, 318</sup> (**99**) appeared to be the best candidates. Of the readily available cyclopentadienylcobalt(II) precursors,  $[(C_5Me_5)CoCl]_2$ <sup>152</sup> (**40**) was deemed ideal.

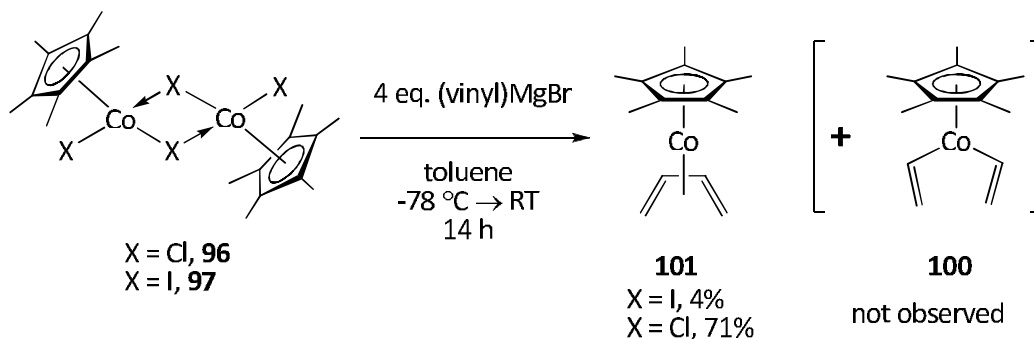
All four starting cobalt halide complexes were prepared by following literature procedures. One complication arising from using cobalt(III) dihalo dimers **96** and **97** is thermal instability in coordinating solvents, undergoing slow ligand disproportionation, affording the cobalticenium cation and cobalt dihalide at ambient temperature.<sup>313</sup>

### A. Vinyl Grignard Addition to Cobalt(III) Precursors

All attempts to generate a stable cobalt vinyl complex by treatment of dihalo cobalt(III) dimers **96** and **97** with two equivalents of vinylmagnesium

bromide (per cobalt) were unsuccessful. The addition of four equivalents of vinylmagnesium bromide to a purple slurry of diiodocobalt dimer **97** afforded a mixture of diamagnetic products (Equation 4-13). The  $^1\text{H}$  NMR spectrum of the residue largely consisted of broadened resonances that were not suggestive of the formation of the expected bis(vinyl) cobalt complex **100**. However, a low yield of the corresponding cobalt(I)  $\eta^4$ -butadiene adduct **101** was found and identified by comparison to authentic material.<sup>24</sup> When the reaction was repeated with the dichloro congener **96**, the butadiene adduct **101** was the dominant product, this time in good yield. Again, no evidence for the formation of bis(vinyl) cobalt complex **100** was found. This method of preparing butadiene adduct **101** represents a more convenient preparation of the complex as it requires fewer steps compared to the literature procedure, which entails the initial preparation of the labile  $(\text{C}_5\text{Me}_5)\text{Co}(\text{C}_2\text{H}_4)_2$  complex.<sup>319</sup>

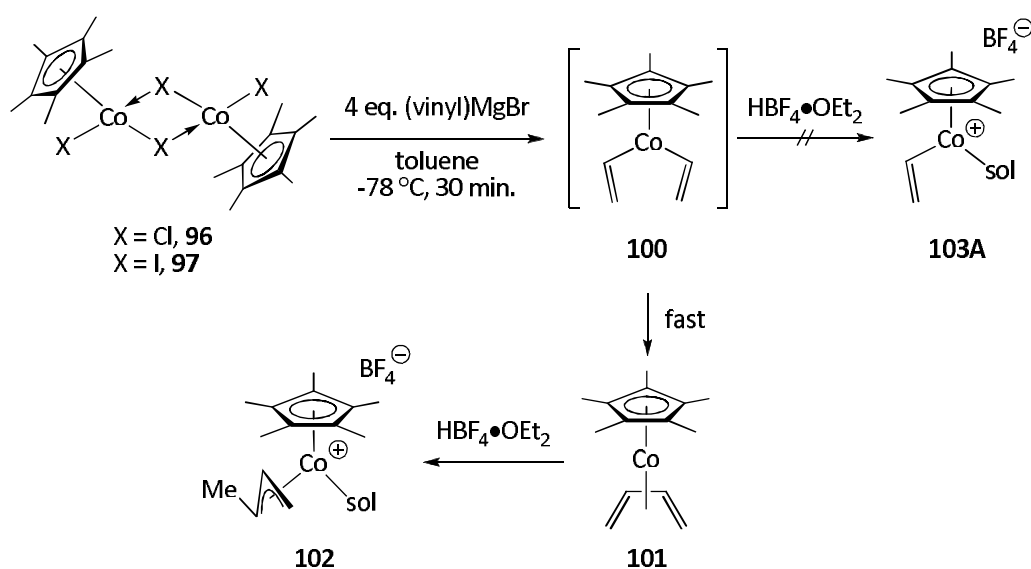
**Equation 4-13**



The formation and isolation of the butadiene adduct **101** from the treatment of vinyl anion to either dihalo dimers **96** and **97**, however, implies that

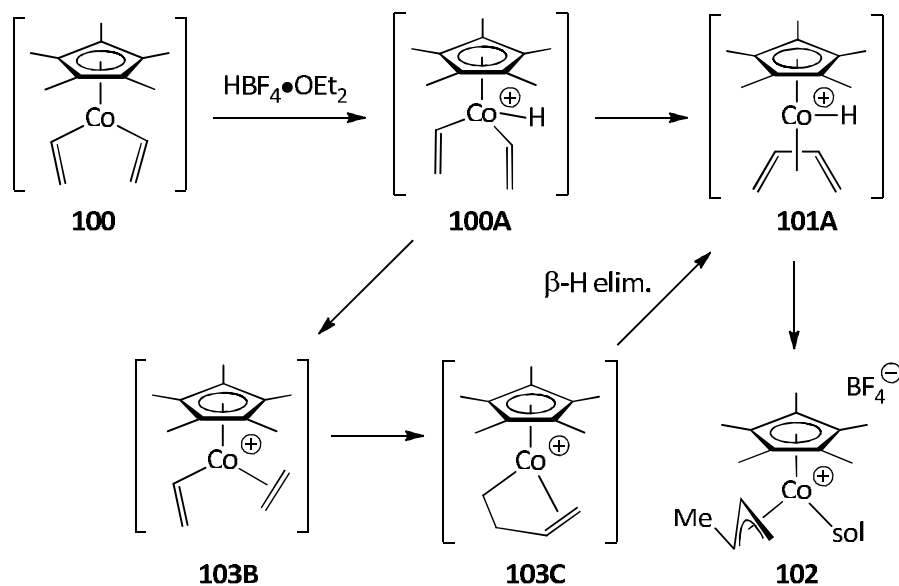
the bis(vinyl) complex **100** is certainly formed, albeit transiently at  $-78\text{ }^{\circ}\text{C}$ . This hypothesis suggests that the addition of a strong protic acid at some point during the reaction could result in the protolytic loss of ethylene and formation of the desired cationic cobalt vinyl complex. Interestingly, treatment of a sample of dihalo dimer **96** or **97** at low temperature with four equivalents of vinylmagnesium bromide, followed by the addition of  $\text{HBF}_4 \cdot \text{OEt}_2$ , afforded the cationic  $(\text{C}_5\text{Me}_5)\text{Co}(\eta^3\text{-crotyl})$  complex **102** in variable yield along with other unidentified products (Scheme 4-25). No evidence for the formation of the cationic vinyl complex **103A** was found. This finding indicates that once the bis(vinyl) complex **100** is formed, reductive coupling to form the  $\eta^4$ -butadiene adduct **101** is both kinetically fast and thermodynamically favoured, even at low temperatures.

**Scheme 4-25**



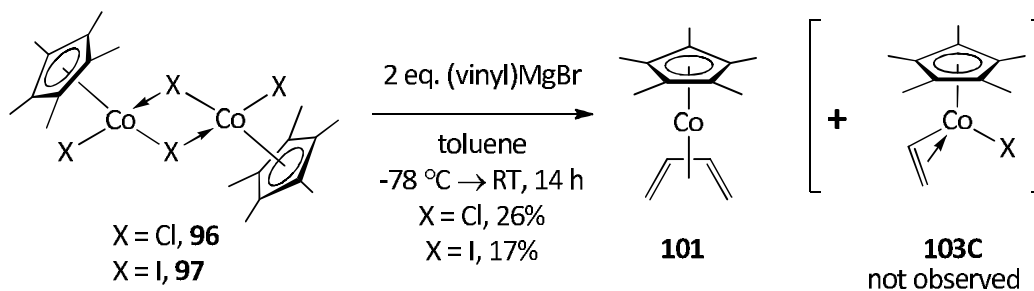
The protonation of complex **100** could also induce reductive elimination of the vinyl ligands (Scheme 4-26). Protonated complex **100A** can undergo direct reductive coupling, followed by proton migration, to yield crotyl complex **102**. Alternatively, reductive elimination of complex **100A** to form the vinyl-ethyl complex **103B**, followed by migratory insertion and  $\beta$ -hydride elimination, can also lead to complex **101A**.

**Scheme 4-26**



The fast reductive coupling of bis(vinyl) complex **100** to form the  $\eta^4$ -butadiene adduct **101** is also observed when only two equivalents of vinylmagnesium bromide are added to one equivalent of dihalo dimer **96** or **97** (Equation 4-14). The isolated yield of butadiene adduct **101** is again lower when diiodo dimer **97** is used compared to when dichloro dimer **96** is used.

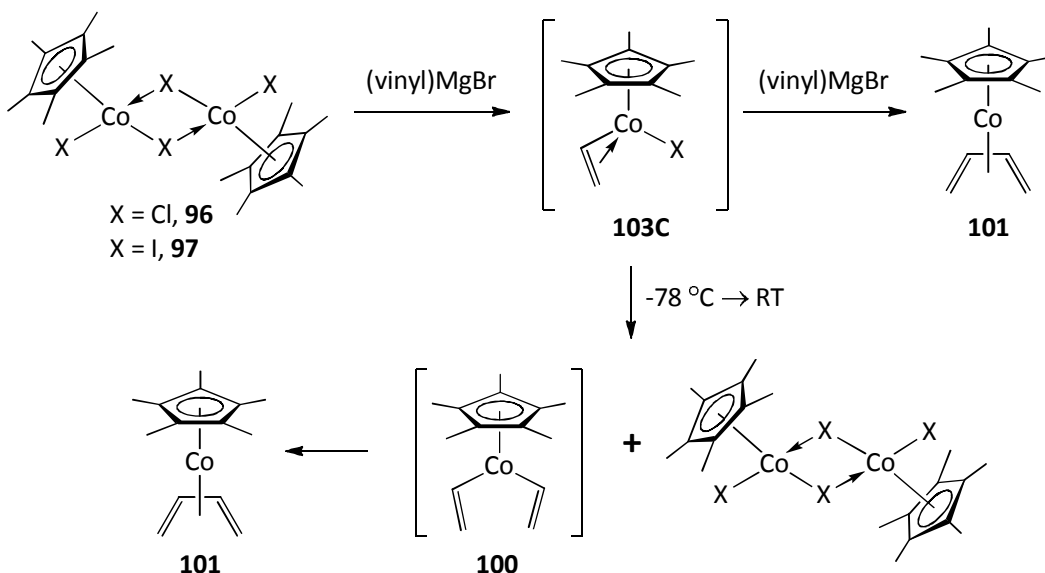
**Equation 4-14**



The formation of the  $\eta^4$ -butadiene complex **101** from this reaction stoichiometry most likely arises from rapid disproportionation of the intermediate cobalt vinyl halide complex **103C**, which returns starting material and the unstable bis(vinyl) complex **100** (Scheme 4-27). It is also possible that the intermediate cobalt vinyl halide complex **102** simply reacts *faster* with vinylmagnesium bromide than with dihalo dimers **96** or **97**.

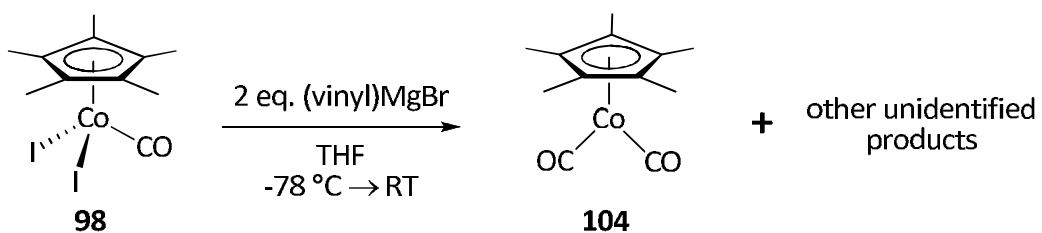
Because of the rapid reductive coupling of the cobalt bis(vinyl) complex **100**, other strategies were investigated to prepare isolable cobalt  $\sigma$ -vinyl or  $\eta^2$ -vinyl complexes. To impede reductive coupling, an additional ligand was installed on the cobalt centre to occupy a coordination site. Alternative half-sandwich cobalt(III) containing starting materials such as  $(\text{C}_5\text{Me}_5)\text{Co}(\text{L})_2$  ( $\text{L} = \text{CO}$ , **98**;  $\text{L} = \text{PPh}_3$ , **99**) were selected from which to prepare the vinyl complex. These cobalt(III) compounds do not suffer from the same limitations as dihalo dimers **96** and **97**, surviving indefinitely in coordinating solvents such as THF without competing disproportionation at ambient temperature.

**Scheme 4-27**



Cobalt(II) carbonyl complex **98** was thus treated with two equivalents of vinylmagnesium bromide at low temperature. Following extraction with hexane, the crude product residue was analyzed using  $^1\text{H}$  NMR spectroscopy and revealed a complex mixture. However, infra-red spectroscopic analysis of the product residue revealed two prominent stretches in the carbonyl region at  $2000\text{ cm}^{-1}$  and  $1937\text{ cm}^{-1}$ , which are consistent with the formation of  $(\text{C}_5\text{Me}_5)\text{Co}(\text{CO})_2$  (Equation 4-15).<sup>320, 321</sup>

**Equation 4-15**

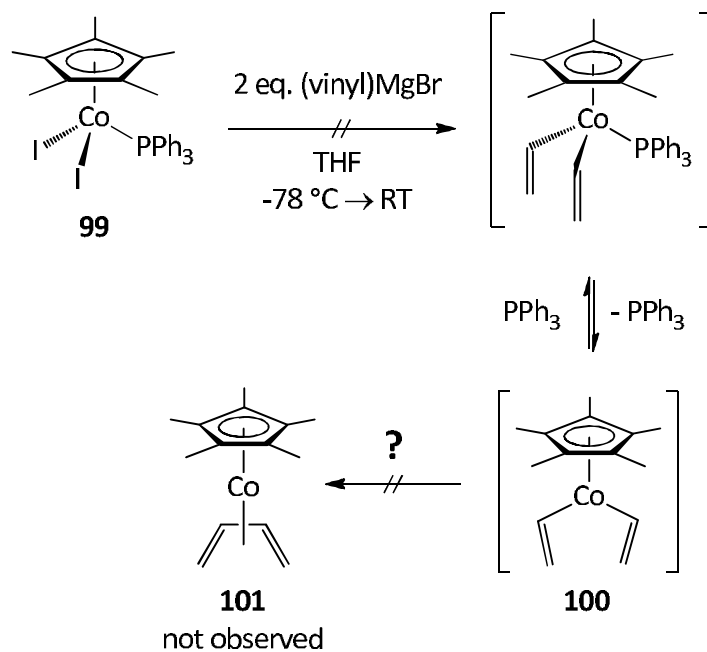


The formation of dicarbonyl complex **104** suggests that disproportionation of an advanced carbonyl-containing intermediate is occurring in order to afford both the dicarbonyl functionality as well as the formal reduction of the cobalt centre.

Since it is possible that the carbonyl ligand elicits participation in unforeseen reactions with the added vinyl anion, the phosphine adduct was examined instead. Cobalt phosphine complex **99** was treated with two equivalents of vinylmagnesium bromide at low temperature. Following extraction using hexane, the crude product residue was analyzed by  $^1\text{H}$  NMR spectroscopy and revealed significantly broadened resonances, but nothing that would suggest formation of the targeted cobalt(III) bis(vinyl) complex (Scheme 4-28).

Interestingly, reductive coupling to produce the  $\eta^4$ -butadiene adduct **101** is possible, although no evidence for its formation was detected. However, it is also possible that single electron transfer from the vinyl Grignard reagent to the cobalt(III) centre dominates, forming a paramagnetic cobalt(II) intermediate. The addition of Grignard reagents to sterically demanding organic substrates typically occurs via radical pathways, which are initiated by single electron transfer from the Grignard reagent to the substrate.<sup>322</sup>

Scheme 4-28



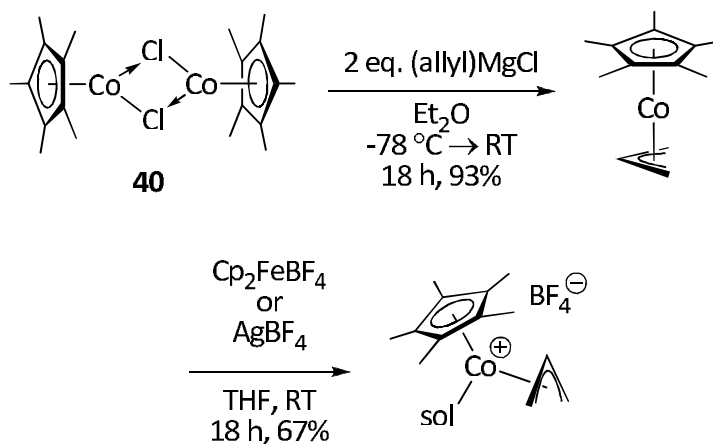
## B. Vinyl Grignard Addition to Cobalt(II) Precursors

One alternative pathway proposed was the addition of vinylmagnesium halide to a half-sandwich cobalt(II) precursor, followed by oxidation to cobalt(III). Nehl has demonstrated the successful application of this route to prepare allyl complexes, treating  $[(C_5Me_5)CoCl]_2$  with allylmagnesium chloride followed by oxidation with ferrocenium tetrafluoroborate, giving the cationic  $(C_5Me_5)Co(\eta^3\text{-allyl})$  complex in moderate yield (Scheme 4-29).<sup>103</sup>

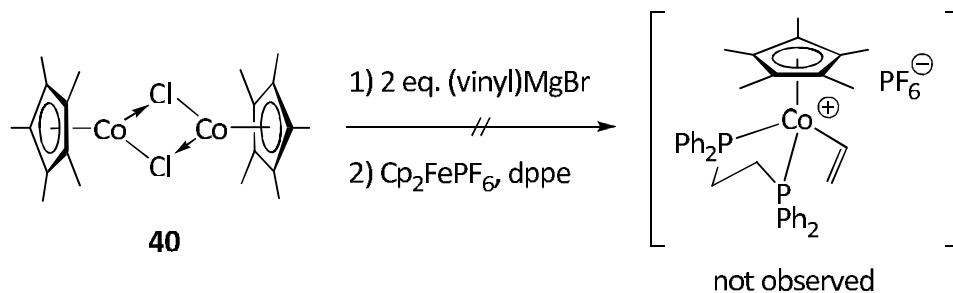
The analogous reaction was undertaken using vinylmagnesium bromide and  $[(C_5Me_5)CoCl]_2$ . The resulting cobalt(II) vinyl complexes were expected to be highly reactive, based on low electron count, and could be dimeric or

monomeric, with a weakly bound solvent molecule. Isolation and characterization of these vinyl complexes might be accomplished by the addition of donor ligands, such as triphenylphosphine or (diphenylphosphino)ethane (dppe), to displace the solvento ligand or dissociate the dimer, followed by oxidation (Equation 4-16). Unfortunately,  $^1\text{H}$  NMR spectra of the product residues after oxidation consisted only of broad resonances, indicative of persistent paramagnetic material.

**Scheme 4-29**



**Equation 4-16**



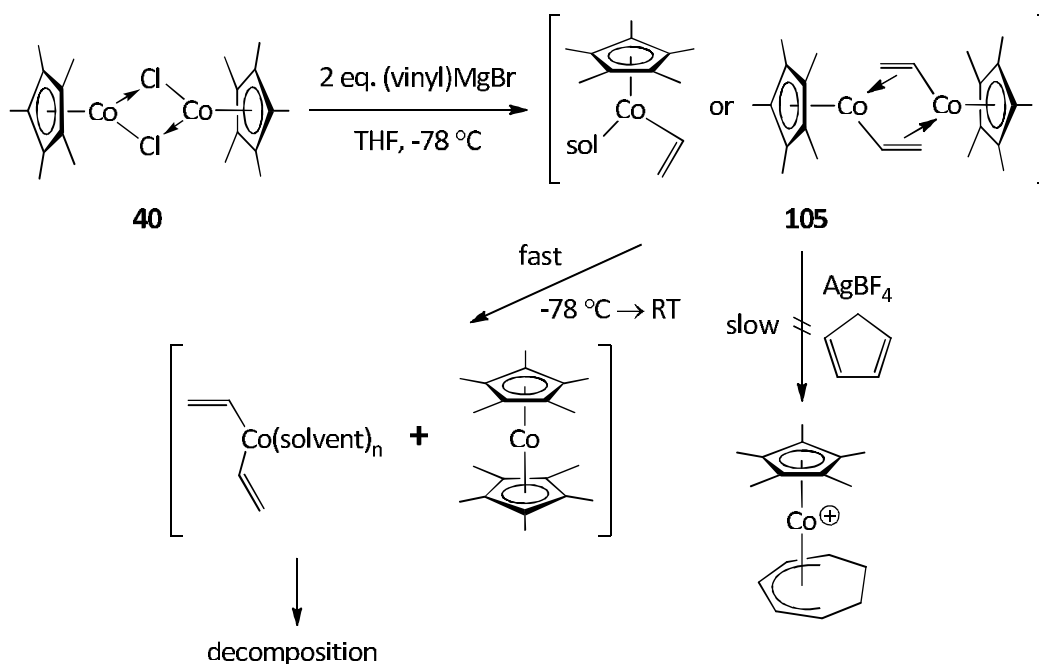
While the synthesis and complete characterization of the cobalt vinyl precursors was unsuccessful, another pathway was envisioned whereby the cobalt  $\eta^2$ -vinyl cation would be produced *in situ* and then “quenched” with cyclopentadiene. If the vinyl cation were an intermediate along the pathway of carbon-carbon bond activation, then cyclopentadiene coordination should result in the formation of a cobalt  $\eta^5$ -cycloheptadienyl complex. Since these seven-membered carbocycles have been independently synthesized and characterized in this group via [3 + 2 + 2] allyl-alkyne cycloaddition and [5 + 2] cyclopentenyl-alkyne ring expansion, any isolable products from the reaction of cobalt vinyl complexes with cyclopentadiene could be spectroscopically compared with authentic samples.

Consequently, cobalt(II) dimer **40** was treated with two equivalents of vinyl Grignard (one equivalent per cobalt) at low temperature for some hours, followed by the addition of two equivalents of an oxidant (either silver tetrafluoroborate or ferrocenium tetrafluoroborate) and excess monomeric cyclopentadiene. Upon warming to ambient temperature over 16 hours, analysis of the residue by NMR spectroscopy revealed only the presence of a paramagnetic compound or compounds, the composition of which has not yet been determined.

Various alternative reaction pathways are possible to rationalize the transience of the intermediate cobalt(II) vinyl species. The most likely mode of decomposition is ligand redistribution of the monomeric or dimeric cobalt vinyl

intermediate to afford (decamethyl)cobaltocene<sup>323</sup> and a highly unsaturated bis(vinyl) complex (Scheme 4-30).

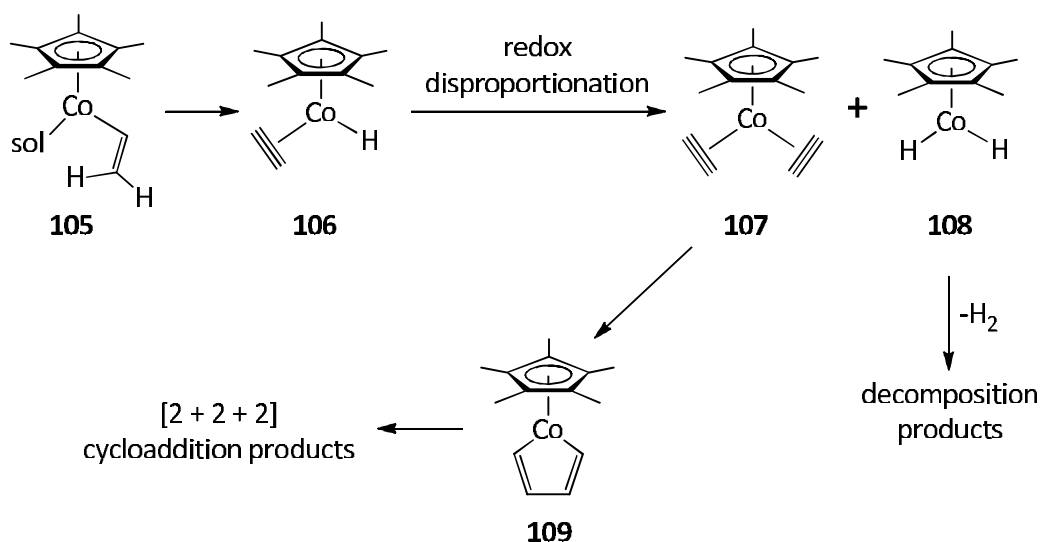
**Scheme 4-30**



An alternative decomposition pathway is  $\beta$ -hydride elimination from the intermediate vinyl complex **105**, converting the  $\eta^2$ -vinyl to the  $\eta^2$ -acetylene ligand (Scheme 4-31). Transfer of a vinyl hydrogen atom to the cobalt centre produces the hydrido-acetylene complex **106**, which may undergo redox disproportionation with another equivalent of **106** to afford the bis(alkyne) complex **107** and the dihydride complex **108**. Half-sandwich cobalt(I) bis(alkyne) complexes bearing small alkynes are difficult to isolate due to rapid oxidative coupling to form the corresponding metalacyclopentadiene complexes **109**,

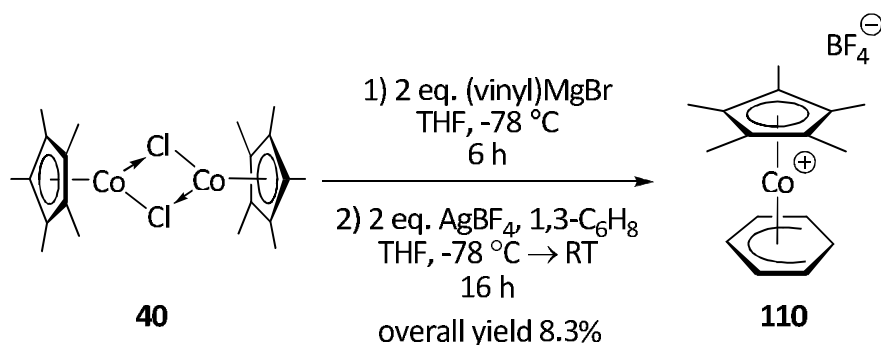
which are themselves intermediates along the cobalt catalyzed [2 + 2 + 2] alkyne cyclotrimerization reaction pathway.<sup>3, 4, 105-107, 303, 304, 324, 325</sup> The dihydride complex **108** can lose dihydrogen forming a highly unsaturated cobalt(I) cluster or set of solvento complexes.

**Scheme 4-31**



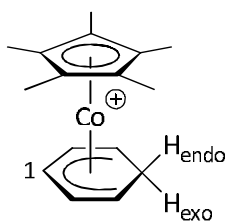
Although the use of phosphine or monomeric cyclopentadiene to trap the intermediate cobalt vinyl complex was unsuccessful, the addition of 1,3-cyclohexadiene furnished an isolable product. Treatment of the crude vinylation reaction mixture with excess 1,3-cyclohexadiene at low temperature, followed by oxidation using silver tetrafluoroborate, afforded the cationic  $\eta^5$ -hexadienyl complex **110** in very poor yield (Equation 4-17). The product was purified by column chromatography and recrystallized from a mixture of dichloromethane/diethyl ether.

Equation 4-17



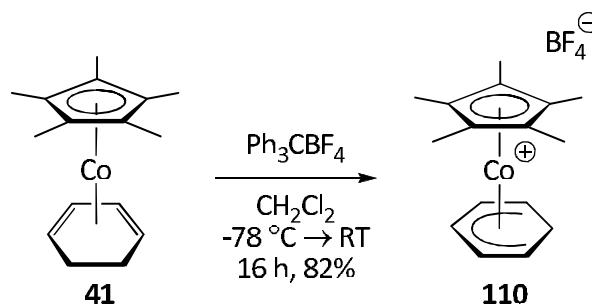
Relevant <sup>1</sup>H NMR data are summarized in Figure 4-7 and Table 4-1. The <sup>1</sup>H NMR spectrum consists of a downfield triplet at δ 6.80, coupled to another triplet slightly upfield at δ 5.09, in turn mutually coupled to another triplet at δ 3.29. Each downfield triplet possesses a coupling constant of <sup>3</sup>J<sub>HH</sub> = 6.5 Hz. A set of methylene protons are located at 1.45 ppm and 2.82 ppm and are strongly and mutually coupled (<sup>2</sup>J<sub>HH</sub> = 15.7 Hz). The structure of the cationic η<sup>5</sup>-cyclohexadienyl complex **110** was confirmed by an independent synthesis: hydride abstraction from cobalt η<sup>4</sup>-cyclohexadiene complex **41** using trityl tetrafluoroborate (Equation 4-18). The resulting product is spectroscopically indistinguishable from the η<sup>5</sup>-cyclohexadienyl complex **110**.

Figure 4-7: <sup>1</sup>H Numbering Scheme for Cobalt η<sup>5</sup>-Cyclohexadienyl Cation **110**



**Table 4-1:**  $^1\text{H}$  NMR Spectroscopic Data for Cobalt  $\eta^5$ -Cyclohexadienyl Cation **110**

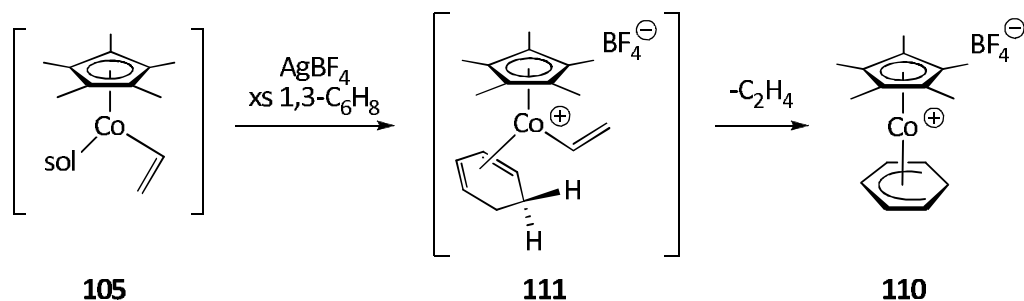
Position	$\delta$ $^1\text{H}$
1	6.80 (t, $J = 6.5$ Hz)
2	5.09 (t, $J = 6.5$ Hz)
3	3.29 (t, $J = 6.5$ Hz)
4	2.82 (d, $J = 15.7$ Hz, $\text{H}_{\text{exo}}$ ) 1.45 (d, $J = 15.7$ , $\text{H}_{\text{endo}}$ )
$\text{C}_5(\text{CH}_3)_5$	1.97 (s)

**Equation 4-18**

The formation of the  $\eta^5$ -cyclohexadienyl complex **110** from chlorocobalt(II) dimer **40** is unusual, though the compound arises only as a byproduct in low yield. A possible rationale for the formation of the  $\eta^5$ -cyclohexadienyl adduct **110** begins with formation of the unsaturated cobalt(II) vinyl complex **105** at low temperature (Scheme 4-32). Upon addition of a

stoichiometric amount of silver tetrafluoroborate and excess 1,3-cyclohexadiene at low temperature, presumably oxidation of the cobalt and coordination of diene occur to form cobalt vinyl-cyclohexadiene complex **111**. No evidence for the intermediacy of **111** exists. Allylic carbon-hydrogen bond activation and elimination of ethylene furnish the observed cationic  $\eta^5$ -cyclohexadienyl product **110**.

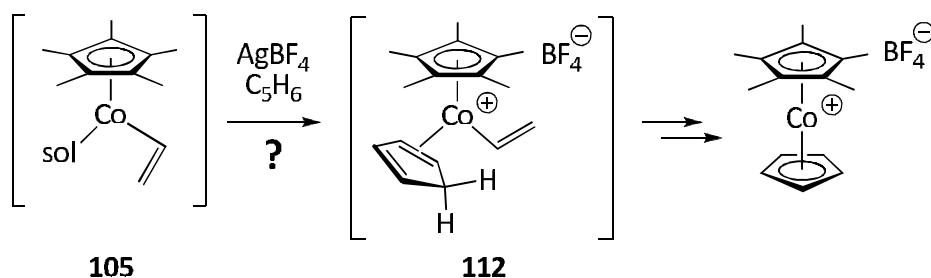
**Scheme 4-32**



A similar mechanism could also rationalize the product from cyclopentadiene addition (Scheme 4-33). Addition of silver tetrafluoroborate and monomeric cyclopentadiene to the crude vinylated reaction mixture might afford the vinyl-cyclopentadiene complex **112**, which could undergo allylic carbon-hydrogen bond activation of the bound cyclopentadiene moiety followed by ethylene extrusion to afford an unsymmetrical cobalticenium salt. However, no evidence for the formation of the cobalticenium salt was found in the reaction residue. While plausible, this mechanism does not account for the

majority of the paramagnetic product mixture when either cyclopentadiene or cyclohexadiene is added.

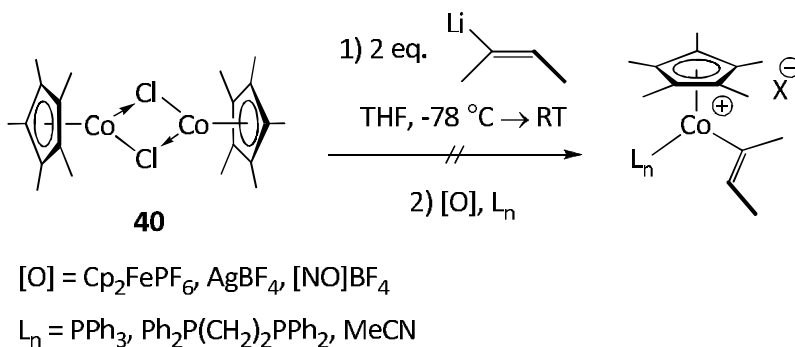
**Scheme 4-33**



The lack of coherent reactivity of vinyl complex **105** with cyclopentadiene upon oxidation can be attributed simply to the lack of substituents on the vinyl ligand. Dzwiniel has shown that protonation of (C<sub>5</sub>H<sub>5</sub>)Co(RC<sub>5</sub>H<sub>5</sub>) (R = Me, **31**; R = *t*-Bu, **32**) with strong acid and excess acetylene leads to allyl-alkyne cycloaddition (Equation 2-7), whereas substituted alkynes, such as 2-butyne, leads to ring-expansion (Scheme 4-20). This observation suggests that the unsubstituted vinyl ligand may be less reactive towards ring-expansion than other pathways, and that the corresponding cobalt-vinyl complex derived from 2-butyne would be a better candidate. We envisioned that the addition of the 2-butenyl anion to either cobalt(II) or cobalt(III) precursor should afford the desired cobalt  $\eta^2$ -butenyl intermediates. The addition of monomeric cyclopentadiene to a cationic unsaturated derivative should afford seven-membered ring products.

The lithiated derivative of 2-bromo-2-butene was generated by standard lithium-halide exchange procedures using either one equivalent of *n*-butyllithium or two equivalents of *tert*-butyllithium. Treatment of two equivalents 2-lithio-2-butene with chlorocobalt dimer **40** at low temperature was followed by oxidation with a range of oxidants in the presence of several different Lewis bases (Equation 4-19). Under all reactions conditions tested, only persistently paramagnetic residues were obtained.

**Equation 4-19**



One additional strategy was investigated for the synthesis of cobalt  $\eta^2$ -vinyl complexes: oxidative addition of an alkenyl bromide followed by halide abstraction to generate the corresponding cation. Such an approach has been reported for the synthesis of (C<sub>5</sub>R<sub>5</sub>)Co( $\eta^3$ -allyl)X (where R = H, Me; X = halide) from the corresponding (C<sub>5</sub>R<sub>5</sub>)Co(ethylene)<sub>2</sub> and substituted allylic bromides.<sup>116</sup>

Treatment of a solution of (C<sub>5</sub>Me<sub>5</sub>)Co(C<sub>2</sub>H<sub>4</sub>)<sub>2</sub> at ambient temperature with either excess vinyl bromide or excess 2-bromo-2-butene returned only starting

material. Performing the exchange reaction at elevated temperatures resulted only in the decomposition of the starting bis(ethylene) complex. Performing the reaction under photochemical conditions (Hanovia 450W lamp, UV, Pyrex, ambient temperature) resulted in rapid decomposition of the starting material within 15 min as evidenced by the quick colour change from red to green, characteristic of the formation of cobalt(II). This is supported by  $^1\text{H}$  NMR spectroscopy of the crude product residue which revealed broadened resonances which are characteristic of paramagnetic residue. The crude product residue was chromatographed using neutral alumina (Activity I) and hexane in order to remove the paramagnetic products and establish the fate of the starting alkenyl bromide. Proton NMR spectroscopy of the chromatographed residue, however, revealed a complicated mixture, demonstrating that under the reaction conditions the alkenyl bromide decomposes. It is plausible that the rate of decomposition of the alkenyl bromide is faster than oxidative addition to the cobalt(I) complex, leading to the formation of paramagnetic cobalt complexes.

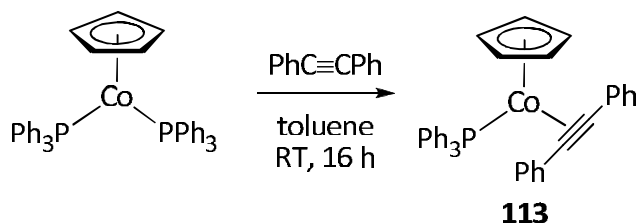
### **C. Strong Acid Addition to Cobalt Mono-Alkyne Complex**

Green has demonstrated that the addition of strong acid to a bis(alkyne) molybdenum(II) complex generates a 1-metalacyclopropene complex (Equation

4-12).<sup>298</sup> A similar synthetic approach using a half-sandwich cobalt mono-alkyne complex was thus undertaken.

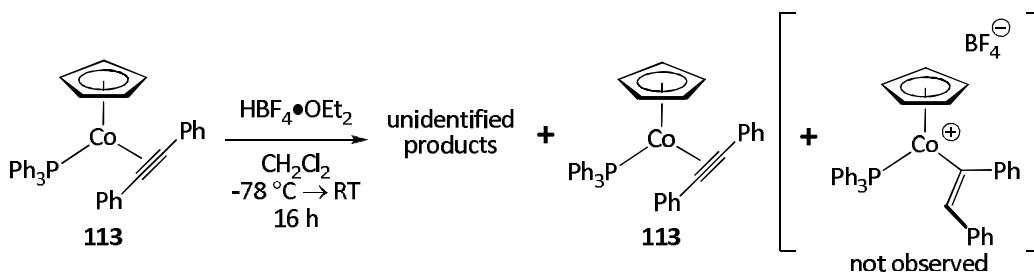
A paucity of known half-sandwich cobalt mono-alkyne complexes limited the choice of precursors to  $(C_5H_5)Co(PPh_3)(\eta^2-PhCCPh)$  **113**. The starting material was prepared according to the literature procedure by *in situ* exchange of diphenylacetylene with  $(C_5H_5)Co(PPh_3)_2$  (Equation 4-21).<sup>309</sup>

#### Equation 4-20



The mono-alkyne complex **113** was thus treated with  $HBF_4 \cdot OEt_2$  at low temperature (Equation 4-21). After warming to ambient temperature, the solvent was removed and the crude product residue analyzed using  $^1H$ ,  $^{13}C$ , and  $^{31}P$  NMR spectroscopy. Both the  $^1H$  and  $^{31}P$  spectral data of the crude residue showed that some starting material was present, albeit with significant broadening of the resonances, along with multiple  $C_5H_5$  resonances, indicating the formation of multiple products. No further characterization was attempted.

Equation 4-21



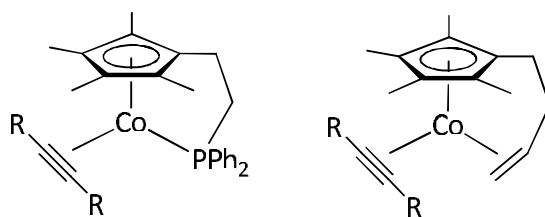
The presence of unreacted starting material is mystifying based on the addition of a stoichiometric amount of strong acid. It is plausible that the protonation of mono-alkyne complex **113** is slow at low temperature (Scheme 4-34). Once the desired cationic cobalt vinyl complex is formed, triphenylphosphine may dissociate from the coordination sphere of the metal and be protonated by residual acid, thus preventing re-coordination of the phosphine. The fate of the resulting unsaturated cationic cobalt vinyl complex is unknown.

Although in principle such complexes could be stabilized by using a more electron-donating ligand, such as pentamethylcyclopentadienyl, this is not preceded here: the preparation of  $(\text{C}_5\text{Me}_5)\text{Co}(\text{PPh}_3)(\eta^2\text{-PhCCPh})$  or other analogues has not been reported.



complex. One possible solution to this problem is a cyclopentadienyl ligand possessing a tethered electron-donating ligand, such as ethylene or phosphines, which should kinetically inhibit phosphine dissociation (Figure 4-8). Both Okuda<sup>326</sup> and Cole-Hamilton<sup>327</sup> have reported cobalt complexes bearing such tethered cyclopentadienyl ligands. An alternative strategy to tethered ligands is the use of strongly electron-donating ligands, such as N-heterocyclic carbenes, which should not dissociate under the reaction conditions.

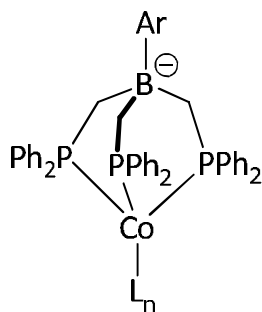
**Figure 4-8:** Potential Targets for the Preparation of Cobalt Mono-Alkyne Complexes



An alternative to the ubiquitous cyclopentadienyl template is the anionic tripodal tris(phosphino)borato series of ligands (Figure 4-9). Compared to the cyclopentadienyl ligand, the tris(phosphino)borato ligands and tripodal phosphine ligands in general possess several attractive features, including i) increased nucleophilicity of the metal centre; ii) better control of the coordination number, stoichiometry, and stereochemistry of the metal complex; iii) slower and more controlled intra- and intermolecular exchange reactions; iv) formation of stable complexes in a variety of metal oxidation states; and v)

useful and detailed structural and bonding information derived from metal-to-phosphorous and phosphorous-to-phosphorous coupling constants in NMR spectra.<sup>328</sup>

**Figure 4-9:** Anionic Tripodal Tris(phosphine)borato Complex of Cobalt



The low yields obtained when bulky disubstituted alkynes are used for the ring-expansion of cobalt cyclopentenyl complexes can in principle be resolved by using the tris(phosphine)borato series of ligands, which can potentially dissociate a phosphine arm to accommodate the steric bulk of the alkyne. Peters has already prepared both iron<sup>329</sup> and cobalt<sup>330</sup> complexes bearing this tripodal ligand and has used the iron complexes to investigate dinitrogen and carbon dioxide activation.<sup>331-333</sup>

## Chapter 5. Experimental Procedures

### Reagents and Methods.

All manipulations on air sensitive compounds were performed under argon or nitrogen atmospheres using standard Schlenk techniques or a MBraun LABmaster SP dry box. Diethyl ether was distilled from sodium/benzophenone ketyl under nitrogen. Dichloromethane and acetonitrile were distilled from calcium hydride and degassed. Hexane and pentane were distilled from potassium/benzophenone ketyl. Acetone was dried over boric oxide, degassed *via* three freeze-pump-thaw cycles, vacuum transferred and stored under nitrogen. Acetylene was passed sequentially through columns consisting of concentrated sulfuric acid and sodium hydroxide. All other reagents were used without further purification.  $^1\text{H}$  NMR and  $^{13}\text{C}$  NMR spectra were recorded on either a Varian Unity-Inova 300 ( $^1\text{H}$ , 300 MHz), Varian Unity-Inova 400 ( $^1\text{H}$ , 400 MHz;  $^{13}\text{C}$ , 100 MHz), Varian Mercury 400 ( $^1\text{H}$ , 400 MHz;  $^{13}\text{C}$ , 100 MHz), Varian Unity-Inova 500 ( $^1\text{H}$ , 500 MHz;  $^{13}\text{C}$ , 125 MHz), or Varian DirectDrive 500 ( $^1\text{H}$ , 500 MHz;  $^{13}\text{C}$ , 125 MHz). High-resolution mass spectra were obtained on an Applied Biosystems Mariner Biospectrometry Workstation (electrospray ionization) and a Kratos Analytical MS-50B (electron impact). Elemental analyses were performed by the University of Alberta Microanalysis Laboratories.

## Further Notes on Spectroscopic Methods.

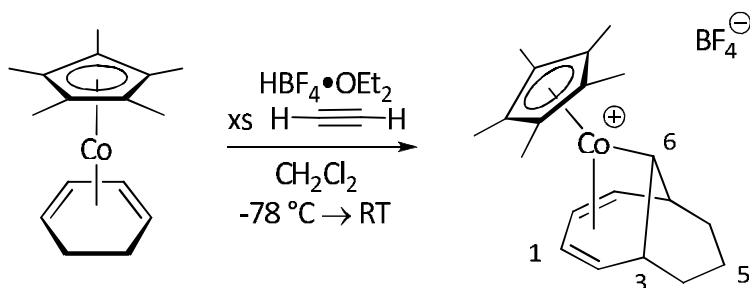
Chemical shifts are reported relative to residual protiated solvent. For  $^1\text{H}$  NMR spectral data, values of the coupling constants are obtained directly. Although generally measured to  $\pm 0.1$  Hz,  $J$  values are self-consistent to only  $\pm 1$  Hz. Data for  $^1\text{H}$ - $^1\text{H}$  COSY,  $^1\text{H}$ - $^{13}\text{C}$  HMQC,  $^1\text{H}$ - $^{13}\text{C}$  HSQC, and  $^1\text{H}$ - $^{13}\text{C}$  HMBC are presented such that correlations are listed only once. GCOSY, GHMQC, GHSQC and GHMBC denote the standard COSY, HMQC, HSQC and HMBC experiments were acquired using field gradients.

## Materials.

The following compounds were prepared by published procedures:  $\text{C}_5\text{Me}_5\text{Li}$ ,<sup>334</sup>  $[(\text{C}_5\text{Me}_5)\text{CoCl}]_2$ ,<sup>152</sup>  $(\text{C}_5\text{Me}_5)\text{Co}(\eta^4\text{-cyclohexadiene})$ ,<sup>132</sup>  $(\text{C}_5\text{Me}_5)\text{Co}(\eta^4\text{-cyclooctadiene})$ ,<sup>121</sup>  $(t\text{-Bu}_2\text{C}_5\text{H}_3)\text{Li}$ ,<sup>165, 166, 335</sup>  $(\text{C}_5\text{H}_5)\text{Co}(\text{CO})\text{I}_2$ ,<sup>314</sup>  $[(\text{C}_5\text{H}_5)\text{CoI}_2]_n$ ,<sup>314</sup>  $(\text{C}_5\text{H}_5)\text{Co}(\text{PPh}_3)\text{I}_2$ ,<sup>314</sup>  $(\text{C}_5\text{Me}_5)\text{Co}(\text{PPh}_3)\text{I}_2$ ,<sup>314, 336</sup>  $[(\text{C}_5\text{Me}_5)\text{CoX}_2]_n$  ( $X = \text{Cl, I}$ ),<sup>153-156, 337</sup>  $(\text{C}_5\text{Me}_5)\text{Co}(\eta^4\text{-butadiene})$ ,<sup>103, 319</sup> and  $(\text{C}_5\text{H}_5)\text{Co}(\text{PPh}_3)(\text{PhCCPh})$ .<sup>311, 312</sup>

Sodium amalgam was prepared by dissolving small pieces of sodium in mercury until a homogenous mixture was achieved. The concentration of sodium in mercury did not exceed 1% by weight.

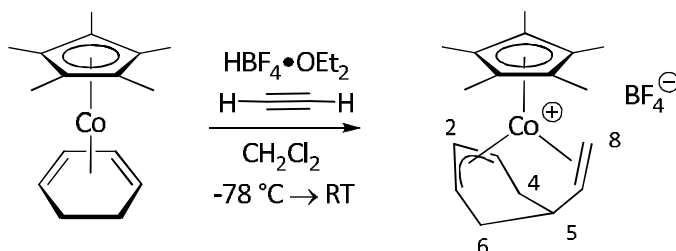
## Chapter 2 Experimental Section



### **$[(C_5Me_5)Co(\eta^1, \eta^4\text{-bicyclo[4.3.1]deca-2,4-dien-10-ide})]BF_4$ (42)**

A red solution of  $(C_5Me_5)Co(1,3\text{-cyclohexadiene})$  (311.1 mg, 1.14 mmol) in degassed dichloromethane (20 mL) was cooled to  $-78^\circ C$ . Acetylene was bubbled through the solution for 10 min and  $HBF_4 \cdot OEt_2$  (160  $\mu L$ , 1.16 mmol) was added. The reaction mixture was held at  $-78^\circ C$  for 24 hours, then warmed to  $-50^\circ C$  for 48 hours and then  $-30^\circ C$  for 4 hours before removing the solvent *in vacuo*. The residue was purified by chromatography on silica gel (3% methanol/dichloromethane v/v) and crystallized from dichloromethane/diethyl ether to afford 302 mg (64%) of a red powder.  $^1H$  NMR (500 MHz,  $CDCl_3$ ):  $\delta$  5.78 (m, 2<sup>nd</sup> order pattern,  $H_1$ ),  $\delta$  3.80 (m, 2<sup>nd</sup> order pattern, 2H,  $H_2$ ),  $\delta$  2.83 (m, 2<sup>nd</sup> order pattern, 2H,  $H_3$ ),  $\delta$  1.81 (s, 15H,  $C_5(CH_3)_5$ ),  $\delta$  1.34 (t,  $J = 8.5$  Hz, 1H,  $H_6$ ),  $\delta$  0.9-1.1 (m, 4H,  $H_4/H_4'$ ),  $\delta$  0.5 (m, 2H,  $H_5$ );  $^{13}C$  NMR (125.3 MHz,  $CDCl_3$ ):  $\delta$  100.6, 99.9, 61.9, 32.9, 30.4, 14.7, 9.56, -16.1; gCOSY (300 MHz,  $CDCl_3$ )  $\delta$  5.78  $\leftrightarrow$   $\delta$  3.80;  $\delta$  3.80  $\leftrightarrow$   $\delta$  2.83;  $\delta$  2.83  $\leftrightarrow$   $\delta$  1.34,  $\delta$  1.05;  $\delta$  1.05  $\leftrightarrow$   $\delta$  0.5; gHMQC (500 MHz,  $CDCl_3$ ):  $\delta$  99.9  $\leftrightarrow$   $\delta$  5.78;  $\delta$  61.9  $\leftrightarrow$   $\delta$  3.80;  $\delta$  32.9  $\leftrightarrow$   $\delta$  2.83;  $\delta$  30.4  $\leftrightarrow$   $\delta$

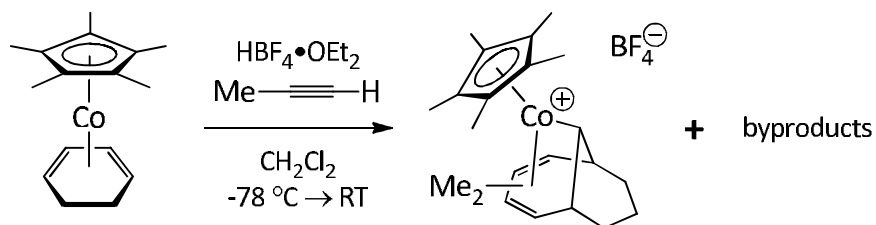
1.05;  $\delta$  14.7  $\leftrightarrow$   $\delta$  0.5;  $\delta$  9.56  $\leftrightarrow$   $\delta$  1.81;  $\delta$  -16.1  $\leftrightarrow$   $\delta$  1.34; Electrospray MS  $m/z$  calculated for  $C_{20}H_{28}Co$  ( $M^+ - BF_4$ ): 327.15175; found: 327.15213; Analysis calculated for  $C_{20}H_{28}CoPF_6$ : C, 50.89%; H, 5.97%; found: C, 51.01%; H, 6.03%.



### **$[(C_5Me_5)Co(\eta^3, \eta^2-5\text{-vinylcyclohex-2-en-1-yl})]BF_4$ (43)**

A red solution of  $(C_5Me_5)Co(1,3\text{-cyclohexadiene})$  (0.240 g, 0.87 mmol) in degassed dichloromethane (20 mL) was cooled to  $-78\text{ }^\circ\text{C}$ . Acetylene was bubbled through the solution for 45 seconds and  $HBF_4 \cdot OEt_2$  (120  $\mu\text{L}$ , 0.87 mmol) was added. The mixture was stirred for 3 hours at low temperature and then warmed to ambient temperature. The solvent was removed *in vacuo* and the mixture chromatographed on silica gel (3% methanol/dichloromethane v/v) and then crystallized from dichloromethane/diethyl ether mixture to afford 0.317 mg (93.3%) of a red powder.  $^1\text{H NMR}$  (400 MHz,  $CDCl_3$ ):  $\delta$  5.32 (dt,  $J = 7.0, 1.6$  Hz, 1H,  $H_3$ ),  $\delta$  4.83 (t,  $J = 7.0$  Hz, 1H,  $H_1$ ),  $\delta$  4.64 (dd,  $J = 14.0, 8.0$  Hz, 1H,  $H_7$ ),  $\delta$  4.54 (d,  $J = 14.0$  Hz, 1H,  $H_{8a}$ ),  $\delta$  4.30 (dd,  $J = 7.0$  Hz, 1H,  $H_2$ ),  $\delta$  3.97 (d,  $J = 8.0$  Hz, 1H,  $H_{8b}$ ),  $\delta$  2.22 (dt,  $J = 14.5, 3.5$  Hz, 1H,  $H_{4a}$ ),  $\delta$  1.88 (m, partially obscured, 1H,  $H_5$ ),  $\delta$  1.68 (s, 15H,  $C_5Me_5$ ),  $\delta$  1.56 (d,  $J = 13.5$  Hz, 1H,  $H_{4b}$ ),  $\delta$  1.20 (dt,  $J = 16.0, 3.5$  Hz,

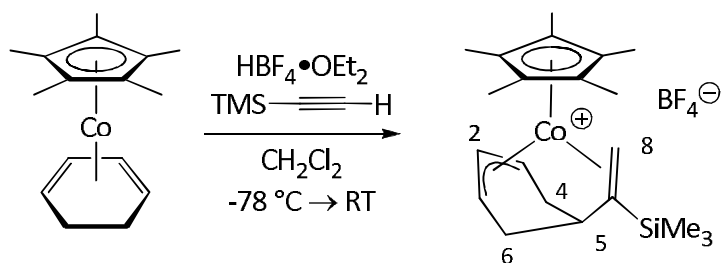
1H, H<sub>6a</sub>),  $\delta$  0.57 (d,  $J$  = 15.5 Hz, 1H, H<sub>6b</sub>);  $^{13}\text{C}\{^1\text{H}\}$  (100.58 MHz,  $\text{CDCl}_3$ ):  $\delta$  100.6, 99.6, 90.0, 85.9, 83.2, 75.0, 37.6, 36.4, 24.0, 9.7; gCOSY (400 MHz,  $\text{CDCl}_3$ ):  $\delta$  5.32  $\leftrightarrow$   $\delta$  4.30, 2.22, 1.56;  $\delta$  4.83  $\leftrightarrow$   $\delta$  4.30, 1.20, 0.57;  $\delta$  4.64  $\leftrightarrow$   $\delta$  4.54, 3.97;  $\delta$  1.88  $\leftrightarrow$   $\delta$  4.64, 4.54, 2.22, 1.56, 1.20, 0.57; gHMQC (400 MHz,  $\text{CDCl}_3$ ):  $\delta$  5.32  $\leftrightarrow$   $\delta$  83.2;  $\delta$  4.83  $\leftrightarrow$   $\delta$  85.9;  $\delta$  4.64  $\leftrightarrow$   $\delta$  100.6;  $\delta$  4.54, 3.97  $\leftrightarrow$   $\delta$  75.0;  $\delta$  4.3  $\leftrightarrow$  90.0;  $\delta$  2.22, 1.56  $\leftrightarrow$   $\delta$  37.6;  $\delta$  1.88  $\leftrightarrow$   $\delta$  36.4;  $\delta$  1.68  $\leftrightarrow$   $\delta$  9.7;  $\delta$  1.20, 0.57  $\leftrightarrow$   $\delta$  24.0; Electrospray MS  $m/z$  calculated for  $\text{C}_{18}\text{H}_{26}\text{Co}$  ( $\text{M}^+\text{-BF}_4$ ): 301.1360; found: 301.13643; Analysis calculated for  $\text{C}_{18}\text{H}_{26}\text{CoBF}_4$ : C, 55.7%; H, 6.75%; found: C, 55.7%; H, 6.60%.



**[[ $\text{C}_5\text{Me}_5$ Co(dimethyl- $\eta^1, \eta^4$ -bicyclo[4.3.1]deca-2,4-dien-10-ide)] $\text{BF}_4$  (42-Me<sub>2</sub>)**

A red solution of  $(\text{C}_5\text{Me}_5)\text{Co}(\eta^4\text{-cyclohexadiene})$  (0.105 g, 0.38 mmol) in degassed dichloromethane (20 mL) was cooled to  $-78$  °C. Excess propyne was bubbled through the solution for 10 minutes and  $\text{HBF}_4 \cdot \text{OEt}_2$  (52  $\mu\text{L}$ , 0.38 mmol) were added via syringe. The mixture was stirred overnight while warming to ambient temperature. The solvent was removed *in vacuo* and the mixture chromatographed on silica gel (3% methanol/dichloromethane v/v) to afford 113 mg dark red oil. The assignment of the product was based on electrospray mass

spectrometry and partial  $^1\text{H}$  NMR data of the product mixture. The  $^1\text{H}$  NMR spectrum of the product mixture showed multiple broadened resonances, indicating a persistent paramagnetic impurity which could not be separated from the bulk sample.  $^1\text{H}$  NMR (400 MHz,  $\text{CDCl}_3$ ):  $\delta$  2.65 (s, 3H, Me);  $\delta$  2.31 (s, 3H, Me), 1.72 (s, 15H,  $\text{C}_5\text{Me}_5$ ); Electro spray MS  $m/z$  calculated for  $\text{C}_{22}\text{H}_{32}\text{Co}$  ( $\text{M}^+ - \text{BF}_4$ ): 355.1831; found: 335.1845.

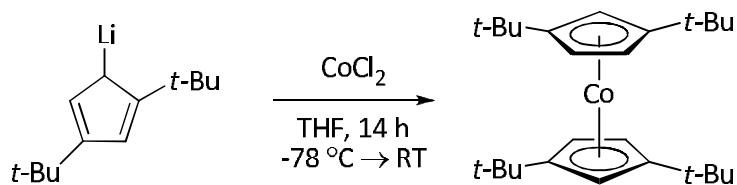


**$[(\text{C}_5\text{Me}_5)\text{Co}(\eta^3, \eta^2\text{-5-(1-trimethylsilylvinyl)cyclohex-2-en-1-yl)]\text{BF}_4$  (47)**

A red solution of  $(\text{C}_5\text{Me}_5)\text{Co}(\eta^4\text{-cyclohexadiene})$  (0.240 g, 0.87 mmol) in degassed dichloromethane (20 mL) was cooled to  $-78\text{ }^\circ\text{C}$ . Ethynyltrimethylsilane (0.6 mL, 4.24 mmol) and  $\text{HBF}_4 \cdot \text{OEt}_2$  (120  $\mu\text{L}$ , 0.87 mmol) were added via syringe. The mixture was stirred overnight while warming to ambient temperature. The solvent was removed *in vacuo* and the mixture chromatographed on silica gel (3% methanol/dichloromethane v/v) and then crystallized from dichloromethane/diethyl ether mixture to afford 241 mg (60%) of a red powder.  $^1\text{H}$  NMR (400 MHz,  $\text{CDCl}_3$ ):  $\delta$  5.55 (d,  $J = 6.0$  Hz, 1H,  $\text{H}_1$ );  $\delta$  5.04 (s,  $\text{H}_{8a/8b}$ );  $\delta$  4.70 (t,  $J = 5.6$  Hz, 1H,  $\text{H}_3$ );  $\delta$  4.19 (t,  $J = 6.0$  Hz, 1H,  $\text{H}_2$ );  $\delta$  4.09 (s, 1H,  $\text{H}_{8a}/\text{H}_{8b}$ );  $\delta$  2.37

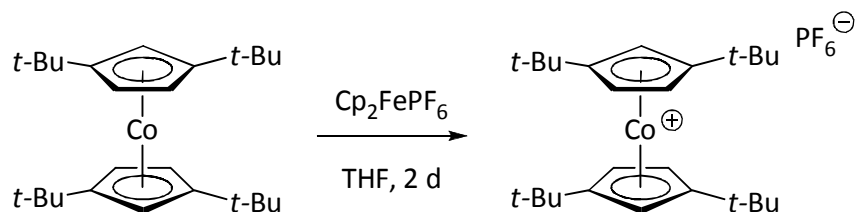
(dt,  $J = 14.4, 3.6$  Hz, 1H, H<sub>6a</sub>);  $\delta$  1.66 (s, 15H, C<sub>5</sub>Me<sub>5</sub>);  $\delta$  1.60 (obscured under C<sub>5</sub>Me<sub>5</sub> peak, H<sub>5</sub>);  $\delta$  1.51 (d,  $J = 14.4$  Hz, 1H, H<sub>6b</sub>);  $\delta$  1.18 (d,  $J = 16.0$  Hz, 1H, H<sub>4a</sub>);  $\delta$  0.4 (d,  $J = 16.0$  Hz, 1H, H<sub>4b</sub>);  $\delta$  0.34 (s, 9H, SiMe<sub>3</sub>); <sup>13</sup>C NMR (100.58 MHz, CDCl<sub>3</sub>):  $\delta$  121.7, 100.1, 90.0, 83.0, 82.03, 82.01, 40.8, 38.8, 23.8, 10.2, 2.2; gCOSY (400 MHz, CDCl<sub>3</sub>):  $\delta$  5.55  $\leftrightarrow$   $\delta$  4.19, 2.37;  $\delta$  4.70  $\leftrightarrow$   $\delta$  4.19, 0.40;  $\delta$  2.37  $\leftrightarrow$   $\delta$  1.72, 1.51;  $\delta$  1.72  $\leftrightarrow$   $\delta$  1.18, 0.40;  $\delta$  1.18  $\leftrightarrow$   $\delta$  0.40; gHSQC (400 MHz, CDCl<sub>3</sub>):  $\delta$  5.55  $\leftrightarrow$   $\delta$  82.01;  $\delta$  5.04, 4.09  $\leftrightarrow$   $\delta$  82.03;  $\delta$  4.70  $\leftrightarrow$   $\delta$  83.0;  $\delta$  4.19  $\leftrightarrow$   $\delta$  90.0;  $\delta$  2.37, 1.51  $\leftrightarrow$   $\delta$  38.8 (C<sub>4</sub> or C<sub>6</sub>);  $\delta$  1.66  $\leftrightarrow$   $\delta$  10.2;  $\delta$  1.72  $\leftrightarrow$   $\delta$  40.8;  $\delta$  1.18  $\leftrightarrow$   $\delta$  23.8;  $\delta$  0.40  $\leftrightarrow$   $\delta$  23.76;  $\delta$  0.34  $\leftrightarrow$   $\delta$  2.2; Electrospray MS  $m/z$  calculated for C<sub>21</sub>H<sub>34</sub>CoSi (M<sup>+</sup>-BF<sub>4</sub>): 373.1762; found: 373.1759; All attempts to obtain satisfactory elemental analysis of the sample were unsuccessful, the values obtained were not within the acceptable ranges ( $\pm 0.4\%$ ).

## Chapter 3 Experimental Section



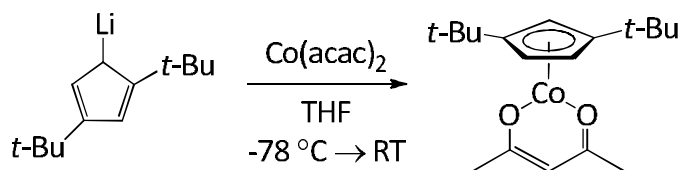
### **$(t\text{-Bu}_2\text{C}_5\text{H}_3)_2\text{Co}$ (62)**

A Schlenk flask was charged with  $\text{CoCl}_2$  (74.1 mg, 0.57 mmol) in 10 mL THF and cooled to  $-78\text{ }^\circ\text{C}$ . A pale yellow solution of lithium 1,3-di-tert-butylcyclopentadienide (105 mg, 0.57 mmol) in 15 mL degassed THF was added the mixture via syringe over a period of 10 minutes. The pale blue suspension changed to a deep red colour after the addition was complete. The resulting red mixture was stirred for 14 hours while warming to ambient temperature, whereupon the solvent was removed *in vacuo*. The mixture was dissolved in hexane and filtered through diatomaceous earth, affording 85.4 mg (72%) of a dark red powder. EI MS  $m/z$  calculated for  $\text{C}_{26}\text{H}_{42}\text{Co}$ : 413.26185; found: 413.26164; Analysis calculated for  $\text{C}_{26}\text{H}_{42}\text{Co}$ : C, 75.1%; H, 10.24%; found: C, 74.9%; H, 10.31%.



**[(*t*-Bu<sub>2</sub>C<sub>5</sub>H<sub>3</sub>)<sub>2</sub>Co]PF<sub>6</sub> (**63**)**

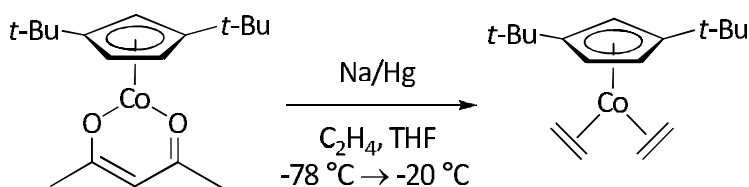
To a deep red solution of cobalticenium complex **62** (20 mg, 0.048 mmol) in 10 mL degassed THF was added Cp<sub>2</sub>FePF<sub>6</sub> (16 mg, 0.048 mmol). The resulting brown mixture was stirred for 2 days, whereupon the solvent was removed *in vacuo*. The product mixture was triturated with hexanes until no yellow colour was present in the filtrate. The product was recrystallized from a THF/hexane mixture to afford 13.2 mg (49%) of a yellow powder. <sup>1</sup>H NMR (400 MHz, acetone-d<sup>6</sup>): δ 5.89 (t, *J* = 1.6 Hz, 1H, H<sub>1</sub>); δ 5.73 (d, *J* = 1.6 Hz, 2H, H<sub>2</sub>); δ 1.43 (s, 18H, *t*-Bu); Analysis calculated for C<sub>26</sub>H<sub>42</sub>CoPF<sub>6</sub>: C, 55.9%; H, 7.58%; found: C, 55.6%; H, 7.39%.



**(*t*-Bu<sub>2</sub>C<sub>5</sub>H<sub>3</sub>)Co(C<sub>5</sub>H<sub>7</sub>O<sub>2</sub>) (**64**)**

A Schlenk flask was charged with Co(acac)<sub>2</sub> (749 mg, 2.91 mmol) in 10 mL THF and cooled to -78 °C. A pale yellow solution of lithium 1,3-di-*tert*-

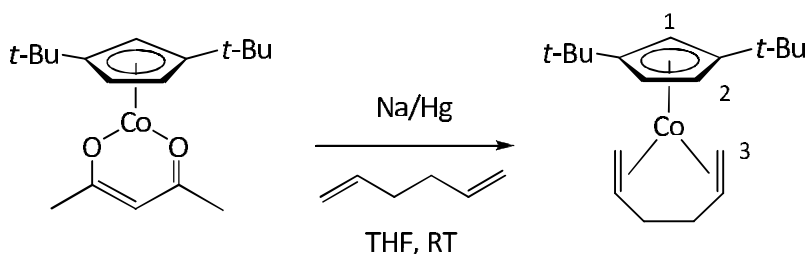
butylcyclopentadienide (519 mg, 2.82 mmol) in 15 mL degassed THF was added to the flask via syringe over a period of 10 minutes, immediately producing a deep red mixture. The resulting red mixture was stirred for 14 hours while warming to ambient temperature, whereupon the solvent was removed *in vacuo*. The mixture was dissolved in hexane and filtered through diatomaceous earth, affording 659 mg (70%) of a dark red oil. EI MS *m/z* calculated for  $C_{18}H_{28}O_2Co$ : 335.14212; found: 335.14224; Analysis calculated for  $C_{18}H_{26}O_2Co$ : C, 64.5%; H, 8.42%; found: C, 64.3%; H, 8.53%.



**$(t\text{-Bu}_2C_5H_3)Co(C_2H_4)_2$  (**65**)**

A dark red solution of  $(t\text{-Bu}_2C_5H_3)Co(acac)$  **64** (201.6 mg, 0.6 mmol) in 15 mL THF was added to a thick-walled reaction bomb containing sodium amalgam (160 mg sodium, 6.9 mmol; 22 g mercury) at ambient temperature. The bomb was cooled to  $-78\text{ }^\circ\text{C}$  and ethylene was introduced for 10 minutes, after which the vessel was sealed and warmed to  $-25\text{ }^\circ\text{C}$  and maintained at that temperature for 48 hours. The solvent was removed *in vacuo* and the oily mixture was quickly extracted with pentane and filtered through diatomaceous earth to afford 149.3

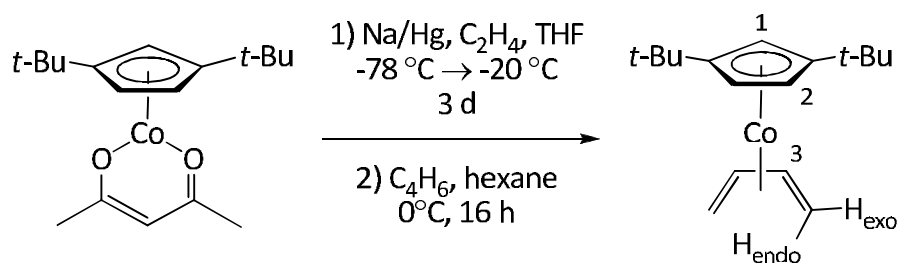
mg (~85%) of a dark red oil. Due to the thermal sensitivity of the product, complete removal of the solvent was not possible. The product was stored at -30 °C to minimize decomposition.  $^1\text{H}$  NMR (400 MHz,  $\text{C}_6\text{D}_6$ ):  $\delta$  3.77 (d,  $J$  = 2.5 Hz, 2H, CH-CH);  $\delta$  3.44 (t,  $J$  = 2.4 Hz, 1H, CH);  $\delta$  2.61 (m, 2<sup>nd</sup> order, 4H,  $\text{C}_2\text{H}_4$ );  $\delta$  1.40 (s, 18H, *t*-Bu);  $\delta$  0.67 (m, 2<sup>nd</sup> order, 4H,  $\text{C}_2\text{H}_4$ ).



**(*t*-Bu<sub>2</sub>C<sub>5</sub>H<sub>3</sub>)Co(1,5-hexadiene) (66)**

A dark red solution of *t*-Bu<sub>2</sub>CpCo(acac) **64** (105 mg, 0.31 mmol) in 15 mL degassed THF was added to a mixture of 160 mg sodium (7.0 mmol) and 19.5 g mercury at ambient temperature. 1,5-hexadiene (0.5 mL, 4.2 mmol) was then added via syringe and the mixture stirred overnight. The initially dark brown solution becomes a deep red mixture with visible precipitation. The solvent was removed *in vacuo* and the mixture extracted with hexane and filtered through diatomaceous earth. The solvent was removed *in vacuo*, affording 94 mg (95%) of a red oil.  $^1\text{H}$  NMR (400 MHz,  $\text{C}_6\text{D}_6$ ):  $\delta$  3.88 (m, 2H, H<sub>4</sub>);  $\delta$  3.75 (d,  $J$  = 2.2 Hz, 2H, H<sub>1</sub>); 3.47 (t,  $J$  = 2.2 Hz, 1H, H<sub>1</sub>);  $\delta$  2.39 (d,  $J$  = 8.3 Hz, 2H, H<sub>3<sub>exo</sub></sub>);  $\delta$  2.26 (m, 2H,

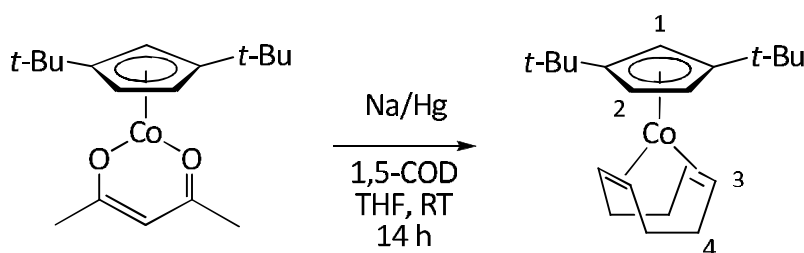
H<sub>5a</sub>/H<sub>5b</sub>);  $\delta$  1.37 (s, 18H, *t*-Bu);  $\delta$  1.20 (m, 2H, H<sub>4</sub>);  $\delta$  1.09 (d,  $J$  = 12.1 Hz, 2H, H<sub>3endo</sub>); <sup>13</sup>C NMR (100 MHz, C<sub>6</sub>D<sub>6</sub>):  $\delta$  113.1, 80.2, 79.2, 63.3, 40.2, 32.4, 32.3, 31.0; gCOSY (400 MHz, C<sub>6</sub>D<sub>6</sub>):  $\delta$  3.88  $\leftrightarrow$   $\delta$  2.39, 2.26, 1.20, 1.09;  $\delta$  3.75  $\leftrightarrow$   $\delta$  3.47;  $\delta$  2.39  $\leftrightarrow$   $\delta$  1.09;  $\delta$  2.26  $\leftrightarrow$   $\delta$  1.20; gHMQC (400 MHz, C<sub>6</sub>D<sub>6</sub>):  $\delta$  80.2  $\leftrightarrow$   $\delta$  3.75;  $\delta$  79.2  $\leftrightarrow$   $\delta$  3.47;  $\delta$  63.3  $\leftrightarrow$   $\delta$  3.88;  $\delta$  40.2  $\leftrightarrow$   $\delta$  2.39, 1.09;  $\delta$  32.4  $\leftrightarrow$   $\delta$  2.26, 1.20;  $\delta$  32.3  $\leftrightarrow$   $\delta$  1.37; EI MS  $m/z$  calculated for C<sub>19</sub>H<sub>31</sub>Co: 318.1758; found: 318.17554; Analysis calculated for C<sub>19</sub>H<sub>31</sub>Co: C, 71.7%; H, 9.81%; found: C, 71.4%; H, 9.77%.



### (*t*-Bu)<sub>2</sub>C<sub>5</sub>H<sub>3</sub>Co(C<sub>4</sub>H<sub>6</sub>) (67)

A dark red solution of (*t*-Bu)<sub>2</sub>C<sub>5</sub>H<sub>3</sub>Co(acac) **64** (147.6 mg, 0.44 mmol) in 15 mL THF was added to a thick-walled reaction bomb containing a mixture of 120 mg sodium (5.2 mmol) and 19 g mercury at room temperature. The bomb was cooled to -78 °C and ethylene was introduced for 10 minutes, after which the vessel was sealed and warmed to -25 °C and maintained at that temperature for 48 hours. The solvent was removed *in vacuo* and the oily mixture extracted with

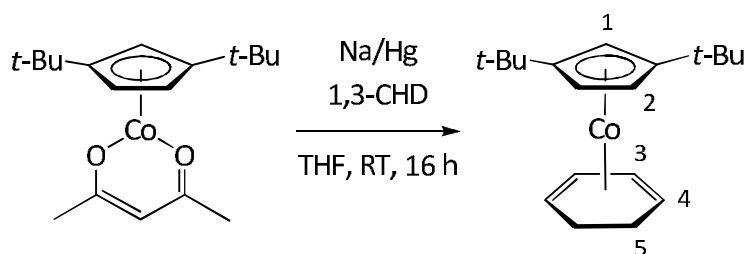
hexane. The solution was then introduced into a thick-walled reaction bomb and cooled to 0 °C. Excess butadiene was condensed into the reaction bomb and the mixture stirred for 16 hours while warming to ambient temperature. The solvent was removed *in vacuo* and the mixture extracted with pentane and filtered through diatomaceous earth to afford 87 mg (68%) of a deep red oil. <sup>1</sup>H NMR (500 MHz, C<sub>6</sub>D<sub>6</sub>): δ 4.95 (m, 2<sup>nd</sup> order, 2H, H<sub>3</sub>); δ 4.43 (t, *J* = 2.0 Hz, 1H, H<sub>1</sub>); δ 4.19 (d, *J* = 2.0 Hz, 2H, H<sub>2</sub>); δ 1.82 (m, 2<sup>nd</sup> order, 2H, H<sub>exo</sub>); δ 1.23 (s, 18H, *t*-Bu); δ -0.38 (m, 2<sup>nd</sup> order, 2H, H<sub>endo</sub>); gCOSY (500 MHz, C<sub>6</sub>D<sub>6</sub>): δ 4.95 (H<sub>3</sub>) ↔ δ 1.82 (H<sub>exo</sub>), -0.38 (H<sub>endo</sub>); δ 1.82 (H<sub>exo</sub>) ↔ δ -0.38 (H<sub>endo</sub>); EI MS *m/z* calculated for C<sub>17</sub>H<sub>27</sub>Co: 290.14447; found: 290.14436; Analysis calculated for C<sub>17</sub>H<sub>27</sub>Co: C, 70.3%; H, 9.37%; found: C, 70.1%; H, 9.26%.



### **(*t*-Bu<sub>2</sub>C<sub>5</sub>H<sub>3</sub>)Co(1,5-cyclooctadiene) (68)**

A dark red solution of *t*-Bu<sub>2</sub>CpCo(acac) **64** (175.8 mg, 0.52 mmol) in 15 mL THF was added to a mixture of 170 mg sodium (7.4 mmol) and 25.4 g mercury at ambient temperature. 1,5-Cyclooctadiene (0.5 mL, 4.1 mmol) was then added

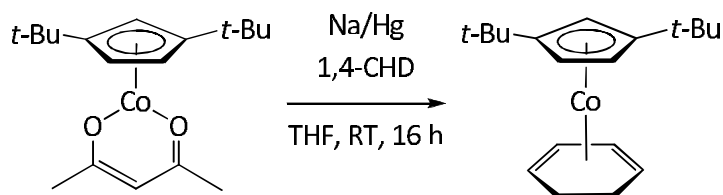
via syringe and the mixture stirred overnight. The initially dark red solution becomes an orange mixture with visible precipitation. After 14 hours, the solvent was removed *in vacuo* and the mixture extracted with hexane and filtered through diatomaceous earth. The solvent was removed to afford 179 mg (95%) of a red oil.  $^1\text{H}$  NMR (500 MHz,  $\text{C}_6\text{D}_6$ ):  $\delta$  3.78 (d,  $J = 2.5$  Hz, 2H,  $\text{H}_2$ ); 3.51 (m, 2<sup>nd</sup> order, 4H,  $\text{H}_3$ ); 3.41 (t,  $J = 2.0$  Hz, 1H,  $\text{H}_1$ ); 2.50 (m, 2<sup>nd</sup> order, 4H,  $\text{H}_{4\text{exo}}$ ); 1.70 (m, 2<sup>nd</sup> order, 4H,  $\text{H}_{4\text{endo}}$ ); 1.41 (s, 18H, *t*-Bu);  $^{13}\text{C}$  NMR (100 MHz,  $\text{C}_6\text{D}_6$ ):  $\delta$  113.4, 80.3, 77, 63.4, 32.4, 32.3, 31.7; gCOSY (400 MHz,  $\text{C}_6\text{D}_6$ ):  $\delta$  3.78 ( $\text{H}_2$ )  $\leftrightarrow$   $\delta$  3.41 ( $\text{H}_1$ );  $\delta$  3.51 ( $\text{H}_3$ )  $\leftrightarrow$   $\delta$  2.50, 1.70 ( $\text{H}_{4\text{endo}}$ ,  $\text{H}_{4\text{exo}}$ ); EI MS  $m/z$  calculated for  $\text{C}_{17}\text{H}_{27}\text{Co}$ : 344.1944; found: 344.1947; Analysis calculated for  $\text{C}_{21}\text{H}_{33}\text{Co}$ : C, 73.2%; H, 9.66%; found: C, 72.7%; H, 9.74%.



### **( $t\text{-Bu}_2\text{C}_5\text{H}_3$ )Co(1,3-cyclohexadiene) (69) (Method A)**

A dark red solution of  $t\text{-Bu}_2\text{CpCo}(\text{acac})$  **64** (63 mg, 0.19 mmol) in 15 mL THF was added to a mixture of 190 mg sodium (8.3 mmol) and 23.2 g mercury at room temperature. 1,3-Cyclohexadiene (0.5 mL, 5.3 mmol) was then added via syringe and the mixture stirred overnight. The initially dark red solution becomes an

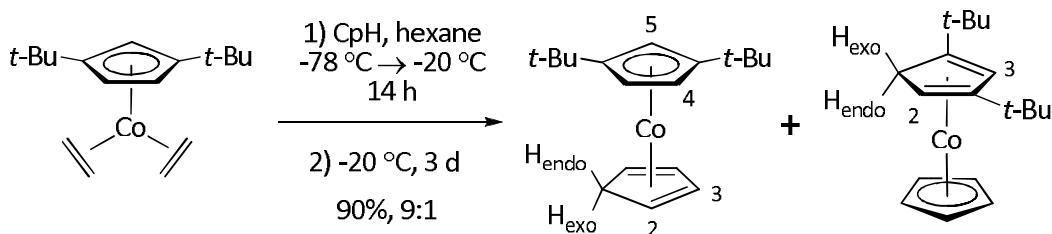
orange mixture with visible precipitation. The solvent was removed *in vacuo* and the mixture extracted with hexane and filtered through diatomaceous earth. The solvent was removed to afford 42 mg (71%) of a red oil. Upon standing at -35 °C, the oil solidifies but all attempts to recrystallize the sample have been unsuccessful.  $^1\text{H}$  NMR (400 MHz,  $\text{C}_6\text{D}_6$ ):  $\delta$  4.85 (m, 2<sup>nd</sup> order, dd in appearance, 2H,  $\text{H}_3$ ); 4.38 (t,  $J = 1.9$  Hz, 1H,  $\text{H}_1$ ); 4.33 (d,  $J = 1.9$  Hz, 2H,  $\text{H}_2$ ); 3.05 (m, 2<sup>nd</sup> order, 2H,  $\text{H}_4$ ); 1.59 (m, 2<sup>nd</sup> order, extracted coupling constant  $J = 11.1$  Hz, 2H,  $\text{H}_{5\text{endo}}$ ); 1.21 (s, 18H, *t*-Bu); 0.93 (m, 2<sup>nd</sup> order, extracted coupling constant  $J = 10.8$  Hz, 2H,  $\text{H}_{5\text{exo}}$ ); gCOSY (400 MHz,  $\text{C}_6\text{D}_6$ ):  $\delta$  4.85 ( $\text{H}_3$ )  $\leftrightarrow$   $\delta$  3.05 ( $\text{H}_4$ );  $\delta$  4.38 ( $\text{H}_1$ )  $\leftrightarrow$   $\delta$  4.33 ( $\text{H}_2$ ),  $\delta$  3.05 ( $\text{H}_4$ )  $\leftrightarrow$   $\delta$  1.59 ( $\text{H}_{\text{endo}}$ ), 0.93 ( $\text{H}_{\text{exo}}$ );  $\delta$  1.59 ( $\text{H}_{\text{endo}}$ )  $\leftrightarrow$   $\delta$  0.93 ( $\text{H}_{\text{exo}}$ ); EI MS  $m/z$  calculated for  $\text{C}_{19}\text{H}_{29}\text{Co}$ : 316.1601; found: 316.1600; Analysis calculated for  $\text{C}_{19}\text{H}_{29}\text{Co}$ : C, 72.1; H, 9.24; found: C, 71.7; H, 9.11.



### **( $t\text{-Bu}_2\text{C}_5\text{H}_3$ )Co(1,3-cyclohexadiene) (69) (Method B)**

A dark red solution of  $t\text{-Bu}_2\text{CpCo}(\text{acac})$  **64** (94 mg, 0.28 mmol) in 15 mL THF was added to a mixture of 280 mg sodium (12.2 mmol) and 30.5 g mercury at room temperature. 1,4-Cyclohexadiene (0.5 mL, 5.3 mmol) was then added via syringe and the mixture stirred overnight. The initially dark red solution becomes an

orange mixture with visible precipitation. The solvent was removed *in vacuo* and the mixture extracted with hexane and filtered through diatomaceous earth. The solvent was removed and afforded 76 mg (86%) of a red oil. Upon standing at -35 °C, the oil solidifies but all attempts to recrystallize the sample have been unsuccessful.



**(*t*-Bu<sub>2</sub>C<sub>5</sub>H<sub>3</sub>)Co(η<sup>4</sup>-C<sub>5</sub>H<sub>6</sub>) (72A) and (*t*-Bu<sub>2</sub>C<sub>5</sub>H<sub>4</sub>)Co(C<sub>5</sub>H<sub>5</sub>) (72B) (Method A)**

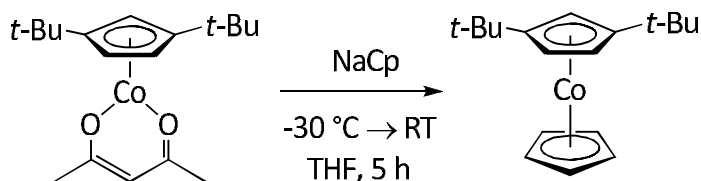
A dark brown solution of (*t*-Bu<sub>2</sub>C<sub>5</sub>H<sub>3</sub>)Co(C<sub>2</sub>H<sub>4</sub>)<sub>2</sub> **64** (140 mg, 0.48 mmol) in 15 mL pentane was added to a thick-walled reaction bomb and cooled to -78 °C. Monomeric cyclopentadiene (0.5 mL, 6.1 mmol) was added via syringe and the mixture stirred while warming to -20 °C over a period of 14 hours, after which it was held at -20 °C for three days. The volatile components were removed *in vacuo* and the mixture re-dissolved in pentane and filtered through diatomaceous earth. The solution was removed *in vacuo* to afford 130 mg (90%) of a dark red oil containing a 9 : 1 ratio of **72A** and **72B**. Upon standing at -35 °C, the oil solidified but repeated attempts to recrystallize the mixture were unsuccessful. **72A**: <sup>1</sup>H NMR (400 MHz, C<sub>6</sub>D<sub>6</sub>): δ 5.27 (m, 2<sup>nd</sup> order, 2H, H<sub>3</sub>); δ 4.48 (d, *J* = 1.6 Hz, 2H, H<sub>4</sub>); δ 4.14 (t, *J* = 1.6 Hz, 1H, H<sub>5</sub>); δ 2.75 (dt, *J* = 13.6, 2.0

Hz, 1H, H<sub>exo</sub>);  $\delta$  2.42 (br. s, 2H, H<sub>2</sub>);  $\delta$  2.09 (dt,  $J$  = 13.6, 1.7 Hz, 1H, H<sub>endo</sub>);  $\delta$  1.16 (s, 18H, *t*-Bu); <sup>13</sup>C NMR (400 MHz, C<sub>6</sub>D<sub>6</sub>):  $\delta$  110.5, 76.7, 74.7, 73.3, 41.7, 39.4, 31.9, 30.9; gCOSY (400 MHz, C<sub>6</sub>D<sub>6</sub>):  $\delta$  5.27  $\leftrightarrow$   $\delta$  2.75, 2.42, 2.09;  $\delta$  4.48  $\leftrightarrow$   $\delta$  4.14; gHMQC (400 MHz, C<sub>6</sub>D<sub>6</sub>):  $\delta$  76.7  $\leftrightarrow$   $\delta$  5.27;  $\delta$  74.7  $\leftrightarrow$   $\delta$  4.48;  $\delta$  73.3  $\leftrightarrow$   $\delta$  4.14;  $\delta$  41.7  $\leftrightarrow$   $\delta$  2.75, 2.09;  $\delta$  39.4  $\leftrightarrow$   $\delta$  2.42;  $\delta$  31.9  $\leftrightarrow$   $\delta$  1.16. **72B**: <sup>1</sup>H NMR (400 MHz, C<sub>6</sub>D<sub>6</sub>):  $\delta$  5.05 (d,  $J$  = 1.8 Hz, 1H, H<sub>3</sub>);  $\delta$  4.64 (s, 5H, C<sub>5</sub>H<sub>5</sub>);  $\delta$  2.57 (dd,  $J$  = 13.4, 2.5 Hz, 1H, H<sub>endo</sub>);  $\delta$  2.43 (apparent dt,  $J$  = 2.3, 1.8 Hz, 1H, H<sub>2</sub>);  $\delta$  2.13 (dd,  $J$  = 13.2, 2.0 Hz, 1H, H<sub>exo</sub>);  $\delta$  1.26 (s, 9H, *t*-Bu);  $\delta$  0.92 (s, 9H, *t*-Bu); gCOSY (400 MHz, C<sub>6</sub>D<sub>6</sub>):  $\delta$  5.05  $\leftrightarrow$   $\delta$  2.43;  $\delta$  2.57  $\leftrightarrow$   $\delta$  2.43, 2.13; <sup>13</sup>C NMR (100 MHz, C<sub>6</sub>D<sub>6</sub>):  $\delta$  109.2, 80.0, 72.1, 69.4, 40.9, 35.7, 31.9, 31.1, 29.7, 28.9, gHMQC (400 MHz, C<sub>6</sub>D<sub>6</sub>):  $\delta$  80.0  $\leftrightarrow$   $\delta$  4.64;  $\delta$  72.1  $\leftrightarrow$   $\delta$  5.05;  $\delta$  40.9  $\leftrightarrow$   $\delta$  2.57, 2.13;  $\delta$  35.7  $\leftrightarrow$   $\delta$  2.43;  $\delta$  31.1  $\leftrightarrow$  0.92;  $\delta$  28.9  $\leftrightarrow$   $\delta$  1.26; EI MS  $m/z$  calculated for C<sub>18</sub>H<sub>27</sub>Co (M<sup>+</sup>): 302.1445; found: Parent peak not found; EI MS  $m/z$  calculated for C<sub>18</sub>H<sub>26</sub>Co (M<sup>+</sup>-H): 301.13666; found: 301.13596.

**(*t*-Bu<sub>2</sub>C<sub>5</sub>H<sub>3</sub>)Co( $\eta^4$ -C<sub>5</sub>H<sub>6</sub>) (72A) and (*t*-Bu<sub>2</sub>C<sub>5</sub>H<sub>4</sub>)Co(C<sub>5</sub>H<sub>5</sub>) (72B) (Method B)**

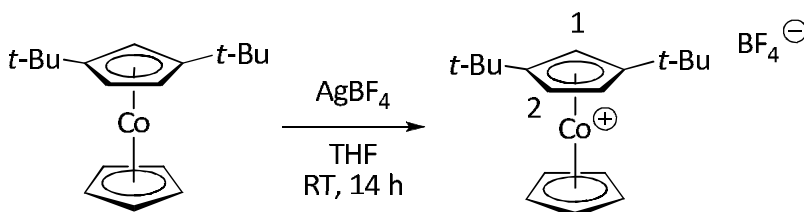
A deep red solution of (*t*-Bu<sub>2</sub>C<sub>5</sub>H<sub>3</sub>)Co(hexadiene) **66** (120 mg, 0.38 mmol) in 20 mL hexane was added to a thick-walled reaction bomb. Monomeric cyclopentadiene (0.5 mL, 6.1 mmol) was added via syringe and the mixture stirred for two days while at ambient temperature. The volatile components were removed *in vacuo* and the mixture re-dissolved in pentane and filtered through diatomaceous earth. The solvent was removed *in vacuo* to afford **34.2**

mg (30%) of a dark red oil, containing a 8 : 1 ratio of **72A** and **72B**. Upon standing at -35 °C, the oil solidified but repeated attempts to recrystallize the mixture were unsuccessful.



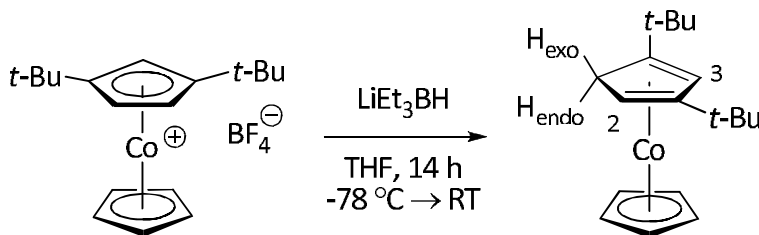
### **(*t*-Bu<sub>2</sub>C<sub>5</sub>H<sub>3</sub>)Co(C<sub>5</sub>H<sub>5</sub>) (**73**)**

A solution of NaCp (49 mg, 0.56 mmol) in 15 mL THF was cooled to -30 °C and added to a dark red solution of (*t*-Bu<sub>2</sub>C<sub>5</sub>H<sub>3</sub>)Co(acac) **64** in THF (167 mg, 0.50 mmol). The resulting mixture darkened in colour and was stirred for 5 hours while warming to ambient temperature. The solvent was removed *in vacuo* and the residue filtered through diatomaceous earth using hexane. The solvent was removed *in vacuo* and the resulting dark red oil was left to stand at -30 °C, whereupon the oil solidified to afford 140 mg (93%) of a dark red semi-solid. EI MS *m/z* calculated for C<sub>18</sub>H<sub>26</sub>Co: 301.13673; found: 301.13284; Analysis calculated for C<sub>18</sub>H<sub>26</sub>Co: C, 71.8%; H, 8.70%; found: C, 71.6%; H, 8.68%.



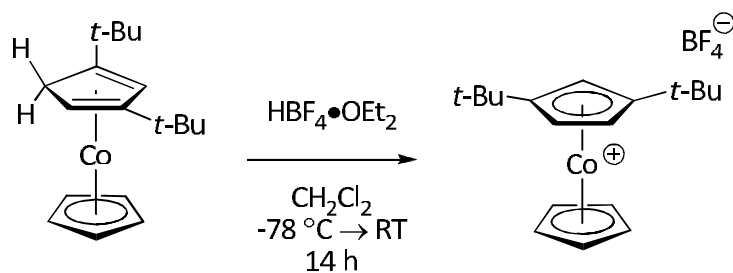
### **$[(t\text{-Bu}_2\text{C}_5\text{H}_3)\text{Co}(\text{C}_5\text{H}_5)]\text{BF}_4$ (74) (Route A)**

A red solution of  $(t\text{-Bu}_2\text{C}_5\text{H}_3)\text{Co}(\text{C}_5\text{H}_5)$  **73** in 10 mL THF (261 mg, 0.87 mmol) was added to a slurry of  $\text{AgBF}_4$  (180.1 mg, 0.93 mmol) in 10 mL THF at ambient temperature. Upon addition, the deep red solution immediately became brown and, over a 30 minute period, took on a greenish tint. The mixture was stirred for 14 hours and the solvent was removed *in vacuo*. The mixture extracted using  $\text{CH}_2\text{Cl}_2$  and filtered through diatomaceous earth. The solvent was removed *in vacuo* and the product recrystallized from a  $\text{CH}_2\text{Cl}_2/\text{Et}_2\text{O}$  mixture to afford 316 mg (94%) of orange needles.  $^1\text{H}$  NMR (400 MHz, acetone- $d_6$ ):  $\delta$  5.94 (s, 5H, Cp);  $\delta$  5.82 (t,  $J = 1.6$  Hz, 1H,  $\text{H}_1$ );  $\delta$  5.79 (d,  $J = 1.6$  Hz, 2H,  $\text{H}_2$ );  $\delta$  1.36 (s, 18H,  $t\text{-Bu}$ );  $^{13}\text{C}$  NMR (100 MHz, acetone- $d_6$ ):  $\delta$  120.9, 85.7, 79.8, 78.5, 32.4, 32.3,  $\text{C}(\text{CH}_3)_3$  and  $\text{C}(\text{CH}_3)_3$  obscured by solvent; Electrospray MS  $m/z$  calculated for  $\text{C}_{18}\text{H}_{26}\text{Co}$  ( $\text{M}^+ - \text{BF}_4$ ): 303.13160; found: 301.13609; Analysis calculated for  $\text{C}_{18}\text{H}_{26}\text{CoBF}_4$ : C, 55.7%; H, 6.75%; found: C, 56.0%; H, 6.57%.



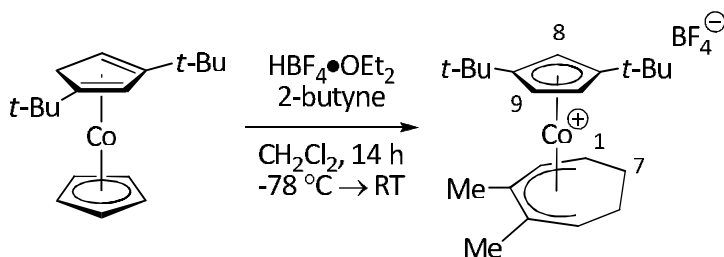
### **$(\text{C}_5\text{H}_5)\text{Co}(\eta^4\text{-}t\text{-Bu}_2\text{C}_5\text{H}_4)$ (72B)**

A pale orange solution of  $[(t\text{-Bu}_2\text{C}_5\text{H}_3)\text{Co}(\text{C}_5\text{H}_5)]\text{BF}_4$  **74** (0.172 g, 0.44 mmol) in 15 mL THF was cooled to  $-78\text{ }^\circ\text{C}$  and treated with 450  $\mu\text{L}$  of  $\text{LiEt}_3\text{BH}$  (1.0M, 0.45 mmol). The solution darkened to a deep red colour and was warmed to ambient temperature over 14 hours. The solvent was removed *in vacuo* and the mixture extracted with hexane and filtered through diatomaceous earth to afford 111 mg (83%) of a dark red oil.



### **[(*t*-Bu<sub>2</sub>C<sub>5</sub>H<sub>3</sub>)Co(C<sub>5</sub>H<sub>5</sub>)]BF<sub>4</sub> (74) (Route B)**

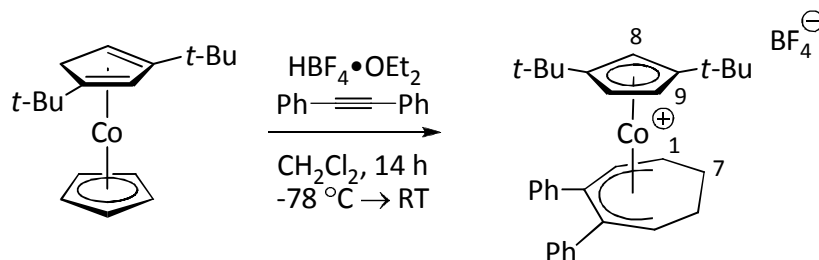
A deep red solution of (C<sub>5</sub>H<sub>5</sub>)Co( $\eta^4$ -*t*-Bu<sub>2</sub>C<sub>5</sub>H<sub>4</sub>) **72B** (0.055 g, 0.18 mmol) in 15 ml dichloromethane was cooled to -78 °C and treated with HBF<sub>4</sub>•OEt<sub>2</sub> (25  $\mu$ L, 0.18mmol). The solution lightened in colour immediately and was stirred for 14 hours while warming to ambient temperature. The solvent was removed *in vacuo* and the mixture chromatographed on silica gel (3% methanol/dichloromethane v/v) and recrystallized from a dichloromethane/diethyl ether mixture afforded 52.4 mg (75%) of a yellow-orange powder.



### **[(*t*-Bu<sub>2</sub>C<sub>5</sub>H<sub>3</sub>)Co(2,3-dimethylhepta-2,4-dien-1-yl)]BF<sub>4</sub> 75**

A deep red solution of (C<sub>5</sub>H<sub>5</sub>)Co( $\eta^4$ -*t*-Bu<sub>2</sub>C<sub>5</sub>H<sub>4</sub>) **72B** (0.075 g, 0.25 mmol) and 2-butyne (99  $\mu$ L, 1.26 mmol) in 20 mL dichloromethane was cooled to -78 °C and treated with HBF<sub>4</sub>•OEt<sub>2</sub> (35  $\mu$ L, 0.26 mmol) via syringe. The orange solution immediately turned dark red upon acid addition and was stirred for 14 hours while warming to ambient temperature. The solvent was removed *in vacuo* and

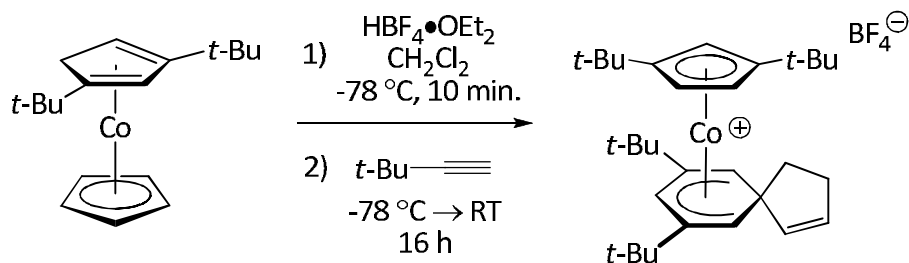
the mixture dissolved with acetone and filtered through diatomaceous earth. The sample was chromatographed through silica gel (3% MeOH/CH<sub>2</sub>Cl<sub>2</sub> v/v) to afford 19 mg of a red oily solid. The product mixture was characterized by <sup>1</sup>H NMR spectroscopy. However, the broadened resonances in the spectrum were indicative of a persistent paramagnetic impurity. Dzwiniel and Stryker prepared the *tert*-butylcyclopentadienyl congener of cycloheptadienyl complex **75**; the <sup>1</sup>H NMR resonances compares well with the spectral data of the *tert*-butylcyclopentadienyl congener.<sup>131</sup> Partial <sup>1</sup>H NMR (400 MHz, CDCl<sub>3</sub>): δ 5.73 (br s, 1H, H<sub>1/2</sub>); δ 5.53 (br m, 1H, H<sub>8/9</sub>); δ 5.17-5.20 (br m, 1H, H<sub>1/2/5</sub>, partially overlapped); δ 4.96 (br s, 1H, H<sub>8/9</sub>); δ 4.82 (br s, 1H, H<sub>8/9</sub>); δ 2.56 (br s, 3H, Me); δ 2.81 (br m, 1H, H<sub>7endo</sub>); δ 2.40 (br d, *J* = 11.8 Hz, 1H, H<sub>7exo</sub>); δ 2.29 (br s, 3H, Me); δ 1.82 (br m, 1H, H<sub>6endo</sub>); δ 1.32 (br s, 9H, *t*-Bu); δ 1.30 (br s, 9H, *t*-Bu); δ 0.41 (br m, 1H, H<sub>6exo</sub>); gCOSY (400 MHz, CDCl<sub>3</sub>): δ 5.73 (H<sub>1/2</sub>) ↔ δ 5.17-5.20 (H<sub>1/2</sub>), δ 5.53 (H<sub>8/9</sub>) ↔ δ 4.96 (H<sub>8/9</sub>), 4.82 (H<sub>8/9</sub>); δ 5.20 (H<sub>5</sub>) ↔ δ 2.81 (H<sub>6endo</sub>); δ 5.18 (H<sub>1/2</sub>) ↔ δ 1.82 (H<sub>7endo</sub>), 0.41 (H<sub>7exo</sub>); δ 2.81 (H<sub>7endo</sub>) ↔ δ 1.82 (H<sub>6endo</sub>); δ 1.82 (H<sub>6endo</sub>) ↔ δ 0.42 (H<sub>6exo</sub>); Electrospray MS *m/z* calculated for C<sub>22</sub>H<sub>34</sub>Co (M<sup>+</sup>-BF<sub>4</sub>): 357.19870; found: 357.19881.



**[(*t*-Bu<sub>2</sub>C<sub>5</sub>H<sub>3</sub>)Co(2,3-diphenylhepta-2,4-dien-1-yl)]BF<sub>4</sub> (**77**)**

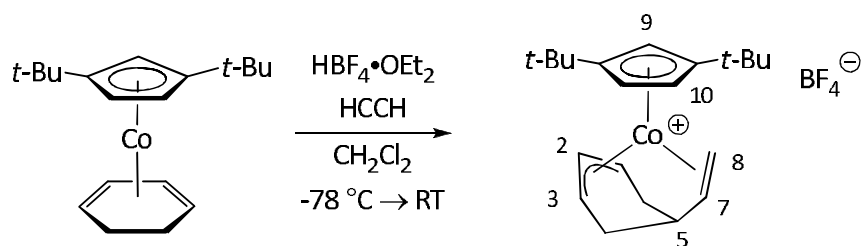
A deep red solution of (C<sub>5</sub>H<sub>5</sub>)Co( $\eta^4$ -*t*-Bu<sub>2</sub>C<sub>5</sub>H<sub>4</sub>) **72B** (0.054 g, 0.18 mmol) and diphenylacetylene (0.088 mg, 0.50 mmol) in 20 mL dichloromethane was cooled to -78 °C and treated with HBF<sub>4</sub>•OEt<sub>2</sub> (25  $\mu$ L, 0.18 mmol) via syringe. The orange solution immediately turned dark red upon acid addition and was stirred for 14 hours while warming to ambient temperature. The solvent was removed *in vacuo* and the mixture dissolved with acetone and filtered through diatomaceous earth. The sample was chromatographed through silica gel (3% MeOH/CH<sub>2</sub>Cl<sub>2</sub> v/v) to afford 25 mg of a red oily solid. The product mixture was characterized by <sup>1</sup>H NMR spectroscopy. However, the broadened resonances in the spectrum were indicative of a persistent paramagnetic impurity. Dzwiniel and Stryker prepared the *tert*-butylcyclopentadienyl congener of cycloheptadienyl complex **77**; the <sup>1</sup>H NMR resonances compared well to the spectral data of the *tert*-butylcyclopentadienyl congener.<sup>131</sup> The identity of the product was confirmed by X-ray diffraction analysis of a sample recrystallized from a dichloromethane/diethyl ether. Partial <sup>1</sup>H NMR (500 MHz, CDCl<sub>3</sub>):  $\delta$  7.52 (br d, *J* = 6.4 Hz, 2H, H<sub>Ph</sub>);  $\delta$  7.37-7.42 (br m, 4H, H<sub>Ph</sub>);  $\delta$  7.22-7.27 (br m, 4H, H<sub>Ph</sub>, partially obscured by solvent);  $\delta$  6.29 (br s, 1H, H<sub>8</sub> or H<sub>9</sub>);  $\delta$  5.77 (br m, 2H, H<sub>1,2</sub>);  $\delta$  5.50 (br d, *J* = 8.3 Hz, 1H, H<sub>5</sub>);  $\delta$  5.19 (br s, 1H, H<sub>8</sub> or H<sub>9</sub>);  $\delta$  5.07 (br s, 1H, H<sub>8</sub> or H<sub>9</sub>);  $\delta$  3.31 (br m, 1H, H<sub>7endo</sub>);  $\delta$  2.03-2.23 (br m, 2H, H<sub>7exo,6endo</sub>);  $\delta$  0.62 (br m, 1H, H<sub>6exo</sub>); gCOSY (400 MHz, CDCl<sub>3</sub>):  $\delta$  5.77 (H<sub>1</sub>)  $\leftrightarrow$   $\delta$  2.19 (H<sub>7exo,6endo</sub>);  $\delta$  3.31 (H<sub>1</sub>)  $\leftrightarrow$

$\delta$  2.19 (H<sub>7exo, 6endo</sub>); 2.19 (H<sub>7exo,6endo</sub>)  $\leftrightarrow$  0.62 (H<sub>6exo</sub>); Electrospray MS  $m/z$   
calculated for C<sub>32</sub>H<sub>38</sub>Co (M<sup>+</sup>-BF<sub>4</sub>): 481.23000; found: 481.23036.



**$[(t\text{-Bu}_2\text{C}_5\text{H}_3)\text{Co}(2,3\text{-diphenylhepta-2,4-dien-1-yl})]\text{BF}_4$  (**78**)**

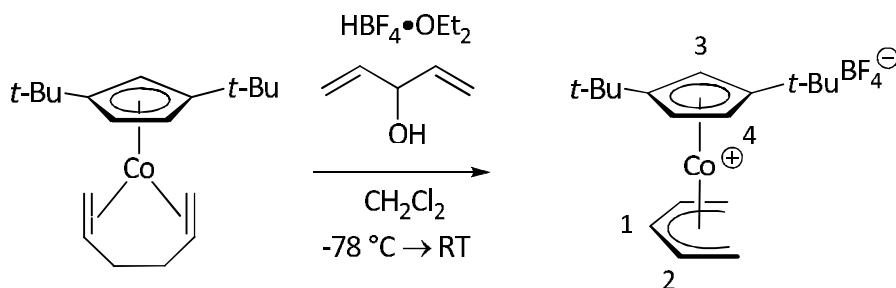
A dark red solution of  $(\text{C}_5\text{H}_5)\text{Co}(\eta^4\text{-}t\text{-Bu}_2\text{C}_5\text{H}_4)$  **72B** (0.089 g, 0.29 mmol) in 15 mL dichloromethane was cooled to  $-78^\circ\text{C}$  and  $\text{HBF}_4 \cdot \text{OEt}_2$  (40  $\mu\text{L}$ , 0.29 mmol) was added via syringe. The orange solution immediately turned dark red upon acid addition and was stirred for 10 minutes before excess *tert*-butylacetylene (100  $\mu\text{L}$ , 0.81 mmol) was added. The mixture was stirred for 16 hours while warming to ambient temperature. The solvent was removed *in vacuo* and the mixture dissolved with acetone and filtered through diatomaceous earth. The solvent was removed *in vacuo* to afford 45 mg of a red oily solid. Characterization of this product was provided solely by X-ray diffraction analysis of a sample recrystallized from a dichloromethane/diethyl ether mixture. The  $^1\text{H}$  NMR spectrum of the product showed multiple broadened signals that were indicative of a persistent paramagnetic impurity. Chromatography through silica gel (3%  $\text{MeOH}/\text{CH}_2\text{Cl}_2$  v/v) could not separate the paramagnetic impurity from the bulk sample.



**[(*t*-Bu<sub>2</sub>C<sub>5</sub>H<sub>3</sub>)Co( $\eta^3, \eta^2$ -5-vinylcyclohex-2-en-1-yl)]BF<sub>4</sub> (**80**)**

A dark red solution of (*t*-Bu<sub>2</sub>C<sub>5</sub>H<sub>3</sub>)Co( $\eta^4$ -cyclohexadiene) **69** (0.050 g, 0.16 mmol) in 15 mL dichloromethane was cooled to -78 °C. Acetylene was bubbled through the solution for 10 minutes and HBF<sub>4</sub>•OEt<sub>2</sub> (25  $\mu$ L, 0.18 mmol) was added via syringe. The orange solution immediately turned dark red upon acid addition and was stirred for 16 hours while warming to ambient temperature. The solvent was removed *in vacuo* and the mixture dissolved with acetone and filtered through diatomaceous earth. The solvent was removed *in vacuo* to afford 86 mg (90%) of a red oily solid. <sup>1</sup>H NMR (400 MHz, acetone-d<sup>6</sup>):  $\delta$  6.69 (t,  $J$  = 7 Hz, 1H, H<sub>1</sub> or H<sub>3</sub>);  $\delta$  5.94 (t,  $J$  = 2.2 Hz, 1H, H<sub>10a</sub>/H<sub>10b</sub>);  $\delta$  5.79 (t,  $J$  = 2.2 Hz, 1H, H<sub>10a</sub>/H<sub>10b</sub>);  $\delta$  5.68 (t,  $J$  = 7.0 Hz, 1H, H<sub>1</sub> or H<sub>3</sub>);  $\delta$  5.50 (t,  $J$  = 7.0 Hz, 1H, H<sub>2</sub>);  $\delta$  5.32 (ddd,  $J$  = 14.2, 8.4, 1.9 Hz, 1H, H<sub>7</sub>);  $\delta$  5.17 (t,  $J$  = 2.2 Hz, 1H, H<sub>8</sub>);  $\delta$  5.15 (d,  $J$  = 8.4 Hz, 1H, H<sub>8a</sub>);  $\delta$  4.70 (d,  $J$  = 14.4 Hz, 1H, H<sub>8b</sub>);  $\delta$  2.42 (dt,  $J$  = 15.2, 4.6 Hz, 1H, H<sub>4a</sub>/H<sub>4b</sub> or H<sub>6a</sub>'/H<sub>6b</sub>');  $\delta$  1.97 (br m, 1H, H<sub>5</sub>);  $\delta$  1.66 (d,  $J$  = 15.2 Hz, 1H, H<sub>4a</sub>/H<sub>4b</sub> or H<sub>6a</sub>'/H<sub>6b</sub>');  $\delta$  1.44 (s, 9H, *t*-Bu);  $\delta$  1.33 (s, 9H, *t*-Bu);  $\delta$  1.27 (d,  $J$  = 16.3 Hz, 1H, H<sub>4a</sub>/H<sub>4b</sub> or H<sub>6a</sub>'/H<sub>6b</sub>');  $\delta$  0.64 (d,  $J$  = 16.3 Hz, 1H, H<sub>4a</sub>/H<sub>4b</sub> or H<sub>6a</sub>'/H<sub>6b</sub>'); <sup>13</sup>C NMR (100 MHz, acetone-d<sup>6</sup>):  $\delta$  119.3, 115.5, 98.4, 87.7, 84.5, 84.1, 82.8, 79.8, 68.4, 37.3,

35.5, 31.4, 23.1, C(CH<sub>3</sub>)<sub>3</sub> carbons obscured by solvent; gHSQC (400 MHz, acetone-d<sup>6</sup>): δ 98.4 ↔ δ 5.32; δ 87.7 ↔ δ 5.79; δ 84.5 ↔ δ 5.17 or 5.94; δ 84.1 ↔ δ 5.17 or 5.94; δ 82.8 ↔ δ 5.50; δ 79.8 ↔ δ 6.69; δ 68.4 ↔ δ 4.7 and 5.15; δ 37.3 ↔ δ 1.66 and 2.42; δ 35.5 ↔ δ 1.97; δ 23.1 ↔ δ 0.64 and 1.27; Electrospray MS *m/z* calculated for C<sub>21</sub>H<sub>32</sub>Co (M<sup>+</sup>-BF<sub>4</sub>): 430.18654; found: 430.18659; Analysis calculated for C<sub>21</sub>H<sub>32</sub>CoBF<sub>4</sub>: C, 58.6%; H, 7.50%; found: C, 58.3%; H, 7.36%.

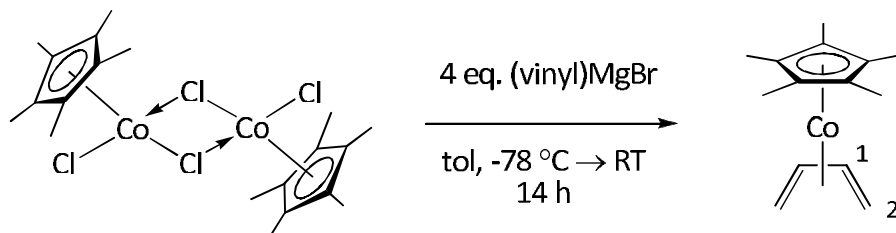


### [(*t*-Bu<sub>2</sub>C<sub>5</sub>H<sub>3</sub>)Co(penta-2,4-dien-1-yl)][BF<sub>4</sub>] (**81**)

A red solution of (C<sub>5</sub>H<sub>3</sub><sup>t</sup>Bu<sub>2</sub>)Co(1,5-hexadiene) **66** (174 mg, 0.55 mmol) in 15 mL dichloromethane was cooled to -78 °C and HBF<sub>4</sub>•OEt<sub>2</sub> (75 μL, 0.55 mmol) was added via syringe. After a period of 15 minutes, 1,4-pentadien-3-ol was added to the solution and the entire mixture warmed to ambient temperature over 18 hours while stirring. The solvent was removed under reduced pressure and the mixture chromatographed on silica gel (3% methanol/dichloromethane v/v) and then recrystallized from a mixture of dichloromethane/diethyl ether to afford 134 mg (63%) of red crystals. <sup>1</sup>H NMR (400 MHz, CDCl<sub>3</sub>): δ 7.10 (t, *J* = 6.9 Hz, 1H, H<sub>1</sub>); 5.82 (m, 2<sup>nd</sup> order, 1H, H<sub>2</sub>); 5.53 (d, *J* = 1.8 Hz, 2H, H<sub>4</sub>); 5.27 (t, *J* = 1.8 Hz,

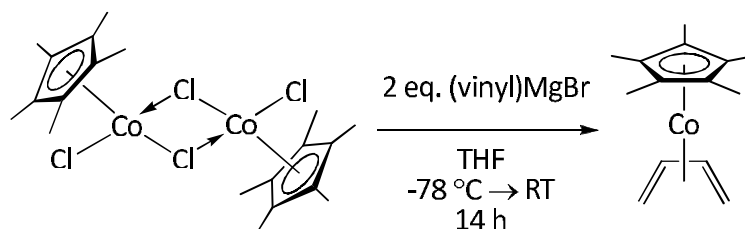
1H, H<sub>3</sub>); 4.18 (dd, *J* = 9.3 Hz, 2.4 Hz, 2H, H<sub>exo</sub>); 1.64 (dd, *J* = 12.0 Hz, 2.4 Hz, 2H, H<sub>endo</sub>); 1.4 (s, 18H, CMe<sub>3</sub>); <sup>13</sup>C NMR (100 MHz, CDCl<sub>3</sub>): δ 120.1, 100.4, 96.1, 82.7, 81.2, 59.7, 53.5, 31.3; gCOSY (400 MHz, CDCl<sub>3</sub>): δ 7.10 (H<sub>1</sub>) ↔ δ 5.82 (H<sub>2</sub>); δ 5.82 (H<sub>2</sub>) ↔ δ 4.18 (H<sub>exo</sub>), δ 1.64 (H<sub>endo</sub>); δ 5.53 (H<sub>3</sub>) ↔ δ 5.27 (H<sub>4</sub>); δ 4.18 (H<sub>exo</sub>) ↔ δ 1.64 (H<sub>endo</sub>); gHMQC (400 MHz, CDCl<sub>3</sub>): δ 7.10 ↔ δ 100.4; δ 5.82 ↔ δ 96.1; δ 5.53 ↔ δ 82.7; δ 5.27 ↔ δ 81.24; δ 4.18, 1.64 ↔ δ 59.7; δ 1.4 ↔ δ 31.3; Electrospray MS *m/z* calculated for C<sub>18</sub>H<sub>28</sub>Co (M<sup>+</sup>-BF<sub>4</sub>): 303.15175; found: 301.15171; Analysis calculated for C<sub>18</sub>H<sub>28</sub>CoBF<sub>4</sub>: C, 55.4%; H, 7.23%; found: C, 55.6%; H, 7.26%.

## Chapter 4 Experimental Section



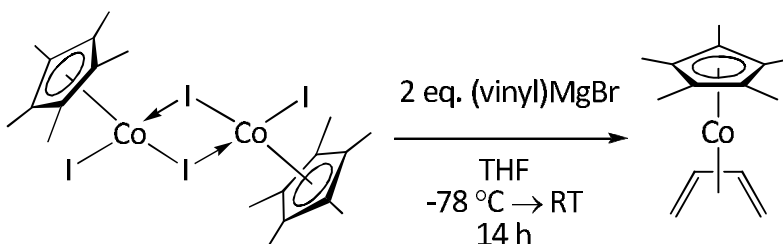
### $(C_5Me_5)Co(\eta^4-C_4H_6)$ (101) (Method A)

A green slurry of  $[(C_5Me_5)CoCl_2]_2$  **96** (25.7 mg, 0.049 mmol) in 10 mL toluene was cooled to  $-78\text{ }^\circ\text{C}$  and treated with vinylmagnesium bromide (0.4 mL, 0.56 M, 0.22 mmol). The mixture changed quickly from green to brown in colour and was stirred while warming to ambient temperature over a period of 14 hours. The solvent was removed *in vacuo* and the residue extracted with hexanes and filtered through diatomaceous earth. The oily residue was recrystallized from cold pentane to afford 17 mg (0.068 mmol, 71%) of a dark red powder. The NMR data is consistent with literature values.  $^1\text{H}$  NMR (500 MHz,  $C_6D_6$ ):  $\delta$  4.33 (m, 2<sup>nd</sup> order, 2H,  $H_1$ );  $\delta$  1.71 (s, 15H,  $C_5Me_5$ );  $\delta$  1.22 (m, 2<sup>nd</sup> order, 2H,  $H_{exo}$ );  $\delta$  -0.21 (m, 2<sup>nd</sup> order, 2H,  $H_{endo}$ ); gCOSY (400 MHz,  $C_6D_6$ ):  $\delta$  4.33  $\leftrightarrow$   $\delta$  1.22, -0.21;  $\delta$  1.22  $\leftrightarrow$   $\delta$  -0.21;  $^{13}\text{C}$  NMR (100.58 MHz,  $C_6D_6$ ):  $\delta$  89.4, 80.8 ( $C_5Me_5$ ), 35.8, 10.4.



### **$(C_5Me_5)Co(\eta^4-C_4H_6)$ (101) (Method B)**

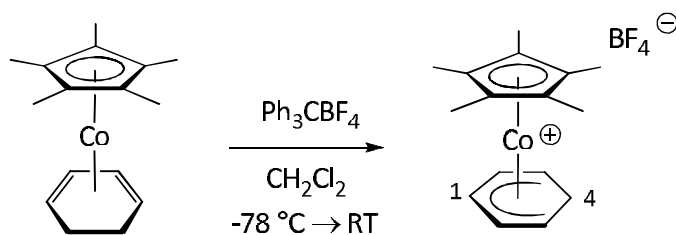
A green slurry of  $[(C_5Me_5)CoCl_2]_2$  **96** (21.2 mg, 0.040 mmol) in 10 mL THF was cooled to  $-78\text{ }^\circ\text{C}$  and treated with vinylmagnesium bromide (0.150 mL, 0.56 M, 0.084 mmol). The mixture changed from green to brown in colour and was stirred while warming to ambient temperature over a period of 14 hours. The solvent was removed *in vacuo* and the residue extracted with hexanes and filtered through diatomaceous earth. The solvent was removed *in vacuo* to afford 5.2 mg (0.021 mmol, 26%) of a dark red solid.



### **$(C_5Me_5)Co(\eta^4-C_4H_6)$ (101) (Method C)**

A purple slurry of  $[(C_5Me_5)CoI_2]_2$  **97** (75.4 mg, 0.084 mmol) in THF was quickly cooled to  $-78\text{ }^\circ\text{C}$  and treated with vinylmagnesium bromide (0.310 mL, 0.56 M, 0.17 mmol). The mixture changed from purple to brown in colour and was

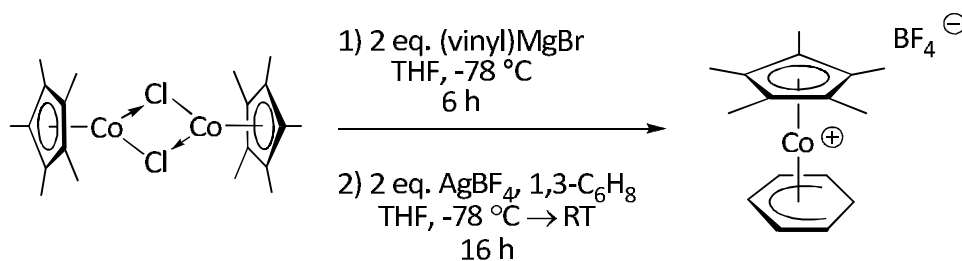
stirred while warming to ambient temperature over a period of 14 hours. The solvent was removed *in vacuo* and the residue extracted with hexanes and filtered through diatomaceous earth. The solvent was removed *in vacuo* to afford 7.1 mg (0.029 mmol, 17%) of a dark red solid.



#### **[(C<sub>5</sub>Me<sub>5</sub>)Co(η<sup>5</sup>-C<sub>6</sub>H<sub>7</sub>)]BF<sub>4</sub> (110) (Method A)**

A red solution of (C<sub>5</sub>Me<sub>5</sub>)Co(η<sup>4</sup>-cyclohexadiene) **41** (0.135 g, 0.49 mmol) in 20 mL dichloromethane was cooled to -78 °C. Trityl tetrafluoroborate (162 mg, 0.49) was added at low temperature and the red solution was slowly warmed to ambient temperature over 16 hours. The solvent was removed *in vacuo* and the residue crystallized from a mixture of dichloromethane and diethyl ether to afford 145 mg (82%) of red crystals. <sup>1</sup>H NMR (400 MHz, CDCl<sub>3</sub>): δ 6.80 (t, *J* = 5.3 Hz, 1H, H<sub>1</sub>); δ 5.09 (t, *J* = 5.9 Hz, 2H, H<sub>2</sub>); δ 3.29 (t, *J* = 6.5 Hz, 2H, H<sub>3</sub>); δ 2.82 (dt, *J* = 15.8, 6.6 Hz, 1H, H<sub>exo</sub>); δ 1.97 (s, 15H, CH<sub>3</sub>); δ 1.45 (d, *J* = 15.7, 1H, H<sub>endo</sub>); <sup>13</sup>C NMR (100.58 MHz, CDCl<sub>3</sub>): δ 98.4 (C<sub>5</sub>Me<sub>5</sub>), 95.9, 90.8, 52.3, 24.0, 10.0; gCOSY (400 MHz, CDCl<sub>3</sub>): δ 6.80 ↔ δ 5.09, 3.29; δ 5.09 ↔ δ 6.80, 3.29, 1.45; δ 3.29 ↔ δ 6.80, 5.09, 2.82, 1.45; δ 2.82 ↔ δ 3.29, 1.45; gHMQC (400 MHz, CDCl<sub>3</sub>): δ 6.80 ↔ δ 90.8; δ 5.09 ↔ δ 95.9; δ 3.29 ↔ δ 52.3; δ 2.82, 1.45 ↔ δ 24.0; δ 1.97 ↔

$\delta$  10.0; ; Electrospray MS  $m/z$  calculated for  $C_{16}H_{22}Co$  ( $M^+-BF_4$ ): 273.1048; found: 273.10479; Analysis calculated for  $C_{16}H_{22}CoBF_4$ : C, 53.37%; H, 6.16%; found: C, 53.02%; H, 6.18%.



#### **$[(C_5Me_5)Co(\eta^5-C_6H_7)]BF_4$ (110) (Method B)**

A green solution of  $[(C_5Me_5)CoCl]_2$  **40** (202 mg, 0.44 mmol) in 15 mL THF was cooled to -78 °C and treated with vinylmagnesium bromide (1.6 mL, 0.50 M, 0.90 mmol) via syringe over a period of 5 minutes. The resulting mixture was stirred for 6 hours while maintained at low temperature. A suspension of AgBF<sub>4</sub> (187 mg, 0.96 mmol) and 1,3-cyclohexadiene (0.55 mL, 5.77 mmol) in 10 mL THF was cooled to -78 °C and transferred via syringe to the reaction flask. The resulting mixture was stirred for another 16 hours while warming to ambient temperature. The volatile components were removed *in vacuo* and the product extracted using dichloromethane and filtered through diatomaceous earth. The solvent was removed *in vacuo* and the product recrystallized from a dichloromethane/diethyl ether mixture to afford 28.4 mg (8.3%) of a dark red powder.

## Notes and References

1. Hegedus, L. S., *Transition Metals in the Synthesis of Complex Organic Molecules*. 2nd ed.; University Science Books: Sausalito, CA, 1999.
2. Schlosser, M.; Hegedus, L. S.; Lipshutz, B. H.; Marshall, J. A.; Nakamura, E.; Negishi, E.; Reetz, M. T.; Semmelhack, M. F.; Smith, K.; Yamamoto, H., *Organometallics in Synthesis - A Manual*. 2nd ed.; John Wiley & Sons: New York, 2002.
3. Schore, N. E. *Chem. Rev.*, **1988**, *88*, 1081-1119.
4. Ojima, I.; Tzamarioudaki, M.; Li, Z.; Donovan, R. J. *Chem. Rev.*, **1996**, *96*, 635-662.
5. Fruhauf, H. W. *Chem. Rev.*, **1997**, *97*, 523-596.
6. Dewar, M. J. S. *Bull. Soc. Chim. Fr.*, **1951**, *18*, C71-C79.
7. Chatt, J.; Duncanson, L. A. *J. Chem. Soc.*, **1953**, 2939-2947.
8. Freking, G.; Frohlich, N. *Chem. Rev.*, **2000**, *100*, 717-774.
9. Templeton, J. L. *Adv. Organomet. Chem.*, **1989**, *29*, 1-100.
10. Reger, D. L.; Belmore, K. A.; Mintz, E.; McElligott, P. J. *Organometallics*, **1984**, *3*, 1759-1761.
11. Silvestre, J.; Hoffmann, R. *Helv. Chim. Acta*, **1985**, *68*, 1461-1506.
12. Schilling, B. E. R.; Hoffmann, R.; Lichtenberger, D. L. *J. Am. Chem. Soc.*, **1979**, *101*, 585-591.

13. Nesmeyanov, A. N.; Aleksandrov, G. G.; Antonova, A. B.; Anisimov, K. N.; Kolobova, N. E.; Struchkov, Y. T. *J. Organomet. Chem.*, **1976**, *110*, C36-C38.
14. Antonova, A. B.; Kolobova, N. E.; Petrovskii, P. V.; Lokshin, B. V.; Obezyuk, N. S. *J. Organomet. Chem.*, **1977**, *137*, 55-67.
15. Wakatsuki, Y.; Koga, N.; Yamazaki, H.; Morokuma, K. *J. Am. Chem. Soc.*, **1994**, *116*, 8105-8111.
16. Collman, J. P.; Hegedus, L. S.; Norton, J. R.; Finke, R. G., *Principles and Applications of Organotransition Metal Chemistry*. University Science: Mill Valley, California, 1987.
17. Harrington, P. J., *Comprehensive Organometallic Chemistry II*. Elsevier: New York, 1995; Vol. 12, p 923.
18. Oppolzer, W., *Comprehensive Organometallic Chemistry II*. Elsevier: New York, 1995; Vol. 12, p 905.
19. Krysan, D. J., *Comprehensive Organometallic Chemistry II*. Elsevier: New York, 1995; Vol. 12, p 959.
20. Crabtree, R. H., *The Organometallic Chemistry of the Transition Metals*. Fourth ed.; Wiley-Interscience: Yale University, New Haven, Connecticut, 2005.
21. Tsuji, J., In *Handbook of Organopalladium Chemistry for Organic Synthesis*, Negishi, E., Ed. John Wiley & Sons: New York, 2000; Vol. 2, p 1669.

22. Tsuji, J., *Transition Metal Reagents and Catalysts*. John Wiley & Sons: New York, 2000.
23. Schweibert, K. E.; Stryker, J. M. *J. Am. Chem. Soc.*, **1995**, *117*, 8275-8276.
24. Etkin, N.; Dzwiniel, T. L.; Schwiebert, K. E.; Stryker, J. M. *J. Am. Chem. Soc.*, **1998**, *120*, 9702-9703.
25. Dzwiniel, T. L.; Etkin, N.; Stryker, J. M. *J. Am. Chem. Soc.*, **1999**, *121*, 10640-10641.
26. Chin, C. S.; Won, G.; Chong, D.; Kim, M.; Lee, H. *Acc. Chem. Res.*, **2002**, *35*, 218-225.
27. Older, C. M.; McDonald, R.; Stryker, J. M. *J. Am. Chem. Soc.*, **2005**, *127*, 14202-14203.
28. Tsukada, N.; Sugawara, S.; Nakaoka, K.; Inoue, Y. *J. Org. Chem.*, **2003**, *68*, 5961-5966.
29. Green, M. L. H.; Taylor, S. H. *J. Chem. Soc., Dalton Trans.*, **1975**, 1142-1149.
30. Older, C. M.; Stryker, J. M. *Organometallics*, **2000**, *19*, 2661-2663.
31. Older, C. M.; Stryker, J. M. *Organometallics*, **2000**, *19*, 3266-3268.
32. Lutsenko, Z. L.; Rubezhov, A. Z. *Bull. Acad. Sci. USSR*, **1982**, 1259-1261.
33. Lutsenko, Z. L.; Kisin, A. V.; Kuznetsova, M. G.; Rubezhov, A. Z. *Bull. Acad. Sci. USSR* **1981**, 1141-1144.
34. Lutsenko, Z. L.; Petrovskii, P. V.; Bezrukova, A. A.; Rubezhov, A. Z. *Bull. Acad. Sci. USSR*, **1988**, 735-739.

35. Lutsenko, Z. L.; Kisin, A. V.; Kuznetsova, M. G.; Bezrukova, A. A.;  
Khandkarova, V. S.; Rubezhov, A. Z. *Inorg. Chim. Acta* **1981**, *53*, L28.
36. Lutsenko, Z. L.; Aleksandrov, G. G.; Petrovskii, P. V.; Shubina, E. S.;  
Andrianov, V. G.; Struchkov, Y. T.; Rubezhov, A. Z. *J. Organomet. Chem.*,  
**1985**, *281*, 349-364.
37. Betz, P.; Jolly, P. W.; Kruger, C.; Zakrzewski, U. *Organometallics*, **1991**, *10*,  
3520-3525.
38. Sanchez-Castro, M. E.; Ramirez-Monroy, A.; Paz-Sandoval, M. A.  
*Organometallics*, **2005**, *24*, 2875-2888.
39. Older, C. M. *Ph.D. Dissertation*, University of Alberta, **2000**.
40. Fischer, R. A.; Herrmann, W. A. *J. Organomet. Chem.*, **1989**, *377*, 275-279.
41. Greco, A.; Green, M.; Stone, F. G. A. *J. Chem. Soc. A*, **1971**, 3476-3481.
42. Bottrill, M.; Green, M.; O'Brien, E.; Smart, L. E.; Woodward, P. J. *J. Chem.  
Soc., Dalton Trans.*, **1980**, 292-298.
43. Davidson, J. L.; Green, M.; Stone, F. G. A. *J. Chem. Soc., Dalton Trans.*,  
**1976**, 2044-2053.
44. Bogdanovic, B.; Heimbach, P.; Kroner, M.; Wilke, G. *Justus Liebigs Ann.  
Chem.*, **1969**, *727*, 183.
45. Brenner, W.; Heimbach, P.; Hey, H. J.; Muller, G.; Wilke, G. *Justus Liebigs  
Ann. Chem.*, **1969**, *727*, 161-182.
46. Heimbach, P.; Brenner, W. *Angew. Chem.*, **1966**, *78*, 983-984.
47. Heimbach, P.; Brenner, W. *Angew. Chem. Int. Ed. Engl.*, **1966**, *5*, 961-962.

48. Heimbach, P. *Angew. Chem. Int. Ed. Engl.*, **1966**, *5*, 961.
49. Wilke, G. *Angew. Chem. Int. Ed. Engl.*, **1963**, *2*, 105-115.
50. Baker, R. *Chem. Rev.*, **1973**, *73*, 487-530.
51. Billington, D. C. *Chem. Soc. Rev.*, **1985**, 93-120.
52. Corey, E. J.; Hamanaka, E. J. *Am. Chem. Soc.*, **1967**, *89*, 2758-2759.
53. Corey, E. J.; Semmelhack, M. F. *J. Am. Chem. Soc.*, **1967**, *89*, 2755-2757.
54. Corey, E. J.; Wat, E. J. *Am. Chem. Soc.*, **1967**, *89*, 2757-2758.
55. Chiusoli, G. P. *Acc. Chem. Res.*, **1973**, *6*, 422-427.
56. Oppolzer, W.; Bedoya-Zurita, M.; Switzer, C. Y. *Tetrahedron Lett.*, **1988**, *29*, 6433-6436.
57. Oppolzer, W.; Xu, J.-Z.; Stone, C. *Helv. Chim. Acta*, **1991**, *74*, 465-468.
58. Oppolzer, W.; Gaudin, J. M.; Birkinshaw, T. N. *Tetrahedron Lett.*, **1988**, *29*, 4705-4708.
59. Oppolzer, W.; Gaudin, J. M. *Helv. Chim. Acta*, **1987**, *70*, 1477-1481.
60. Chiusoli, G. P.; Cassar, L. *Angew. Chem. Int. Ed. Engl.*, **1967**, *6*, 124-133.
61. Camps, F.; Coll, J.; Moreto, J. M.; Torras, J. *Tetrahedron Lett.*, **1985**, *26*, 6397-6398.
62. Camps, F.; Coll, J.; Moreto, J. M.; Torras, J. *Tetrahedron Lett.*, **1987**, *40*, 4745-4748.
63. Camps, F.; Coll, J.; Llebaria, A.; Moreto, J. M. *Tetrahedron Lett.*, **1988**, *29*, 5811-5814.

64. Camps, F.; Coll, J.; Moreto, J. M.; Torras, J. *J. Org. Chem.*, **1989**, *54*, 1969-1978.
65. Camps, F.; Llebaria, A.; Moreto, J. M.; Pages, L. *Tetrahedron Lett.*, **1992**, *33*, 109-112.
66. Camps, F.; Moreto, J. M.; Pages, L. *Tetrahedron Lett.*, **1992**, *48*, 3147.
67. Pages, L.; Llebaria, A.; Camps, F.; Molins, E.; Miravittles, C.; Moreto, J. M. *J. Am. Chem. Soc.*, **1992**, *114*, 10449-10461.
68. Llebaria, A.; Moreto, J. M. *J. Organomet. Chem.*, **1993**, *451*, 1-13.
69. Villar, J. M.; Delgado, A.; Llebaria, A.; Moreto, J. M. *Tetrahedron: Asymmetry*, **1995**, *6*, 665-668.
70. Villar, J. M.; Delgado, A.; Llebaria, A.; Moreto, J. M.; Molins, E.; Miravittles, C. *Tetrahedron*, **1996**, *52*, 10525-10546.
71. Vilaseca, F.; Pages, L.; Villar, J. M.; Llebaria, A.; Delgado, A.; Moreto, J. M. *J. Organomet. Chem.*, **1998**, *551*, 107-115.
72. Garcia-Grande, G.; Moreto, J. M. *J. Am. Chem. Soc.*, **1999**, *121*, 878-879.
73. Camps, F.; Llebaria, A.; Moreto, J. M.; Pages, L. *Tetrahedron Lett.*, **1992**, *33*, 113-114.
74. Nadal, M. L.; Bosch, J.; Vila, J. M.; Klein, G.; Ricart, S.; Moreto, J. M. *J. Am. Chem. Soc.*, **2005**, *127*, 10476-10477.
75. Cui, D.-M.; Tsuzuki, T.; Miyake, K.; Ikeda, S.-I.; Sato, Y. *Tetrahedron*, **1998**, *54*, 1063-1072.
76. Ikeda, S.-I.; Kondo, K.; Sato, Y. *J. Org. Chem.*, **1996**, *61*, 8248-8255.

77. Ikeda, S.-I.; Cui, D.-M.; Sato, Y. *J. Org. Chem.*, **1994**, *59*, 6877-6878.
78. Ikeda, S.-I.; Sato, Y. *J. Am. Chem. Soc.*, **1994**, *116*, 5975-5976.
79. Ikeda, S.-I.; Miyashita, H.; Sato, Y. *Organometallics*, **1988**, *17*, 4316-4318.
80. Widenhoefer, R. A. *Acc. Chem. Res.*, **2002**, *35*, 905-913.
81. Kawanami, Y.; Yamamoto, K. *Synlett.*, **1995**, 1232-1234.
82. Uno, T.; Wakayanagi, S.; Sonoda, Y.; Yamamoto, K. *Synlett.*, **2003**, 1997-2000.
83. Tsukada, N.; Sugawara, S.; Inoue, Y. *Org. Lett.*, **2000**, *2*, 655-657.
84. Okada, K.; Oshima, K.; Utimoto, K. *J. Am. Chem. Soc.*, **1996**, *118*, 6076-6077.
85. Miller, J. A.; Negishi, E. *Tetrahedron Lett.*, **1984**, *25*, 5863-5866.
86. Negishi, E.; Takahashi, T. *Synthesis*, **1988**, 1-18.
87. Araki, S.; Imai, A.; Shimizu, K.; Butsugan, Y. *Tetrahedron Lett.*, **1992**, *33*, 2581-2582.
88. Mikhailov, B. M. *Pure Appl. Chem.*, **1974**, *39*, 505-524.
89. Mikhailov, B. M. *Organomet. Chem. Rev.*, **1972**, *8(A)*, 1-65.
90. Pearson, A. J., In *Iron Compounds in Organic Synthesis*, Academic Press: San Diego, 1994; pp 37-44.
91. Welker, M. E. *Chem. Rev.*, **1992**, *92*, 97-112.
92. Rosenblum, M. *J. Organomet. Chem.*, **1986**, *300*, 191-218.
93. Abram, T. S.; Baker, R.; Exon, C. M.; Rao, V. B. *J. Chem. Soc., Perkin Trans. 1*, **1982**, 285-294.

94. Schwiebert, K. E. *Ph.D. Dissertation*, Indiana University, **1993**.
95. Appleton, T. G.; Clark, H. C.; Poller, R. C.; Puddephatt, R. J. *J. Organomet. Chem.*, **1972**, *39*, C13-C16.
96. Sbrana, G.; Braca, G.; Benedetti, E. *J. Chem. Soc., Dalton Trans.*, **1975**, 754-761.
97. Barrado, G.; Hricko, M. M.; Miguel, D.; Riera, V.; Wally, H.; Garcia-Granda, S. *Organometallics*, **1998**, *17*, 820-826.
98. Biasotto, F.; Etienne, M.; Dahan, F. *Organometallics*, **1995**, *14*, 1870-1874.
99. Davidson, J. L.; Green, M.; Stone, C.; Welch, A. J. *J. Chem. Soc., Dalton Trans.*, **1976**, 2044.
100. Tang, J.; Shinokubo, H.; Oshima, K. *Organometallics*, **1998**, *17*, 290-292.
101. Bartlett, R. A.; Olmstead, M. M.; Power, P. P.; Shoner, S. C. *Organometallics*, **1988**, *7*, 1801-1806.
102. Morris, R. J.; Girolami, G. S. *Organometallics*, **1989**, *8*, 1478-1485.
103. Nehl, H. *Chem. Ber.*, **1993**, *126*, 1519-1527.
104. Nehl, H. *Chem. Ber.*, **1994**, *127*, 2535-2537.
105. Vollhardt, K. P. C. *Acc. Chem. Res.*, **1977**, *10*, 1-8.
106. Vollhardt, K. P. C. *Angew. Chem. Int. Ed. Engl.*, **1984**, *23*, 539-556.
107. Vollhardt, K. P. C. *Angew. Chem.*, **1984**, *96*, 525-541.
108. Chang, H. T.; Jegamohan, M.; Cheng, C. H. *Org. Lett.*, **2007**, *9*, 505-508.
109. Garcia, P.; Moulin, s.; Micio, Y.; Leboeuf, D.; Gandon, V.; Aubert, C.; Malacria, M. *Chem. Eur. J.*, **2009**, *15*, 2129-2139.

110. Heller, B.; Hapke, M. *Chem. Soc. Rev.*, **2007**, *36*, 1085-1094.
111. Butenschon, H. *Angew. Chem. Int. Ed.*, **2008**, *47*, 5287-5290.
112. Yet, L. *Chem. Rev.*, **2000**, *100*, 2963-3008.
113. Nakamura, I.; Yamamoto, Y. *Chem. Rev.*, **2004**, *104*, 2127-2198.
114. Tsukada, N.; Sakaiharu, Y.; Inoue, Y. *Tetrahedron Lett.*, **2007**, *48*, 4019-4021.
115. Older, C. M.; McDonald, R.; Stryker, J. M. *J. Am. Chem. Soc.*, **2005**, *127*, 14202-14203.
116. Dzwiniel, T. L. University of Alberta, **1999**.
117. Witherell, R. D. *Ph.D. Dissertation*, University of Alberta, **2007**.
118. Schweibert, K. E. *Ph.D. Dissertation*, Indiana University, **1993**.
119. Nicholls, J. C.; Spencer, J. L. *Organometallics*, **1994**, *13*, 1781-1787.
120. Bennett, M. A.; Nicholls, J. C.; Rahman, A. K. F.; Redhouse, A. D.; Spencer, J. L.; Willis, A. C. *J. Chem. Soc., Chem. Commun.*, **1989**, 1328-1330.
121. Cracknell, R. B.; Nicholls, J. C.; Spencer, J. L. *Organometallics*, **1996**, *15*, 446-448.
122. Witherell, R. D.; Ylijoki, K. E. O.; Stryker, J. M. *J. Am. Chem. Soc.*, **2008**, *130*, 2176-2177.
123. Margulis, T. N.; Schiff, L.; Rosenblum, M. *J. Am. Chem. Soc.*, **1965**, *87*, 3269-3270.
124. Domingos, A. J. P.; Johnson, B. F. G.; Lewis, J. J. *Chem. Soc., Dalton Trans.*, **1974**, 145-149.

125. Johnson, B. F. G.; Lewis, J.; Randall, G. L. P. *J. Chem. Soc. A*, **1971**, 422-429.
126. Charles, A. D.; Diversi, P.; Johnson, B. F. G.; Karlin, K. D.; Lewis, J.; Rivera, A. V.; Sheldrick, G. M. *J. Organomet. Chem.*, **1977**, *128*, C31-C34.
127. Charles, A. D.; Diversi, P.; Johnson, B. F. G. *J. Chem. Soc., Dalton Trans.*, **1981**, 1906-1917.
128. Eisenstadt, A.; Winstein, S. *Tetrahedron Lett.*, **1970**, *11*, 4603-4606.
129. Eisenstadt, A. *J. Organomet. Chem.*, **1972**, *38*, C32-C34.
130. Bluemel, J.; Hertkorn, N.; Kanellakopoulos, B.; Koehler, F. H.; Lachmann, J.; Mueller, G.; Wagner, F. E. *Organometallics*, **1993**, *12*, 3896-3905.
131. Dzwiniel, T. L.; Stryker, J. M. *J. Am. Chem. Soc.*, **2004**, *126*, 9184-9185.
132. Buchmann, B.; Piantini, U.; von Philipsborn, W.; Salzer, A. *Helv. Chim. Acta*, **1987**, *70*, 1487-1506.
133. Jameson, G. B.; Salzer, A. *Organometallics*, **1982**, *1*, 689-694.
134. Kreiter, C. G.; Michels, E.; Kaub, J. *Z. Naturforsch. Teil B*, **1986**, *41*, 722-730.
135. Kane-Maguire, L. A. P.; Mouncher, P. A.; Salzer, A. *J. Organomet. Chem.*, **1988**, *347*, 383-390.
136. Evans, J.; Johnson, B. F. G.; Lewis, J. *J. Chem. Soc., Dalton Trans.*, **1972**, 2668-2675.
137. Angermund, K. P.; Betz, P.; Butenschon, H. *Chem. Ber.*, **1993**, *126*, 713-724.
138. Siegbahn, P. E. M. *J. Phys. Chem.*, **2002**, *99*, 12723-12729.

139. Wierschke, S. G.; Chandrasekhar, J.; Jorgensen, W. L. *J. Am. Chem. Soc.*, **1985**, *107*, 1496-1500.
140. Lambert, J. B.; Wang, G. T.; Finzel, R. B.; Teramura, D. H. *J. Am. Chem. Soc.*, **1987**, *109*, 7838-7845.
141. Geiger, W. E.; Gennett, T.; Lane, G. A.; Salzer, A.; Rheingold, A. L. *Organometallics*, **1986**, *5*, 1352-1359.
142. Benn, R.; Cibura, K.; Hofmann, P.; Jonas, K.; Rufinska, A. *Organometallics*, **1985**, *4*, 2214-2221.
143. Lehmkuhl, H.; Nehl, H. *Chem. Ber.*, **1984**, *117*, 3443-3456.
144. King, R. B.; Stone, F. G. A. *Inorg. Synth.*, **1963**, *7*, 99-115.
145. Sheats, J. E. *Organomet. Chem. Rev.*, **1979**, *7*, 461-521.
146. Tane, J. P.; Vollhardt, K. P. C. *Angew. Chem. Int. Ed. Engl.*, **1982**, *21*, 617-618.
147. Fischer, E. O.; Herberich, G. E. *Chem. Ber.*, **1961**, *94*, 1517-1523.
148. Fischer, E. O.; Fellmann, W.; Herberich, G. E. *Chem. Ber.*, **1962**, *95*, 2254-2258.
149. Furlani, C.; Collamati, I. *Chem. Ber.*, **1962**, *95*, 2928-2933.
150. Maryin, V. P.; Petrovskii, P. V. *J. Organomet. Chem.*, **1992**, *441*, 125-141.
151. Malkov, A. V.; Petrovskii, P. V.; Fedin, E. I.; Leonova, E. V. *Bull. Acad. Sci. USSR*, **1987**, *6*, 1270-1276.
152. Koelle, U.; Fuss, B.; Belting, M.; Raabe, E. *Organometallics*, **1986**, *5*, 980-987.

153. Koelle, U.; Fuss, B. *Chem. Ber.*, **1984**, *117*, 743-752.
154. Koelle, U.; Fuss, B. *Chem. Ber.*, **1984**, *117*, 753-762.
155. Koelle, U.; Khouzami, F.; Fuss, B. *Angew. Chem.*, **1982**, *94*, 132.
156. Koelle, U.; Khouzami, F.; Fuss, B. *Angew. Chem. Int. Ed. Engl.*, **1982**, *21*, 131-132.
157. Schneider, J. J.; Czap, N.; Spickermann, D.; Lehmann, C. W.; Fontani, M.; Laschi, F.; Zanello, P. *J. Organomet. Chem.*, **1999**, *590*, 7-14.
158. Baumann, F.; Dormann, E.; Ehleiter, Y.; Kaim, W.; Karcher, J.; Kelemen, M.; Krammer, R.; Saurenz, D.; Stalke, D.; Wachter, C.; Wolmershauser, G.; Sitzmann, H. *J. Organomet. Chem.*, **1999**, *587*, 267-283.
159. Schneider, J. J.; Wolf, D.; Janiak, C.; Heinemann, O.; Rust, J.; Kruger, C. *Chem. Eur. J.*, **1998**, *4*, 1982-1991.
160. Jonas, K.; Deffense, E.; Habermann, D. *Angew. Chem.*, **1983**, *95*, 729.
161. Jonas, K.; Deffense, E.; Habermann, D. *Angew. Chem. Int. Ed. Engl.*, **1983**, *22*, 716-717.
162. Jonas, K.; Kruger, C. *Angew. Chem.*, **1980**, *92*, 513-531.
163. Jonas, K.; Kruger, C. *Angew. Chem. Int. Ed. Engl.*, **1980**, *19*, 520-537.
164. Cibura, K. *Ph.D. Dissertation*, Ruhr Universität Bochum, **1985**.
165. Howie, R. A.; McQuillan, G. P.; Thompson, D. W.; Lock, G. A. *J. Organomet. Chem.*, **1986**, *303*, 213-220.
166. Stone, K. J.; Little, R. D. *J. Org. Chem.*, **1984**, *49*, 1849-1853.

167. Paradies, J.; Erker, G.; Fröhlich, R. *Angew. Chem. Int. Ed.*, **2006**, *45*, 3079-3082.
168. Bunel, E. E.; Valle, L.; Manriquez, J. M. *Organometallics*, **1985**, *4*, 1680-1682.
169. Smith, M. E.; Andersen, R. A. *J. Am. Chem. Soc.*, **1996**, *118*, 11119-11128.
170. Cabon, Y.; Carmichael, D.; Forissier, K.; Mathey, F.; Ricard, L.; Seeboth, N. *Organometallics*, **2007**, *26*, 5468-5472.
171. Beevor, R. G.; Frith, S. A.; Spencer, J. L. *J. Organomet. Chem.*, **1981**, *221*, C25-C27.
172. Spencer, J. L., In *Organometallic Syntheses*, Eisch, J. J.; King, R. B., Eds. Academic: New York, 1965; Vol. 3, p 109.
173. Jonas, K. *Angew. Chem. Int. Ed. Engl.*, **1985**, *24*, 295-311.
174. Green, M. L. H.; Pratt, L.; Wilkinson, G. *J. Chem. Soc.*, **1959**, 3753-3767.
175. Nakamura, E.; Ammal, S. C.; Stryker, J. M. *Unpublished work*.
176. Ylijoki, K. E. O.; Witherell, R. D.; Kirk, A. D.; Böcklein, S.; Lofstrand, V. A.; McDonald, R.; Ferguson, M. J.; Stryker, J. M. *Organometallics*, **2009**, *28*, 6807-6822.
177. Kirk, A. D. *M.Sc. Dissertation*, University of Alberta, **2007**.
178. Cracknell, R. B.; Orpen, A. G.; Spencer, J. L. *J. Chem. Soc., Chem. Commun.*, **1984**, 326-327.
179. Cracknell, R. B.; Orpen, A. G.; Spencer, J. L. *J. Chem. Soc., Chem. Commun.*, **1986**, 1005-1006.

180. Brookhart, M.; Lincoln, D. M.; Volpe, A. F.; Schmidt, G. F. *Organometallics*, **1989**, *8*, 1212-1218.
181. Brookhart, M.; Lincoln, D. M.; Bennett, M. A.; Pelling, S. *J. Am. Chem. Soc.*, **1990**, *112*, 2691-2694.
182. Brookhart, M.; Green, M. L. H.; Pardy, R. B. A. *Chem. Commun.*, **1983**, 691-692.
183. Schmidt, G. F.; Brookhart, M. *J. Am. Chem. Soc.*, **1985**, *107*, 1443-1444.
184. Schroder, D.; Schwarz, H. *Angew. Chem. Int. Ed. Engl.*, **1995**, *34*, 1973-1995.
185. Periana, R. A.; Bergman, R. G. *J. Am. Chem. Soc.*, **1984**, *106*, 7272-7273.
186. Periana, R. A.; Bergman, R. G. *J. Am. Chem. Soc.*, **1986**, *108*, 7346-7355.
187. Rybtchinski, B.; Vigalok, A.; Yehoshoa, B. D.; Milstein, D. *J. Am. Chem. Soc.*, **1996**, *118*, 12406-12415.
188. Halpern, J. *Acc. Chem. Res.*, **1982**, *15*, 238-244.
189. Labinger, J. A.; Bercaw, J. E. *Organometallics*, **1988**, *7*, 926-928.
190. Lovering, E. G.; Laidler, K. J. *Can. J. Chem.*, **1960**, *38*, 2367-2372.
191. Shilov, A. E.; Shul'pin, G. B. *Chem. Rev.*, **1997**, *97*, 2879-2932.
192. Takahashi, T.; Kanno, K.-i., In *Topics in Organometallic Chemistry*, Takahashi, T., Ed. Springer: Berlin, 2005; Vol. 8, p 217.
193. Murakami, M.; Ito, Y., In *Topics in Organometallic Chemistry*, Murai, S., Ed. Springer: Berlin, 1999; Vol. 3, pp 97-129.
194. Jun, C.-H. *Chem. Soc. Rev.*, **2004**, *33*, 610-618.

195. Tipper, C. H. F. *J. Chem. Soc.*, **1955**, 2045-2046.
196. Jun, C.-H.; Kang, J.-B.; Lim, Y.-G. *Tetrahedron Lett.*, **1995**, *36*, 277-280.
197. Wender, P. A.; Gamber, G. G.; Hubbard, R. D.; Zhang, L. *J. Am. Chem. Soc.*, **2002**, *124*, 2876-2877.
198. Wender, P. A.; Gamber, G. G.; Hubbard, R. D.; Pham, S. M.; Zhang, L. *J. Am. Chem. Soc.*, **2005**, *127*, 2836-2837.
199. Wender, P. A.; Haustedt, L. O.; Lim, J.; Love, J. A.; Williams, T. J.; Yoon, J.-Y. *J. Am. Chem. Soc.*, **2006**, *128*, 6302-6303.
200. Yu, Z.-X.; Wender, P. A.; Houk, K. N. *J. Am. Chem. Soc.*, **2004**, *126*, 9154-9155.
201. Yu, Z.-X.; Cheong, P. H.-Y.; Liu, P.; Legault, C. Y.; Wender, P. A.; Houk, K. N. *J. Am. Chem. Soc.*, **2008**, *130*, 2378-2379.
202. Wegner, H. A.; de Meijere, A.; Wender, P. A. *J. Am. Chem. Soc.*, **2005**, *127*, 6530-6531.
203. Ogoshi, H.; Setsune, J.; Yoshida, J. *J. Chem. Soc., Chem. Commun.*, **1975**, 234-235.
204. Hidai, M.; Orisaku, M.; Uchida, Y. *Chem. Lett.*, **1980**, 753-754.
205. Dzhemilev, U. M.; Khusnutdinov, R. I.; Shchadneva, N. A.; Tolstikov, G. A. *Izv. Akad. Nauk SSSR Ser. Khim.*, **1990**, 1598-1601.
206. Dzhemilev, U. M.; Khusnutdinov, R. I.; Shchadneva, N. A.; Tolstikov, G. A. *Bull. Acad. Sci. USSR Div. Chem. Sci.*, **1990**, *39*, 1447.
207. Koga, Y.; Narasaki, K. *Chem. Lett.*, **1999**, 705-706.

208. Taber, D. F.; Kanai, K.; Jiang, Q.; Bui, G. *J. Am. Chem. Soc.*, **2000**, *122*, 6807-6808.
209. Matsuda, T.; Tsuboi, T.; Murakami, M. *J. Am. Chem. Soc.*, **2007**, *129*, 12596-12597.
210. Walczak, M. A. A.; Wipf, P. *J. Am. Chem. Soc.*, **2008**, *130*, 6924-6925.
211. Jiao, L.; Ye, S.; Yu, Z.-X. *J. Am. Chem. Soc.*, **2008**, *130*, 7178-7179.
212. Kim, S. Y.; Lee, S. I.; Choi, S. Y.; Chung, Y. K. *Angew. Chem. Int. Ed.*, **2008**, *47*, 4914-4917.
213. Rubin, M.; Rubina, M.; Gevorgyan, V. *Chem. Rev.*, **2007**, *107*, 3117-3179.
214. Atkinson, E. R.; Levins, P. L.; Dickelman, T. E. *Chem. Ind.*, **1964**, 934.
215. Lu, Z.; Jun, C.-H.; de Gala, S. R.; Sigalas, M.; Eisenstein, O.; Crabtree, R. H. *J. Chem. Soc., Chem. Commun.*, **1993**, 1877-1880.
216. Eisch, J. J.; Piotrowski, A. M.; Han, K. I.; Kruger, C.; Tsay, Y. H. *Organometallics*, **1985**, *4*, 224-231.
217. Perthuisot, C.; Jones, W. D. *Organometallics*, **1994**, *16*, 2016.
218. Perthuisot, C.; Edelbach, B. L.; Zubris, D. L.; Jones, W. D. *Organometallics*, **1997**, *16*, 2016-2023.
219. Edelbach, B. L.; Lachicotte, R. J.; Jones, W. D. *J. Am. Chem. Soc.*, **1998**, *120*, 2843-2853.
220. Gordon, A. J.; Ford, R. A., In *The Chemist's Companion*, Wiley: New York, 1972; p 113.

221. Liebeskind, L. S.; Baysdon, S. L.; South, M. S.; Blount, J. F. *J. Organomet. Chem.*, **1980**, *202*, C73-C76.
222. Liebeskind, L. S.; Baysdon, S. L.; South, M. S.; Iyer, S.; Leeds, J. P. *Tetrahedron*, **1985**, *41*, 5839-5853.
223. Suggs, J. W.; Jun, C.-H. *J. Am. Chem. Soc.*, **1984**, *106*, 3054-3056.
224. Suggs, J. W.; Jun, C.-H. *J. Am. Chem. Soc.*, **1986**, *108*, 4679-4681.
225. Wentzel, M. T.; Reddy, V. J.; Hyster, T. K.; Douglas, C. J. *Angew. Chem. Int. Ed.*, **2009**, *48*, 6121-6123.
226. Parshall, G. W. *J. Am. Chem. Soc.*, **1974**, *96*, 2360-2366.
227. Favero, G.; Morvillo, A.; Turco, A. *J. Organomet. Chem.*, **1983**, *241*, 251-257.
228. Morvillo, A.; Turco, A. *J. Organomet. Chem.*, **1981**, *208*, 103-113.
229. Favero, G.; Turco, A. *J. Organomet. Chem.*, **1976**, *105*, 389-392.
230. Burmeister, J. L.; Edwards, L. M. *J. Chem. Soc. A*, **1971**, 1663-1666.
231. Bianchini, C.; Masi, D.; Meli, A.; Sabat, M. *Organometallics*, **1986**, *5*, 1670-1675.
232. Churchill, D.; Shin, J. H.; Hascall, T.; Hahn, J. M.; Bridgewater, B. M.; Parkin, G. *Organometallics*, **1999**, *18*, 2403-2406.
233. Taw, F. L.; White, P. S.; Bergman, R. G.; Brookhart, M. *J. Am. Chem. Soc.*, **2002**, *124*, 4192-4193.
234. Taw, F. L.; Mueller, A. H.; Bergman, R. G.; Brookhart, M. *J. Am. Chem. Soc.*, **2003**, *125*, 9808-9813.

235. Nakazawa, H.; Kawasaki, T.; Miyoshi, K.; Suresh, C. H.; Koga, N.  
*Organometallics*, **2004**, *23*, 117-126.
236. Nakazawa, H.; Kamata, K.; Itazaki, M. *Chem. Commun.*, **2005**, 4004-4006.
237. Nakazawa, H.; Itazaki, M.; Kamata, K.; Ueda, K. *Chem. Asia J.*, **2007**, *2*,  
882-888.
238. Atesin, T. A.; Li, T.; Lachaize, S.; Garcia, J. J.; Jones, W. D. *Organometallics*,  
**2008**, *27*, 3811-3817.
239. Ohnishi, Y.-Y.; Nakao, Y.; Sato, H.; Nakao, Y.; Hiyama, T.; Sakaki, S.  
*Organometallics*, **2009**, *28*, 2583-2594.
240. Nakao, Y.; Oda, S.; Yada, A.; Hiyama, T. *Tetrahedron*, **2006**, *62*, 7567-7576.
241. Nakao, Y.; Oda, S.; Hiyama, T. *J. Am. Chem. Soc.*, **2004**, *126*, 13904-13905.
242. Hirata, Y.; Yukawa, T.; Kashiwara, N.; Nakao, Y.; Hiyama, T. *J. Am. Chem.  
Soc.*, **2009**, *131*, 10964-10973.
243. Gozin, M.; Aizenberg, M.; Liou, S.-Y.; Weisman, A.; Ben-David, Y.; Milstein,  
D. *Nature*, **1994**, *370*, 42-44.
244. Gandelman, M.; Vigalok, A.; Shimon, L. J. W.; Milstein, D.  
*Organometallics*, **1997**, *16*, 3981-3986.
245. Albrecht, M.; Spek, A. L.; van Koten, G. *J. Am. Chem. Soc.*, **2001**, *123*,  
7233-7246.
246. Albrecht, M.; Gossage, R. A.; Spek, A. L.; van Koten, G. *J. Am. Chem. Soc.*,  
**1999**, *121*, 11898-11899.

247. Jazzar, R. F. R.; Macgregor, S. A.; Mahon, M. F.; Richards, S. P.; Whittlesey, M. K. *J. Am. Chem. Soc.*, **2002**, *124*, 4944-4945.
248. Park, Y. J.; Park, J.-Y.; Jun, C.-H. *Acc. Chem. Res.*, **2008**, *41*, 222-234.
249. Benfield, F. W. S.; Green, M. L. H. *J. Chem. Soc., Dalton Trans.*, **1974**, 1324-1331.
250. Eilbracht, P.; Dahler, P. *Chem. Ber.*, **1980**, *113*, 542-554.
251. Hemond, R. C.; Hughes, R. P.; Locker, H. B. *Organometallics*, **1986**, *5*, 2391-2392.
252. Jones, W. D.; Maguire, J. A. *Organometallics*, **1987**, *6*, 1301-1311.
253. Older, C. M.; Stryker, J. M. *Organometallics*, **1998**, *17*, 5596-5598.
254. Older, C. M.; Stryker, J. M. *J. Am. Chem. Soc.*, **2000**, *122*, 2784-2797.
255. Schock, L. E.; Marks, T. J. *J. Am. Chem. Soc.*, **1988**, *110*, 7701-7715.
256. Bunel, E.; Burger, B. J.; Bercaw, J. E. *J. Am. Chem. Soc.*, **1988**, *110*, 976-978.
257. Eshuis, J. J. W.; Tan, Y.; Teuben, J. H.; Renkema, J. *J. Mol. Catal.*, **1990**, *62*, 277-287.
258. Watson, P. L.; Parshall, G. W. *Acc. Chem. Res.*, **1985**, *18*, 51-56.
259. McNeill, K.; Andersen, R. A.; Bergman, R. G. *J. Am. Chem. Soc.*, **1997**, *119*, 11244.
260. Takemori, T.; Suzuki, H. *Organometallics*, **1996**, *15*, 4346-4348.
261. Ermer, S. P.; Struck, G. E.; Bitler, S. P.; Richards, R.; Bau, R.; Flood, T. C. *Organometallics*, **1993**, *12*, 2634-2643.

262. Tjaden, E. B.; Stryker, J. M. *J. Am. Chem. Soc.*, **1990**, *112*, 6420-6422.
263. Hosokawa, T.; Maitlis, P. M. *J. Am. Chem. Soc.*, **1972**, *94*, 3238-3240.
264. Larock, R. C.; Varaprath, S. *J. Org. Chem.*, **1984**, *49*, 3432-3435.
265. Flood, T. C.; Bitler, S. P. *J. Am. Chem. Soc.*, **1984**, *106*, 6076-6077.
266. McNeill, K.; Andersen, R. A.; Bergman, R. G. *J. Am. Chem. Soc.*, **1997**, *119*, 11244-11254.
267. Itazaki, M.; Yoda, C.; Nishihara, Y.; Osakada, K. *Organometallics*, **2004**, *23*, 5402-5409.
268. Grubbs, R. H.; Miyashita, A.; Liu, M.-I. M.; Burk, P. L. *J. Am. Chem. Soc.*, **1978**, *100*, 2418-2425.
269. Grubbs, R. H.; Miyashita, A. *J. Am. Chem. Soc.*, **1978**, *100*, 7418-7420.
270. Grubbs, R. H.; Miyashita, A. *J. Am. Chem. Soc.*, **1978**, *100*, 1300-1302.
271. Grubbs, R. H.; Miyashita, A.; Liu, M.-I. M.; Burk, P. L. *J. Am. Chem. Soc.*, **1977**, *99*, 3863-3864.
272. Grubbs, R. H.; Miyashita, A. *J. Chem. Soc., Chem. Commun.*, **1977**, 864-865.
273. Takahashi, T.; Fujimori, T.; Seki, T.; Saburi, M.; Uchida, Y.; Rousset, C. J.; Negishi, E. *J. Chem. Soc., Chem. Commun.*, **1990**, 182-183.
274. Takahashi, T.; Tamura, M.; Saburi, M.; Uchida, Y.; Negishi, E. *J. Chem. Soc., Chem. Commun.*, **1989**, 852-853.
275. Takahashi, T.; Kageyama, M.; Denisov, V.; Hara, R.; Negishi, E. *Tetrahedron Lett.*, **1993**, *34*, 687-690.

276. Tillack, A.; Baumann, W.; Ohff, A.; Lefeber, C.; Spannenberg, A.; Kempe, R.; Rosenthal, U. *J. Organomet. Chem.*, **1996**, *520*, 187-193.
277. Xi, Z.; Sato, K.; Gao, Y.; Lu, J.; Takahashi, T. *J. Am. Chem. Soc.*, **2003**, *125*, 9568-9569.
278. Takahashi, T.; Kuzuba, Y.; Kong, F.; Nakajima, K.; Xi, Z. *J. Am. Chem. Soc.*, **2005**, *127*, 17188-17189.
279. Takahashi, T.; Song, Z.; Sato, K.; Kuzuba, Y.; Nakajima, K.; Kanno, K.-i. *J. Am. Chem. Soc.*, **2007**, *129*, 11678-11679.
280. Takahashi, T.; Song, Z.; Hsieh, Y.-F.; Nakajima, K.; Kanno, K.-i. *J. Am. Chem. Soc.*, **2008**, *130*, 15236-15237.
281. Casty, G. L.; Stryker, J. M. *Organometallics*, **1997**, *16*, 3083-3085.
282. Selnau, H. E.; Merola, J. S. *J. Am. Chem. Soc.*, **1991**, *113*, 4008-4009.
283. Byrne, E. K.; Theopold. *J. Am. Chem. Soc.*, **1987**, *109*, 1282-1283.
284. Brookhart, M.; Grant, B. E.; Lenges, C. P.; Prosenc, M. H.; White, P. S. *Angew. Chem. Int. Ed.*, **2000**, *39*, 1676-1679.
285. Doherty, M. D.; Grant, B. E.; White, P. S.; Brookhart, M. *Organometallics*, **2007**, *26*, 5950-5960.
286. Ingleson, M.; Fan, H.; Pink, M.; Tomaszewski, J.; Caulton, K. G. *J. Am. Chem. Soc.*, **2006**, *128*, 1804-1805.
287. Casey, C. P.; Brady, J. T.; Boller, T. M.; Weinhold, F.; Hayashi, R. K. *J. Am. Chem. Soc.*, **1998**, *120*, 12500-12511.

288. Allen, S.; Beevor, R. G.; Green, M.; Norman, N. C.; Orpen, A. G.; Williams, I. D. *J. Chem. Soc., Dalton Trans.*, **1985**, 435-450.
289. Allen, S. R.; Green, M.; Orpen, A. G.; Williams, I. D. *J. Chem. Soc., Chem. Commun.*, **1982**, 826-828.
290. Green, M.; Norman, N. C.; Orpen, A. G. *J. Am. Chem. Soc.*, **1981**, *103*, 1267-1269.
291. Brauers, G.; Feher, F. J.; Green, M.; Hogg, J. K.; Orpen, A. G. *J. Chem. Soc., Dalton Trans.*, **1996**, 3387-3396.
292. Feng, S. G.; Templeton, J. L. *Organometallics*, **1992**, *11*, 2168-2175.
293. Frohnapfel, D. S.; Enriquez, A. E.; Templeton, J. L. *Organometallics*, **2000**, *19*, 221-227.
294. Chisholm, M. H.; Clark, H. C. *J. Am. Chem. Soc.*, **1972**, *94*, 1532-1539.
295. Davidson, J. L.; Vasapollo, G.; Manojlovic-Muir, L.; Muir, K. W. *J. Chem. Soc., Chem. Commun.*, **1982**, 1025-1026.
296. Allen, S. R.; Beevor, R. G.; Green, M.; Norman, N. C.; Orpen, A. G. *J. Chem. Soc., Chem. Commun.*, **1985**, 435-436.
297. Reger, D. L.; Belmore, K. A.; Mintz, E.; McElligott, P. J. *Organometallics*, **1984**, *3*, 134-140.
298. Conole, G. C.; Green, M.; McPartlin, M.; Reeve, C.; Wollhouse, C. M. *J. Chem. Soc., Chem. Commun.*, **1988**, 1310-1313.
299. Casey, C. P.; Selmecky, A. D.; Nash, J. R.; Yi, C. S.; Powell, D. R.; Hayashi, R. *J. Am. Chem. Soc.*, **1996**, *118*, 6698-6706.

300. Casey, C. P.; Brady, J. T. *Organometallics*, **1998**, *17*, 4620-4629.
301. Schore, N. E., In *Comprehensive Organic Synthesis*, Trost, B. M.; Fleming, I.; Paquette, L. A., Eds. Pergamon: Oxford, 1991; Vol. 5, p 1129.
302. Grotjahn, D. B., In *Comprehensive Organic Synthesis*, Trost, B. M.; Fleming, I.; Paquette, L. A., Eds. Pergamon: Oxford, 1991; Vol. 5, p 1129.
303. Lautens, M.; Klute, W.; Tam, W. *Chem. Rev.*, **1996**, *96*, 49-92.
304. Fletcher, A. J.; Christie, S. D. R. *J. Chem. Soc., Perkin Trans. 1*, **2000**, 1657-1668.
305. O'Connor, J. M.; Bunker, K. D. *J. Organomet. Chem.*, **2003**, *671*, 1-7.
306. Feilong, J.; Fehlner, T. P.; Rheingold, A. L. *J. Am. Chem. Soc.*, **1987**, *109*, 1860-1861.
307. Foerstner, J.; Kakoschke, A.; Goddard, R.; Rust, J.; Wartchow, R.; Butenschon, H. *J. Organomet. Chem.*, **2001**, *617-618*, 412-422.
308. Butenschon, H.; Kettenbach, R. T.; Kruger, C. *Angew. Chem. Int. Ed. Engl.*, **1992**, *31*, 1066-1068.
309. Wakatsuki, Y.; Yamazaki, H. *Inorg. Synth.*, **1989**, *26*, 189-200.
310. Okuda, J.; Zimmermann, K. H.; Herdtweck, E. *Angew. Chem. Int. Ed. Engl.*, **1991**, *30*, 430-431.
311. Yamazaki, H.; Hagihara, N. *J. Organomet. Chem.*, **1970**, *21*, 431-443.
312. Yamazaki, H.; Hagihara, N. *J. Organomet. Chem.*, **1967**, *7*, P22-P23.
313. Roe, D. M.; Maitlis, P. M. *J. Chem. Soc. A*, **1971**, 3173-3175.

314. King, R. B.; Efraty, A.; Douglas, W. M. *J. Organomet. Chem.*, **1973**, *56*, 345-355.
315. Plitzko, K. D.; Boekelheide, V. *Organometallics*, **1988**, *7*, 1573-1582.
316. Contakes, S. M.; Klausmeyer, K. K.; Rauchfuss, T. B.; Carmona, D.; Lamat, M. P.; Oro, L. A. *Inorg. Synth.*, **2004**, *34*, 166-171.
317. Bolinger, C. M.; Weatherill, T. D.; Rauchfuss, T. B.; Rheingold, A. L. *Inorg. Chem.*, **1986**, *25*, 634-43.
318. Kergoat, R.; De Lima, L. C. G.; Jegat, C.; Le Berre, N.; Kubicki, M. M.; Guerchais, J. E.; L'Haridon, P. *J. Organomet. Chem.*, **1990**, *389*, 71-84.
319. Schneider, J. J. Z. *Naturforsch. Teil B.*, **1995**, *50*, 1055-1060.
320. Frith, S. A.; Spencer, J. L. *Inorg. Synth.*, **1990**, *28*, 273-280.
321. Frith, S. A.; Spencer, J. L. *Inorg. Synth.*, **1985**, *23*, 15-21.
322. Holm, T.; Crossland, I., In *Grignard Reagents*, Richey, H. G., Ed. Wiley: Chichester, 2000; pp 1-26.
323. Kölle, U.; Khouzami, F. *Chem. Ber.*, **1981**, *114*, 2929-2937.
324. Agenet, N.; Gandon, V.; Vollhardt, K. P. C.; Malacria, M.; Aubert, C. *J. Am. Chem. Soc.*, **2007**, *129*, 8860-8871.
325. Hilt, G.; Vogler, T.; Hess, W.; Galbiati, F. *Chem. Commun.*, **2005**, 1474-1475.
326. Okuda, J.; Zimmermann, K. H. *Chem. Ber.*, **2006**, *122*, 1645-1647.

327. McConnell, A. C.; Pogorzelec, P. J.; Slawin, A. M. Z.; Williams, G. L.; Elliott, P. I. P.; Haynes, A.; Marr, A. C.; Cole-Hamilton, D. J. *Dalton Trans.*, **2006**, 91-107.
328. Cotton, F. A.; Hong, B. *Prog. Inorg. Chem.*, **1992**, *40*, 179-289.
329. Mehn, M. P.; Brown, S. D.; Paine, T. K.; Brennessel, W. W.; Cramer, C. J.; Peters, J. C.; Que, L. *Dalton Trans.*, **2006**, 1347-1351.
330. Jenkins, D. M.; Di Bilio, A. J.; Allen, M. J.; Betley, T. A.; Peters, J. C. *J. Am. Chem. Soc.*, **2002**, *124*, 15336-15350.
331. Lu, C. C.; Saouma, C. T.; Day, M. W.; Peters, J. C. *J. Am. Chem. Soc.*, **2007**, *129*, 4-5.
332. Betley, T. A.; Peters, J. C. *J. Am. Chem. Soc.*, **2004**, *126*, 6252-6254.
333. Daida, E. J.; Peters, J. C. *Inorg. Chem.*, **2004**, *43*, 7474-7485.
334. Threlkel, R. S.; Bercaw, J. E.; Seidler, P. F.; Stryker, J. M.; Bergman, R. G., In *Organic Syntheses*, Vedejs, E., Ed. Organic Syntheses Inc.: New York, 1987; Vol. 65, p 42.
335. Clark, T. J.; Nile, T. A. *Synlett.*, **1990**, 589-590.
336. Diversi, P.; Ingrosso, G.; Lucherini, A.; Porzio, W.; Zocchi, M. *Inorg. Chem.*, **1980**, *19*, 3590-3597.
337. Grundy, S. L.; Maitlis, P. M. *J. Chem. Soc., Chem. Commun.*, **1982**, 379-380.

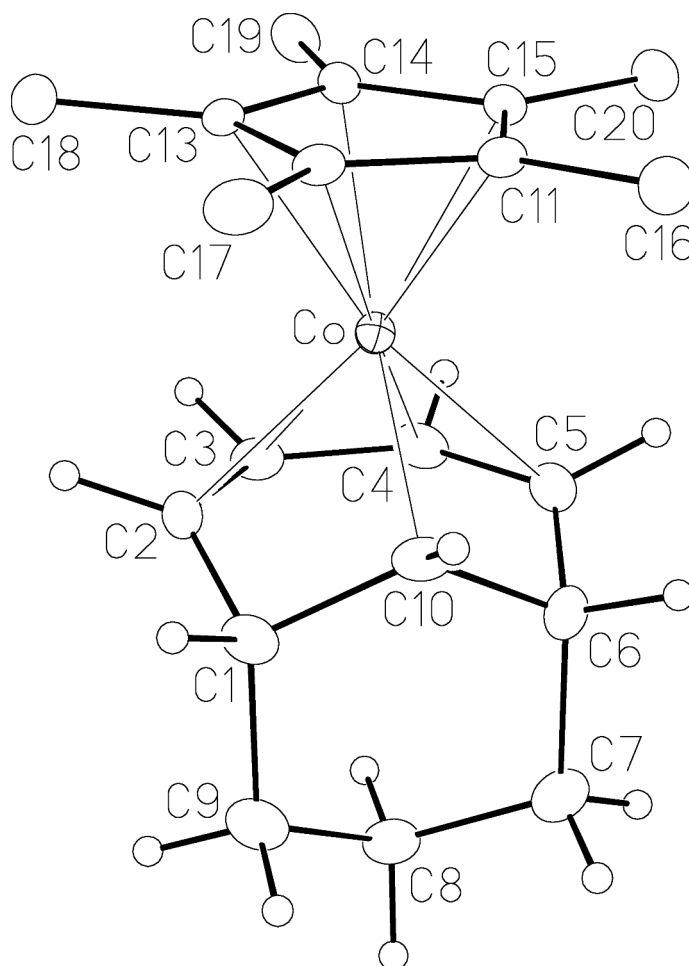
## Appendix 1. Structure Report JMS0545: Bicyclic Complex 42

**Compound:**  $[(\eta^5\text{-C}_5\text{Me}_5)\text{Co}(\eta^4,\eta^1\text{-bicyclo[4.3.1]deca-2,4-dien-10-ide})][\text{BPh}_4]$

**Formula:**  $\text{C}_{44}\text{H}_{48}\text{BCo}$

**Supervisor:** J. M. Stryker

**Crystallographer:** R. McDonald



Perspective view of the  $[(\eta^5\text{-C}_5\text{Me}_5)\text{Co}(\eta^4,\eta^1\text{-bicyclo[4.3.1]deca-2,4-dien-10-ide})]^+$  complex ion showing the atom labelling scheme. Non-hydrogen atoms are represented by Gaussian ellipsoids at the 20% probability level. Hydrogen atoms are shown with arbitrarily small thermal parameters for the bicyclo[4.3.1]deca-2,4-dien-10-ide groups, and are not shown for the pentamethylcyclopentadienyl groups.

## Crystallographic Experimental Details

### A. Crystal Data

formula	C <sub>44</sub> H <sub>48</sub> BCo
formula weight	646.56
crystal dimensions (mm)	0.46 x 0.42 x 0.17
crystal system	monoclinic
space group	Cc (No. 9)
unit cell parameters <sup>a</sup>	
<i>a</i> (Å)	17.1557 (16)
<i>b</i> (Å)	10.2282 (10)
<i>c</i> (Å)	20.2926 (19)
β (deg)	105.3284 (14)
<i>V</i> (Å <sup>3</sup> )	3434.1 (6)
<i>Z</i>	4
ρ <sub>calcd</sub> (g cm <sup>-3</sup> )	1.251
μ (mm <sup>-1</sup> )	0.530

### B. Data Collection and Refinement Conditions

diffractometer	Bruker PLATFORM/SMART 1000
CCD <sup>b</sup>	
radiation (λ [Å]) (0.71073)	graphite-monochromated Mo Kα
temperature (°C)	-80
scan type	ω scans (0.3°) (15 s exposures)
data collection 2θ limit (deg)	52.82
total data collected ≤ <i>l</i> ≤	13196 (-21 ≤ <i>h</i> ≤ 21, -12 ≤ <i>k</i> ≤ 12, -25 25)
independent reflections	6991 ( <i>R</i> <sub>int</sub> = 0.0277)
number of observed reflections ( <i>NO</i> )	6205 [ <i>F</i> <sub>o</sub> <sup>2</sup> ≥ 2σ( <i>F</i> <sub>o</sub> <sup>2</sup> )]
structure solution method	direct methods ( <i>SHELXS-86</i> <sup>c</sup> )
refinement method ( <i>SHELXL-93</i> <sup>d</sup> )	full-matrix least-squares on <i>F</i> <sup>2</sup>
absorption correction method	multi-scan ( <i>SADABS</i> )
range of transmission factors	0.9153–0.7925
data/restraints/parameters	6991 [ <i>F</i> <sub>o</sub> <sup>2</sup> ≥ -3σ( <i>F</i> <sub>o</sub> <sup>2</sup> )] / 0 / 420
Flack absolute structure parameter <sup>e</sup>	0.002 (8)
goodness-of-fit ( <i>S</i> ) <sup>f</sup>	1.001 [ <i>F</i> <sub>o</sub> <sup>2</sup> ≥ -3σ( <i>F</i> <sub>o</sub> <sup>2</sup> )]
final <i>R</i> indices <sup>g</sup>	
<i>R</i> <sub>1</sub> [ <i>F</i> <sub>o</sub> <sup>2</sup> ≥ 2σ( <i>F</i> <sub>o</sub> <sup>2</sup> )]	0.0323
<i>wR</i> <sub>2</sub> [ <i>F</i> <sub>o</sub> <sup>2</sup> ≥ -3σ( <i>F</i> <sub>o</sub> <sup>2</sup> )]	0.0724
largest difference peak and hole	0.367 and -0.167 e Å <sup>-3</sup>

<sup>a</sup>Obtained from least-squares refinement of 7454 reflections with  $4.68^\circ < 2\theta < 52.08^\circ$ .

<sup>b</sup>Programs for diffractometer operation, data collection, data reduction and absorption correction were those supplied by Bruker.

<sup>c</sup>Sheldrick, G. M. *Acta Crystallogr.* **1990**, *A46*, 467–473.

<sup>d</sup>Sheldrick, G. M. *SHELXL-93*. Program for crystal structure determination. University of Göttingen, Germany, 1993.

<sup>e</sup>Flack, H. D. *Acta Crystallogr.* **1983**, *A39*, 876–881; Flack, H. D.; Bernardinelli, G. *Acta Crystallogr.* **1999**, *A55*, 908–915; Flack, H. D.; Bernardinelli, G. *J. Appl. Cryst.* **2000**, *33*, 1143–1148. The Flack parameter will refine to a value near zero if the structure is in the correct configuration and will refine to a value near one for the inverted configuration.

$fS = [\sum w(F_o^2 - F_c^2)^2 / (n - p)]^{1/2}$  ( $n$  = number of data;  $p$  = number of parameters varied;  $w = [\sum^2(F_o^2) + (0.0323P)^2]^{-1}$  where  $P = [\text{Max}(F_o^2, 0) + 2F_c^2]/3$ ).

$gR_1 = \sum ||F_o| - |F_c|| / \sum |F_o|$ ;  $wR_2 = [\sum w(F_o^2 - F_c^2)^2 / \sum w(F_o^4)]^{1/2}$ .

## Appendix 2. Structure Report JMS0534: Vinylcyclohexenyl Complex

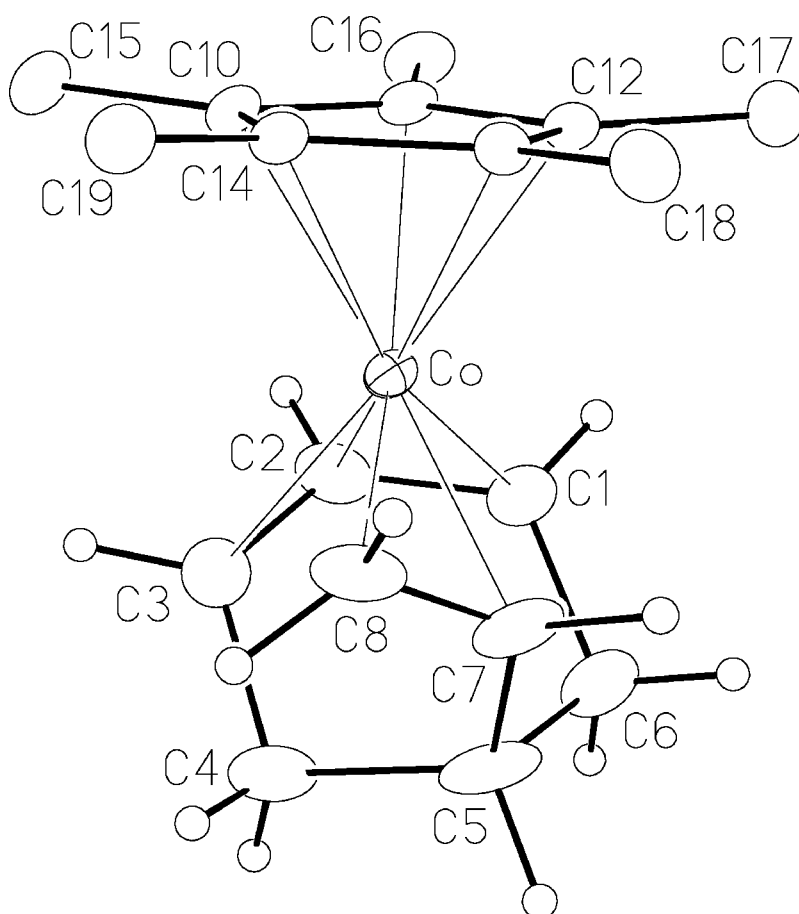
43

**Compound:**  $[(\eta^5\text{-C}_5\text{Me}_5)\text{Co}(\eta^3,\eta^2\text{-5-vinylcyclohex-2-en-1-yl})][\text{BF}_4]$

**Formula:**  $\text{C}_{18}\text{H}_{26}\text{BCoF}_4$

**Supervisor:** J. M. Stryker

**Crystallographer:** R. McDonald



Perspective view of the  $[(\eta^5\text{-C}_5\text{Me}_5)\text{Co}(\eta^3,\eta^2\text{-5-vinylcyclohex-2-en-1-yl})]^+$  complex ion showing the atom labelling scheme. Non-hydrogen atoms are represented by Gaussian ellipsoids at the 20% probability level. Hydrogen atoms of the 5-vinylcyclohex-2-en-1-yl ligand are shown with arbitrarily small thermal parameters; hydrogens of the pentamethylcyclopentadienyl ligand are not shown.

## Crystallographic Experimental Details

### A. Crystal Data

formula	C <sub>18</sub> H <sub>26</sub> BCoF <sub>4</sub>
formula weight	388.13
crystal dimensions (mm)	0.56 x 0.12 x 0.10
crystal system	monoclinic
space group [No.	<i>P</i> 2 <sub>1</sub> / <i>n</i> (an alternate setting of <i>P</i> 2 <sub>1</sub> / <i>c</i> 14])
unit cell parameters <sup>a</sup>	
<i>a</i> (Å)	8.9199 (9)
<i>b</i> (Å)	13.9572 (14)
<i>c</i> (Å)	14.0250 (14)
β (deg)	92.0720 (16)
<i>V</i> (Å <sup>3</sup> )	1744.9 (3)
<i>Z</i>	4
ρ <sub>calcd</sub> (g cm <sup>-3</sup> )	1.477
μ (mm <sup>-1</sup> )	1.019

### B. Data Collection and Refinement Conditions

diffractometer	Bruker PLATFORM/SMART 1000
CCD <sup>b</sup>	
radiation (λ [Å]) (0.71073)	graphite-monochromated Mo Kα
temperature (°C)	-80
scan type	ω scans (0.3°) (25 s exposures)
data collection 2θ limit (deg)	52.76
total data collected ≤ <i>l</i> ≤	12455 (-11 ≤ <i>h</i> ≤ 10, -17 ≤ <i>k</i> ≤ 17, -17 17)
independent reflections	3558 ( <i>R</i> <sub>int</sub> = 0.0347)
number of observed reflections ( <i>NO</i> )	2931 [ <i>F</i> <sub>o</sub> <sup>2</sup> ≥ 2σ( <i>F</i> <sub>o</sub> <sup>2</sup> )]
structure solution method	direct methods ( <i>SHELXS-86</i> <sup>c</sup> )
refinement method ( <i>SHELXL-93</i> <sup>d</sup> )	full-matrix least-squares on <i>F</i> <sup>2</sup>
absorption correction method	multi-scan ( <i>SADABS</i> )
range of transmission factors	0.9049–0.5991
data/restraints/parameters	3558 [ <i>F</i> <sub>o</sub> <sup>2</sup> ≥ -3σ( <i>F</i> <sub>o</sub> <sup>2</sup> )] / 20 <sup>e</sup> / 239
goodness-of-fit ( <i>S</i> ) <sup>f</sup>	1.052 [ <i>F</i> <sub>o</sub> <sup>2</sup> ≥ -3σ( <i>F</i> <sub>o</sub> <sup>2</sup> )]
final <i>R</i> indices <sup>g</sup>	
<i>R</i> <sub>1</sub> [ <i>F</i> <sub>o</sub> <sup>2</sup> ≥ 2σ( <i>F</i> <sub>o</sub> <sup>2</sup> )]	0.0602
<i>wR</i> <sub>2</sub> [ <i>F</i> <sub>o</sub> <sup>2</sup> ≥ -3σ( <i>F</i> <sub>o</sub> <sup>2</sup> )]	0.1677
largest difference peak and hole	1.174 and -0.648 e Å <sup>-3</sup>

<sup>a</sup>Obtained from least-squares refinement of 5568 reflections with  $5.32^\circ < 2\theta < 52.60^\circ$ .

<sup>b</sup>Programs for diffractometer operation, data collection, data reduction and absorption correction were those supplied by Bruker.

<sup>c</sup>Sheldrick, G. M. *Acta Crystallogr.* **1990**, *A46*, 467–473.

<sup>d</sup>Sheldrick, G. M. *SHELXL-93*. Program for crystal structure determination. University of Göttingen, Germany, 1993.

<sup>e</sup>All F–B bond lengths within both constituents (present in 75:25 ratio) of the disordered tetrafluoroborate ion were set to be equal to the same value, which was allowed to vary during refinement (the same was true for the 1,3 F…F distances).

$fS = [\sum w(F_o^2 - F_c^2)^2 / (n - p)]^{1/2}$  ( $n$  = number of data;  $p$  = number of parameters varied;  $w = [\sum^2(F_o^2) + (0.0904P)^2 + 3.4742P]^{-1}$  where  $P = [\text{Max}(F_o^2, 0) + 2F_c^2]/3$ ).

$gR_1 = \sum ||F_o| - |F_c|| / \sum |F_o|$ ;  $wR_2 = [\sum w(F_o^2 - F_c^2)^2 / \sum w(F_o^4)]^{1/2}$ .

### Appendix 3. Structure Report JMS0616:

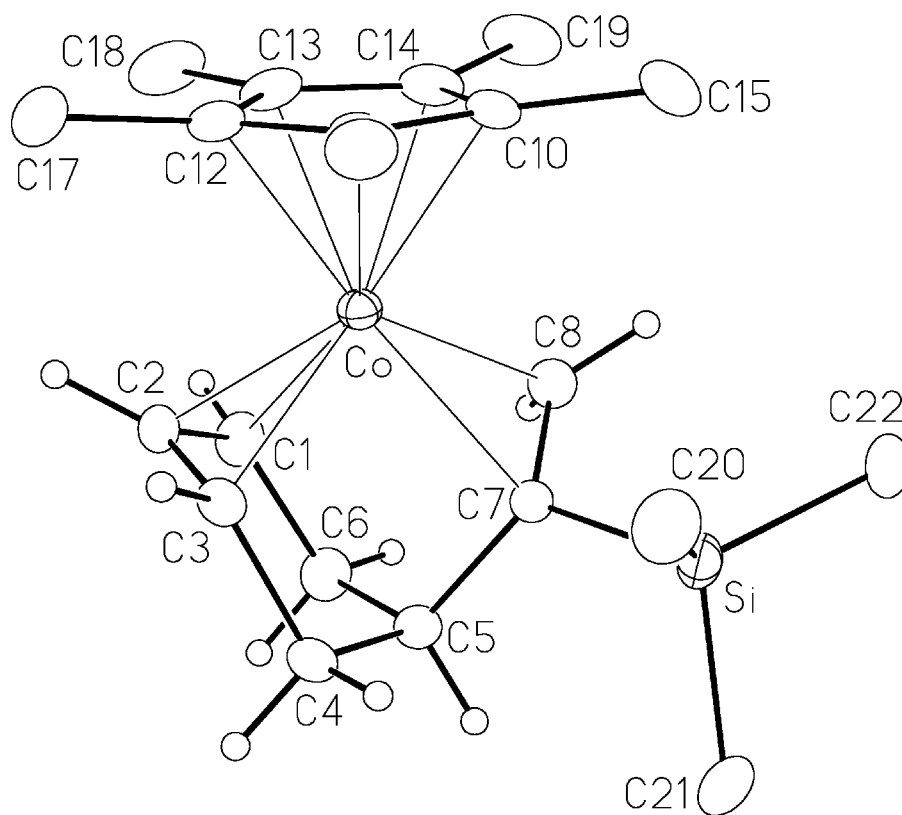
#### Trimethylsilylvinylcyclohexenyl Complex 47

**Compound:**  $[(\eta^5\text{-C}_5\text{Me}_5)\text{Co}(\eta^3,\eta^2\text{-5-(1-trimethylsilylvinyl)cyclohex-2-en-1-yl})][\text{PF}_6]$

**Formula:**  $\text{C}_{21}\text{H}_{34}\text{CoF}_6\text{PSi}$

**Supervisor:** J. M. Stryker

**Crystallographer:** R. McDonald



Perspective view of the  $[(\eta^5\text{-C}_5\text{Me}_5)\text{Co}(\eta^3,\eta^2\text{-5-(1-trimethylsilylvinyl)cyclohex-2-en-1-yl})]^+$  complex ion showing the atom labelling scheme. Non-hydrogen atoms are represented by Gaussian ellipsoids at the 20% probability level. Hydrogen atoms are shown with arbitrarily small thermal parameters except for trimethylsilyl and pentamethylcyclopentadienyl hydrogens, which are not shown.

## Crystallographic Experimental Details

### A. Crystal Data

formula	C <sub>21</sub> H <sub>34</sub> CoF <sub>6</sub> PSi
formula weight	518.47
crystal dimensions (mm)	0.44 x 0.27 x 0.20
crystal system	orthorhombic
space group	<i>Pca</i> 2 <sub>1</sub> (No. 29)
unit cell parameters <sup>a</sup>	
<i>a</i> (Å)	16.1683 (17)
<i>b</i> (Å)	8.8323 (9)
<i>c</i> (Å)	16.3923 (17)
<i>V</i> (Å <sup>3</sup> )	2340.9 (4)
<i>Z</i>	4
$\rho_{\text{calcd}}$ (g cm <sup>-3</sup> )	1.471
$\mu$ (mm <sup>-1</sup> )	0.906

### B. Data Collection and Refinement Conditions

diffractometer	Bruker PLATFORM/SMART 1000
CCD <sup>b</sup>	
radiation ( $\lambda$ [Å])	graphite-monochromated Mo K $\alpha$
(0.71073)	
temperature (°C)	-80
scan type	$\omega$ scans (0.4°) (10 s exposures)
data collection $2\theta$ limit (deg)	52.82
total data collected	13799 ( $-17 \leq h \leq 20$ , $-11 \leq k \leq 10$ , $-20$
$\leq l \leq$	20)
independent reflections	4786 ( $R_{\text{int}} = 0.0379$ )
number of observed reflections ( <i>NO</i> )	3979 [ $F_o^2 \geq 2\sigma(F_o^2)$ ]
structure solution method	Patterson search/structure
expansion	( <i>DIRDIF-99</i> ) <sup>c</sup>
refinement method	full-matrix least-squares on $F^2$
( <i>SHELXL-93</i> ) <sup>d</sup>	
absorption correction method	multi-scan ( <i>SADABS</i> )
range of transmission factors	0.8396–0.6913
data/restraints/parameters	4786 [ $F_o^2 \geq -3\sigma(F_o^2)$ ] / 0 / 276
Flack absolute structure parameter <sup>e</sup>	-0.005 (19)
goodness-of-fit ( <i>S</i> ) <sup>f</sup>	1.020 [ $F_o^2 \geq -3\sigma(F_o^2)$ ]
final <i>R</i> indices <sup>g</sup>	
<i>R</i> <sub>1</sub> [ $F_o^2 \geq 2\sigma(F_o^2)$ ]	0.0461
<i>wR</i> <sub>2</sub> [ $F_o^2 \geq -3\sigma(F_o^2)$ ]	0.1267
largest difference peak and hole	0.714 and -0.311 e Å <sup>-3</sup>

<sup>a</sup>Obtained from least-squares refinement of 4344 reflections with  $4.62^\circ < 2\theta < 46.32^\circ$ .

<sup>b</sup>Programs for diffractometer operation, data collection, data reduction and absorption correction were those supplied by Bruker.

<sup>c</sup>Beurskens, P. T.; Beurskens, G.; de Gelder, R.; Garcia-Granda, S.; Israel, R.; Gould, R. O.; Smits, J. M. M. (1999). The *DIRDIF-99* program system. Crystallography Laboratory, University of Nijmegen, The Netherlands.

<sup>d</sup>Sheldrick, G. M. *SHELXL-93*. Program for crystal structure determination. University of Göttingen, Germany, 1993.

<sup>e</sup>Flack, H. D. *Acta Crystallogr.* **1983**, *A39*, 876–881; Flack, H. D.; Bernardinelli, G. *Acta Crystallogr.* **1999**, *A55*, 908–915; Flack, H. D.; Bernardinelli, G. *J. Appl. Cryst.* **2000**, *33*, 1143–1148. The Flack parameter will refine to a value near zero if the structure is in the correct configuration and will refine to a value near one for the inverted configuration.

$fS = [\sum w(F_o^2 - F_c^2)^2 / (n - p)]^{1/2}$  ( $n$  = number of data;  $p$  = number of parameters varied;  $w = [\sum^2(F_o^2) + (0.0757P)^2 + 0.8370P]^{-1}$  where  $P = [\text{Max}(F_o^2, 0) + 2F_c^2]/3$ ).

$gR_1 = \sum ||F_o| - |F_c|| / \sum |F_o|$ ;  $wR_2 = [\sum w(F_o^2 - F_c^2)^2 / \sum w(F_o^4)]^{1/2}$ .

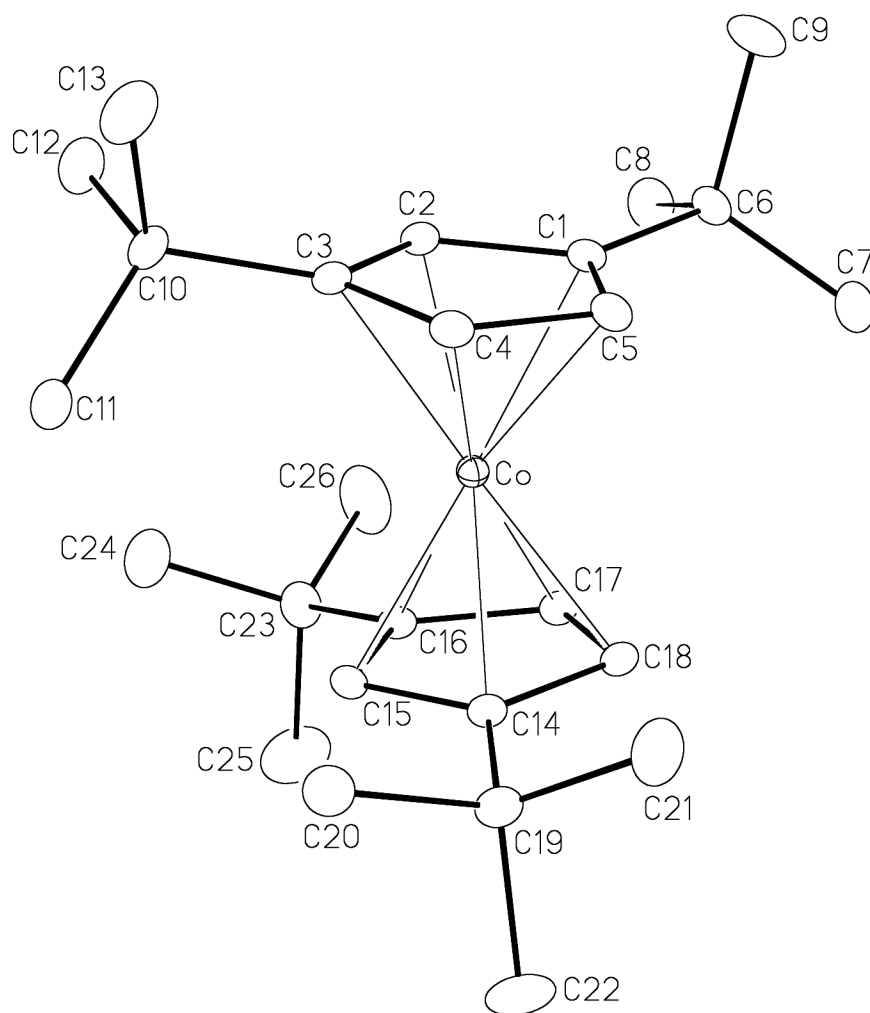
## Appendix 4. Structure Report JMS0855: Cobalticenium Complex 63

**Compound:**  $[(C_5H_3^tBu_2)Co][BF_4] \cdot CHCl_3$

**Formula:**  $C_{27}H_{43}BCl_3CoF_4$  ( $C_{26}H_{42}BCoF_4 \cdot CHCl_3$ )

**Supervisor:** J. M. Stryker

**Crystallographer:** M. J. Ferguson



Perspective view of the  $[(C_5H_3^tBu_2)Co]^+$  ion showing the atom labelling scheme. Non-hydrogen atoms are represented by Gaussian ellipsoids at the 20% probability level. Hydrogen atoms are not shown.

## Crystallographic Experimental Details

### A. Crystal Data

formula	C <sub>27</sub> H <sub>43</sub> BCl <sub>3</sub> CoF <sub>4</sub>
formula weight	619.70
crystal dimensions (mm)	0.63 x 0.42 x 0.28
crystal system	orthorhombic
space group	<i>Pna</i> 2 <sub>1</sub> (No. 33)
unit cell parameters <sup>a</sup>	
<i>a</i> (Å)	21.0272 (16)
<i>b</i> (Å)	14.9919 (11)
<i>c</i> (Å)	9.6529 (7)
<i>V</i> (Å <sup>3</sup> )	3043.0 (4)
<i>Z</i>	4
$\rho_{\text{calcd}}$ (g cm <sup>-3</sup> )	1.353
$\mu$ (mm <sup>-1</sup> )	0.867

### B. Data Collection and Refinement Conditions

diffractometer	Bruker D8/APEX II CCD <sup>b</sup>
radiation ( $\lambda$ [Å])	graphite-monochromated Mo K $\alpha$
(0.71073)	
temperature (°C)	-100
scan type	$\omega$ scans (0.4°) (10 s exposures)
data collection $2\theta$ limit (deg)	54.98
total data collected	21137 ( $-27 \leq h \leq 25$ , $-19 \leq k \leq 17$ , $-12$
$\leq l \leq$	12)
independent reflections	6895 ( $R_{\text{int}} = 0.0226$ )
number of observed reflections ( <i>NO</i> )	6351 [ $F_o^2 \geq 2\sigma(F_o^2)$ ]
structure solution method	direct methods ( <i>SIR97</i> <sup>c</sup> )
refinement method	full-matrix least-squares on $F^2$
( <i>SHELXL-97</i> <sup>d</sup> )	
absorption correction method	multi-scan ( <i>SADABS</i> )
range of transmission factors	0.7927–0.6112
data/restraints/parameters	6895 [ $F_o^2 \geq -3\sigma(F_o^2)$ ] / 0 / 325
Flack absolute structure parameter <sup>e</sup>	-0.003(11)
goodness-of-fit ( <i>S</i> ) <sup>f</sup>	1.067 [ $F_o^2 \geq -3\sigma(F_o^2)$ ]
final <i>R</i> indices <sup>g</sup>	
<i>R</i> <sub>1</sub> [ $F_o^2 \geq 2\sigma(F_o^2)$ ]	0.0320
<i>wR</i> <sub>2</sub> [ $F_o^2 \geq -3\sigma(F_o^2)$ ]	0.0846
largest difference peak and hole	0.517 and -0.293 e Å <sup>-3</sup>

<sup>a</sup>Obtained from least-squares refinement of 9882 reflections with  $4.74^\circ < 2\theta <$

55.72°.

<sup>b</sup>Programs for diffractometer operation, data collection, data reduction and absorption correction were those supplied by Bruker.

<sup>c</sup>Altomare, A.; Burla, M. C.; Camalli, M.; Cascarano, G. L.; Giacovazzo, C.; Guagliardi, A.; Moliterni, A. G. G.; Polidori, G.; Spagna, R. *J. Appl. Cryst.* **1999**, *32*, 115–119.

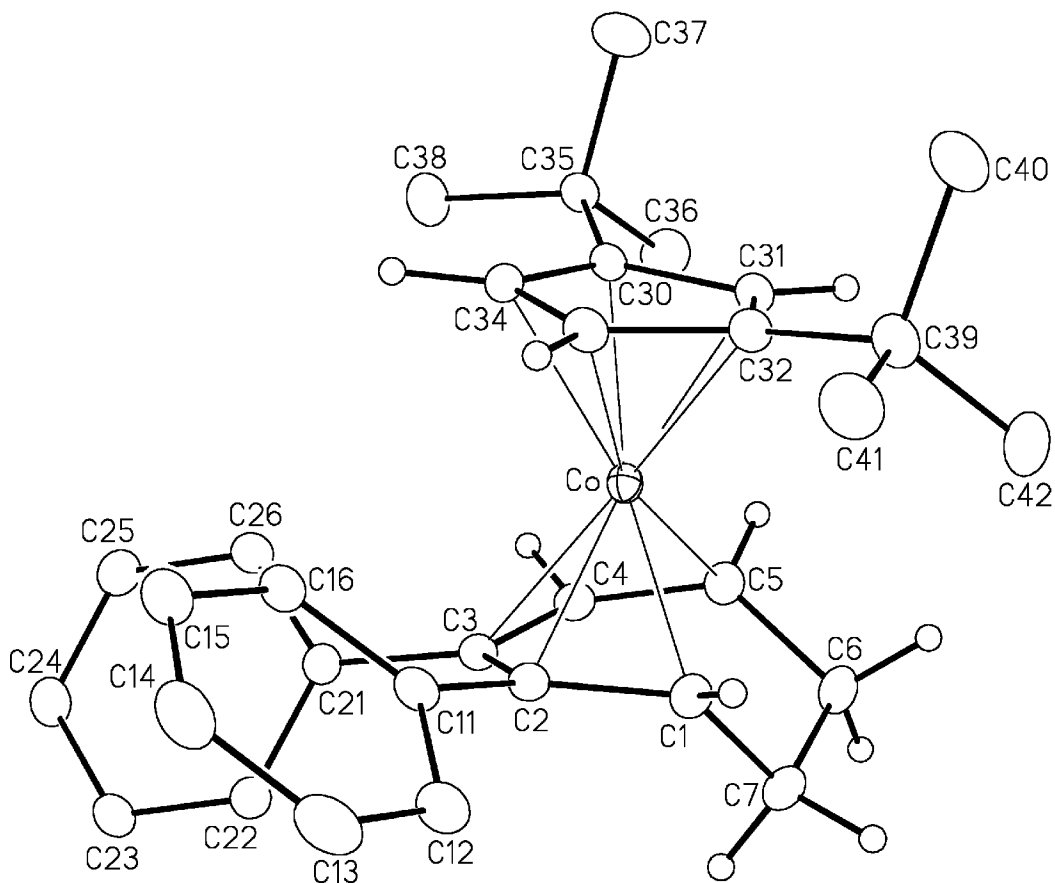
<sup>d</sup>Sheldrick, G. M. *Acta Crystallogr.* **2008**, *A64*, 112–122.

<sup>e</sup>Flack, H. D. *Acta Crystallogr.* **1983**, *A39*, 876–881; Flack, H. D.; Bernardinelli, G. *Acta Crystallogr.* **1999**, *A55*, 908–915; Flack, H. D.; Bernardinelli, G. *J. Appl. Cryst.* **2000**, *33*, 1143–1148. The Flack parameter will refine to a value near zero if the structure is in the correct configuration and will refine to a value near one for the inverted configuration.

$fS = [\sum w(F_o^2 - F_c^2)^2 / (n - p)]^{1/2}$  ( $n$  = number of data;  $p$  = number of parameters varied;  $w = [\sum^2(F_o^2) + (0.0455P)^2 + 0.7284P]^{-1}$  where  $P = [\text{Max}(F_o^2, 0) + 2F_c^2]/3$ ).

$gR_1 = \sum ||F_o| - |F_c|| / \sum |F_o|$ ;  $wR_2 = [\sum w(F_o^2 - F_c^2)^2 / \sum w(F_o^4)]^{1/2}$ .





Perspective view of the second of two crystallographically independent  $[(C_5H_3^tBu_2)Co(2,3\text{-diphenylhepta-}2,4\text{-dien-}1\text{-yl})]^+$  ions (*molecule B*) showing the atom labelling scheme. Non-hydrogen atoms are represented by Gaussian ellipsoids at the 20% probability level. Hydrogen atoms are shown with arbitrarily small thermal parameters, and are not shown for the *tert*-butyl and phenyl groups.

## Crystallographic Experimental Details

### A. Crystal Data

formula	C <sub>32</sub> H <sub>38</sub> BCoF <sub>4</sub>
formula weight	568.36
crystal dimensions (mm)	0.41 x 0.25 x 0.19
crystal system	triclinic
space group	$P\bar{1}$ (No. 2)
unit cell parameters <sup>a</sup>	
<i>a</i> (Å)	9.9168 (13)
<i>b</i> (Å)	10.6310 (14)
<i>c</i> (Å)	30.343 (4)
<i>α</i> (deg)	93.6758 (16)
<i>β</i> (deg)	90.4395 (16)
<i>γ</i> (deg)	117.0461 (14)
<i>V</i> (Å <sup>3</sup> )	2840.8 (6)
<i>Z</i>	4
$\rho_{\text{calcd}}$ (g cm <sup>-3</sup> )	1.329
$\mu$ (mm <sup>-1</sup> )	0.650

### B. Data Collection and Refinement Conditions

diffractometer	Bruker PLATFORM/SMART 1000
CCD <sup>b</sup>	
radiation ( $\lambda$ [Å])	graphite-monochromated Mo K $\alpha$
(0.71073)	
temperature (°C)	-100
scan type	$\omega$ scans (0.3°) (20 s exposures)
data collection $2\theta$ limit (deg)	52.80
total data collected	22379 ( $-12 \leq h \leq 12$ , $-13 \leq k \leq 13$ , $-37$
$\leq l \leq$	37)
independent reflections	11548 ( $R_{\text{int}} = 0.0307$ )
number of observed reflections ( <i>NO</i> )	OBS [ $F_o^2 \geq 2\sigma(F_o^2)$ ]
structure solution method	direct methods ( <i>SIR97</i> <sup>c</sup> )
refinement method	full-matrix least-squares on $F^2$
( <i>SHELXL</i> -	97 <sup>d</sup> )
absorption correction method	Gaussian integration (face-indexed)
range of transmission factors	0.8865–0.7765
data/restraints/parameters	11548 [ $F_o^2 \geq -3\sigma(F_o^2)$ ] / 0 / 685
goodness-of-fit ( <i>S</i> ) <sup>e</sup>	1.030 [ $F_o^2 \geq -3\sigma(F_o^2)$ ]
final <i>R</i> indices <sup>f</sup>	
<i>R</i> <sub>1</sub> [ $F_o^2 \geq 2\sigma(F_o^2)$ ]	0.0481
<i>wR</i> <sub>2</sub> [ $F_o^2 \geq -3\sigma(F_o^2)$ ]	0.1351
largest difference peak and hole	0.903 and -0.502 e Å <sup>-3</sup>

<sup>a</sup>Obtained from least-squares refinement of 8152 reflections with  $4.62^\circ < 2\theta < 51.90^\circ$ .

<sup>b</sup>Programs for diffractometer operation, data collection, data reduction and absorption correction were those supplied by Bruker.

<sup>c</sup>Altomare, A.; Burla, M. C.; Camalli, M.; Cascarano, G. L.; Giacovazzo, C.; Guagliardi, A.; Moliterni, A. G. G.; Polidori, G.; Spagna, R. *J. Appl. Cryst.* **1999**, *32*, 115–119.

<sup>d</sup>Sheldrick, G. M. *Acta Crystallogr.* **2008**, *A64*, 112–122.

<sup>e</sup> $S = [\sum w(F_o^2 - F_c^2)^2 / (n - p)]^{1/2}$  ( $n$  = number of data;  $p$  = number of parameters varied;  $w = [\sum^2(F_o^2) + (0.0710P)^2 + 1.5190P]^{-1}$  where  $P = [\text{Max}(F_o^2, 0) + 2F_c^2]/3$ ).

<sup>f</sup> $R_1 = \sum ||F_o| - |F_c|| / \sum |F_o|$ ;  $wR_2 = [\sum w(F_o^2 - F_c^2)^2 / \sum w(F_o^4)]^{1/2}$ .

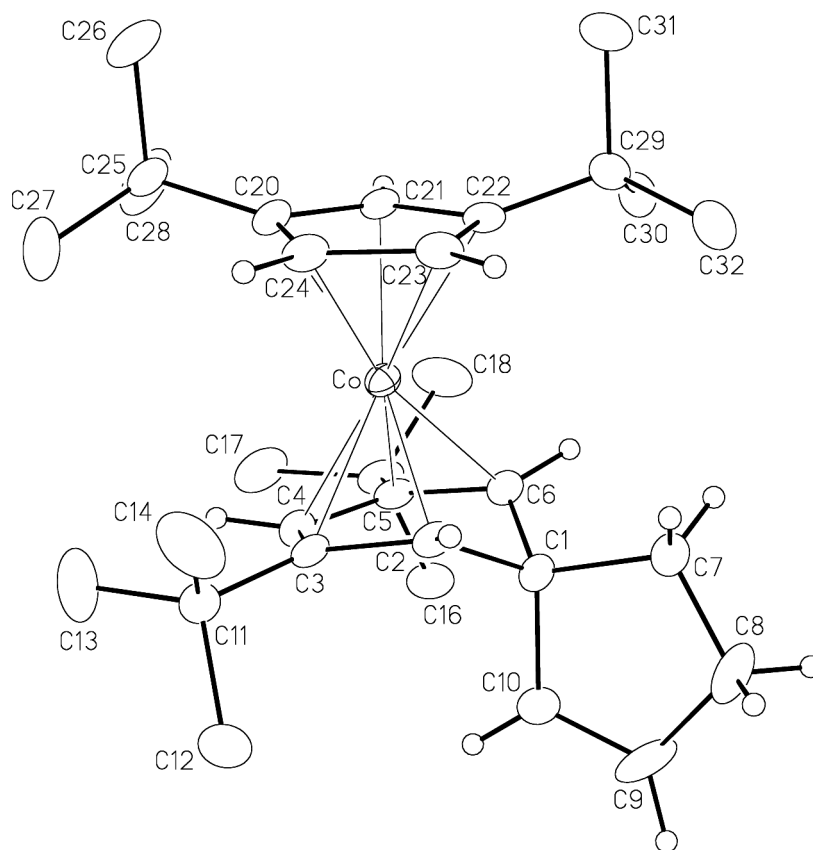
## Appendix 7. Structure Report JMS0931: Spirocyclic Complex 78

**Compound:**  $[(C_5H_3^tBu_2)Co(7,9\text{-di-}tert\text{-butylspiro[4.5]deca-1,6,9\text{-trien-8-yl})][BF_4]$

**Formula:**  $C_{31}H_{48}BCoF_4$

**Supervisor:** J. M. Stryker

**Crystallographer:** M. J. Ferguson



Perspective view of the  $[(C_5H_3^tBu_2)Co(7,9\text{-di-}tert\text{-butylspiro[4.5]deca-1,6,9\text{-trien-8-yl})]^+$  ion showing the atom labelling scheme. Non-hydrogen atoms are represented by Gaussian ellipsoids at the 20% probability level. Hydrogen atoms are shown with arbitrarily small thermal parameters, and are not shown for the *tert*-butyl groups.

## Crystallographic Experimental Details

### A. Crystal Data

formula	C <sub>31</sub> H <sub>46</sub> BCoF <sub>4</sub>
formula weight	564.42
crystal dimensions (mm)	0.31 x 0.21 x 0.10
crystal system	monoclinic
space group	C2/c
unit cell parameters <sup>a</sup>	
<i>a</i> (Å)	32.889 (10)
<i>b</i> (Å)	10.392 (3)
<i>c</i> (Å)	17.673 (6)
β (deg)	99.526 (5)
<i>V</i> (Å <sup>3</sup> )	5957 (3)
<i>Z</i>	8
ρ <sub>calcd</sub> (g cm <sup>-3</sup> )	1.259
μ (mm <sup>-1</sup> )	0.619

### B. Data Collection and Refinement Conditions

diffractometer	Bruker PLATFORM/SMART 1000
CCD <sup>b</sup>	
radiation (λ [Å]) (0.71073)	graphite-monochromated Mo Kα
temperature (°C)	-100
scan type	ω scans (0.3°) (30 s exposures)
data collection 2θ limit (deg)	50.50
total data collected ≤ <i>l</i> ≤	18363 (-39 ≤ <i>h</i> ≤ 39, -12 ≤ <i>k</i> ≤ 12, -21 21)
independent reflections	5391 ( <i>R</i> <sub>int</sub> = 0.1115)
number of observed reflections ( <i>NO</i> )	2945 [ <i>F</i> <sub>o</sub> <sup>2</sup> ≥ 2σ( <i>F</i> <sub>o</sub> <sup>2</sup> )]
structure solution method	direct methods ( <i>SIR97</i> <sup>c</sup> )
refinement method ( <i>SHELXL-97</i> <sup>d</sup> )	full-matrix least-squares on <i>F</i> <sup>2</sup>
absorption correction method	Gaussian integration (face-indexed)
range of transmission factors	0.9407–0.8313
data/restraints/parameters	5391 [ <i>F</i> <sub>o</sub> <sup>2</sup> ≥ -3σ( <i>F</i> <sub>o</sub> <sup>2</sup> )] / 0 / 334
goodness-of-fit ( <i>S</i> ) <sup>e</sup>	1.029 [ <i>F</i> <sub>o</sub> <sup>2</sup> ≥ -3σ( <i>F</i> <sub>o</sub> <sup>2</sup> )]
final <i>R</i> indices <sup>f</sup>	
<i>R</i> <sub>1</sub> [ <i>F</i> <sub>o</sub> <sup>2</sup> ≥ 2σ( <i>F</i> <sub>o</sub> <sup>2</sup> )]	0.0681
<i>wR</i> <sub>2</sub> [ <i>F</i> <sub>o</sub> <sup>2</sup> ≥ -3σ( <i>F</i> <sub>o</sub> <sup>2</sup> )]	0.2162
largest difference peak and hole	0.747 and -0.746 e Å <sup>-3</sup>

<sup>a</sup>Obtained from least-squares refinement of 2036 reflections with  $4.62^\circ < 2\theta < 45.14^\circ$ .

<sup>b</sup>Programs for diffractometer operation, data collection, data reduction and absorption correction were those supplied by Bruker.

<sup>c</sup>Altomare, A.; Burla, M. C.; Camalli, M.; Cascarano, G. L.; Giacovazzo, C.; Guagliardi, A.; Moliterni, A. G. G.; Polidori, G.; Spagna, R. *J. Appl. Cryst.* **1999**, *32*, 115–119.

<sup>d</sup>Sheldrick, G. M. *Acta Crystallogr.* **2008**, *A64*, 112–122.

<sup>e</sup> $S = [\sum w(F_o^2 - F_c^2)^2 / (n - p)]^{1/2}$  ( $n$  = number of data;  $p$  = number of parameters varied;  $w = [\sum^2(F_o^2) + (0.1128P)^2]^{-1}$  where  $P = [\text{Max}(F_o^2, 0) + 2F_c^2]/3$ ).

<sup>f</sup> $R_1 = \sum ||F_o| - |F_c|| / \sum |F_o|$ ;  $wR_2 = [\sum w(F_o^2 - F_c^2)^2 / \sum w(F_o^4)]^{1/2}$ .



## Crystallographic Experimental Details

### A. Crystal Data

formula	C <sub>19</sub> H <sub>29</sub> BCl <sub>3</sub> CoF <sub>4</sub>
formula weight	509.51
crystal dimensions (mm)	0.59 x 0.17 x 0.06
crystal system	monoclinic
space group	<i>P</i> 2 <sub>1</sub> / <i>c</i> (No. 14)
unit cell parameters <sup>a</sup>	
<i>a</i> (Å)	16.3194 (10)
<i>b</i> (Å)	10.1645 (6)
<i>c</i> (Å)	14.3631 (9)
β (deg)	97.3680 (10)
<i>V</i> (Å <sup>3</sup> )	2362.9 (2)
<i>Z</i>	4
ρ <sub>calcd</sub> (g cm <sup>-3</sup> )	1.432
μ (mm <sup>-1</sup> )	1.099

### B. Data Collection and Refinement Conditions

diffractometer	Bruker D8/APEX II CCD <sup>b</sup>
radiation (λ [Å]) (0.71073)	graphite-monochromated Mo Kα
temperature (°C)	-100
scan type	ω scans (0.3°) (20 s exposures)
data collection 2θ limit (deg)	50.50
total data collected ≤ <i>l</i> ≤	16384 (-19 ≤ <i>h</i> ≤ 19, -12 ≤ <i>k</i> ≤ 12, -17 17)
independent reflections	4281 ( <i>R</i> <sub>int</sub> = 0.0303)
number of observed reflections ( <i>NO</i> )	3599 [ <i>F</i> <sub>o</sub> <sup>2</sup> ≥ 2σ( <i>F</i> <sub>o</sub> <sup>2</sup> )]
structure solution method	direct methods ( <i>SHELXS-97</i> <sup>c</sup> )
refinement method ( <i>SHELXL-97</i> <sup>c</sup> )	full-matrix least-squares on <i>F</i> <sup>2</sup>
absorption correction method	numerical ( <i>SADABS</i> )
range of transmission factors	0.9410–0.5642
data/restraints/parameters	4281 [ <i>F</i> <sub>o</sub> <sup>2</sup> ≥ -3σ( <i>F</i> <sub>o</sub> <sup>2</sup> )] / 6 <sup>d</sup> / 269
goodness-of-fit ( <i>S</i> ) <sup>e</sup>	1.067 [ <i>F</i> <sub>o</sub> <sup>2</sup> ≥ -3σ( <i>F</i> <sub>o</sub> <sup>2</sup> )]
final <i>R</i> indices <sup>f</sup>	
<i>R</i> <sub>1</sub> [ <i>F</i> <sub>o</sub> <sup>2</sup> ≥ 2σ( <i>F</i> <sub>o</sub> <sup>2</sup> )]	0.0454
<i>wR</i> <sub>2</sub> [ <i>F</i> <sub>o</sub> <sup>2</sup> ≥ -3σ( <i>F</i> <sub>o</sub> <sup>2</sup> )]	0.1377
largest difference peak and hole	0.950 and -0.596 e Å <sup>-3</sup>

<sup>a</sup>Obtained from least-squares refinement of 7303 reflections with 4.74° < 2θ <

49.94°.

<sup>b</sup>Programs for diffractometer operation, data collection, data reduction and absorption correction were those supplied by Bruker.

<sup>c</sup>Sheldrick, G. M. *Acta Crystallogr.* **2008**, *A64*, 112–122.

<sup>d</sup>The C–Cl and Cl···Cl distances of the minor orientation of the disordered solvent chloroform molecule were restrained to be the same as those of the major orientation by use of the *SHELXL* SAME instruction.

<sup>e</sup> $S = [\sum w(F_o^2 - F_c^2)^2 / (n - p)]^{1/2}$  ( $n$  = number of data;  $p$  = number of parameters varied;  $w = [\sum^2(F_o^2) + (0.0745P)^2 + 3.1099P]^{-1}$  where  $P = [\text{Max}(F_o^2, 0) + 2F_c^2]/3$ ).

<sup>f</sup> $R_1 = \sum ||F_o| - |F_c|| / \sum |F_o|$ ;  $wR_2 = [\sum w(F_o^2 - F_c^2)^2 / \sum w(F_o^4)]^{1/2}$ .